BMR JOURNAL of Australian Geology & Geophysics

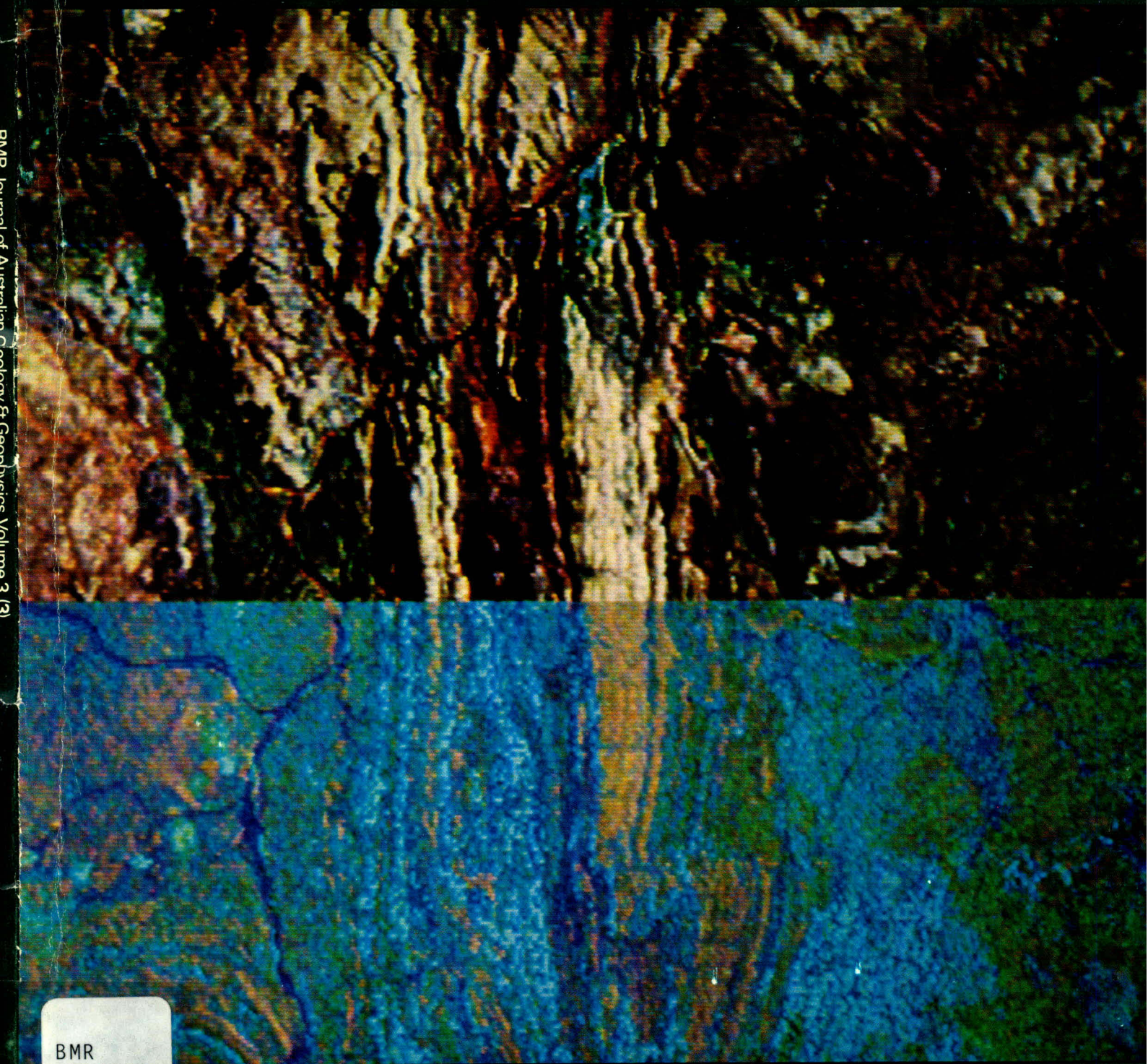

VOLUME 3, NUMBER 3, SEPTEMBER 1978

Department of National Development, Australia

Minister: The Hon. K. E. Newman, M.P.
Secretary: A. J. Woods

Bureau of Mineral Resources, Geology and Geophysics

Director: L. C. Noakes, O.B.E.
Editor, BMR Journal: J. F. Truswell

The BMR Journal of Australian Geology and Geophysics is a quarterly journal of research and related activities. Contributions are from officers of the BMR, from BMR officers working in collaboration with others, or requested work sponsored by the BMR. In addition to articles the Journal may include shorter notes and discussion of papers published in it. Discussion of papers is invited from anyone.

Annual subscription to the Journal is at the rate of $10 (Australian). Individual numbers, if available, cost $3. Subscriptions, etc., made payable to the Receiver of Public Moneys in Australian dollars, should be sent to the Director, Bureau of Mineral Resources, Geology & Geophysics, P.O. Box 378, Canberra, A.C.T. 2601, Australia. The Journal can also be obtained from the offices of the Department of National Development in Sydney and Melbourne.

Other matters concerning the Journal should be sent to the Director, marked for the attention of the Editor, BMR Journal.

BMR JOURNAL of Australian Geology & Geophysics

Volume 3, Number 3
September 1978

AUSTRALIAN GOVERNMENT PUBLISHING SERVICE
CANBERRA 1978

Front cover:

Part of LANDSAT image 2292-23594 covering the Mammoth Mines region of northwest Queensland. The scene, photographed from an interactive video display screen, illustrates (at a scale of about 1:100 000) two processes that can be applied to LANDSAT data to assist geological interpretation. The cover illustration was computer-processed by the CSIRO Division of Mineral Physics to display the upper part as a false colour composite of MSS bands 4, 5 and 7, and the lower part as a colour-ratio composite of MSS ratios 4/5, 5/6, 6/7. The potential of LANDSAT for assisting mineral and petroleum exploration is discussed in a paper in this number.

ISSN 0312-9608

Printed by Graphic Services Pty Ltd, 516-518 Grand Junction Road, Northfield, S.A. 5085

Ages of granites and associated mineralisation in the Herberton tinfield of northeast Queensland

L. P. Black, D. H. Blake, & J. A. Olatunji[1]

Rb-Sr isotopic data reveal a close temporal association between ore deposits and the emplacement of Upper Palaeozoic granitic intrusions in the Herberton tinfield of northeast Queensland. Three main granite types are present: Elizabeth Creek type, consisting mainly of leucocratic biotite adamellite and ranging in age from 292 or 299 m.y. to 320 m.y.; Herbert River type, mainly granodiorite and isotopically dated at 278 to 315 m.y.; and 280 m.y. old Mareeba type, which consists mainly of biotite adamellite. Six mineralising events have been detected, all but the youngest being related to Elizabeth Creek Granite. The oldest, about 320 m.y. ago, was associated with intrusion of apparently small granite bodies southwest and southeast of Irvinebank. The next, at 314 m.y., accompanied the intrusion of the main mass of Elizabeth Creek Granite in the Emuford-Watsonville-Coolgarra area. A slightly later event, at 309 m.y., was associated with the emplacement of petrographically similar granite near Herberton. Mineralisation in the Wolfram Camp and Bamford Hill areas appears to have taken place about 303 m.y. ago. All of these events were characterised by greisen formation. A subsequent mineralisation in the Herberton area, at about 297 m.y., is related to a fine-grained phase of Elizabeth Creek Granite, and is characterised by chloritic alteration. The youngest dated event, in which hydrothermal alteration led to the production of fine-grained green biotite, occurred at about 284 m.y., and may be related to an intrusion of Mareeba-type granite. None of the major economic products (Sn, W, Cu, Pb, Ag) were confined to a single mineralising event: tin deposits, for example, were formed during at least five of the six episodes, and tungsten during at least four.

Introduction

Important Sn, W, Cu, Pb, and Ag mineralisation in the Herberton tinfield of northeast Queensland is clearly related to granitic intrusion. In this paper Rb-Sr ages for both the orebodies and the intrusions are presented and discussed, in an attempt to determine the age of the mineralisation. The area studied (Fig. 1) is those parts of the Herberton, Chillagoe, and Mareeba Gold and Mineral Fields covered by the Herberton and Mount Garnet 1-mile Sheets (Blake, 1972) and the eastern parts of the Almaden and Chillagoe 1-mile Sheets (de Keyser & Wolff, 1964). For convenience, this area is here termed the Herberton tinfield. Regional geological mapping of this area was commenced by members of the Bureau of Mineral Resources and Geological Survey of Queensland in 1956 (Best, 1962). Branch (1966) also covered the area in his study of acid magmatism in northeast Queensland. More recently, one of us (J.A.O.) has studied the area around Herberton in considerable detail. Isotopic dating was begun by Richards & others (1966), and has been continued since then by Black (e.g., Black & Richards, 1972a, b; Black, 1978; Oversby & others, 1976).

Geological setting

The Herberton tinfield lies within the northern part of the Palaeozoic Tasman Geosyncline, to the east of the Precambrian Georgetown Inlier. The Chillagoe Formation, consisting mainly of limestone and chert, forms the westernmost part of the geosyncline near Chillagoe and Almaden. This formation is overlain to the east by the Hodgkinson Formation, a thick turbidite sequence of greywacke and siltstone which forms the bulk of the Hodgkinson Basin (de Keyser & Lucas, 1968). These rocks range in age from Silurian to Devonian or possibly Lower Carboniferous, and are tightly folded. The two formations, and also the Precambrian inlier to the west, are intruded and overlain by extensive Upper Palaeozoic acid igneous rocks of rather uniform composition. These occur as high-level granite intrusions, ring complexes with both intrusive and extrusive components, and predominantly ignimbritic volcanics which are considered by Branch (1966, 1967) to occupy huge cauldron subsidence areas. Of these, only the granites are thought to have played a major role in ore formation.

Analytical techniques

Granite samples were collected from blast sites and fresh outcrops. Most analysed samples of orebody material were collected by sledgehammer from disused mine workings; a few in the Herberton area came from drill core. Subsequent procedures were based on the techniques outlined in Page & others (1976) and Williams & others (1976), and incorporated a mixed Rb^{85}-Sr^{84} spike. Regression of all total-rock data is based on the work of McIntyre & others (1966). Following Black (1978), slightly lower precision estimates (0.5%) have been applied to the mica ages than those reported (0.3%) for the joint Australian National University/Bureau of Mineral Resources laboratory by Williams & others (1976)—because of the generally lower common Sr content and consequently less stable Sr-ion signals for the micas of this study. Mica ages are therefore considered to be correct to ± 3 m.y. All precision limits are quoted at the 95 percent confidence level. Replicate analyses for two samples (74490207, 74490208) and analyses of two samples (74490241, 74490242) from a single locality appear in Table 2, and these indicate that the precision limits are probably realistic. The value $1.42 \times 10^{-11} y^{-1}$ (Neumann & Huster, 1972; Steiger & Jäger, 1977) has been used for the decay constant of Rb^{87}. To enable meaningful comparisons, all previously reported Rb-Sr ages from the area have been recalculated using this decay constant, making them about 2 percent younger.

1. Geology Department, Ahmadu Bello University, Zaria, Nigeria.

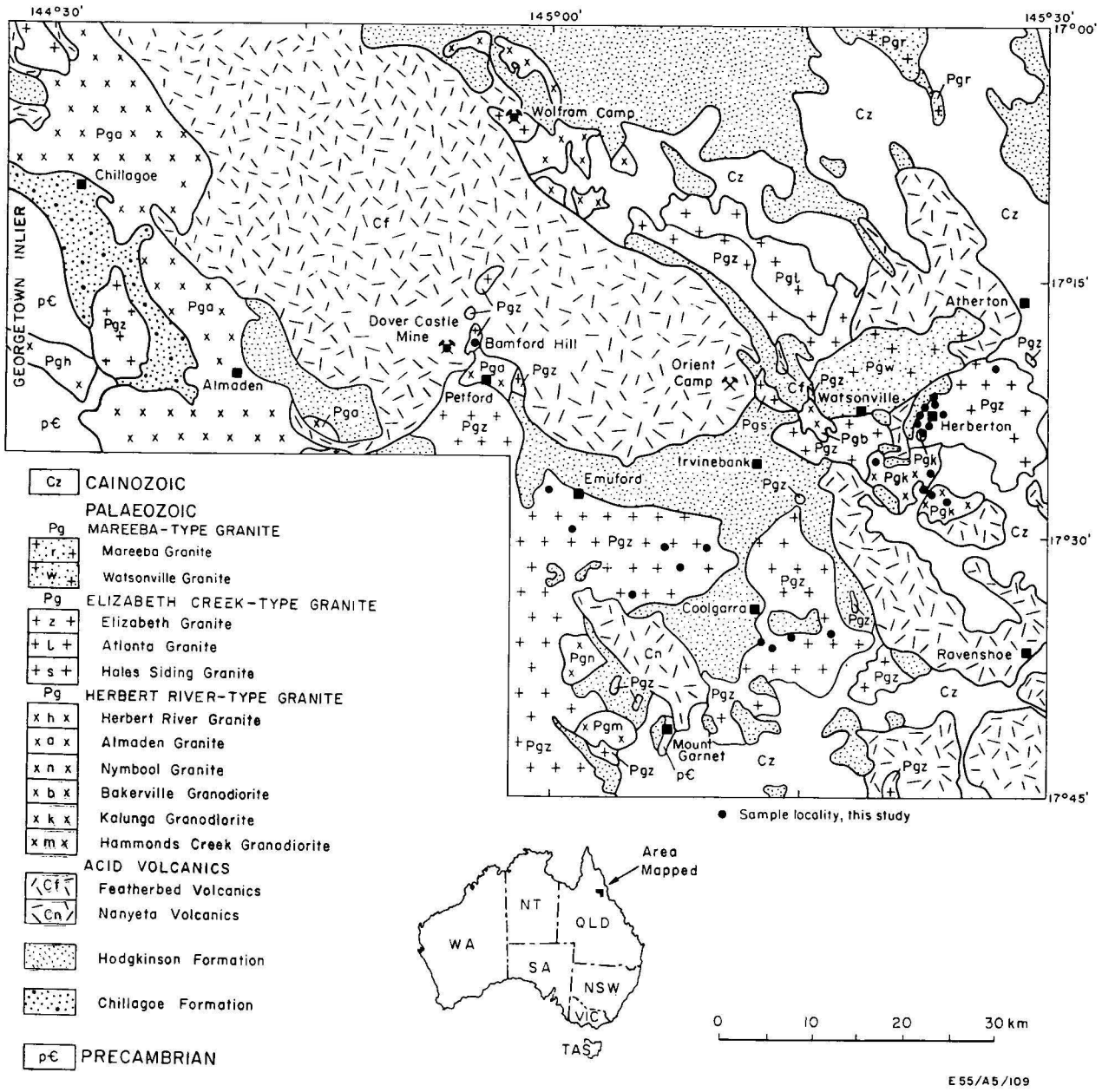

Figure 1. Geological map of the Herberton tinfield area.

Granites

Three main types of Upper Palaeozoic granitic rocks, the Elizabeth Creek, Herbert River, and Mareeba types, are present in the Herberton tinfield. Isotopic ages for these granites are summarised in Table 3.

Elizabeth Creek-type granite

This is the most extensive of the granite types, and is considered by Blake (1972), and Blake & Smith (1970) to be responsible for the Sn, W, Mo, Sb, Bi, As, and most of the Cu, Pb, Ag, and Zn mineralisation. It includes the Elizabeth Creek Granite, Atlanta Granite, and Hales Siding Granite of Blake (1972), and the Elizabeth Creek Granite of de Keyser & Wolff (1964), all of which consist predominantly of biotite adamellite. Typical features are pale pink to orange or pale grey colours; colour index less than 5; grain-size ranging from fine to coarse, with fine-grained varieties commonly containing both feldspar phenocrysts and quartz blebs; abundant aplite veins and greisens; general absence of xenoliths; almost ubiquitous accessory fluorite. The Elizabeth Creek-type granite ranges in age (after Black, 1978) from perhaps 292 m.y. at Bamford Hill and Wolfram Camp, through 299 m.y. near Petford, to 320 m.y. for several occurrences southwest and southeast of Irvinebank. However, the main intrusive event, represented by most of the Elizabeth Creek type-granite in the Emuford-Watsonville-Coolgarra area, took place about 314 m.y. ago.

Detailed work in a restricted area around Herberton has enabled the Elizabeth Creek Granite here to be sub-

divided into two distinct varieties, ECG I and ECG II. Field relations shown that ECG II intrudes ECG I. Low-lying outcrops along the Wild River south of Herberton Railway Station are typical of ECG I. This variety, which is generally closely jointed and deeply weathered, consists of medium to coarse-grained granite having an average modal composition of 32 percent quartz, 40 percent microcline, 24 percent unzoned plagioclase (An_{20-25}), and 2 percent partly chloritised biotite. Accessories include opaques, zircon, apatite, and fluorite. The second variety of Elizabeth Creek Granite (ECG II), which generally is not as weathered as ECG I, forms conspicuous hillocks such as at Pot Luck Hill west of Herberton. It is fine to medium-grained and non-porphyritic, and has an average modal composition of 35 percent quartz, 35 percent potash feldspar, 24 percent plagioclase, 3 percent biotite, and 1 percent muscovite. Main accessories are magnetite, sphene, topaz, and fluorite. Unlike that in ECG I, the plagioclase in ECG II is compositionally zoned from oligoclase margins to andesine cores. The two types of granite are associated with different types of alteration. Typical greisens are largely confied to ECG I, whereas ECG II is characterised by chloritic alteration. This aspect of the granites is discussed more fully in a later section.

The two-fold division of the Elizabeth Creek Granite near Herberton is supported by the latest isotopic evidence. The best age estimate for ECG I is considered to be 310 m.y., the age obtained on biotite from unaltered ECG I (74490233) in the Carrington Falls area, 8 km northeast of Herberton. This is in agreement with a previously determined model I total-rock age of 314 ± 11 m.y. (Black, 1978). A biotite age of 307 m.y. for ECG I (74490234) from the Happy Jack mine, Herberton, may be slightly too young, as the host granite here is a little altered. The isotopic evidence shows that ECG I at Herberton is closely comparable in age to the 314 m.y. old Elizabeth Creek Granite exposed in the Emford-Watsonville-Coolgarra area. Biotite from a single sample of ECG II at Herberton (74490238) yields a significantly younger age of 300 m.y. Black (1978) has shown that Elizabeth Creek Granite of similar age is exposed to the west, near Petford, where a fine-grained phase has been dated at 299 ± 6 m.y., and that a zone of Elizabeth Creek Granite of comparable or perhaps slightly younger age extends 40 km northwards from Petford, through the Featherbed Volcanics, to Bamford Hill and Wolfram Camp.

Herbert River-type granite

This granite type is considered by Best (1962), de Keyser & Wolff (1964), and Branch (1966) to be the source of the Cu, Pb, Ag, and Au mineralisation in the Chillagoe district, where it is mapped as Herbert River Granite and Almaden Granite. In the Herberton tinfield, however, where it includes the Kalunga Granodiorite, Hammonds Creek Granodiorite, Bakerville Granodiorite, and possibly the Nymbool Granite, the Herbert River-type granite is apparently unrelated to any economic mineralisation (Blake, 1972). Predominant rock types are biotite granodiorite that commonly contains some hornblende, and adamellite containing abundant dark fine-grained xenoliths and commonly also some pyroxene. Aplite veins occur locally but there are no associated greisens.

Sample		*Rb (ug/g)*	*Sr (ug/g)*	Sr^{87}/Sr^{86}	Rb^{87}/Sr^{86}	*Age (m.y.)*
Western intrusion			Kalunga Granodiorite			
67490025*	total rock	274.0	128.2	.73576	6.189	
67490026*	total rock	248.4	104.1	.73739	6.910	
67490027*	total rock	174.4	131.5	.72648	3.836	
67490027*	biotite	945.2	4.662	3.6825	755.8	276
67490062*	total rock	336.6	52.21	.78584	18.76	
67490063*	total rock	314.5	115.1	.74102	7.914	
67490064*	total rock	267.2	93.09	.74243	8.315	
67490064R1	total rock (aplite)	300.5	24.35	.84739	36.13	~267
74490102	total rock	261.3	98.33	.74039	7.698	
74490102	biotite	968.9	3.762	4.878	1047	280
Eastern intrusion						
67490061*	total rock	231.1	144.7	.72906	4.622	
67490061*	biotite	679.0	5.377	2.5163	429.1	296
67490061*	biotite	710.1	6.592	2.2451	370.7	292
74490108	total rock	233.3	131.3	.73181	5.142	
74990108	biotite	958.9	7.524	2.5331	433.7	295
74490109	total rock	244.3	130.7	.73237	5.412	
74490110	total rock	224.2	143.6	.72901	4.519	
74490110	biotite	730.4	4.553	3.1238	572.7	296
74490111	total rock (aplite)	311.0	23.53	.86154	38.75	~272
?Eastern intrusion						
74490104	total rock	192.6	160.9	.72504	3.463	
74490104	biotite	737.1	15.88	1.3145	142.0	299
			Elizabeth Creek Granite			
74490212B	biotite	4430	7.309	29.612	6699	303
74490216	biotite	6288	8.680	120.45	26592	316
74490233	biotite (ECG I)	5658	9.531	1.5288	185.2	310
74490233	total rock (ECG I)	215.4	80.41	.74521	7.758	
74490234	biotite (ECG I)	1979	4.119	15.557	3403	307
74490238	biotite (ECG II)	725.5	5.487	2.6878	455.8	300
74490238	total rock (ECG II)	519.9	13.13	1.2586	120.5	
			Granite at Dover Castle mine			
74490206B	biotite	1146	9.069	2.4250	426.2	282
74490206B	biotite	1210	8.964	2.5396	459.7	280

* Samples analysed by Black (1978).

Table 1. Rb-Sr isotopic compositions of Herberton tinfield granite samples.

Isotopic data indicate an age range of about 278-315 m.y. for the Herbert River-type granite (Black, 1978). The extensive intrusions in the Chillagoe-Almaden area are dated at about 300 m.y., and the Bakerville Granodiorite (301 ± 5 m.y.) is of similar age. A single biotite analysis sugests that the Hammonds Creek Granodiorite may be slightly younger, at 293 m.y. The age obtained for the Nymbool Granite, 315 m.y., is similar to that of the nearby Elizabeth Creek Granite.

New isotopic data for the Kalunga Granodiorite are presented in Table 1. These indicate, as was suggested by Black (1978), that the Kalunga Granodiorite comprises two main intrusions, a western and an eastern body. The western body consists mainly of grey medium-grained granodiorite in which hornblende is generally very subordinate to biotite; some adamellite, which does not usually contain hornblende, is also present. The eastern body consists of coarser granodiorite in which hornblende is commonly more abundant than biotite. Basic xenoliths are present in both bodies but are more common in the eastern intrusion. Both intrusions are cut by aplite veins. The eastern intrusion has given biotite ages of 294, 296, and 297 m.y. and a less precise total-rock age of 272 ± 47 m.y. A biotite age of 299 m.y. indicates that Kalunga Granodiorite exposed 1.5 km southwest of Herberton was probably emplaced at the same time. Biotite ages of 276 m.y. and 280 m.y. indicate that the western intrusion (total rock age 282 ± 15 m.y.) is somewhat younger. The isotopic data suggest that the aplites (samples 67490064R1, 7449011) are considerably younger, at 270 m.y., than both these intrusions, if it is assumed that the aplite and granodiorite had similar initial Sr^{87}/Sr^{86} values.

Mareeba-type granite

This is represented in the area by the Watsonville Granite (Blake, 1972), which does not appear to be mineralised, and possibly by a granite intruding Featherbed Volcanics at the Dover Castle mine, 6 km northwest of Petford (sample 74490206B, this study). The Watsonville Granite consists predominantly of medium-grained non-porphyritic biotite adamellite. Xenoliths and aplite veins are relatively uncommon, and there are no associated greisens.

The Mareeba-type granite gives isotopic ages of about 280 m.y. (Black, 1978): a total rock isochron age of 282 ± 9 m.y. for Mareeba Granite from well to the north of the Herberton tinfield is supported by both muscovite (278 m.y. and 281 m.y.) and biotite (279 m.y. and 282 m.y. ages; the Watsonville Granite has given total-rock and biotite ages of 289 ± 16 m.y. and 281 m.y., respectively. Duplicate biotite analyses on the granite (74490206B) at the Dover Castle mine give ages of 280 m.y. and 282 m.y.

Economic mineralisation

Economic mineralisation in the Herberton tinfield has been discussed in many previous publications, e.g., Best (1962), Blake (1972), and Black & Richards (1972c). Detailed studies of that near Herberton have recently been reported by Olatunji (1975).

The ore deposits are noted more for diversity than tonnage. Cassiterite has been the most economically important mineral virtually throughout the entire life of the field—15 percent of Australia's total Sn production has been won from the area. Significant concentrations of W, Ag, Pb, Mo, and Cu have also been mined. Minor deposits include Au, fluorspar, Zn, limestone, SiO_2, Sb, Bi, and mica. Over 2500 lode mines and prospects, few of which are currently being worked, have been located (Blake, 1972).

Economic mineralisation is widespread in the Hodgkinson Formation and Elizabeth Creek Granite, and also occurs in two of the Upper Palaeozoic acid volcanic formations, the Featherbed and the Nanyeta Volcanics. All this mineralisation can be related, on field evidence, to the Elizabeth Creek Granite. In the Emuford-Irvinebank area, for instance, spacially associated orebodies lie in successive zones characterised by W, Sn, Cu, and Pb mineralisation about a body of this granite (Blake & Smith, 1970). The non-ideal nature of this zonation is probably caused by the presence of many separate emanative centres for the ores (Taylor, 1971; Blake & Smith, 1971).

Greisens are commonly associated with the Elizabeth Creek Granite in the Herberton tinfield, especially where the granite is mineralised. They form both well-defined veins and more irregular bodies, and consist predominantly of quartz and pale mica, most of which is probably muscovite. They were probably formed during the final crystallisation stages in the various intrusions of Elizabeth Creek Granite.

Age of mineralisation

Isotopic data for mineralised samples appear in Table 2 and are summarised, together with granite ages, in Table 3. Most of this isotopic work was done on mica separates. Initial Sr^{87}/Sr^{86} values required to calculate individual mica ages were obtained from mica-total rock tie-lines or, if this was not possible, by assuming an initial ratio of 0.710, the general value found by Black (1978) for most of the Upper Palaeozoic granites in the region.

The total age spread for the newly dated mineralised samples is 315 to 284 m.y. In addition, some samples of granite associated with greisen and Mo and probably W mineralisation from southwest and southeast of Irvinebank have been dated previously at about 320 m.y. (Black, 1978). Altogether, four ages of greisen formation, each associated with some mineralisation, can be distinguished.

1. Greisens dated at 320 m.y. from southwest and southeast of Irvinebank.

2. Greisens dated at about 314 m.y. Ten greisen samples from the Emuford-Watsonville-Coolgarra area give ages between 311 and 315 m.y., indicating that these greisens were probably formed during the time of maximum development of the Elizabeth Creek Granite in this area (Black, 1978, fig. 2).

3. Greisens dated at 307 to 310 m.y. Statistically indistinguishable ages within this range have been given by eight greisen samples from near Herberton. The mean age of this group is significantly different from the previous group at the 99.9 percent confidence level. These Herberton greisens were probably formed during the crystallisation of the coarse-grained ECG I (sample 74490233) at Herberton.

4. Greisens dated at about 300 m.y. Ages of about 303 m.y. are given by muscovite from greisens at Bamford Hill and Wolfram Camp, in areas of 'young' Elizabeth Creek Granite. Greisen from the Dingo mine, 9 km northeast of Coolgarra, gives a slightly younger age, 299 m.y., which compares closely with a biotite age of 303 m.y. for a medium-grained adamellite phase of the Elizabeth Creek Granite (74490212B) at this locality.

Sample No. (prefix 74490)		Alteration/type	Mine	Product	Location	Rb (ug/g)	Sr (ug/g)	Sr^{87}/Sr^{86}	Rb^{87}/Sr^{86}	Age (m.y.)
201B	muscovite	greissen	Sparklet	Sn	3.5 km S of Emuford	1834	3.749	17.020	3667	313
205B	muscovite	greissen	?	W	3.5 km W of Emuford	2648	5.203	19.166	4123	315
207C	muscovite	greissen	Forget-me-not	W, Mo, Bi	Bamford Hill	1393	4.117	7.7917	1654	301
						1379	4.132	7.729	1625	303
						1384	4.158	7.6621	1615	302
208B	muscovite	greissen	Forget-me-not	W, Mo, Bi	Wolfram Camp	1392	3.762	9.1135	1947	303
						1546	4.208	9.0845	1931	305
209A	muscovite	greissen	?	W	10 km ESE of Coolgarra	1784	4.653	10.279	2144	314
212C	muscovite	greissen	Dingo	Sn	9 km NE of Coolgarra	1752	3.331	18.339	4137	299
218	biotite	greissen	Devon	W	5 km SE of Coolgarra	3317	5.536	32.701	7145	315
219	biotite	greissen	Treasure	W, Mo	13 km W of Coolgarra	3950	5.713	69.919	15508	314
220	muscovite	greissen	?	W	11 km NW of Coolgarra	1930	5.140	9.9004	2059	314
221	muscovite	greissen	Tungstic Knob	W	9 km NW of Coolgarra	1891	7.187	5.8210	1139	315
224	muscovite	greissen	Archer	Sn	2 km WSW of Herberton	2393	4 086	28.332	6260	310
229	biotite	greissen	Boundary	Sn	1.5 km S of Watsonville	1480	11.46	2.7098	445.8	315
235	biotite	greissen	?	?Sn	1 km W of Herberton	2516	4.679	20.977	4631	308
235	total rock	greissen	?	?Sn	1 km W of Herberton	939.5	2.0195	14.478	3154	307
236	biotite	green biotite	Telegraph	Sn	1 km SSW of Herberton	34.61	.74016	1.2876	142.7	284
237	biotite	chlorite	Pot Luck	Sn	1 km SW of Herberton	260.9	5.199	1.3765	154.4	297
237	total rock	chlorite	Pot Luck	Sn	1 km SW of Herberton	383.9	40.63	.84091	27.64	
240	muscovite	greisen	Happy Jack	Sn, Cu, Mo	1 km NE of Herberton	1960	4.125	15.211	3320	307
241	muscovite	greisen	?	?Cu, Sn	2 km N of Herberton	1849	15.01	2.5651	420.5	310
242	muscovite	greisen	?	?Cu, Sn	2 km N of Herberton	677.5	9.528	1.7041	225.3	310
243	muscovite	greisen	?	?Sn	1 km E of Herberton	1881	8.252	4.7659	919.3	310
244	muscovite	greisen	?	Cu, Ag	2 km NNE of Herberton	1835	6.584	6.0650	1227	307
245	dark mica	greisen	John Bull	W	4 km SW of Coolgarra	3430	9.297	9.5426	1986	313
246	dark mica	greisen	Black Prince	Sn	10 km SSW of Irvinebank	3067	5.666	22.136	4839	311
247	dark mica	greisen	?	W	3 km S of Coolgarra	3153	4.859	48.043	10551	315
248	muscovite	?greisen	Jimbilly	Sn	6 km NNW of Coolgarra	1823	9.894	3.7969	692.7	313

Table 2. Rb-Sr isotopic compositions of mineralised samples from the Herberton tinfield.

Age (m.y.)	*Granite Emplacement*	*Alteration*	*Product*
320	Some Elizabeth Creek Granite southwest and southeast of Irvinebank	greisen	Mo, W?
314-315	Elizabeth Creek Granite in Emuford-Watsonville-Coolgarra area, Nymbool Granite	greisen	Sn, Cu, Pb, W, Mo?
309-310	Elizabeth Creek Granite (ECG I) near Herberton	greisen	Sn, Cu, W
303	?Elizabeth Creek Granite at Bamford Hill and Wolfram Camp	greisen	W, Mo, Bi
300-297	Fine-grained Elizabeth Creek Granite between Petford and Wolfram Camp, ECG II near Herberton, Almaden and Herbert River Granites near Chillagoe, Bakerville Granodiorite, old phase of the Kalunga Granodiorite	chlorite	Sn, Cu
280	Mareeba Granite, Watsonville Granite, young phase of the Kalunga Granodiorite, small granite body at Dover Castle mine	green biotite	Sn, Pb

Table 3. Isotopic ages of granites and mineralisation.

The greisen data indicate a general close age correlation between greisen and adjacent Elizabeth Creek Granite, supporting the view that greisen formation took place at the time of crystallisation of the host granite. However, the situation at Bamford Hill and Wolfram Camp seems to be anomalous in this respect. Granite at Bamford Hill, for instance, appears to be younger (292 ± 6 m.y.; Black, 1978) than the greisen (302 m.y.) it encloses. The Rb-Sr age for muscovite from the greisen has been measured in triplicate with good agreement (see Table 2), and this is supported by a K-Ar age of 301 m.y. (Table 4). Isotopic updating is unlikely to have produced such good agreement between different isotopic systems. Hence the greisen was almost certainly formed at 302 m.y. Its anomalous age relationship might relate only to an over-optimistic estimate of precision limits for the granite. Alternatively, it might have real geological significance and indicate, for example, that the greisen is related to an older phase of the Elizabeth Creek Granite than that which actually encloses it. Similarly, at Wolfram Camp duplicate Rb-Sr ages of 303 m.y. and 305 m.y. for muscovite from greisen agree with a K-Ar age of 304 m.y. (Table 4) for the same muscovite, but are older than a mean total-rock Rb-Sr age of 291 m.y. (Black, 1978) for surrounding granite. Whatever the explanation for the discrepancy between granite and greisen ages in these two areas, the greisen and associated W, Mo, and Bi deposits of Wolfram Camp and Bamford Hill appear to be reliably dated at about 303 m.y.

In addition to greisens, there is widespread chloritic alteration in the Herberton and Watsonville area (Blake, 1972). This chloritic alteration is well developed, for instance, at the Archer, Big Ben, Sandra Mary and Pot Luck mines near Herberton. A drill-core sample (74490237) from the Pot Luck mine was used in this study. It represents a fracture-controlled alteration zone of mainly massive chlorite. A separate of biotite mixed with chlorite from altered granite at the outer fringe of the alteration was used for dating. The age obtained, 297 m.y., is similar to that of ECG II, which encloses the fracture fillings, and is much younger than greisens associated with ECG I. Although only a single determination, it is consistent with the field evidence, and is considered to provide a reasonable estimate of the time of the chloritic-type alteration.

Sample	*% K*	*$^{*}Ar^{40}/K^{40}$*	*% Ar^{40} atmospheric*	*Age (m.y.)*
74490207	8.92	0.018685	2.3	301 ± 4
74490208	8.84	0.018770	1.8	304 ± 4

Analyses by A. W. Webb of the Australian Mineral Development Laboratories. Ages are calculated using the decay constants recommended by Beckinsale & Gale (1969), corrected for the K^{40} abundance value of Garner & others (1975).

Table 4. K-Ar ages on muscovite samples from the Herberton tinfield.

The third type of alteration dated, characterised by secondary biotite, occurs near Herberton in ECG II at Pot Luck Hill and in ECG I at the Boska and Telegraph mines. The alteration-rock of these localities is present in fractures, and consists of iron-stained greisen fragments set in a matrix of biotite. It is thought to have formed by brecciation of greisen and subsequent hydrothermal alteration of the breccia matrix to secondary biotite (Olatunji, 1975). The biotite sample analysed, from a fracture in salmon-pink coarse-grained ECG I at the Telegraph mine, gives an age of 284 m.y. This age is similar to that of the nearby Watsonville Granite and the younger phase of the Kalunga Granodiorite. This similarity may be more than coincidence, and we suggest that the secondary biotite was formed by hydrothermal alteration during the emplacement of these granites, the last major intrusive event in the area.

Origin of mineralisation

The isotopic data indicate a close temporal correlation of economic mineralisation with major granite emplacement in the Herberton tinfield. Granite dated at 320 m.y. (Black, 1977) and associated greisen southwest and southeast of Irvinebank are representatives of the earliest recorded event. Most of the greisen formation in the Emuford-Watsonville-Coolgarra area was essentially contemporaneous with the emplacement of medium to coarse-grained Elizabeth Creek Granite about 314 m.y. ago. Further east, in the Herberton area, the greisens, and probably also ECG I, are slightly but significantly younger, at 309 m.y. The W, Mo, and Bi deposits of Wolfram Camp and Bamford Hill were formed at about 303 m.y., and mark the end of greisen formation in the area. Hydrothermal activity leading to the development of chloritic alteration took place near Herberton during or slightly after the emplacement of the host ECG II, about 300 m.y. ago. A body of Elizabeth Creek Granite of similar age is present in the west, near Petford. Hydrothermal alteration characterised by the formation of secondary biotite probably occurred at about 280 m.y., during the emplacement of the Watsonville Granite, the younger body of Kalunga Granodiorite, and the granite intruding the Featherbed Volcanics at the Dover Castle mine.

The chloritic hydrothermal alteration and all but possibly the earliest greisens are associated with cassiterite mineralisation. Cassiterite also occurs with the dated secondary green biotite at the Telegraph mine. Hence Sn mineralisation is linked with at least five of the six intrusive events now recognised in the area (see Table 3). W and Mo appear to be related to the four greisen forming events, at 320 m.y. (southwest and southeast of Irvinebank), 314 m.y. (Emuford-Watsonville-Cool-

garra), 309 m.y. (Herberton), and 303 m.y. (Bamford Hill and Wolfram Camp). In the Herberton area Cu mineralisation is related to ECG I (309 m.y.) at the Happy Jack and You and I mines and in the northeast part of Captain Hill, and to ECG II (300 m.y.) at the Big Ben mine. It is related to earlier Elizabeth Creek Granite (314 m.y.) at the Boundary mine, Watsonville.

New isotopic data (Black, 1978) indicate that the Featherbed Volcanics range in age from about 270 m.y. to 310 m.y. The part of this unit containing the Orient Camp group of Ag-Pb mines is dated at 311 ± 16 m.y. and there is no geochronological reason to suggest that these Ag-Pb deposits could not form the outer part of the district mineralogical zonation about the mass of 314 m.y. old Elizabeth Creek Granite to the south (Blake & Smith, 1970, 1971). In contrast, the Pb-bearing Sn deposits at the Dover Castle mine northwest of Petford occur in Featherbed Volcanics dated at 301 ± 9 m.y., and are consequently inferred to be related to a younger granite. Thus, like those of Cu and Sn, the Pb deposits in the area are probably of more than one age.

Data from the Pb-isotopic study of Black & Richards (1972c) indicate that part of the orebody lead in northeastern Queensland has been derived by hydrothermal-fluid leaching from country rock. Eighty percent of the lead ore in the Dargalong Ag-Pb mines in Precambrian rocks southwest of Chillagoe appears to be of this origin. The lead isotope composition of the Ag-Pb-Cu orebodies in the Palaeozoic rocks of the Chillagoe-Almaden area does not match that of the nearby and supposedly related Almaden Granite. Thus the contact metasomatic theory widely advocated for the origin of these orebodies can apply only if they also contain a significant proportion of leached country-rock lead. That this is the case has yet to be established.

The multiple mineralising events documented here present a possible alternative explanation for the reversed zoning observed in some mines of the area. Such zoning was postulated by Blake & Smith (1970, 1971, see also Taylor, 1971) to be a secondary effect relating to oxidation above the water table, but could also be an effect of two or more superimposed mineralisation events. Multiple mineralisation could also explain some of the irregularities of the district zoning (see Blake & Smith, 1970; fig. 2).

The present study has firmly established that the mineralisation in the Herberton tinfield is closely related to the emplacement of Elizabeth Creek type-granites, and possibly also, to a lesser extent, to Mareeba-type granite (Watsonville Granite). The granites provided the heat source and possibly the bulk of hydrothermal fluids for ore-formation, although some of the ore components themselves, such as Pb, could be partly derived by leaching from country rock during migration of the hydrothermal fluids.

Acknowledgements

We express our thanks to R. W. Page, John Ferguson, K. R. Walker, W. B. Dallwitz, C. D. Branch, and J. R. Richards for constructive criticism of the manuscript. J.A.O. acknowledges R. G. Taylor and C. Cuff for their invaluable suggestions and encouragement during his field work in the Herberton district. M. W. Mahon, T. K. Zapasnik, and J. L. Duggan provided technical assistance in sample preparation and processing. The diagram was prepared by Rosa Fabbo of the BMR Drawing Office. J.A.O. acknowledges the financial support of a Commonwealth Countries Scholarship and Fellowship (Australian Development Assistance Agency and the Federal Scholarship Board of Nigeria) for his doctoral study at James Cook University.

References

BECKINSALE, R. D., & GALE, N. H., 1969—A reappraisal of the decay constants and branching ratios of ^{40}K. *Earth and Planetary Science Letters*, **6**, 289-94.

BEST, J. G., 1962—Atherton, Queensland—1:250 000 Geological Series. *Bureau of Mineral Resources, Australia, Explanatory Notes* **SE/55-5**.

BLACK, L. P., 1978—Isotopic ages of rocks from the Georgetown - Mount Garnet - Herberton area, North Queensland. *Bureau of Mineral Resources, Australia, Report* **200**; *BMR Microform* **MF 28**.

BLACK, L. P., & RICHARDS, J. R., 1972a—Rb-Sr study of some igneous rocks near Chillagoe and Herberton, northeastern Queensland. *Journal of the Geological Society of Australia*, **19**, 271-9.

BLACK, L. P., & RICHARDS, J. R., 1972b—Rock lead isotopes in northeast Queensland. *Journal of the Geological Society of Australia*, **19**, 320-30.

BLACK, L. P., & RICHARDS, J. R., 1972c—Isotopic composition and possible genesis of ore leads in north-eastern Queensland, Australia. *Economic Geology*, **67**, 1168-79.

BLAKE, D. H., 1972—Regional and economic geology of the Herberton/Mount Garnet area-Herberton tinfield, North Queensland. *Bureau of Mineral Resources, Australia, Bulletin* **124**.

BLAKE, D. H., & SMITH, J. W., 1970—Mineralogical zoning in the Herberton Tinfield, North Queensland, Australia. *Economic Geology*, **65**, 993-97.

BLAKE, D. H., & SMITH, J. W., 1971—Mineralogical zoning in the Herberton Tinfield, North Queensland, Australia—Discussion. *Economic Geology*, **66**, 815.

BRANCH, C. D., 1966—Volcanic cauldrons, ring complexes, and associated granites of the Georgetown Inlier, Queensland. *Bureau of Mineral Resources, Australia, Bulletin* **76**.

BRANCH, C. D., 1967—Genesis of magma for acid calc-alkaline volcano-plutonic formations. *Tectonophysics*, **4**, 83-100.

GARNER, E. L., MURPHY, T. J., GRAMLICH, J. W., PAULSEN, P. J., & BARNES, I. L., 1975—Absolute isotopic abundance ratios and the atomic weight of a reference sample of potassium. *Journal of Research U.S. National Bureau of Standards, A, Physics and Chemistry*, **79A**, 713-25.

KEYSER, F. de, & LUCAS, K. G., 1968—Geology of the Hodgkinson and Laura Basins, north Queensland. *Bureau of Mineral Resources, Australia, Bulletin* **84**.

KEYSER, F. de, & WOLFF, K. W., 1964—The geology and mineral resources of the Chillagoe area, Queensland. *Bureau of Mineral Resources, Australia, Bulletin* **70**.

MCINTYRE, G. A., BROOKS, C., COMPSTON, W., & TUREK, A., 1966—The statistical assessment of Rb-Sr isochrons. *Journal of Geophysical Research*, **71**, 5459-68.

NEUMANN, W., & HUSTER, E., 1972—Neubestimming der halbwertszeit des ^{87}Rubidiums durch vergleich von messungen an den getrenntent isotopen ^{87}Rb und ^{85}Rb. *Zeitschrift für Naturforschung*, **27a**, 862-63.

OLATUNJI, J. A., 1975—The geology and mineralisation of west Herberton district, North Queensland. Ph.D. thesis, James Cook University of North Queensland (unpublished).

OVERSBY, B. S., PALFREYMAN, W. D., BLACK, L. P., COOPER, J. A., & BAIN, J. H. C., 1976—Georgetown, Yambo and Coen Inliers—regional geology; *in* KNIGHT, C. L. (Editor), Economic Geology of Australia and Papua New Guinea, I. Metals. *Australasian Institute of Mining and Metallurgy Monograph* **5**, 511-16.

PAGE, R. W., BLAKE, D. H., & MAHON, M. W., 1976—Geochronology and related aspects of acid volcanics, associated granites, and other Proterozoic rocks in The Granites-Tanami region, northwestern Australia. *BMR Journal of Australian Geology and Geophysics*, **1**, 1-13.

RICHARDS, J. R., WHITE, D. A., WEBB, A. W., & BRANCH, C. D., 1966—Isotopic ages of acid igneous rocks in the Cairns hinterland, North Queensland. *Bureau of Mineral Resources, Australia, Bulletin* **88**.

STEIGER, R. H., & JÄGER, E., 1977—Subcommission on geochronology: Convention on the use of decay constants in geo- and cosmochronology. *Earth and Planetary Science Letters*, **36**, 359-62.

TAYLOR, R. G., 1971—Mineralogical zoning in the Herberton Tinfield, north Queensland, Australia—Discussion. *Economic Geology*, **66**, 813-5.

WILLIAMS, I. S., COMPSTON, W., CHAPPELL, B. W., & SHIRAHASE, T., 1976—Rubidium-strontium age determinations on micas from a geologically controlled, composite batholith. *Journal of the Geological Society of Australia*, **22**, 497-506.

LANDSAT: developing techniques and applications in mineral and petroleum exploration

C. J. Simpson

The extensive research into satellite data technology that followed the launch of Landsat-1 (ERTS-1) in 1972 has resulted in progressive improvements to product quality and digital data analysis techniques. Improved image quality has direct significance to the many mineral and petroleum exploration organisations that are now routinely applying conventional photogeological interpretation techniques to Landsat multispectral scanner imagery. Photogeological techniques will continue to be the main means of Landsat interpretation, however, even the best quality imagery may contain less than one quarter of the total data recorded and computer techniques offer the only adequate means of analysing all the data in a Landsat scene. Considerable progress has been made with computer analysis of Landsat digital data and some techniques have definite application to mineral and petroleum exploration. In specific environments direct detection of iron weathering products associated with both hydrothermal alteration and uranium deposits has been achieved. Various computer-enhancement techniques have also been employed to reveal structural and lithological information not obvious on conventional Landsat imagery or aerial photography.

Introduction

On 23 July 1972 the United States National Aeronautics and Space Administration (NASA) launched the first Earth Resources Technology Satellite ERTS-1. The satellite was known by that name until Landsat-2, the second satellite in the series, was launched on 22 January 1975 and ERTS-1 was then renamed Landsat-1. Owing to onboard malfunctions Landsat-1 was officially switched off 6 January 1978. Landsat-3 was launched 5 March 1978 and Landsat-4 is scheduled for launch in 1981.

To assess the value of satellites for monitoring earth resources, scientists from all parts of the globe researched the initial data from Landsat-1 and reported their findings to NASA. Of the forty-eight Australian investigators who were involved in the Australian final report to NASA, twenty-six reported on geological aspects. Despite the fact that the Landsat photographic products used by the Australian investigators were fifth generation (about which they were not particularly enthusiastic), the overall conclusions of the final report (Fisher, 1975), recognised among other things, that the satellite imagery was a valuable addition to conventional techniques of regional small-scale geological mapping.

Since that report there have been very considerable advances, both overseas and in Australia, in the technology, product quality, and knowledge of the capabilities of the satellite data. Some users consider that the potential of satellite remote sensing for geology has been deemed sufficiently encouraging to warrant satellites, instrumentation, and space missions specially designed for geological data collection (Henderson & Swann, 1976).

It seems somewhat ironic that although conventional photogeological techniques are widely employed to interpret satellite imagery, all too often and more so overseas than in Australia, Landsat data are used to the complete exclusion of aerial photography which is probably its most valuable complement. The comment by Houston & others (1977) is particularly relevant '. . . geologists who wish to utilize data generated by remote-sensing platforms must keep in mind that remote sensing is not a panacea. Rather it is an additional tool that supplements present methodology and can often reduce costs in specific applications . . .'.

In general, results of research into Landsat satellite data have been readily available particularly in the proceedings of the several symposia sponsored by NASA (1972, 1973a, 1973b, 1975). Texts on remote sensing (including satellite sensing) specifically for geology are now becoming available (e.g. Smith, 1977). Well illustrated review papers on the applications of Landsat for exploration have been published (Viljoen & others, 1975; Halbouty, 1976); however, literature on successful operational applications of satellite data in mineral and petroleum exploration is still lacking.

Within Australia the application of Landsat imagery to geology was initially slow, primarily because of the poor quality of imagery available, and the limited coverage. The use of Landsat imagery has slowly gained momentum and is now standard practice in many exploration companies. Australia is one of the foremost purchasers of Landsat products outside the USA. Current estimates indicate that more than 60 percent of all the Landsat products purchased in Australia are for mineral and petroleum exploration companies. The applications of Landsat to Australian geology are not well publicised, and although general papers have been published by researchers only very few Australian papers, such as Smith & others (1978), have dealt specifically with Landsat in mineral exploration.

Within the Federal Government both the Bureau of Mineral Resources (BMR), and the Commonwealth Scientific and Industrial Research Organisation (CSIRO) Division of Mineral Physics, are maintaining and developing expertise in the geological applications of Landsat data. In August 1977 the Government announced that the Department of Science would establish a Landsat data receiving station at Alice Springs and a data-processing facility at Canberra. Late in the same year, low cost, high quality imagery of Landsat scenes became available to the Australian user as a result of the research efforts of the CSIRO Division of Mineral Physics.

The following report reviews some of the current uses of, and research into, Landsat data applied to mineral and petroleum exploration. It is based largely on selected papers presented at the Pecora III Symposium (Sioux Falls, South Dakota 30 October-2 November 1977) which was sponsored by The American Association of Petroleum Geologists (AAPG) in

cooperation with the United States Geological Survey (USGS) and NASA. The symposium had as its theme 'Application of satellite data to petroleum and mineral exploration'. Most of the papers presented at the symposium will be published in the Bulletin of the AAPG.

Additional selected information has been incorporated from recent publications and personal discussions with researchers. The report is not exhaustive in its coverage of the subject, but is structured to exemplify the diversity of approaches employed. Some of the comments may not be directly applicable to mineral and petroleum exploration companies. While that group is a major user of Landsat data only limited information on the techniques employed or results achieved is made public.

For geology the most valuable contribution of the extensive research into Landsat has been the spectacular improvement in image quality. It is of particular significance to mineral and petroleum exploration since the most useful technique that has been and will continue to be applied to Landsat data is conventional photogeological interpretation.

Research into Landsat applications and techniques is continuing at a rapid pace (particularly in the USA) and many techniques reported below that are showing, or appear to show, promise may be superseded in the not too distant future. It should be appreciated that the major advances that have occurred in the quality of Landsat products and in basic applications research, have not come about by any changes in the satellite instrumentation. Rather the advances have stemmed from a greater understanding of the nature of the satellite data itself, and techniques for its display and presentation. For that reason the initial part of the report discusses features of the satellite, and some computer techniques and terminology that are currently being applied.

Landsat 1 and 2 satellite characteristics

A summary of the general characteristics of the Landsat 1 and 2 satellites is shown in Table 1; detailed information exists in the Landsat Data Users Handbook (NASA, 1976). Subsequent satellites (i.e. Landsat-3 and the proposed Landsat-4) have some different instrumentation and characteristics which have been documented by Taranik (1978).

Spacecraft altitude	—880-940 km (normally 918 km)
Orbit period	—103 minutes
Coverage cycle	—18 days
Duration of cycle	—251 revolutions
Time of equatorial crossing	—9.42 a.m. (local time)
Instrument ground coverage per track	—185.2 km (east-west)
Instantaneous field of view of MSS	—79 metres x 79 metres
Distance between successive tracks at equator	—2760 km
Distance between adjacent tracks at equator	—159.4 km
Spacecraft heading during imaging	—north to south

Table 1. Characteristics of Landsat 1 and 2.

Landsat 1 and 2 both carry two imaging systems (a return beam vidicon and a multispectral scanner), and a data relay system (for earth-based monitoring instruments). Of the imaging systems, the multispectral scanner (MSS) has assumed major significance for geology because of its better spatial resolution, higher fidelity, and greater number of spectral recording bands. The operation of the scanner is briefly discussed to emphasise the differences between the electronically produced MSS imagery and conventional photography. In the following text photograph refers to any picture produced by direct recording on film of reflected electromagnetic radiation. An **image** is a picture produced by techniques involving electronic detection and recording of electromagnetic radiation.

The MSS effectively images a ground strip 185.2 km wide beneath the spacecraft. Reflected solar energy that reaches the spacecraft from that ground strip is measured in four discrete spectral bands which are given numerical designations (Table 2). Bands 6 and 7 of Landsats 1, 2, and 3 record reflected infrared radiation and not thermal (i.e. heat) infrared radiation. Landsat 3 carries an additional MSS band (Band 8) which senses heat emitted from the earth with infrared wavelengths of 10.4 to 12.6 micrometres.

MSS band	*Wavelength (micrometres)*	*Radiation type*
4	0.5–0.6	visible green
5	0.6–0.7	visible red
6	0.7–0.8	invisible reflected infrared
7	0.8–1.1	invisible reflected infrared

Table 2. Landsat 1 and 2 MSS imaging bandwidths.

Imaging is achieved by means of an oscillating mirror which scans across the ground strip in narrow lines from west to east approximately once every 33 milliseconds. Radiation from the mirror is directed to a solid state detector array which produces a voltage output related to the amount of radiation received. The voltage produced at each detector is sampled every 9.95 microseconds, resulting in approximately 3000 samples over the length of each scan line. Thus the brightness of reflected radiation from small areas on the ground is sampled for each band. Voltages produced from each sample are assigned a digital number corresponding to a **terrain brightness value** (BV) within a range 0 (black) to 63 (white), telemetered to ground receiving stations, and recorded on magnetic tape.

Tape-recorded data for each scene undergoes preprocessing which includes certain digital and radiometric adjustments, re-scaling of data in bands 4, 5, and 6 from a range 0-63 to a range of 0-127 counts, and reformatting to high density tape to produce a Landsat computer-compatible tape (CCT).

NASA uses the CCT's to convert the digital data into a black and white photographic product (image) with special film-writing equipment. The resulting image of each MSS spectral band is made up of 7.5816×10^6 rectangular picture elements called **pixels,** each with a grey tone which relates to the brightness of an effective rectangular area on the earth's surface of dimensions 79 m (north-south) x 56m (east-west).

Black and white images of each band are the basic Landsat products. Despite the pre-processing undertaken by NASA the imagery generally available prior to 1977 contained imperfections resulting from a variety of causes. Electronic detector noise, bad data lines and east-west striping in the imagery were often very detracting. Computer-controlled pre-processing is becoming more exacting and the enhanced imagery now available has removed scan-line defects, bad data are replaced with synthetic values, and some edge and con-

trast enhancement (q.v.) has been applied so that the current products are far superior for photointerpretation.

A colour Landsat image, generally referred to as a **false-colour composite,** can be prepared by registering the black and white positive transparencies of three MSS bands on conventional colour-print material and individually illuminating a band with one of the prime colours. The resulting product is normally referred to as false colour because the image rendition produced by exposing band 4 through blue, band 5 through green, and band 7 through red light has the same colour display as conventional false-colour infrared film. A false-colour composite is shown in part of the front cover of this issue. Different band/colour combinations can be used to enhance specific features.

True colour imagery cannot be produced because blue wavelengths are not recorded by the MSS. The USGS have developed a computer technique for producing **simulated natural colour** imagery. Data from all four MSS bands are used to predict and create a synthetic blue component which is added to the final colour image. The version of Landsat imagery thus produced has colours which approximate those that the human eye would see from orbital altitudes if atmospheric absorption and scattering were eliminated.

Computer manipulation of Landsat data

Most users of Landsat have been employing conventional visual photogeological techniques to interpret the standard (unenhanced) satellite imagery. References on photogeological techniques are readily available and Taranik & Trautwein (1976) have documented systematic approaches to the visual interpretation of satellite imagery. Such techniques when logically applied and integrated with existing geological and geophysical knowledge can provide useful new information, and may effect considerable savings in time and money (Viljoen & others, 1975).

Although visual interpretation techniques applied to standard Landsat imagery may be very productive they utilise only a fraction of the data recorded. Landsat CCT's have four to five times the dynamic range (i.e., the ratio of maximum measurable signal to minimum detectable signal) of the standard MSS images or colour composite images currently produced by the USGS Earth Resources Observation System (EROS) Data Centre (Vincent, 1977). Computer manipulation of all the data imaged per scene has the potential for providing additional geological information that cannot currently be obtained by any other technique.

Since 1972 Landsat research has seen major advances in techniques for computer manipulation of CCT data. The two interrelated fields of image enhancement and digital analysis have made considerable progress. In the following discussions **image enhancement** refers to computer techniques designed to increase image detail and allow more effective image interpretation. **Digital analysis** refers to computer techniques for mathematical manipulation, statistical sorting and classification of Landsat digital data using spectral reflectance or spatial information. Digital analysis techniques are presently incapable of synthesising image textural and pattern information, which is very important in conventional photogeological interpretation.

Despite the advances achieved, the extraction of geological information from Landsat by computer techniques is not widely employed at present. While both cost and availability of facilities no doubt play a large part in the reluctance of the general user to employ computer manipulation techniques, it appears that education is also a major contributing factor. Both the

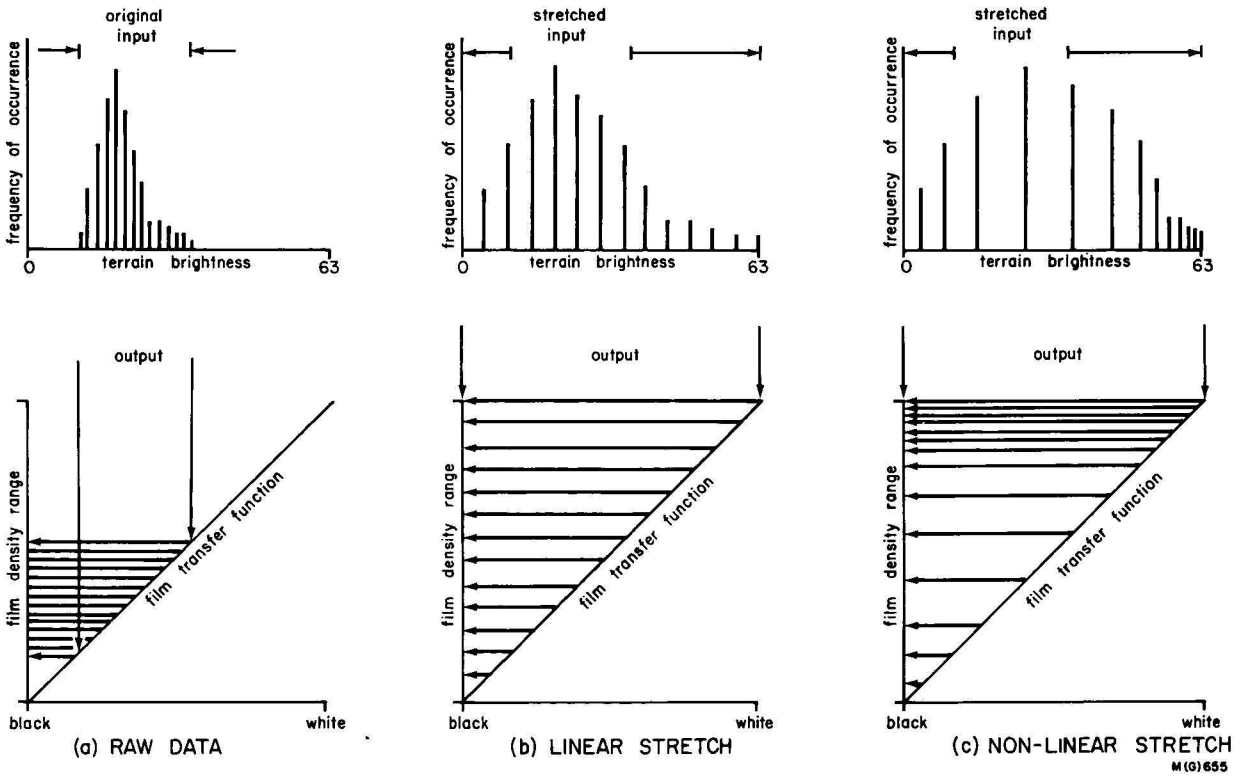

Figure 1. Concept of contrast stretching (modified from Taranik, in press).

USGS and NASA are developing programs to show US users, and potential users, how best to apply the Landsat data to their requirements.

The limited use of computer techniques may reflect current applications in the main since in geology Landsat has been mostly used for the detection of lineaments. Major lineaments can generally be recognised on conventional Landsat photographic products and few users resort to more sophisticated techniques to enhance subtle features. However the potential of computer techniques for lineament enhancement also has been demonstrated by Offield & others (1977), who detected considerably more structural information in computer-enhanced contrast stretched imagery than in conventional Landsat imagery.

Contrast stretching (stretching, or contrast enhancement) is employed to increase the overall scene contrast in the resulting stretched image. Since the MSS system is designed to cover a large dynamic range in scene brightness (oceans, deserts, etc.), any one image will generally occupy only part of that range, resulting in a low-contrast image. In reconstructing an image from digital data stretching spreads the data over the whole of the dynamic range of the output product. Several types of stretches can be employed and are broadly designated as either linear or non-linear (Taranik, 1977b).

The distribution limits of the data composing a scene are determined from a histogram of terrain brightness versus frequency of occurrence. A diagrammatic representation of the distribution of raw unstretched data is shown in Figure 1(a). Since the raw data occupies only a portion of the available terrain brightness range the resulting film product will utilise only a portion of the available dynamic range of the film. During stretching the digital values of the stretch limits are assigned the values of the dynamic range available and all pixel data are given new brightness values to completely occupy that range. In a linear stretch (Fig. 1(b)) the raw data are linearly spaced between the end values (i.e., 0-63 in the diagram) to produce a new distribution. The data in the final scene are distributed in equal density increments over the whole dynamic range of the film. The resulting scene has higher overall contrast, and features are more readily distinguished. Linear stretching produces a more useable product for photointerpretation purposes and has also proven useful for enhancing structure.

A non-linear stretch (Fig. 1(c)) results in an unequal data distribution and a corresponding unequal density distribution in the film product. Various types of non-linear stretches such as logarithmic, gaussian, sinusoidal, and table stretches have been employed by researchers for specific purposes. Such stretches can considerably enhance specific data such as subtle soil-rock differences, or dark terrain detail such as in weathered greenstone belts, but generally they do so at the expense of other spectral information in the scene. Non-linear stretches require a considerable degree of analytical judgment to determine the optimum type of stretch to be employed for the required end result.

The enhanced Landsat imagery produced by the CSIRO and the EROS Data Centre have been subjected to contrast enhancement, usually by linear stretching. The overall effects of contrast stretching is illustrated in Figure 2 which compares a NASA 1972 fifth generation product with a CSIRO enhanced scene of the same area. The effects of various stretching techniques is well illustrated by Soha & others (1976).

Another computer technique that has been successfully employed for enhancement of lineaments on imagery is **spatial filtering** (or edge enhancement). Spatial filtering is a digital process designed to enhance

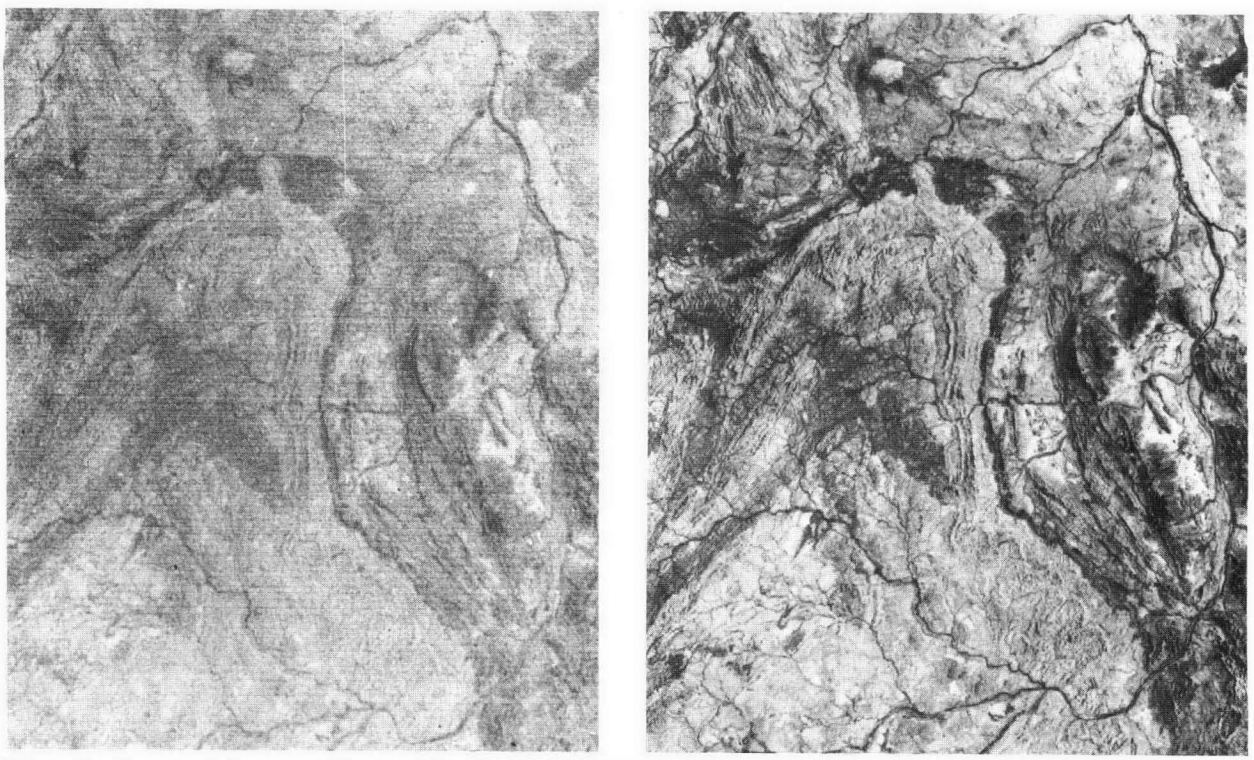

Figure 2. Improved image quality resulting from computer enhancement. Image at 1:500 000 scale at left is part of a 1972 NASA fifth generation product (1152-00073-5 from the Cloncurry region). Right is a CSIRO product enhanced directly from the digital tape of the same scene.

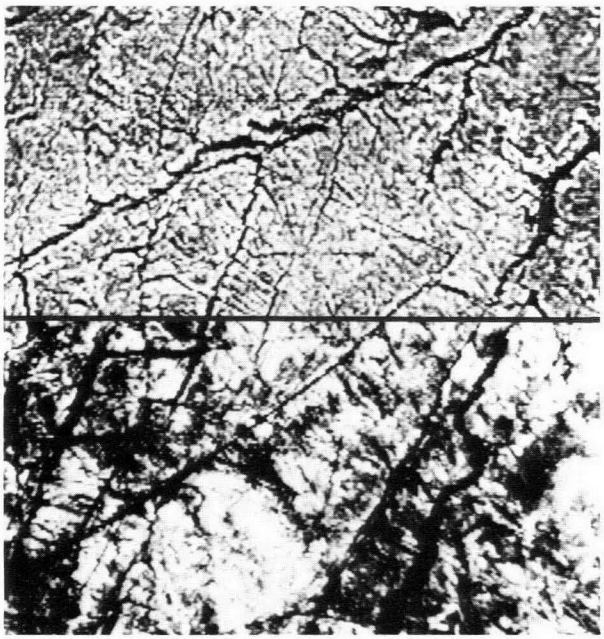

Figure 3. The effect of box filtering applied to enhance structural detail within sandstones of the Kombolgie Formation, NT. The lower portion of the image is normal band 5 data, the upper half has been filtered. (Part of 1500-00370 photographed from a video screen display at about 1:230 000 scale.)

or suppress boundaries between features which have subtle differences in brightness values.

Square or box filters involve computation of the local average brightness within a specified area (i.e., n x m pixels) centred on each pixel. Generally pixel values brighter than the local average are made brighter and those darker than the local average become darker. A low-pass filter emphasises low frequency brightness variation (i.e., large patterns) and a high-pass filter emphasises high frequency variations (i.e., detailed information).

The effect of box filtering is illustrated in Figure 3, which shows an area of fractured Kombolgie Formation in the Milingimbi region of the Northern Territory. The top half of the scene has been processed using a 5 x 5 pixel box filter to enhance structure.

Directional filters compare the pixel values in a given direction, and features at a particular angle to that direction are enhanced. Albert & Steele (1976) employed a first derivative enhancement to emphasise fine structural grain. The filter technique adjusts only specified differences between adjacent pixels in a given direction (either horizontally, vertically or diagonally).

Filtering techniques produce a sharper image, but may produce artifacts. The techniques seem to work best for enhancement of drainage and landform in areas of uniform cover (Taranik, in press).

A technique of computer digital analysis that is being extensively researched by many worker is that of **ratioing.** It is a process whereby the CCT radiance value of each pixel in a MSS band is divided by the radiance values of the corresponding pixel from another MSS band (e.g., ratio MSS 4/5 means that band 4 pixel values have been divided by band 5 pixel values). The ratio values that result are stretched and used instead of the original pixel values to write an image, thus differences between spectral data from two images can be shown in one image. Similarly the images produced from several different band-ratio combinations can be combined optically to produce **colour-ratio composites.** A colour-ratio composite is shown in part of the cover illustration and can be compared with a false-colour composite.

A significant consequence of ratioing is that the brightness variations caused by variations in topographic slope altitude are largely removed, so that responses from the one material will appear the same or similar irrespective of local topographic effects.

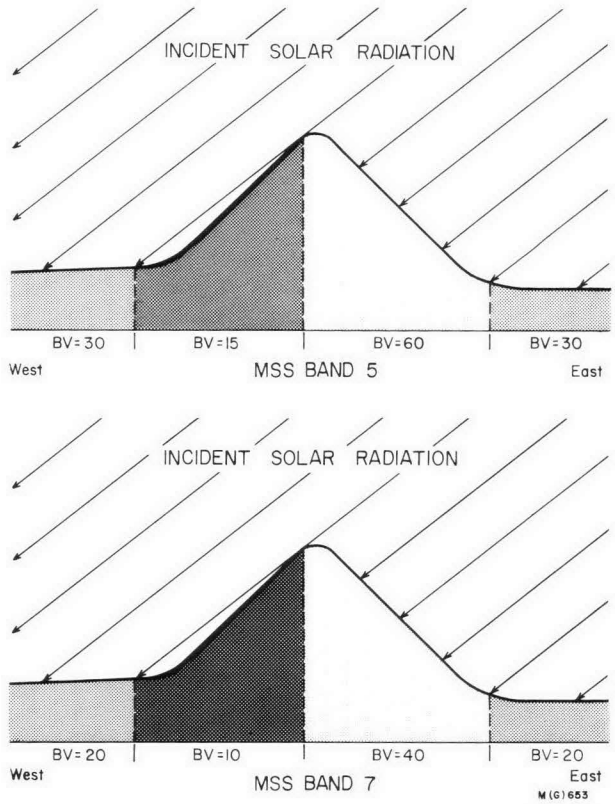

Figure 4. Diagrammatic representation of the effect of topography and illumination on the terrain brightness values (BV's) recorded on two MSS bands from a hill section of homogeneous material.

Figure 4 is a representation of a section through a hill to show the effect of topography and illumination on the terrain brightness values recorded in two different MSS bands. Even though the terrain is assumed to be homogeneous, conventional MSS imagery would show different spectral reflectances. However a MSS 5/7 ratio would result in values of 1.5 for all surfaces and the ratio image would display the hill and surrounds as spectrally homogeneous terrain.

Ratioing can aid lithologic mapping by exploiting reflectance differences between different rocks and soils, and it may also enhance structure especially where accompanied by subtle changes of vegetation character and/or density. The illustration on the cover of this paper shows part of a Landsat scene of the Mammoth Mines area of northwest Queensland. The top portion is a false-colour composite (band 4—blue, band 5—green, band 7—red) while the bottom of the scene is shown as a colour-ratio composite (MSS 4/5—blue,

MSS 5/6—green, MSS 6/7—red). The colour-ratio image allows more definite interpretation of rock type distributions.

Principal components analysis which has been applied in statistical processing, including geostatistics, for some considerable time, is currently receiving attention from Landsat analysts. Principal components analysis processes all data in each band, whereas in contrast stretching and band ratioing the analyst selects the data to be manipulated. The data are dimensionally reduced so that the resulting information can be displayed with minimum redundancy in a three-colour composite image. The technique is useful for discriminating rock and soil types if little prior information is available (Podwysocki & others, 1977).

The computer-assisted techniques discussed above are a few of those in which Landsat data may be manipulated. Additional information of relevance can be found in Rowan & others (1974); Goetz & others (1975); Goetz (1976); Soha & others (1976); Offield (1977); Taranik (in press); Podwysocki & others (1977); and Vincent (1977). The application limits of computer processing have yet to be established, and considerable research will be required to determine the successful and unsuccessful methods among those currently being employed. In the discussion that follows computer-assisted techniques have been emphasised since they are not as well documented as conventional image-interpretation techniques.

Landsat in mineral exploration

To date the major application of Landsat in mineral exploration has been in the detection and analysis of lineaments. The large area of a Landsat scene allows detection of lineaments which are not always obvious on conventional aircraft photography. Kampschuur & Press (1977) note that of the various applications of Landsat to exploration, lineament analysis is the technique which has been most talked about, least successfully demonstrated and has created most scepticism.

Published reports (e.g. NASA 1972, 1973a, 1973b, 1975) on Landsat applications to geology are dominated by lineament studies. The proliferation of lineament studies has demonstrated degrees of success, which may often reflect the effort involved and the approach used. Lineament analysis techniques generally employ conventional photogeological concepts combined with statistical methods (e.g. azimuth-frequency and azimuth-length) in an attempt to determine dominant fracture directions, new structures or extensions to known structures.

Statistical directional analysis of Landsat lineaments cannot be applied over large areas without consideration of the regional geology. This aspect has been discussed by Rivereau (1977), who emphasised the need to be able to separate genuine fracture traces from other linear features before analysis is undertaken. Such differentiation cannot be reliably carried out using Landsat data alone, and requires incorporation of suitable ground and/or airphoto data.

Kampschuur & Press (1977) have been able to correlate the stress directions (determined from thin section study), ground observations of joint measurements, and airphoto fracture mapping, with dominant lineament sets annotated from Landsat. Their work involved target areas in Britain, Spain, France, Morocco, the western Sahara, and Brazil. Assuming that stress directions are normal to major rift zones, deductions can be made on the relative movements, particularly rotation of various continental blocks. Such concepts can be incorporated into syntheses of the relationships between mineralised provinces. Application of satellite data to province studies was also investigated by Offield & others (1977). Lineaments interpreted from Landsat were added to available geological and geophysical data to allow correlation of mineralised areas in southwest Africa and Brazil. The satellite interpretations provided new information to support the concept that prior to rifting the mineralised areas were a single mineral province.

Considerable attention has been placed on techniques for determining possible spatial relationships, if any, between known mineralisation and Landsat lineaments or lineament intersections. To date little published information is available to show that studies of Landsat lineaments have contributed directly to the discovery of mineralisation.

One US company has reported the discovery of lead-zinc mineralisation at considerable depth after drilling a circular feature detected on Landsat imagery (Le Roy Scharon, 1976). Drilling was carried out in an area of reasonably dense vegetation without any ground indication of mineralisation. The feature was similar to another circular feature, observed on Landsat to be associated with known mineralisation at a deposit in the Tennessee Valley. Although the origin or spectral composition of the circular features are not known they are presumed to be related to structure.

A good example of the systematic application of Landsat to assist mineral resource assessment is the method used by the USGS Alaskan Mineral Resources Assessment Program (AMRAP). AMRAP was initiated in 1974 with the intention of producing a rapid yet accurate inventory of Alaska's mineral resources as a basis for long-range national minerals policy and land-use planning (Richter & others, 1975). To achieve the objectives of the program the results of current field work and all published geological, geophysical and geochemical data and interpretations of Landsat imagery of 1:250 000 scale sheet areas are synthesised.

Although Landsat is systematically used in the program, the interpretation techniques employed are continually being upgraded. On a Landsat mosaic of Alaska constructed with unenhanced imagery, linear, arcuate, and circular features are first mapped by conventional techniques and the use of Ronchi rulings. A Ronchi ruling is a coarse diffraction grating which can assist in the detection of linear features. When an image or photograph is viewed through the ruling, linear elements parallel to the grating lines are diffused, and elements perpendicular to the lines are enhanced. Generally the best results for lineament analysis have been obtained with gratings having a line density of 78 lines per cm (Offield, 1975).

In Alaska, computer-enhanced false-colour composite images have proven useful for detecting additional lineaments, arcuate, and circular features. Many of the circular features may correlate with intrusives (Albert, 1975). Lineaments detected on both unenhanced and enhanced imagery are digitised and analysed by computer to determine eight types of data, including azimuth-frequency, mean linear feature length, and the area within a specified distance of a set of linear features (Steele, 1976).

Increasingly the published results of Landsat studies from many countries are reporting the existence of major lineament sets which have rectangular or near rectangular intersects. The current work on the Alaskan lineaments show some orthogonal fracture sets to be

young since they occur in Tertiary-Quaternary terrain. However, they probably reflect more recent imprinting of much older deep-seated structures. The detection of apparently young fracture traces was also reported from the Landsat studies of the Alice Springs region of Australia (Maffi & others, 1974). Evidence from the Alaskan studies suggests that some of the fracture sets may have controlled crustal warping. Known mineral deposits appear to be spatially related to hinge lines (genetic relations, however, have not been established), and volcanic eruptive centres to tension induced along fractures during warping (N. R. D. Albert, USGS, written communication, March 1978).

Considerable research into geological applications of computer manipulation of Landsat data is being carried out by major research organisations (e.g., NASA, USGS), universities, and private exploration companies in the USA. For example, to derive maximum structural and surficial reflectance information for the AMRAP study the USGS is currently evaluating the following types of computer-enhanced imagery: false-colour composites with either linear or non-linear stretches; simulated natural colour; and first derivation single-band (normally MSS 6) black and white images (Albert & Steele, 1976). The images are interpreted by conventional visual techniques.

In the Alaskan environment the false-colour and simulated natural-colour products all contribute to the detection of colour anomalies (i.e., a variation in tone or colour on Landsat imagery that differs significantly from the general background colour). In one quadrangle at least 47 percent of colour anomalies appeared to be related to mineralisation (Albert & Chavez, 1977). On false-colour composites iron oxides associated with alteration zones generally had a yellowish to greenish rendition and on simulated natural colour they appeared reddish to yellow. Simulated natural-colour was found to be more useful for detecting iron-oxide coloration, although both types of imagery may contain 'false alarms' due to other causes. Several areas in Alaska identified from independent data as having exploration potential corresponded to areas of iron-oxide coloration observed on the Landsat simulated natural colour imagery.

Publications of the AMRAP program include maps (e.g., Albert, 1975) which show the locations of Landsat colour anomalies in relation to known and interpreted geology. Where practicable the relations of colour anomalies to mineralisation are established before map publication.

The USGS report by Rowan & others (1974) is an excellent background paper both for an appreciation of the potential of computer analysis of Landsat CCT's, and of the underlying principles involved. The paper outlines the various techniques researched in an attempt to enhance subtle spectral reflectance differences of geologic materials, particularly hydrothermal alteration products associated with limonite-enrichment in the sparsely (10-20%) vegetated Goldfields district of Nevada. On large-scale colour aerial photographs the boundary of the hydrothermal alteration is difficult to define because the colour is not entirely diagnostic. A preliminary evaluation of very small-scale colour photography from Skylab by Rowan & others (1974), suggested that while useful for morphological and structural studies such photographs are not adequate for detecting and mapping mineralised areas. Most of the hydrothermally altered areas were indistinct in Landsat standard MSS, stretched MSS images, and stretched false-colour composites. Although many altered areas are apparent on stretched ratio black and white images they cannot be reliably differentiated.

For discrimination of hydrothermally altered areas, and of regional rock and soil units in the study area, the optimum colour-ratio composite technique appeared to be the combination of diazo-colour transparencies: using blue for MSS 4/5, yellow for MSS 5/6, and magenta for MSS 6/7. Altered areas produce colour anomalies of green to dark green, and brown to red-brown in this combination. Field evaluation showed that, excluding alluvial areas, approximately 80 percent of the colour anomalies are related to hydrothermal alteration (Rowan & others, 1977).

Colour-ratio compositing using the combinations discussed above is being rather arbitrarily employed by many as a standard formula for detecting areas of iron-oxide enrichment. Selection of the optimum ratio image or combination of images can be determined by evaluating ratios calculated from spectra representing the rock units of interest (Rowan & others, 1977). The technique is dependent on the presence of contrasting ferric iron oxide absorption intensities between the altered and unaltered rocks under study. Thus the application of the above combination may not produce the same results if the environment, rock types or alteration products are substantially different.

The study by Rowan & others (1974) showed that the combination of ratioing and stretching' offers a powerful means for discriminating some rock types and exposed iron oxide-enriched alteration zones. Further discrimination may be possible by applying different stretch formulas to ratio values in order to extract more information from dark areas of stretched images. Development of the technique is presently limited by the wide band-widths and small spectral range recorded by the Landsat satellites. More potential is indicated by recording of very narrow bandwidths and selected infrared regions, particularly in the vicinity of the 1.6 and 2.2 micrometre wavelengths (Rowan & others, 1977). The 2.2 micrometre wavelengths correspond to a strong hydroxyl absorption band which can be used to detect clay-rich alteration products (Abrams & others, 1977).

A computer analysis technique to detect hydrothermal alteration on Landsat data was employed by Schmidt & Bernstein (1977) for very arid, vegetation-free, porphyry-copper-bearing regions in the Chagai District of western Pakistan. A simple and unrefined digital analysis classification method was tested, then further developed using known areas of mineralisation for computer training. Within the training area maximum and minimum reflectance limits were chosen for each band for mineralised areas (including intensely hydrothermally altered quartz diorite and pyritic rock) and 16 other categories. The computer program then tested the reflectance of each pixel in each band against the values of the established training area, and classified them accordingly. The results were displayed as computer printout maps, and subsequent field work confirmed that within the investigation area of 2100 km^2 mineralised rocks were generally classified correctly. Five sizable occurrences of hydrothermally altered rock containing abundant sulphides were discovered in locations that Schmidt would not have selected from existing geologic and photogeologic information.

Following this work Dykstra & Birnie (1977) applied a more sophisticated digital analysis classification technique to a larger area (5000 km^2) of the Chagai District. The classification was based on principal com-

ponents analysis, and produced even more reliable results. Known hydrothermal alteration associated with iron oxide enrichment was detected for areas as small as 2 pixels, and several new, potentially prospective areas identified.

The computer classification techniques employed in the Chagai region indicate considerable success in the detection of spectral reflectivity data related to hydrothermal alteration. However it should be emphasised that the region has good outcrop and is almost devoid of vegetation. The presence of vegetation and surficial cover directly influence the spectral reflectivity and hence the reliability of computer classification for geology. Consistent classification results have been obtained with up to 30 percent vegetation cover and sometimes higher (up to 50% for low brush) depending on the vegetation types (L. Rowan, USGS, personal communication, October 1977).

The presence of dense vegetation cover does not altogether rule out the application of computer manipulation for geology and may be an advantage if there are geobotanical relationships. Taranik (1977) used digital analysis classification techniques to successfully delineate areas of nickeliferous laterite in the tropical jungle environment of Gag Island (Indonesia). The exercise was reasonably straightforward, since the markedly lateritic areas do not support vegetation; in that situation a computer could be expected to differentiate between the vegetated and non-vegetated areas more rapidly than the human interpreter using air photography. Similar results could not be obtained by visual inspection of Landsat imagery of Gag Island, because the bare lateritic areas are too small-scale to allow ready detection.

A similar exercise was reported by Bølviken & others (1977), in which Landsat digital analysis techniques were used to detect bare or sparsely vegetated areas (caused by natural heavy-metal poisoning of soils) among densely forested glaciated regions of Norway. Some areas of copper poisoning were characterised by low MSS 7/5 ratio values, thus offering a potential method of differentiating them from sparsely vegetated areas resulting from other causes.

The USGS has carried out enhancement of imagery from the Powder River Basin (Wyoming) to show colour variations that are believed to represent vegetation type and/or density differences. The vegetation patterns resulting from enhancement suggest previously unmapped sedimentary facies changes that may control the distribution of sedimentary uranium deposits. In that specific exercise a single ratio of MSS 5/6 was colour-coded by assigning the three prime colours to high, medium, and low ratio values to produce an enhanced colour composite image with the desired effects (T. Offield, USGS, personal communication, November 1977).

Landsat is receiving considerable attention from uranium exploration organisations because of its potential for preliminary selection of promising ground. The application is based on the association of ferric oxide with sedimentary uranium mineralisation, and the ability of Landsat to detect iron oxides. Offield (1976) discussed Landsat ratioing techniques which have been successfully used for detecting some areas of discoloured ground associated with specific uranium deposits in the USA. Vincent (1977) used digital analysis on Landsat CCT's to identify and isolate the spectral signature of oxidised topsoil associated with known uranium mineralisation. The spectral signature was determined from a theoretical model, which related the ratios of reflectance of ferric oxides, grasses, and arkosic sandstones to ratios of radiance detected by Landsat. After the data from selected CCT's were corrected (by computer) for atmospheric and solar illumination variations, the computer searched all the digital data for the specified signal characteristics. The method proved successful with fewer false alarms than are normally experienced with visual photointerpretation techniques applied to single, or colour composite, ratio images.

Although quite significant information may be interpreted visually from Landsat imagery to assist mineral exploration, the papers discussed above serve to illustrate briefly that various computer digital analysis techniques can also be applied to Landsat CCT data to extract useful geological information.

Landsat in petroleum exploration

The major application in petroleum exploration has been to structural geology, where additional data provided by Landsat when combined with existing ground information, can provide more comprehensive structural concepts to improve target selection. Structure and lineament analysis applicable to Landsat have been discussed above, and there are no additional structural techniques peculiar to petroleum exploration.

Some researchers have developed predictive models for detecting areas of hydrocarbon potential based on the combination of Landsat data and available geological information. Baker (1977) for example incorporates lineaments, drainage analysis, tonal anomalies, and the results of various enhancement techniques to allow the selection of priority areas for further field reconnaissance. The method has been successfully tested on known petroleum provinces.

A phenomenon observed on Landsat, and apparently peculiar to areas of petroleum concentration is the existence of hazy anomalies—subtle tonal areas resembling blurring of the image. The effect was first detailed by Collins & others (1974), who reported that of 35 hazy anomalies detected on Landsat, subsequent investigation confirmed that 33 correlated with producing oilfields or drilled structures. Further airphoto study determined that the anomalies could be recognised only on Landsat imagery, and were best seen in dry weather autumn imagery, although they were also well displayed on wet spring imagery. Ground inspection almost invariably showed the anomalies coincided with local areas of sandy soils.

Considerable effort has been directed to determining the origin of the hazy anomalies which are thought to be related to chemical alteration of soil and rock over areas of natural gas seepage. Some hazy anomalies may be attributed to surface alteration due to man-made activity (Short, 1977).

Marrs & Kaminsky (1977) have applied several computer techniques to enhance hazy anomalies, but with only limited success. In general colour composites of contrast-stretched imagery showed anomalous zones best although not all hazy anomalies could be selectively enhanced.

Subsequent investigation of hazy anomalies by ground mapping and soil analysis (Fe, Mn, Mg, Ca) showed no difference between anomalous zones and surroundings. Despite the uncertainty of their origin, the correlation of hazy anomalies with the presence of subsurface petroleum is so strong that some kind of relationship must be accepted.

Techniques have been developed to detect sea surface oil slicks with Landsat data (Halbouty, 1976). While slicks are mainly of importance in environmental management, the techniques have potential for indicating areas of naturally occurring offshore oil seepage.

The most promising factors of Landsat to oil exploration have been summarised by Short (1977). At present the potential of Landsat data for petroleum exploration appears to be more dependent on conventional visual interpretation of imagery than on computer digital analysis. Irrespective of the techniques used it is predictably only a matter of time before new discoveries, based largely on the logical application of Landsat data, are reported.

Discussion

Since 1972 there have been continual improvements in Landsat data products and increased understanding of the capabilities of the technology.

A review of current activities shows that Landsat can provide basic data of use in some phases of mineral and petroleum exploration. Since the main data distribution is through photographic imagery, benefits flow from competent photogeological interpretation, and integration of derived information with that obtained from conventional sources. The likely contribution of Landsat data to a particular geological investigation cannot be predicted. However, the value of any information obtained by visual interpretation of Landsat imagery must directly relate to the quality of the imagery used. Serious application of Landsat to exploration should be based on the best quality imagery. Computer-enhanced, false-colour composite products fall into that category, and should be considered for application to the particular problem under investigation.

Computer-enhanced imagery of much of Australia is now available from distributors under license to the CSIRO Division of Mineral Physics, North Ryde, NSW. The EROS Data Centre, Sioux Falls, USA, also produces computer-enhanced image products.

Computer manipulation of Landsat CCT data offers considerable additional potential for extraction of useful geological information not available in conventional imagery. For some environments computer manipulation techniques applied to Landsat data may be developed into standard operational exploration methods. Present indications suggest that computer techniques are more applicable in exploration programs or field research when most parameters and variables are known and specific problems have been defined. To extract the most information from the data by interactive computer digital analysis techniques it is essential that the operations are carried out by a geologist who is personally familiar with the area and the problems under study (Lyon, 1977).

Although computer manipulation of Landsat data offers great potential, particularly in mineral exploration, no one technique works all the time and in every area—mainly because of variations in vegetation cover, and differences in geological associations. Considerable research remains to be done to determine which techniques are applicable to particular environments.

Users of Landsat need to assess research developments continually so that they can consider the integration of computer and conventional techniques for most cost-effective data extraction. Unfortunately, access to suitable computer facilities is not readily available to the Landsat user in Australia. Various CSIRO Divisions (Mineral Physics—North Ryde, NSW; Computing Research—Canberra; Land Resources Management—Wembley, WA), the Bureau of Mineral Resources, and some universities are conducting Landsat research on interactive computer manipulation facilities, and are useful sources of information on the status and availability of Australian equipment. Under the Australian Mineral Industries Research Association (AMIRA) program, the CSIRO Division of Mineral Physics is conducting joint research with some exploration companies to develop specialised image processing/interpretation tecnniques for specific geologic targets. The digital enhancement techniques used by the Division have been discussed by Green & others (1978).

Summary of applications

Landsat data have many demonstrated applications to assist mineral and petroleum exploration. At present visual interpretation and/or computer manipulation of Landsat data may assist mineral and petroleum exploration by providing:

improved perspective of exposed surface structural expressions and rock distributions;

direct indications of linear and circular features that can be related to local or regional fractures and lineaments,

subtle indications of subsurface structures expressed through regional drainage control, geomorphic anomalies and lineaments;

structural information (obtained by computer enhancement techniques) not obvious at ground level or on conventional aerial photographs;

rapid delineation of the regional distribution of spectral reflectivity data known to be related to specific rocks, minerals, soils or vegetation;

direct detection of exposed iron-oxide weathering products (such as those often associated with hydrothermal alteration and some uranium deposits);

recognition of distinctive tonal or hazy anomalies that are eventually proved to be related to, or caused by natural petroleum occurrences.

Acknowledgements

I wish to thank Dr K. R. O'Sullivan, CRA Exploration Pty Ltd; Dr J. F. Huntington, CSIRO Division of Mineral Physics; and Mr W. J. Perry, BMR for very valuable discussion and comment during the preparation of this paper. Illustrations for the cover, Figures 2(b) and 3 were kindly supplied by the CSIRO Division of Mineral Physics. Figures 1 and 4 were drawn by G. Bates.

References

ABRAMS, M. J., ASHLEY, R. P., ROWAN, L. C., GOETZ, A. F. H., & KAHLE, A. B., 1977—Mapping of hydrothermal alteration in the Cuprite mining district, Nevada, using aircraft scanner images for the spectral region 0.46 to 2.36 μm. *Geology* **5**, 713-18.

ALBERT, N. R. D., 1975—Interpretation of Earth Resources Technology Satellite imagery of the Nabesna quadrangle, Alaska. *US Geological Survey Miscellaneous Field Studies*, Map **MF-655J**.

ALBERT, N. R. D., & STEELE, W. C., 1976—Interpretation of Landsat imagery of the Tanacross quadrangle, Alaska. *US Geological Survey Miscellaneous Field Studies*, Map **MF-767C**.

ALBERT, N. R. D., & CHAVEZ, P. S., 1977—Computer-enhanced Landsat imagery as a tool for mineral exploration in Alaska. *US Geological Survey Professional Paper* **1015**, 193-200.

BAKER, R. N., 1977—Applications of Landsat data and enhancement techniques to hydrocarbon exploration—subjective geostatistical model. Paper presented at Pecora III Symposium, Sioux Falls, 30 Oct.-2 Nov.

BØLVIKEN, B., HONEY, F., LEVINE, S. R., LYON, R. J. P., & PRELAT, A., 1977—Detection of naturally heavy-metal-poisoned areas by Landsat-1 digital data. *Journal of Geochemical Exploration,* **8**, 457-71.

COLLINS, R. J., MCCOWN, F. P., STONIS, L. P., PETZEL, G., & EVERETT, J. R., 1974—An evaluation of the suitability of ERTS data for the purpose of petroleum exploration. *In Third Earth Resources Technology Satellite—1 Symposium,* **1**, Sect. A. *US NASA Special Publication* **351**, 809-21.

DYKSTRA, J. D., & BIRNIE, R. W., 1977—Reconnaissance geologic mapping in Chagai Hills, Baluchistan, Pakistan, by computer processing of Landsat digital data. Paper presented at Pecora III Symposium. Sioux Falls 30 Oct.-2 Nov.

FISHER, N. H., 1975—A multidisciplinary study of earth resource imagery of Australia, Antarctica and Papua New Guinea—Final report to NASA, March 1975. *Department of Science, Canberra, Australia* (unpublished). NASA—**CR-143154**.

GOETZ, A. F. H., BILLINGSLEY, F. C., GILLESPIE, A. R., ABRAMS, M. J., SQUIRES, R. L., SHOEMAKER, E. M., LUCCHITTA, I., & ELSTON, D. P., 1975—Applications of ERTS images and image processing to regional geologic problems and geologic mapping in northern Arizona. *Jet Propoulsion Laboratory California Institute of Technology.* Technical Report **32-1597**.

GOETZ, A. F. H., 1976—Remote sensing geology: Landsat and beyond. *In* Proceedings CALTECH/JPL conference on image processing technology, data sources and software for commercial and scientific applications. November 3-5, 1976. *Jet Propulsion Laboratory, California Institute of Technology.* Report JPL, **SP 43-30**, 8.1-8.

GREEN, A. A., HUNTINGTON, J. F., & ROBERTS, G. P., 1973 Landsat digital enhancement techniques for mineral exploration in Australia. Paper presented at the Twelfth International Symposium on Remote Sensing of Environment, Manila, 20-26 April 1978.

HALBOUTY, M. T., 1976—Application of Landsat imagery to petroleum and mineral exploration. *American Association of Petroleum Geologists Bulletin,* **60**, 745-93.

HENDERSON, F. B., & SWANN, G. A. (Editors), 1976—Geological remote sensing from space—Report of the ad hoc geological committee on remote sensing from space with recommendations for a Geosat program. *Lawrence Berkeley Laboratory, University of California, Publication* **110**.

HOUSTON, R. S., MARRS, R. W., SHORT, N. M., & LOWMAN, P. D., 1977—Earth observations from remote-sensing platforms; outlook. *In* SMITH, W. L. (Editor), 1977—Remote sensing applications for mineral exploration. *Dowden Hutchinson and Ross, Pennsylvania.*

KAMPSCHUUR, W., & PRESS, N., 1977—The direct relationship of features interpreted from Landsat imagery to plate tectonic concepts in the Atlantic region: Its significance in hydrocarbon exploration. Paper presented at Pecora III Symposium, Sioux Falls, 30 Oct.-2 Nov.

LE ROY SCHARON, H., 1976—Statement before the Committee on Science and Technology. *US House of Representatives 94th Congress* (HR-11573), January 27, **III**, No. **66**, 83-85.

LYON, R. J. P., 1977—Mineral exploration applications of digitally processed Landsat imagery. *US Geological Survey Professional Paper* **1015**, 271-92.

MAFFI, C., SIMPSON, C. J., CROHN, P. W., FRUZZETTI, O. G., & PERRY, W. J., 1974—Geological investigation of earth resources satellite imagery of the Mount Isa, Alice Springs and Canberra areas. *Bureau of Mineral Resources Australia Record* **1974/50** (unpublished).

MARRS, R. W., & KAMINSKY, B., 1977—Detection of petroleum-related soil anomalies from Landsat. Paper presented at Pecora III Symposium, Sioux Falls, 30 Oct.-2 Nov.

NATIONAL AERONAUTICS AND SPACE ADMINISTRATION, 1972—Earth Resources Technology Satellite-1 symposium proceedings. September 27. Goddard Space Flight Centre, Maryland. *National Aeronautics and Space Administration Report* **X-650-73-10**.

NATIONAL AERONAUTICS AND SPACE ADMINISTRATION, 1973a—Symposium on significant results obtained from the Earth Resources Technology Satellite-1. Goddard Space Flight Centre, Maryland, March 5-9. *National Aeronautics and Space Administration* NASA **SP-327**, 1.

NATIONAL AERONAUTICS AND SPACE ADMINISTRATION, 1973b—Third Earth Resources Technology Satellite-1 Symposium. Goddard Space Flight Centre, Washington, December 10-14. *National Aeronautics and Space Administration* NASA **SP-351**, 1.

NATIONAL AERONAUTICS AND SPACE ADMINISTRATION, 1975—Proceedings of the NASA earth resources survey symposium, 9-12 June 1975. L.B.J. Space Centre, Houston. *National Aeronautics and Space Administration* NASA **TMX-58168**.

NATIONAL AERONAUTICS AND SPACE ADMINISTRATION, 1976—LANDSAT DATA USERS HANDBOOK. *National Aeronautics and Space Administration, Goddard Space Flight Centre. Document* **76SDS4258**.

OFFIELD, T. W., 1975—Line-grating diffraction in image analysis: Enhanced detection of linear structures in ERTS images, Colorado Front Range. *Modern Geology* **5**, 101-7.

OFFIELD, T. W., 1976—Remote sensing in uranium exploration. *In* Exploration for uranium ore deposits. *International Atomic Energy Agency, Vienna,* 731-44.

OFFIELD, T. W., ABBOTT, E. A., GILLESPIE, A. R., & LOGUERCIO, S. O., 1977—Structure mapping on enhanced Landsat images of Southern Brazil: Tectonic control of mineralization and speculations on metallogeny. *Geophysics,* **42**, 482-500.

PODWYSOCKI, M. H., GUNTHER, F. J., & BLODGET, H. W., 1977—Discrimination of rock and soil types by digital analysis of Landsat data. *Goddard Space Flight Centre Report* **X-923-77-17**.

RICHTER, D. H., ALBERT, N. R. D., BARNES, D. F., GRISCOM, A., MARSH, S. P., & SINGER, D. A., 1975—The Alaskan Mineral Resource Assessment Program: Background information to accompany folio of geologic and mineral resource maps of the Nabesna quadrangle, Alaska. *US Geological Survey Circular* **718**.

RIVEREAU, J. C., 1977—Contribution of Landsat imagery to geological prospecting over Iberian Peninsula. Paper presented at Pecora III Symposium, Sioux Falls, 30 Oct.-2 Nov.

ROWAN, L. C., WETLAUFER, P. G., GOETZ, A. F. G., BILLINGSLEY, F. C., & STEWART, J. H., 1974—Discrimination of rock types and detection of hydrothermally altered areas in south-central Nevada by the use of computer-enhanced ERTS images. *US Geological Survey Professional Paper* **883**.

ROWAN, L. C., GOETZ, A. F., & ASHLEY, R. P., 1977—Discrimination of hydrothermally altered and unaltered rocks in visible and near infrared multispectral images. *Geophysics,* **42**, 522-35.

SCHMIDT, R. G., & BERNSTEIN, R., 1977—Evaluation of improved digital-processing techniques of Landsat data for sulfide mineral prospecting. *US Geological Survey Professional Paper* **1015**, 201-12.

SHORT, N. M., 1977—Exploration for fossil and nuclear fuels from orbital altitudes. *In* SMITH, W. L. (Editor), REMOTE SENSING APPLICATIONS FOR MINERAL EXPLORATION. *Dowden, Hutchinson, and Ross, Pennsylvania.*

SMITH, R. E., GREEN, A. A., ROBERTS, G. P., & HONEY, F. R., 1978—Use of Landsat-1 imagery as an exploration guide for Keweenawan-type copper deposits. *Remote Sensing of Environment,* **7**, 129-44.

SMITH, W. L. (Editor), 1977—REMOTE SENSING APPLICATIONS FOR MINERAL EXPLORATION. *Dowden, Hutchinson, and Ross, Pennsylvania.*

SOHA, J. M., GILLESPIE, A. R., ABRAMS, M. J., & MADURA, D. P., 1976—Computer techniques for geological applications. *In* Proceedings CALTECH/JPL conference on image processing technology, data sources and software for commercial and scientific applications November 3-5, 1976. *Jet Propulsion Laboratory, California Institute of Technology Report* **JPL SP 43-30**, 4.1-4.21.

STEELE, W. C., 1976—Computer program designed to aid in the analysis of Linear features derived from Landsat data. *US Geological Survey Open-File Report* **76-605**.

TARANIK, J. V., 1977—Characteristics of the Landsat system for mineral and petroleum exploration. Paper presented at Pecora III Symposium, Sioux Falls, 30 Oct.-2 Nov.

TARANIK, J. V., 1978—Characteristics of the Landsat multispectral data system. *US Geological Survey Open-File Report* **78-187**.

TARANIK, J. V., in press—Principles of computer processing of Landsat data for geological applications. *US Geological Survey Open-File Report.*

TARANIK, J. V., & TRAUTWEIN, C. M., 1976—Integration of geological remote sensing techniques in subsurface analysis. *US Geological Survey Open-File Report* **76-402**.

VILJOEN, R. P., VILJOEN, M. J., GROOTENBOER, J., & LONGSHAW, T. G., 1975—ERTS-1 imagery: An appraisal of applications in geology and mineral exploration. *Minerals Science and Engineering*, **7**, 132-68.

VINCENT, R. K., 1977—Uranium exploration with computer-processed Landsat data. *Geophysics*, **42**, 536-41.

A seismic investigation of the eastern margin of the Galilee Basin, Queensland

J. Pinchin

In 1976, four seismic reflection traverses were shot across, and close to, the eastern margin of the Galilee Basin to investigate the structure of the basin's northeast margin with relevance to the extent of the Permian coal measures, and to investigate the relationships and extent of the underlying Devonian Adavale Basin and Devonian-Carboniferous Drummond Basin.

The results show that the basin's northeast margin is steep and faulted, and that there is only a narrow strip in which coal is likely to be found at easily mineable depths. About 30 km southwest of this margin, the sediments are undisturbed, with a southerly dip of about half a degree; here 2000 m of Galilee Basin sedimentary rocks overlie 700 m of Drummond Basin sediments—which extend further to the northwest than was previously thought.

The eastern part of the Galilee Basin is underlain by the fluviatile sediments of the Drummond Basin. The more prospective Adavale Basin does not extend as far north as Jericho No. 1 exploration well.

The Koburra Trough, along the northeast margin of the Galilee Basin, contains a thick sequence of Permo-Carboniferous sediments; results from the 1976 survey indicate that it could be bounded by large anticlinal or monoclinal structures which might provide petroleum traps; it is on this area that exploration should concentrate.

Introduction

During 1976 the Bureau of Mineral Resources conducted a reconnaissance seismic survey over the eastern margin of the Galilee Basin. The survey was carried out to investigate the possibly steep northeast and northwest margins of the Koburra Trough, and the relative extent and relationships of the underlying Adavale and Drummond Basins.

The Galilee Basin is a broad sedimentary downwarp of Late Carboniferous to Triassic age and contains prospective Permian coal measures. The Koburra Trough is the deepest part of the basin and trends north-northwest near the eastern margin of the Galilee Basin. Sedimentary rocks within the trough attain a thickness of at least 6200 m, with 2800 m of these sediments belonging to the Galilee Basin, and the remainder unknown sediments of Carboniferous or possibly Devonian Age.

The eastern margin of the Galilee Basin overlies the western margin of the Devonian-Carboniferous Drummond Basin, and below the southern part of the Galilee Basin lies the Devonian Adavale Basin (Fig. 1). The northerly extent of the Adavale Basin and its relationship to the Drummond Basin is unknown, and information on these matters could be of economic importance, because of the occurrence of a small gas field within the Middle Devonian sequence of the Adavale Basin at Gilmore, and oil and gas shows in the Upper Carboniferous sequence in Lake Galilee No. 1 well.

Previous geophysical investigations

Most of the eastern part of the Galilee Basin has been extensively covered by seismic surveys subsidised under the Petroleum Subsidy Acts, and hence publicly available (Fig. 2), but there are few over the eastern margin. Most surveys obtained good reflections from the top of the Upper Permian coal measures, the 'P horizon', but only later surveys recorded any deeper reflections. The top Permian is, therefore, the deepest horizon that has been regionally mapped; structure contours on this horizon (Fig. 3) show a depth of at least 1400 m in the Koburra Trough, and the steep northeast margin of the Trough.

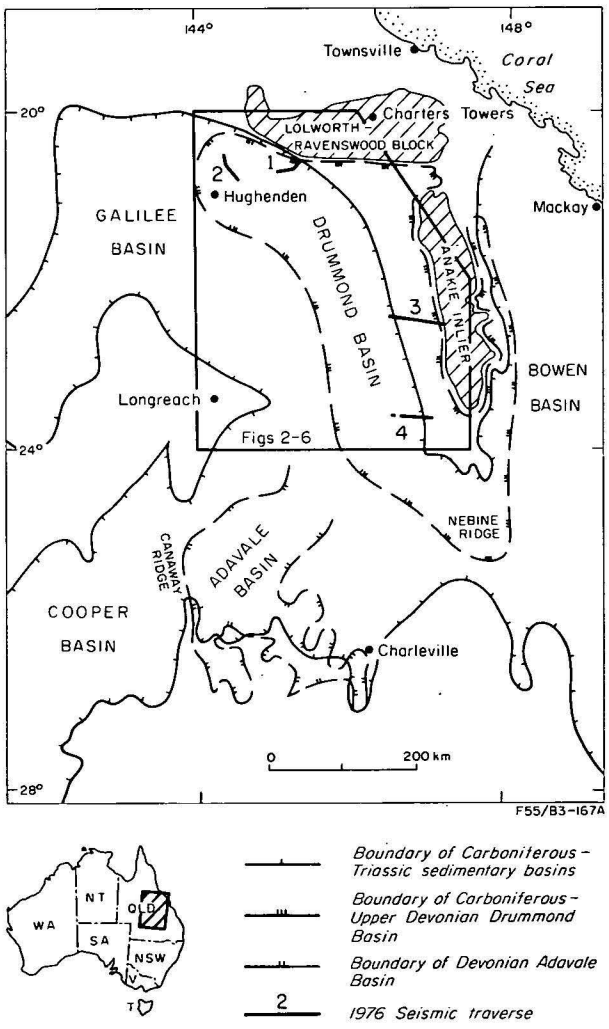

Figure 1. Regional tectonic setting. From Tectonic Map of Australia, 1971, and various BMR Explanatory Notes. Basin boundaries modified by recent seismic survey results.

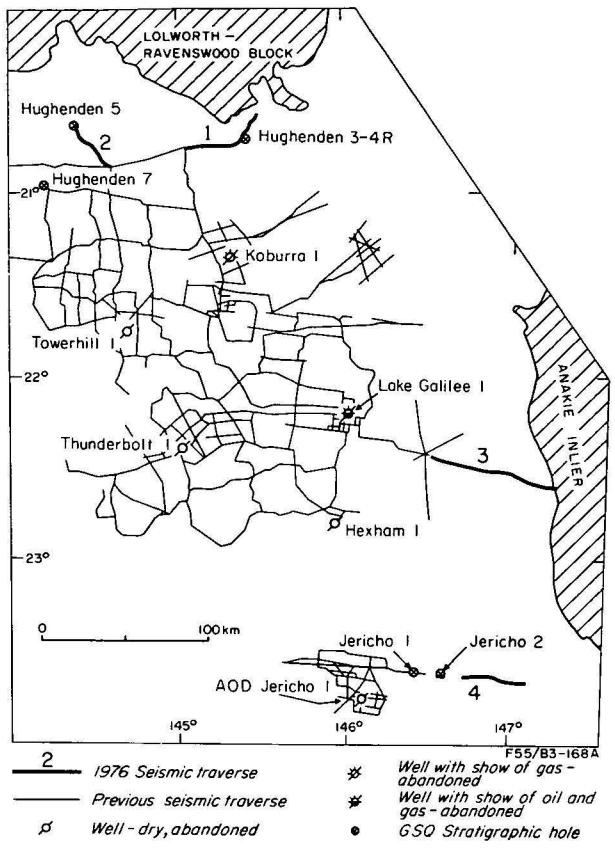

Figure 2. Seismic traverses and exploration wells.

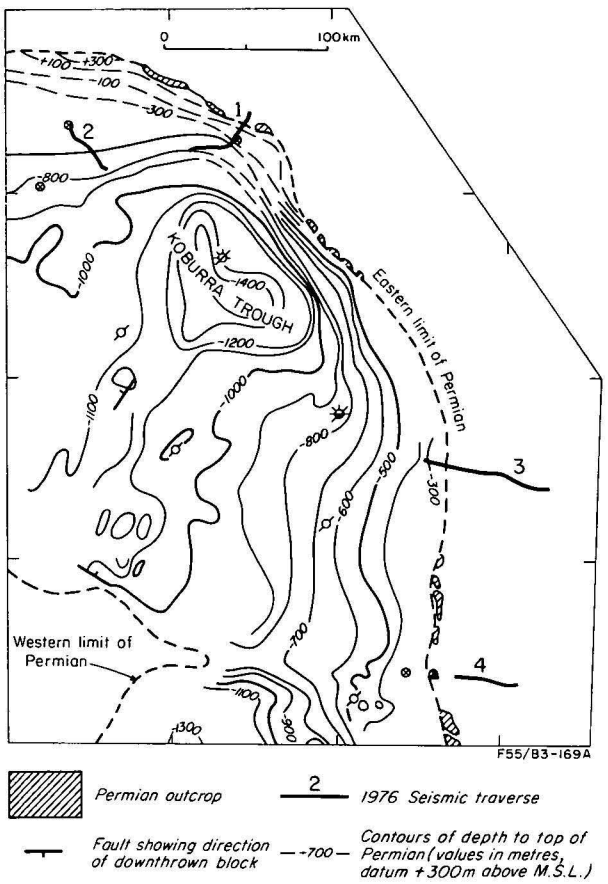

Figure 3. Depth contours to top of Permian.

In 1971, BMR recorded a seismic traverse east of Lake Galilee No. 1 well to investigate the structure of the eastern margin of the Galilee Basin and its relation to the Drummond Basin (Harrison, Anfiloff, & Moss, 1975); it was concluded that the eastern margin of the Galilee Basin is underlain by Middle to Upper Devonian sediments, possibly of the Adavale Basin. However this interpretation was based on scant palynological evidence for the age of these sediments at the bottom of Lake Galilee No. 1 (Playford, Appendix 1a *in* Pemberton, 1965). Recent examinations of the cores from this well, and from other wells in the Galilee Basin throws doubt on this identification (P. Hawkins, pers. comm.).

Regional total magnetic intensity contours are shown in Figure 4. A zone of relatively low amplitude magnetic anomalies coincides with the Koburra Trough, and Hsu (1974) has interpreted magnetic basement depths of 3000 m to 6000 m in this region. At the northwest end of the Koburra Trough, a northeast-trending magnetic lineation separates the low intensity magnetic anomalies over the Trough from higher magnetic intensity to the northwest; Hsu (1974) suggested that this lineation marked the northwest boundary of the Trough.

The Galilee Basin has also been covered by reconnaissance gravity surveys (Gibb, 1968); the Bouguer anomaly map and gravity provinces of Fraser, Darby & Vale (1977) are shown in Figure 5. The Bouguer anomaly values show a general increase in amplitude over the Lolworth-Ravenswood Block in the north and towards the Anakie Inlier in the east (both basement highs located on Fig. 2). The Tangorin Gravity Depression corresponds approximately with the Koburra Trough; but apart from these general observations there is little correlation between Bouguer anomalies and depth to sedimentary basement. One feature, investigated in detail was the Donnybrook Gravity High within the Drummond Gravity Shelf over which a detailed gravity traverse was recorded in 1971. Harrison & others (1975) considered that the anomaly was probably caused by basement uplift, but that a reverse density contrast at depth could alternatively be the cause.

Objectives and program

Four seismic reflection traverses were recorded. Traverses 1 and 2 were surveyed to investigate the possible steep northeast and northwest margins of the Koburra Trough, and to tie the existing seismic network to the stratigraphic bores GSQ Hughenden No. 3-4R and GSQ Hughenden No. 5.

Traverses 3 and 4 were designed to investigate the relationships and relative extents of the Adavale and Drummond Basins in the area east and south of Lake Galilee No. 1 well. There was considerable doubt as to whether the basal sediments in Lake Galilee No. 1 and Jericho No. 1 belong to the Adavale or Drummond Basins. The relative extent of these two basins is regarded as important, because gas has been discovered in the Adavale Basin, but neither gas nor oil has been found in the Drummond Basin. Traverse 3 was shot eastwards from the end of the 1971 BMR seismic traverse to the outcrop of the Anakie Metamorphics, thus providing continuous seismic coverage from Lake Galilee No. 1 across the Drummond Basin to basement outcrop. Traverse 4 provided a similar link between Jericho No. 2 and the Drummond Basin outcrops to the east.

Six-fold common depth point (CDP) seismic reflection techniques were used and gravity measurements at

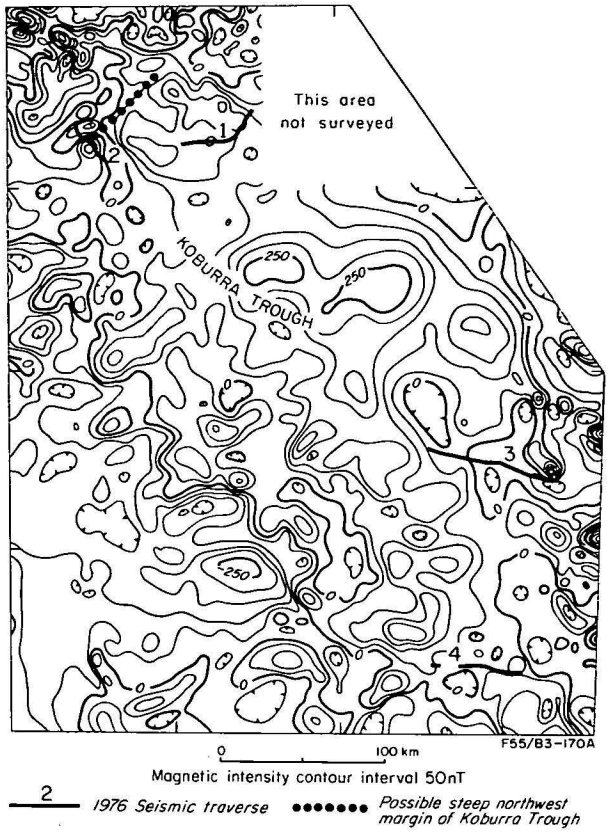

Figure 4. Regional total magnetic intensity.

½ km intervals were taken along all four traverses; details of the field operations are given in Brassil & Anfiloff (1977), and Schmidt, Nelson, & Anfiloff (1977).

Geology

Regional setting

The regional tectonic setting of the area is shown in Figure 1, and details of the geology in Figure 6. The Lolworth-Ravenswood Block and Anakie Inlier are the main basement outcrops in the area. Sedimentary rocks belonging to sedimentary basins of four different ages, the Adavale, Drummond, Galilee, and Eromanga Basins, occupy the area to the south and west of these basement highs.

Rocks of the Early to Middle Devonian Adavale Basin do not crop out anywhere, and the basin is known only from drill-hole and seismic information.

The Late Devonian to mid-Carboniferous Drummond Basin lies south of the Lolworth-Ravenswood Block and mainly west of the Anakie Inlier. Outcrops within this basin are confined to a narrow belt immediately to the west and east of the Anakie Inlier.

Late Carboniferous to Triassic sedimentation in the area was widespread; the sediments were deposited in three separate neighbouring basins—the Galilee, Cooper, and Bowen Basins. Although the Canaway Ridge is taken as the boundary between the Galilee and Cooper Basins, and the Nebine Ridge is considered as the boundary between the Galilee and Bowen Basins, Permo-Triassic sedimentary rocks are continuous across both of these ridges (Mollan, 1969; Senior, 1971; and Vine, 1976).

The Early Jurassic to early Late Cretaceous Eromanga Basin overlies all earlier sedimentary basins

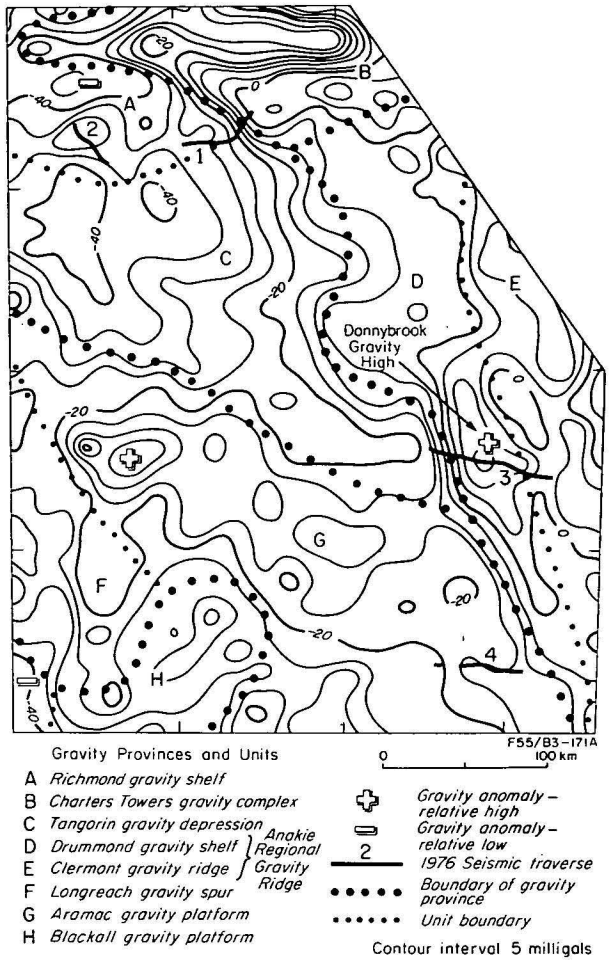

Figure 5. Regional Bouguer anomaly contours.

in the west of the survey area, and the entire region is covered with patches of duricrust and areas of Cainozoic sands, gravels and scattered basalt flows.

Basement

The basement rocks which crop out in the Lolworth-Ravenswood Block and Anakie Inlier consist of Lower Palaeozoic low-grade metasediments, granites, and acid volcanics. Towerhill 1 and Thunderbolt 1 wells are the only exploration wells in the eastern Galilee Basin to reach basement (see Table 1 and Fig. 2); both wells bottomed in Palaeozoic volcanics, which can be correlated either with the pre-Devonian Mount Windsor Volcanics of the Anakie High or with the Devonian-Carboniferous Silver Hills Volcanics of the Drummond Basin (Olgers, 1972).

Well	*Total depth (m)*	*Deepest rock type*
Koburra No. 1	3260	pre-Upper Carboniferous sandstone, shale, siltstone
Towerhill No. 1	1481	pre-Upper Carboniferous acid volcanics
Thunderbolt No. 1	1608	pre-Upper Carboniferous acid volcanics
Lake Galilee No. 1	3406	Middle or Upper Devonian sandstone and shale
Jericho No. 1	2786	pre-Upper Carboniferous acid volcanics
Allandale No. 1 (Lat. 24°25′S Long 145°54′E)	3006	Lower Devonian acid volcanics, possibly Gumbardo Formation

Table 1. Deepest rocks in exploration wells.

Period	*Basin*	Group or Formation		*Lithology*	*Thickness (m)*	*Reference*
Quaternary				Alluvium; soil, sand; basalt; duricrust	50	
		UNCONFORMITY				
Cretaceous	EROMANGA	Rolling Downs Group		Sandstone; siltstone; limestone	1000	Exon & Senior, 1976
Jurassic	EROMANGA	Hooray Sandstone or Gilbert River Formation		Quartzose, sub-labile sandstone	150	Exon, 1966
	EROMANGA	Injune Creek Group		Mudstone; siltstone; sandstone	220	
	EROMANGA	Hutton Sandstone		Quartz sandstone	120	
		UNCONFORMITY				
Triassic	GALILEE	Moolayember Formation	or Warang Sandstone	Mudstone; siltsone; sandstone	150	
	GALILEE	Clematis Sandstone	or Warang Sandstone	Quartzose sandstone; minor cgl	120	
	GALILEE	Rewan Formation	or Warang Sandstone	Mudstone and siltstone	160	Vine & Doutch, 1972
	GALILEE	Betts Creek Beds and Boonderoo Beds		Sandstone; siltstone; coal	100	Vine, 1972
Permian		DISCONFORMITY				
	GALILEE	Joe Joe Group		Sandstone; mudstone; coal	1000	Hawkins, 1977
	UNCONFORMITY (KANIMBLAN OROGENY)					
Carboniferous	DRUMMOND	Ducabrook and Natal Fms		Sandstone; siltstone; tuff	1500	
	DRUMMOND	Star of Hope Formation		Sandstone; tuff; pebble cgl		
	DRUMMOND	Raymond Formation		Quartz sandstone; mudstone	1000	Olgers, 1972
	DRUMMOND	Mt Hall Formation		Sandstone; pebbly conglomerate	600	
	DRUMMOND	Telemon Formation		Sandstone; mudstone; minor 1st	600	
	DRUMMOND	Silver Hills Volcanics		Rhyolite; welded tuff	1500	
	UNCONFORMITY (TABBERABBERAN OROGENY)					
Devonian	ADAVALE	Buckabie Formation		Red sandstone; siltstone; shale	1500	Vine, 1972
	ADAVALE	Etonvale Formation		Siltstone; shale dolomite	500	Tanner, 1968
	ADAVALE	Bury Limestone		Limestone; oolitic fossiliferous	400	
	ADAVALE	Log Creek Formation		Sandstone; dolomite limestone	450	Paten, 1977
	ADAVALE	Eastwood Beds		Interbedded shale and sandstone	500	
	ADAVALE	Gumbardo Formation		Acid volcanics; arkose	400	Auchincloss, 1976
		UNCONFORMITY				
Silurian-Cambrian		Basement rocks including Anakie Metamorphics		Low-grade metamorphics; granites; acid volcanics		

Table 2. Generalised stratigraphy of the area along the eastern margin of the Galilee Basin.

Stratigraphy

The generalised stratigraphy of the area is given in Table 2.

The Adavale Basin mainly contains shallow marine sediments deposited over a platform region (Paten, 1977). Overlying the acid and andesitic volcanics of the Gumbardo Formation is a transgressive sequence of shallow marine sediments including salt and dolomite in the Log Creek and Etonvale Formations. A small gas field was discovered in the Middle Devonian Log Creek Formation at Gilmore, but because of the field's poor reservoir characteristics, size, and distance from market, it has not been brought into production.

The terrestrial sediments of the Drummond Basin were deposited from Late Devonian to Early Carboniferous times in an intermontane trough. Olgers (1972) reports that up to 12 000 m of fluviatile sediments were deposited by generally north-flowing rivers. The initial and final stages of deposition in the basin were accompanied by acid volcanism; the Silver Hills Volcanics form a 1500 m-thick sequence of tuffs and rhyolites at the base of the Drummond Basin, and both the Star of Hope and Ducabrook Formations near the top of the sequence contain numerous tuffs.

Sedimentation in the Galilee Basin was also mainly fluviatile, and continued with minor breaks from the Late Carboniferous until the Late Triassic. There is evidence of glacial conditions in the Late Carboniferous and again in the Early Permian.

During the Late Permian, several distributary river systems flowed southwards into swamps, producing the widespread coal measures. These deposits have the best source-rock potential within the Galilee Basin (Hawkins, 1977).

During the Jurassic and Cretaceous, the fluvial and shallow marine sediments of the Eromanga Basin were deposited in a broad, regional downwarp; covering the area with up to 1800 m of mudstones; sandstones and minor limestone.

Structure

The main geological structures are shown in Figure 6. The Upper Carboniferous and younger sediments are only gently folded and occupy broad downwarps in the

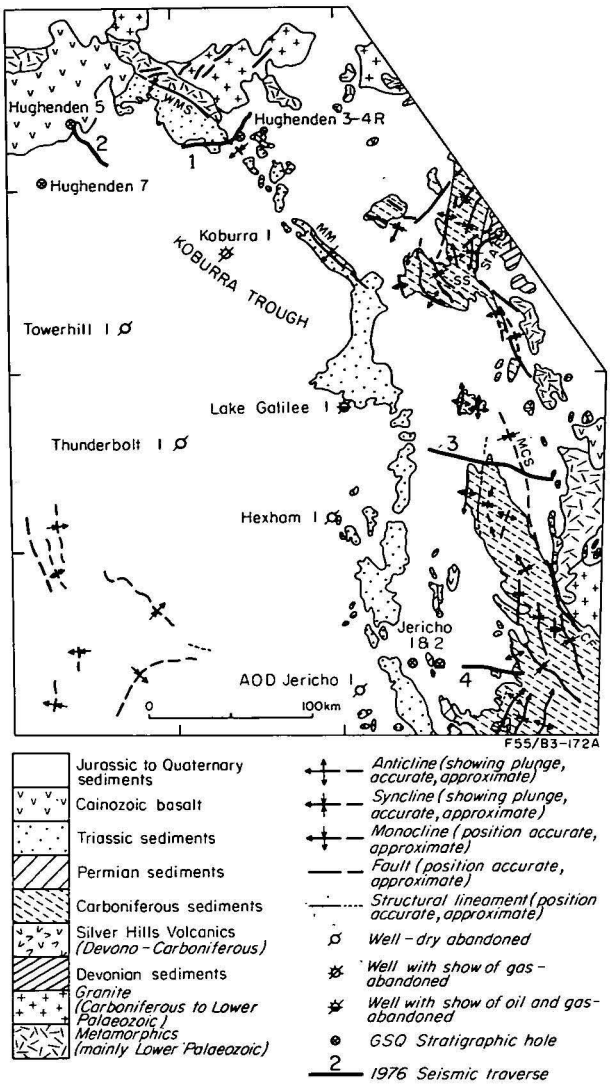

Figure 6. Geology, adapted after Olgers, 1973; Senior, 1974; and Senior & others, 1974.
WMS—White mountains structure; MM—Mingobar Monocline; SS—Scartwater Salient; St AF—Saint Ann's Fault; MCS—Mistake Creek Syncline; CF—Chinaman Fault.

underlying strata. However, the Devonian to Carboniferous sediments of the Adavale and Drummond Basins are folded into a series of generally north-northeast to north-northwest-trending folds, which become tighter towards the east. Olgers (1972) stated that structures in the Drummond Basin were formed during the mid-Carboniferous Kanimblan Orogeny as a result of compression from the east. He also considered that large-scale shearing occurred along northwest and northeast-trending fault zones. He postulated several megashears across the Drummond Basin and Anakie Inlier, and a décollement at the base of the Drummond Basin sequence. The St Anns and Chinaman Faults are high-angle reverse oblique-slip faults and form parts of the megashears.

The boundaries of the Koburra Trough (Fig. 3) have not been precisely defined, but the Trough is known to be about 300 km long along its northwest axis and 100 km across (Allen, 1974). It contains the greatest known thickness of Galilee Basin sediments, 2820 m in Koburra No. 1. The presence of a thick continuous sequence of shallow-water Permian sediments in the Trough indicates that subsidence occurred penecontemporaneously with deposition (Benstead, 1973).

The Mingobar Monocline forms part of the eastern margin of the Koburra Trough. This monocline in the outcropping Triassic and Permian sediments extends, in the subsurface, northwest and southeast of its mapped position (Fig. 6), and appears to be an anticline at depth on the several seismic sections that cross it.

Vine (1972) gave the name Belyando Feature to a lineament that included the White Mountains Structure, the Mingobar Monocline and part of the course of the Beylando River. He suggested that it was a major basement fracture zone and that it marked the western limit of the Drummond Basin. Harrison & others (1975) considered the Drummond Basin sediments to extend 20 km westwards of the Belyando Feature, which appeared to coincide with a shear zone as interpreted from seismic data. This shear zone was postulated to be an extension of the Chinaman Fault.

Results and interpretation

Figures 7 and 8 show a Bouguer anomaly profile, a near-surface seismic refraction profile produced by analysis of the first arrival times, and an interpretation of the seismic reflection section for the traverses. The seismic sections, together with more detailed gravity results will be published by Pinchin, Schmidt & Anfiloff (in prep.).

Traverse 1

The buried river channels interpreted from shallow refraction data (Fig. 7) may be filled with Tertiary sediments of middle-Pliocene age. R. Coventry (in prep.) has correlated the position of these river channels with deep, red soils formed on the lower slopes of the undissected undulating plains in the area during the late Pliocene. Deep, red loamy earths are found in the seismic shot-holes within these channels and the aerial photographs show traces of old river systems.

The shallow refraction data also shows that the youngest sediments at the east end of the line, a partly weathered layer that appears to infill the river channels, are much faulted. The faults were therefore active as recently as the Pliocene.

The three horizons shown in Figure 7 have been traced around the network of seismic lines (Fig. 2) to Koburra No. 1, Towerhill No. 1 and Lake Galilee No. 1 exploration wells. The horizon shown topping the Drummond Basin sequence also ties to the stratigraphic bore GSQ Hughenden No. 3-4R, where Gray (1977) tentatively correlates strata in the bottom of the hole with the Upper Carboniferous Natal Formation.

Faulting makes the basin margin crossed by Traverse 1 fairly steep. The basement rises, mainly by normal faulting, from 2500 m to the surface in a distance of 27 km, giving an average gradient of 5½°; these depth figures are in agreement with Hsu's (1974) calculations of depth to magnetic basement.

The Lower Carboniferous strata do not pinch out, and the Permian sediments do not thin as they approach the basin margin, suggesting that the Drummond and Galilee Basins originally extended further in this direction, and that later uplift or rejuvenation of the Lolworth-Ravenswood Block produced the present margin. However, the Galilee Basin could not have extended much further northeast, because the Lolworth-Ravenswood Block was a source for sediments for the basin (Hawkins, 1977). The uplift of the margin occurred

along a set of parallel monoclines and normal faults. The general structural trend in the area is northwest, so it is probable that the small horst-like block or faulted anticline, crossed by the traverse trends similarly northwest parallel to the White Mountains Structure.

The gravity results (Fig. 7) are consistent with the seismic data: the Bouguer anomaly values rise by about 30 mGal from west to east towards the Lolworth-Ravenswood Block, and the two local increases in gradient of the gravity profile coincide with shallow faults deduced from analysis of the seismic refraction data.

Traverse 2

The buried low-velocity layer interpreted from the shallow refraction data (Fig. 7) could be related to the deep weathering of the Late Cretaceous and Early Tertiary, in which case it would have been buried by later Tertiary terrestrial deposits. However, this is conjectural —the buried weathered zone may be Quaternary.

The shallowest seismic reflection is identified, from its extrapolation to GSQ Hughenden No. 5, as being from the top of the sandstone of the Lower Cretaceous Gilbert River Formation; such sandstones could be expected to yield a strong seismic reflection where they are overlain by mudstone of the Wallumbilla Formation at the base of the Rolling Downs Group. In GSQ Hughenden No. 7, drilled 35 km to the southwest of GSQ Hughenden No. 5 in 1977 (Balfe, in prep.), there is a sharp change in the electric and gamma-ray logs at the boundary between the Wallumbilla and Gilbert River Formations; one would expect a good seismic reflection from this boundary.

The other three reflections, the top Permian, the top of the Late Carboniferous Natal Formation, and basement, are tied to Traverse 1 and to the exploration wells in the area via the network of seismic lines shown in Figure 2.

Figure 7 shows the sediments are undisturbed and dip to the southeast at the slight gradient of ½°. There is no evidence of a steep margin to the Galilee Basin here (cf. Vine & Paine, 1974) on the basis of Hsu's (1974) data. Drummond Basin sediments were not recognised so far northwest before (Fig. 1), and these sediments are believed to have been deposited over a shelf or plain to the west of the intermontane trough that Olgers (1972) considered to be the depositional limits of the basin.

The traverse straddles a broad, low-amplitude gravity high which, since the seismic reflectors are almost flat-lying, must be caused either by gradual density changes within the basement or by large deep structures beyond each end of the traverse (Anfiloff, pers. comm.).

Traverse 3

Interpretation of the shallow refraction data (Fig. 8) shows a weathered zone of fairly constant thickness (ca. 20 m), with a seismic velocity of 1000 m/s, underlain by a refractor with velocity about 2000 m/s. Below this, refractor velocities gradually increase from 3300 m/s in the west to 4500 m/s in the east.

The interpretation of the seismic data presented in Figure 8 is not definitive. However, it matches the known geology and conforms to many of Olgers' (1972) views of the structural development of the Drummond Basin. It does not provide a satisfactory model for the gravity profile, as is explained later. Interpretation is complicated by numerous diffractions and reflected refractions, especially in the more intensely faulted and folded zones. The possible faults at the extreme eastern end of the traverse do not show up on the seismic section, but strong diffraction patterns indicate major discontinuities within the basement rocks.

Olgers in his interpretation of the structure of the Drummond Basin postulated the existence of both thrust-faults and strike-slip faults. The thrust fault shown on this section is in rough alignment with the Chinaman Fault, which is a reverse oblique-slip fault. Olgers interprets a décollement at the base of the Scartwater Salient further north. On the other hand Olgers' Chinaman Megashear (which in places coincides with the Chinaman Fault) passes through this fault zone on Traverse 3, and it seems likely that both low-angle reverse movement and strike-slip movement has occurred here.

The thrust fault is interpreted here as forming during the mid-Carboniferous Kanimblan Orogeny; hence the Drummond Basin sediments, but not the Galilee Basin sediments were affected. This interpretation shows the younger Drummond Basin units to be restricted to the Mistake Creek Syncline, and the older Mount Hall and Telemon Formations to be thicker below the Beresford Upwarp, and to extend far to the west, as suggested by Vine & Doutch (1972). The Beresford Upwarp started to develop in Mount Hall time, and folding and normal faulting continued during deposition; the northern part of the Mistake Creek Syncline crossed by Traverse 3 started to develop after Star of Hope time, and therefore contains a thick Ducabrook Formation. The maximum thicknesses of each unit shown in Figure 8 are in general agreement with those mentioned by Olgers (1972)—except for the Silver Hills Volcanics, which here attains 3000 m, whereas 1500 m was suggested by surface mapping. The different thickness of Mount Hall and Telemon Formations across the thrust fault are due to erosion of the overthrust block prior to deposition of Galilee Basin sediments.

Traverse 3 crosses a Bouguer anomaly high of about 40 mGal, the Donnybrook Gravity High (see Fig. 8). To the east of this high, the Bouguer anomaly values drop steadily to the adjacent low; then, near the eastern end of the traverse, they rise abruptly by about 15 mGal. The seismic results rule out the possibility of a basement uplift as the cause of the Donnybrook Gravity High; in addition, an uplift large enough to produce this gravity high would cause the Silver Hills Volcanics to crop out over the uplift, and they do not. Admittedly, the Beresford Upwarp coincides fairly well with the Donnybrook Gravity High, but the 2 km amplitude of this upwarp could produce, at the most, a third of the observed gravity high, and the adjacent Mistake Creek Syncline, which is a geological structure of similar size, does not correlate well with the observed adjacent gravity low. The gravity profile itself provides evidence against large basement uplift beneath the Donnybrook Gravity High. The observed gravity values over the High are greater than the gravity values over the Anakie Metamorphics at the eastern end of the traverse; therefore, the Donnybrook Gravity High must be caused by a dense body, and not just represent uplifted Anakie Metamorphics. It is postulated here that a dense intrabasement block causes the gravity high; this interpretation is supported by the long wavelength of the high, which indicates a deep-seated origin.

An alternative interpretation based on the concept of low density Silver Hills Volcanics overlain by higher density Drummond Basin sediments is presented by Flavelle & Anfiloff (1976). However, this interpretation

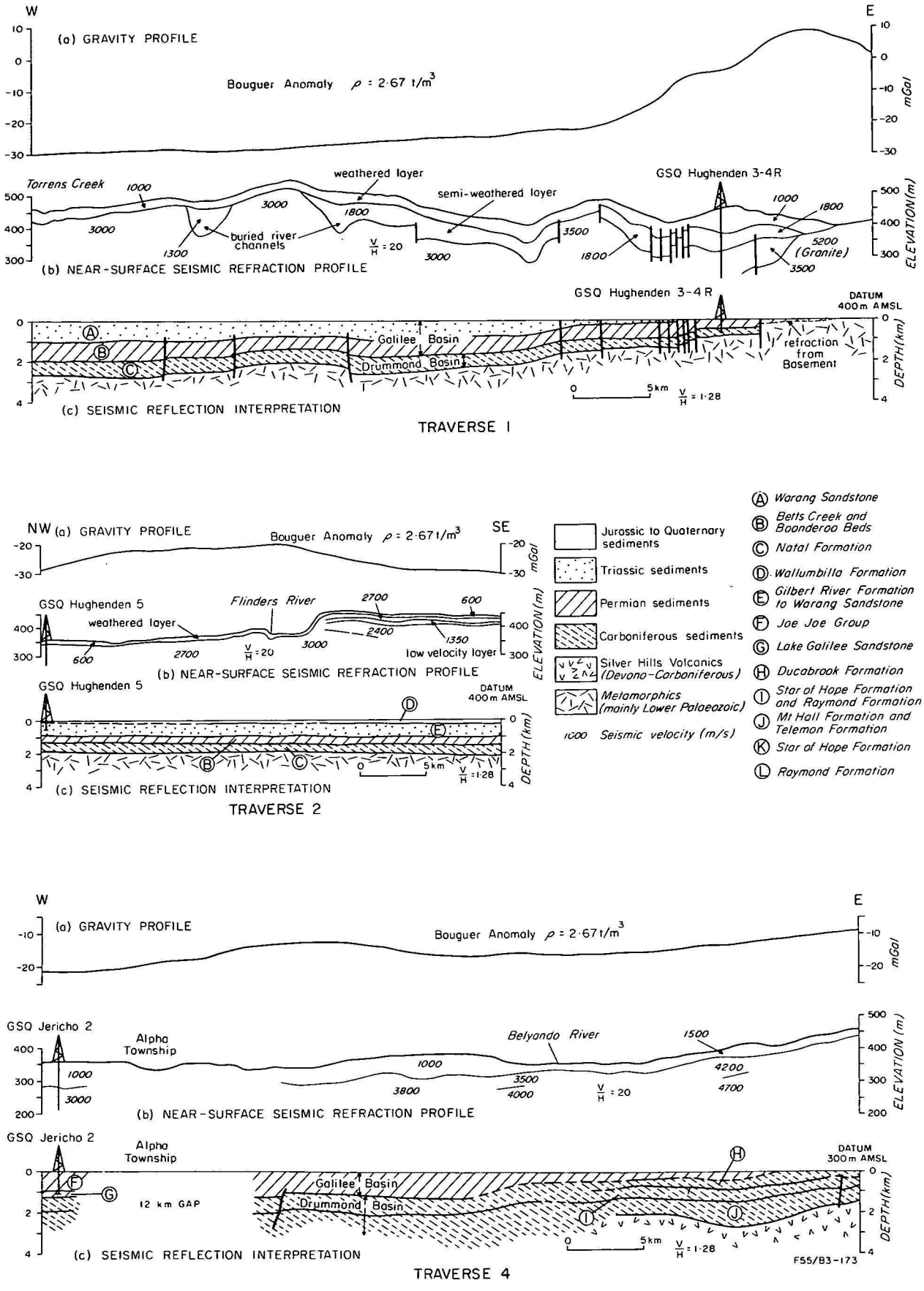

Figure 7. Seismic and gravity results, Traverses 1, 2, and 4.

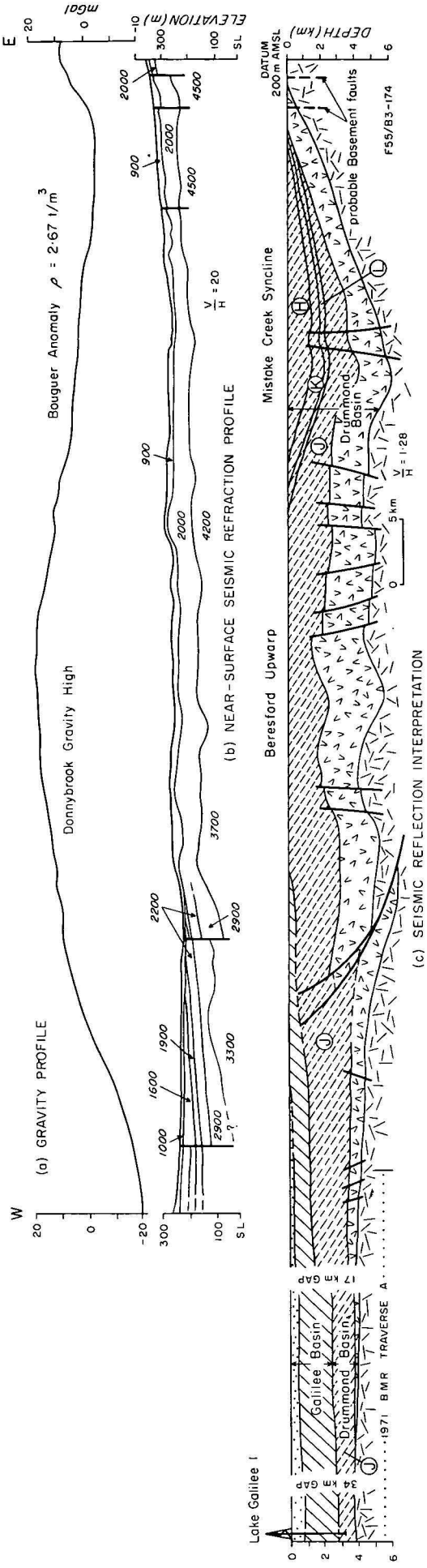

Figure 8. Seismic and gravity results, Traverse 3. For legend see Figure 7.

requires a complex geological history, in conflict with ideas expressed here. Both interpretations are discussed further by Pinchin & others (in prep.).

Traverse 4

Identification of the seismic reflections on this traverse (see Fig. 7) is based on the tie to the stratigraphic bore GSQ Jericho No. 2, the tie to the outcrops of the Drummond Basin in the east, and comparison of the seismic section character to that within the Mistake Creek Syncline on Traverse 3. The strongest reflection, as on Traverse 3, is from near the top of the Mount Hall Formation. No basement reflection has been identified.

The Drummond Basin rocks are not as tightly folded and faulted here as on Traverse 3, but more intense folding east of the traverse is indicated by the surface geology.

Because of the gap in seismic coverage between Traverse 4 and the nearest line of the Jericho Seismic Survey (Alliance, 1964) and because of the distance to be covered, correlation of the reflections on Traverse 4 with those at Jericho No. 1 well is difficult. However, the band of reflections arising from the Mount Hall and Telemon Formations can be followed westwards from Traverse 4 for a considerable distance towards Jericho 1 well. In this well, the Devonian strata consist of volcaniclastics and dacite which are probably related to the Silver Hills Volcanics. Olgers (1972) considered the Drummond Basin to extend to Jericho 1; these seismic results support his conclusions.

The Bouguer anomaly values rise gently from west to east along the traverse, and superimposed on this regional trend is a broad gravity high of only 7 mGal. The long wavelength of this gravity high indicates that it is probably caused by a structure deeper than 3000 m (W. Anfiloff, pers. comm.). Furthermore the seismic section shows no shallow structures that could be identified as possible sources of the gravity anomaly. The steady eastwards rise in Bouguer anomaly values is consistent with the eastwards shallowing of the Galilee Basin indicated by the seismic results.

Conclusions

The northeast margin of the Galilee Basin, adjacent to the Lolworth-Ravenswood Block, is formed by normal onlap onto basement, and is extensively modified by Tertiary faulting along previously existing northwesterly structural trends parallel to the White Mountains Structure and Mingobar Monocline. Traverse 1 crossed a gentle fault-bounded anticline, the amplitude of which increases with depth, indicating fault movement as far back as Early Carboniferous. Structures similar to this could occur further south in the Koburra Trough, where the sedimentary thickness is greater, and could provide the most attractive oil exploration targets in the area.

The steep, faulted nature of the northeast margin probably provides only a narrow strip where coal is likely to be found at shallow depths, and a detailed exploration program would be required to locate any commercial seams.

Rocks of the Drummond Basin are seen to extend further northwest than was previously thought. This raises the questions of the depositional environment west of the intermontane Drummond Basin trough, and the limits of deposition of these Upper Devonian and Lower Carboniferous strata. The Drummond Basin in

the outcrop area is considered to be generally fluviatile and non-prospective for petroleum, but its extension to the west below the Galilee Basin could be of a different facies.

In the Mistake Creek Syncline and Beresford Upwarp (Traverse 3), the Drummond Basin rocks, including a thick sequence of Silver Hills Volcanics, are extensively folded and faulted. This folding ends in the east at a low-angle thrust fault below the Belyando River, west of which there is only gentle folding. The Silver Hills Volcanics are 3000 m thick below the Beresford Upwarp, and thin westwards to pinch out 30 km southeast of Lake Galilee No. 1.

It is thought unlikely that the Adavale Basin extends as far north as Jericho No. 1 well; seismic reflections from the Mount Hall and Telemon Formations can be followed westwards below the Galilee Basin from the Drummond Basin outcrop area to both Lake Galilee No. 1 and Jericho No. 1 exploration wells. Thus it seems likely that the volcaniclastics and dacite in the bottom of Jericho No. 1 are related to the Silver Hills Volcanics. Towerhill No. 1 and Thunderbolt No. 1 wells also bottomed in acid volcanics; if these are also equivalent to the Silver Hills Volcanics, then volcanics accumulated over a wide area, and it is possible that subsequent Drummond Basin sediments were similarly widespread. There is still not enough knowledge about the sediments that underlie the eastern margin of the Galilee Basin to determine the petroleum prospectivity of the area.

The Koburra Trough contains at least 2800 m of Galilee Basin sediments plus 3200 m of pre-Galilee strata, and it may be bounded by anticlinal structures similar to that crossed by Traverse 1. The Koburra Trough looks, at present, to be the most favourable place for petroleum exploration within the Galilee Basin, and its structural history and stratigraphy should be investigated in detail as the next step in the exploration of the basin.

Acknowledgement

The figures were drawn by R. Bates.

References

ALLEN, R. J., 1974—Hydrocarbon significance of Upper Palaeozoic sediments associated with the Koburra Trough, Galilee Basin. *Journal of the Australian Petroleum Exploration Association*, **14**, 59-65.

ALLIANCE OIL DEVELOPMENT, 1964—Seismic survey report, Jericho area, ATP81P, Queensland. *Bureau of Mineral Resources, Petroleum Search Subsidy Act Report* **63/1527** (unpubl.).

AUCHINCLOSS, G., 1976—Adavale Basin. *In* KNIGHT, C. L. (Editor), ECONOMIC GEOLOGY OF AUSTRALIA AND PAPUA NEW GUINEA, 3—Petroleum. *Australasian Institute of Mining and Metallurgy, Melbourne, Monograph* **7**, 309-15.

BALFE, P. E., in prep.—Stratigraphic drilling report—GSQ Hughenden 7. *Queensland Government Mining Journal.*

BENSTEAD, W. L., 1973—Galilee Basin. *Queensland Geological Survey Record* **1973/20** (unpublished).

BRASSIL, F., & ANFILOFF, W., 1977—Galilee Basin seismic and gravity survey, Queensland, 1976. Operational report —Clermont-Alpha area. *Bureau of Mineral Resources, Australia, Record* **1977/26** (unpubl.).

COVENTRY, R. J.—The surficial geology and geomorphic evolution of the Torrens Creek area, North Queensland. Submitted to the *Journal of the Geological Society of Australia.*

EXON, N. F., 1966—Revised Jurassic to Lower Cretaceous stratigraphy in the southeast Eromanga Basin, Queensland. *Queensland Government Mining Journal*, **67**, 775.

EXON, N. F., & SENIOR, B. R., 1976—The Cretaceous of the Eromanga and Surat Basins. *BMR Journal of Australian Geology and Geophysics*, **1**, 33-50.

FLAVELLE, A. J., & ANFILOFF, W., 1976—Non-standard gravity anomalies over sedimentary structures. *Journal of the Australian Petroleum Exploration Association*, **16**, 117-21.

FRASER, A. R., DARBY, F., & VALE, K. R., 1977—Reconnaissance gravity survey of Australia: a qualitative analysis of results. *Bureau of Mineral Resources, Australia, Report* **198**: *BMR Microform* **MF14**.

GIBB, R. A., 1968—North Eromanga and Drummond Basins gravity surveys, Queensland 1959-1963. *Bureau of Mineral Resources, Australia, Report* **131**.

GRAY, A. R. G., 1977—Stratigraphic drilling in the Hughenden 1:250 000 sheet area, 1974-75. *Queensland Government Mining Journal*, **78**, 382-92.

HARRISON, P. L., ANFILOFF, W., & MOSS, F. J., 1975—Galilee Basin seismic and gravity survey, Queensland 1971. *Bureau of Mineral Resources, Australia,* Report **175**.

HAWKINS, P. J., 1977—Galilee Basin—prospect review. *Petroleum Exploration Society of Australia, Queensland Branch, Symposium.* November 1977.

HSU, H. D., 1974—Aeromagnetic interpretation of northern Eromanga and Galilee Basins, Queensland. *Bureau of Mineral Resources, Australia, Record* **1974/42** (unpublished).

MOLLAN, G. M., 1969—Springsure, Queensland, 1:250 000 Geological Series. *Bureau of Mineral Resources, Australia, Explanatory Notes* **SG/55-4** (unpubl.).

OLGERS, F., 1972—Geology of the Drummond Basin, Queensland. *Bureau of Mineral Resources, Australia, Bulletin* **132**.

PATEN, R. J., 1977—The Adavale Basin, Queensland. *Petroleum Exploration Society of Australia, Queensland Branch. Symposium,* Nov. 1977.

PEMBERTON, R. L., 1965—Lake Galilee No. 1 well completion report. *Bureau of Mineral Resources, Australia, Petroleum Search Subsidy Act Report* **64/4076**.

PINCHIN, J., SCHMIDT, D. L., & ANFILOFF, W., in prep.—Eastern Galilee Basin seismic survey, Queensland, 1976. *Bureau of Mineral Resources, Australia, Record.*

SCHMIDT, D. L., NELSON, A., & ANFILOFF, W., 1977—Galilee Basin seismic and gravity survey, Queensland, 1976. Operational report—Pentland-Hughenden area. *Bureau of Mineral Resources, Australia, Record* **1977/27** (unpubl.).

SENIOR, B. R., 1971—Structural interpretation of the Southern Nebine Ridge area, Queensland. *Australasian Oil and Gas Review*, **17**(5).

SENIOR, B. R., 1974—Notes on the geology of the Central Eromanga Basin. *Bureau of Mineral Resources, Australia, Bulletin* **167B**.

SENIOR, B. R., HARRISON, P. L., & MOND, A., 1974—Notes on the Geology of the Northern Eromanga Basin. *Bureau of Mineral Resources, Australia, Bulletin* **167A**.

TANNER, J. J., 1968—Devonian of the Adavale Basin, Queensland, Australia. *International Symposium on Devonian Systems, Calgary, Alberta 1967,* 111-16.

VINE, R. R., & DOUTCH, H. F., 1972—Galilee, Queensland, 1:250 000 Geological Series. *Bureau of Mineral Resources, Australia, Explanatory Notes* **SF/55-10**.

VINE, R. R., & PAINE, A. G. L., 1974—Hughenden, Queensland, 1:250 000 Geological Series. *Bureau of Mineral Resources, Australia, Explanatory Notes* **SF/55-1**.

VINE, R. R., 1972—Relationships between the Adavale and Drummond Basins. *Journal of the Australian Petroleum Exploration Society*, **12**, 58-61.

VINE, R. R., 1976—Galilee Basin. *In* KNIGHT, C. L. (Editor), Economic Geology of Australia and Papua New Gninea, **3**—Petroleum. *Australasian Institute of Mining and Metallurgy, Melbourne, Monograph 7,* 392-5.

Crustal structure of the central Bowen Basin, Queensland

C. D. N. Collins

During May-June 1973, a deep crustal seismic refraction survey was undertaken in the Bowen Basin, Queensland. Blasts from open-cut coal mines in the Basin were used as sources of seismic energy, and recordings were made at twenty-two sites on a 375 km-long line along the axis of the Basin between Gonyella in the north and Moura in the south. A four-layer crust was interpreted from the seismic data, with P-wave velocities of 4.00 ± .22, 5.33 ± .08, 6.39 ± .07 and 7.07 ± .02 km/s respectively. The total thickness of the 4.00 and 5.53 km/s layers is about 6 km under Goonyella, and slightly more under Dingo 130 km north of Moura. Earlier magnetic and gravity work indicates that these two layers thin southwards towards Moura. They comprise folded Permian-Triassic sediments and possibly also Early to Middle Palaeozoic rocks. The 6.39 km/s layer probably represents the igneous or granitised basement. A lower crustal layer with a velocity of 7.07 km/s and thickness ranging between 5 and 6 km has been interpreted. The total crustal thickness at the centre of the traverse is 36 km, and the upper mantle P-wave velocity is 8.10 ± .11 km/s. A southward-dipping Moho may be interpreted, with the crustal thickness increasing from 35 km, 30 km south of Peak Downs, to 37 km near Dingo. The gravity field calculated from the model conflicts with the observed gravity, suggesting a more complex model than that defined by the seismic refraction data alone.

Introduction

The Bowen Basin in central Queensland (Fig. 1) has been known for its extensive coal measures since the last century (Jack, 1879). Though coal has been mined for many years, it was only when markets developed and open-cut methods were introduced in the early 1960s that substantial production began. To extract the coal, the overburden, which is about 30 metres thick, is broken up by blasting and removed by dragline. The charges, which usually range in size from 50 to 300 tonnes of ammonium nitrate explosive, are recorded regularly at the University of Queensland's seismological observatory at Charters Towers 260-640 km away. During May-June 1973, the Bureau of Mineral Resources (BMR) and the University of Queensland undertook a seismic refraction survey to define the crustal structure and upper mantle relief of the basin, using these explosions as seismic energy sources. A reversed refraction line, about 375 km long, was surveyed between the Goonyella and Peak Downs mines in the north, and the Moura and Kianga mines in the south (Fig. 1). Shots were also recorded from the Blackwater mine, 150 km northwest of Moura.

Previous work

The geology of the region has been described in a publication of the Department of National Development (1966), and by Dickens & Malone (1973). Darby (1966) explained the tectonic framework of the region in terms of the genesis of the Tasman Geosyncline. The eastern zone (Fig. 1) corresponds to the zone of central uplift of the geosyncline, with its associated ultrabasic and granitic intrusions; the Bowen Basin was a marginal trough formed at the time of uplift.

The Basin extends from basement outcrop near Collinsville in the north, to Springsure in the south where it is overlapped by Mesozoic rocks of the Great Artesian Basin (Fig. 1). It is probably continuous with the Sydney Basin beneath this younger cover. To the northwest it is bounded by the Anakie High and Drummond Basin, to the east by the Connors Arch and to the west by the Birkhead axis, which separates it from the Galilee Basin.

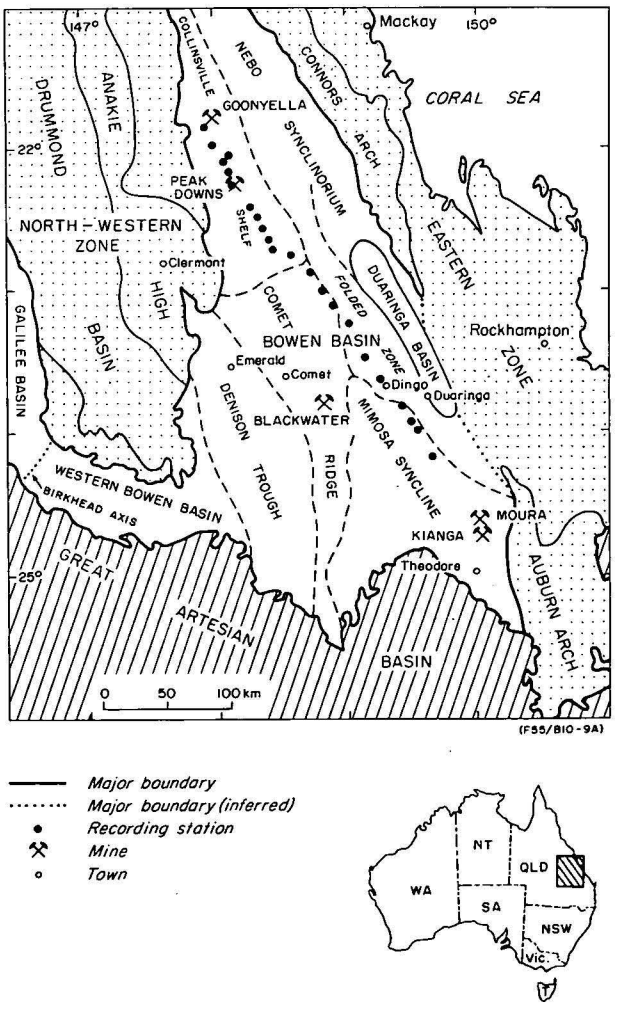

Figure 1. Location of shots and recording stations, and major structural units.

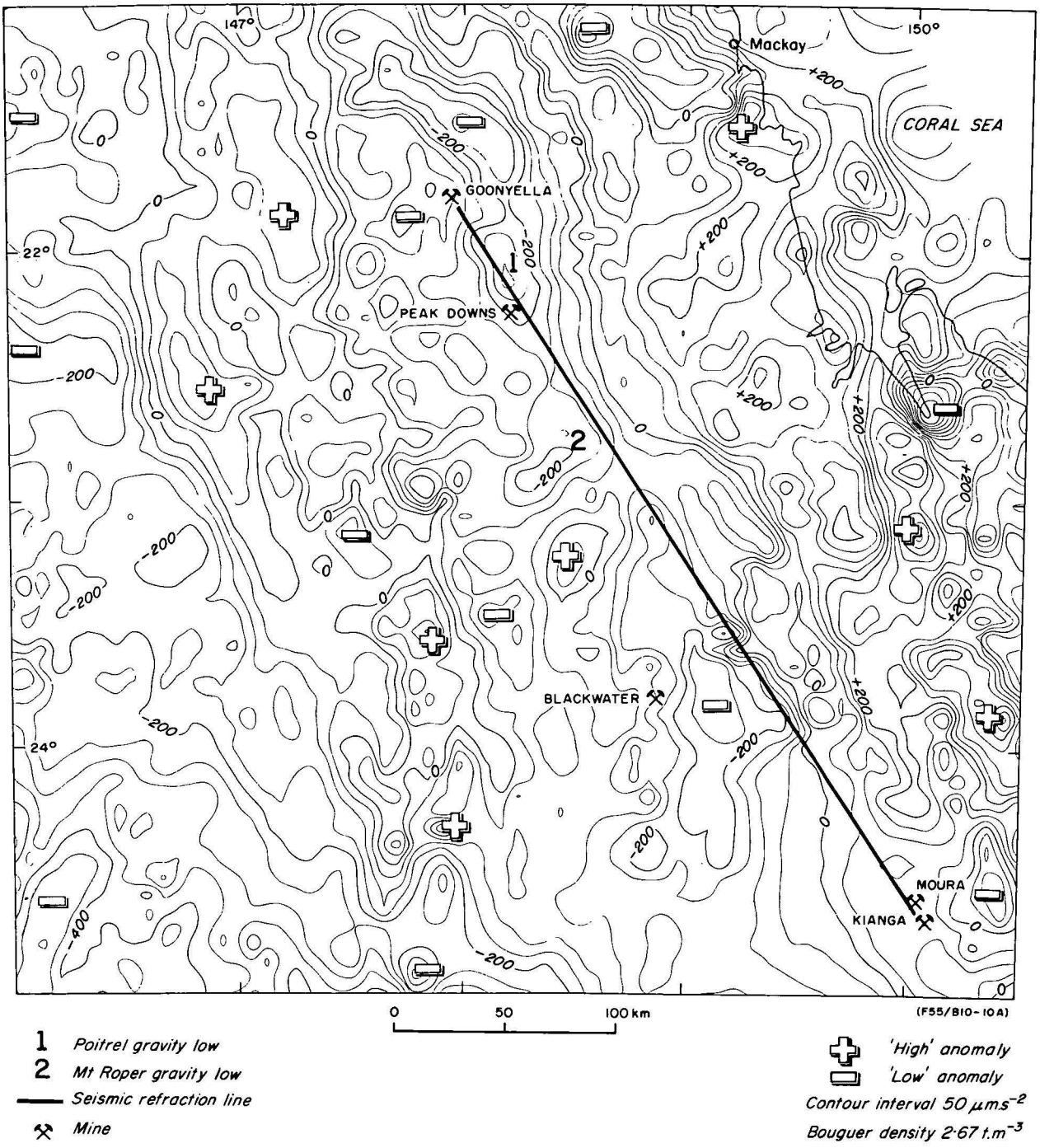

Figure 2. Bouguer anomaly map of the Bowen Basin.

Sedimentation began in the Early Permian, when thick, terrestrial sediments, including numerous coal beds, were deposited. The main centres of deposition were in the Denison Trough and in a trough on the present site of the Connors Arch and Nebo Synclinorium (Fig. 1). Contemporaneous volcanism occurred along the eastern margin. Subsequently, the sea transgressed westwards, and marine and fluviatile sedimentation, accompanied by deepening and expansion of the Denison Trough, continued from the Early to the Late Permian.

Towards the end of the Permian, thick freshwater sediments and extensive coal measures were laid down in the central and western areas of the Basin. In the Early Triassic, the main centre of sedimentation shifted from the area that is now the Nebo Synclinorium to that now occupied by the Mimosa Syncline, where rapid subsidence occurred during the middle to late Triassic. A total thickness of 5500 m of sediments accumulated during this period. Uplift and igneous intrusion in the east proceeded at the same time as the subsidence. Deposition ceased in the Late Triassic, and the sediments were subsequently uplifted and eroded. Tertiary terrestrial sediments are widespread, typically about 200 m thick, but with a maximum thickness of about 1 km in the Duaringa Basin. Contemporaneous basalt flows have been largely removed by erosion.

Previous geophysical surveys in the region were undertaken mainly in the search for minerals, particularly petroleum and coal. Extensive reflection seismic

surveys were carried out, mainly in the southern and southwestern area between Clermont, Springsure, and Theodore (Fig. 1), on the Anakie High, Denison Trough, and Mimosa Syncline—but most of this work is remote from the refraction line described in this paper. Early surveys were reported by Smith (1951), and Shell (Qld) Development (1952). Deep seismic reflections were recorded in the Comet area during a reconnaissance reflection and refraction survey between Emerald and Duaringa (Robertson, 1961, 1965).

Gravity surveys have been conducted by BMR and private companies (Lonsdale, 1965; Darby, 1966); the gravity anomalies (Fig. 2) mostly reflect variations in the depth to basement. Positive anomalies exist over the Anakie High in the west, the Connors Arch and Auburn Arch in the east, and the Comet Ridge in the central Bowen Basin, while negative anomalies are found over the Denison Trough, Mimosa Syncline, and Nebo Synclinorium.

An aeromagnetic survey was undertaken by BMR from 1961 to 1963 (Wells & Milsom, 1966), and estimates of the depths to magnetic basement were in reasonable agreement with those expected from a structural interpretation.

Deep crustal seismic refraction studies have been carried out to the north of the present survey area, across Cape York Peninsula and south as far as Charters Towers (Finlayson, 1968). A three-layer crust was interpreted, with a total crustal thickness along the centre of Cape York Peninsula, and at Charters Towers, of about 45 km, decreasing to about 25 km on either side of the Peninsula. The depth to the intermediate crustal layer was found to be approximately 25 km under the interior of the peninsula, decreasing to 10 km near the coast. A refraction traverse was later extended into the Galilee Basin (Cull & Riesz, 1972) from Charters Towers south to a point about 80 km west of Clermont (Fig. 1). Interpreted depths to the Moho and intermediate layer were 35-40 km, and 20-25 km, respectively. Seismic velocities of about 6 km/s for the upper crust below the sediments, 6.75 km/s for the lower crust and 8.0 km/s for the upper mantle were obtained in both surveys.

Field operations

During the survey reported here shots were recorded from the Utah Development Company mines at Goonyella, Peak Downs, and Blackwater, and the Thiess Peabody Mitsui Coal Pty Ltd (now Thiess Dampier Mitsui Coal Pty Ltd) mines at Moura and Kianga. All mine managements co-operated by facilitating on-site shot timing, and providing information such as shot sizes and positions.

Nineteen shots were recorded, ranging in size from 2.7 tonnes to 300 tonnes, with an average of about 60 tonnes. Typically, the explosive was placed in 6 rows of holes and detonated with a delay of 17 milliseconds between each row. Recordings at Charters Towers observatory showed that the amplitudes of the seismic arrivals depended on the total weight of explosive, and were apparently independent of the delays in the shot. The time of detonation of each shot with respect to VNG radio time signals was obtained, on most occasions, with a manually operated recorder at the shot site. A 200-m ten-geophone spread was used for shot timing at Goonyella. Because of the frequency of shots at Peak Downs mine, an automatic recording system was placed near that mine for the duration of the survey, and used for shot timing.

For the field observations nine BMR automatic seismic tape-recording systems with Willmore Mk 2 seismometers were used; each system recorded a vertical component seismic signal at two gain levels, as well as clock and radio time signals. These recorders occupied 22 stations on a line about 375 km long between Goonyella and Moura (Fig. 1). Station spacing at the northern end was approximately 10 km, and at the southern end approximately 20 km. There were no observations on the southernmost 50 km of the line owing to lack of time. A detailed description of the field work has been given by Connelly & Collins (1973).

Data quality

Shot and station positions were determined to within 0.1 minute of arc, or about 0.2 km. Shot times were read to 0.01 s and corrected for shot-to-timing recorder distance assuming a velocity of 4.0 km/s. This velocity was obtained at Goonyella, and it is expected to be the same at the other mines because of the similar lithology.

Field recording tapes were played back into an analogue chart recorder and the travel-times of seismic arrivals determined from these records. Arrival times at the recording stations could be read to 0.01 s when the arrival was impulsive, for instance, at stations near the shot points; in most other cases, arrivals could be read to 0.1 s. Some arrivals could not be read to this accuracy and were used only as an additional check on the interpreted model.

The gain levels of the recorders near the shot points were set too high, causing saturation; only first arrivals could be read at these stations. Record quality was otherwise generally good, though at the more distant stations the arrivals were in some cases too emergent to be timed accurately.

Interpretation

The travel times were plotted against shot distance after clock error and head parallax corrections had been applied. Figure 3 (a, b, c) shows a plot of travel-times from Goonyella and Peak Downs mines in the north, Moura and Kianga mines in the south, and Blackwater mine near the centre of the traverse. Apparent velocities and intercept times for the various seismic phases were determined by linear regression.

Various velocity-depth models were computed from the travel-time data, assuming planar dipping layers. The reciprocal method of interpretation (Hawkins, 1961) was used where reversed data were available. Where possible, seismic travel-times were tested for consistency from shots at both ends of the traverse, and from Blackwater near the centre of the traverse; a number of possible interpretations were eliminated in this way. Not all seismic arrivals could be identified unambiguously because of a low signal-to-noise ratio on some of the recordings.

Travel times from the models were compared with record sections constructed from the original analogue records (Fig. 4a, b). The data show that the structure may be interpreted as being simple and almost planar; the apparent velocities from both the northern and southern shots are similar for each layer, indicating that the dips are small. The preferred four-layer model is shown in Figure 5. This model was treated by seismic ray tracing programs, which trace seismic ray paths through a given model, and compute the travel

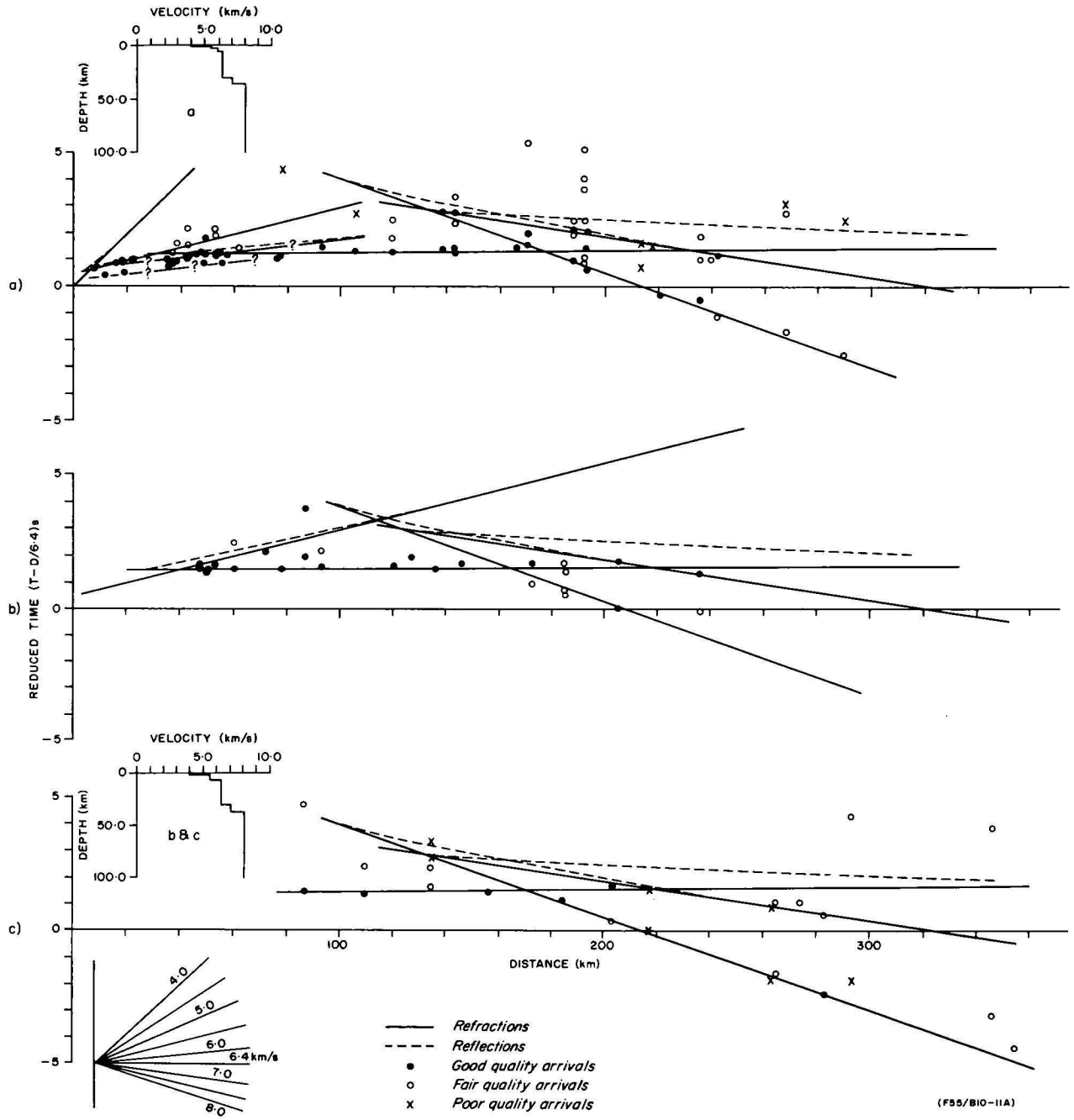

Figure 3. Travel-time curves from shots at (a) Goonyella, (b) Blackwater and (c) Moura and Kianga.

times for the various paths at stations along the surface. GEOTRACE (Cull, 1973) was used for initial interpretation; only horizontal-layered models can be used in this program. SEISRAY, a program to test dipping-layer models, was developed during this interpretation. In general, the agreement is good. Variations from the computed travel-time curves may be due to near-surface conditions at each recording site, and refractor topography.

No first arrivals from the uppermost layer of the model were recorded, except on the 200-m ten-geophone spread used for shot timing at Goonyella. The existence of a low velocity surface layer was inferred from the intercept time of the shallowest layer recorded. An upper limit to its velocity was determined from the travel times to the nearest stations. A velocity of 4.00 ± 0.22 km/s was obtained from the geophone spread and was assumed to apply along the length of the traverse. This agrees with the results of Smith (1951), who found velocities between 3.47 and 4.63 km/s at Comet, near the centre of the traverse; and Robertson (1965), who recorded velocities of 3.57 to 5.06 km/s within the uppermost 1.2 km between Comet and Dingo. A surface layer with a velocity of 4.00 km/s, 1.2 km thick, was therefore adopted in the north, and assumed to be continuous to the south. Recording stations were not placed sufficiently close to the shot-points for any detailed data on near-surface layers to be obtained.

The 5.53 ± 0.08 km/s layer, commencing at a depth of 1.2 km, was derived from good arrivals near Goonyella and Peak Downs, and arrivals from Blackwater. The shot-to-station distance in the south was too great for first arrivals to be recorded from this layer. The

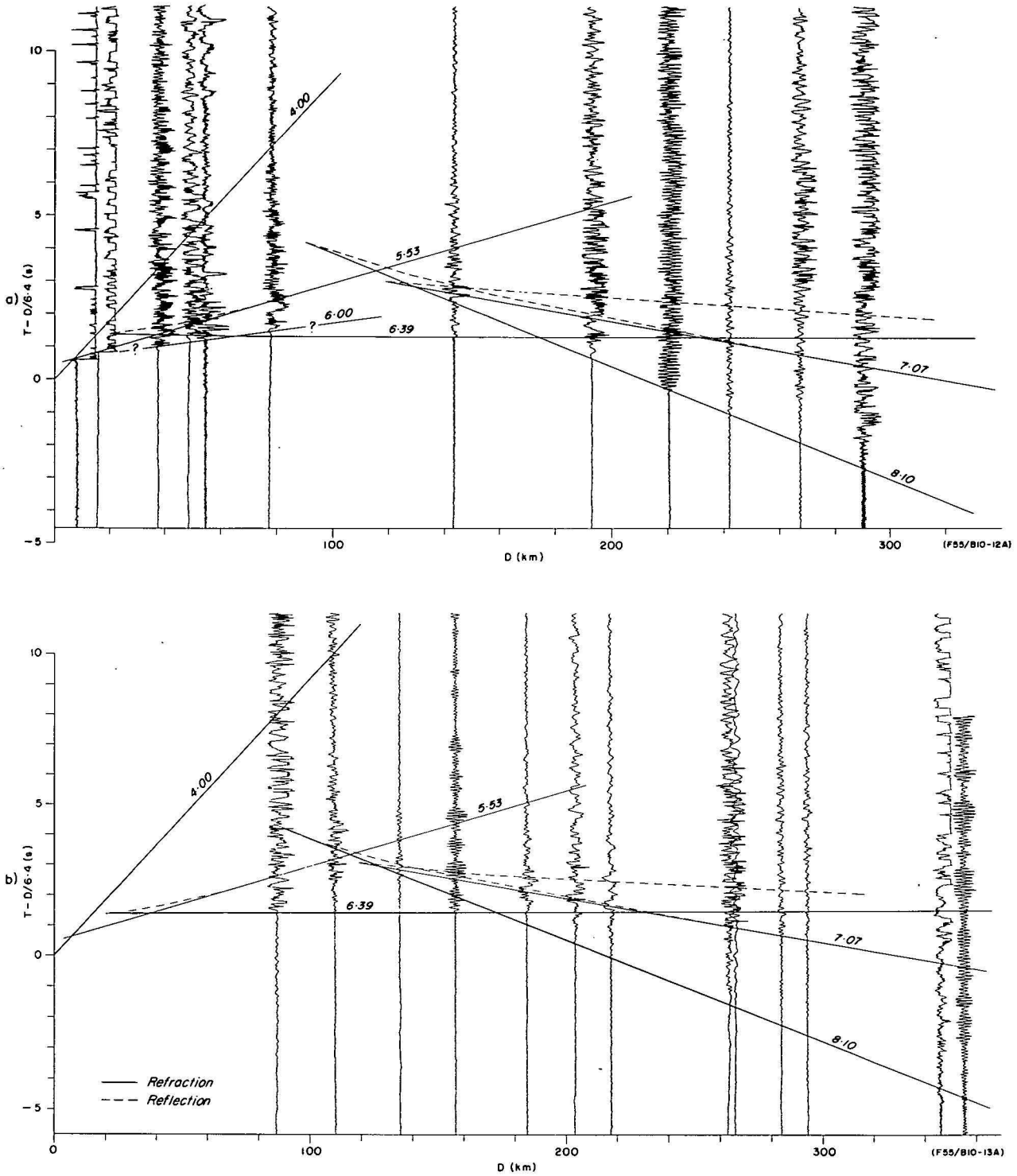

Figure 4. Record sections from shots at (a) Goonyella and Peak Downs and (b) Moura and Kianga.

thickness of the layer is about 5 km under the northern and central parts of the traverse. This agrees with the results of Smith (1951), who found a velocity of 5.49 km/s at a depth of 1.1 km near the axis of the Comet Ridge, and of Robertson (1965), who established a velocity of 5.33 km/s at a depth of 1.2 km between Comet and Dingo. In both cases, the layers dip eastwards, and if continuous, would be deeper under Dingo; however, there is a possible fault zone just west of Dingo, and it may be invalid to extrapolate the structures.

A 6.00 ± .04 km/s layer may be inferred from early arrivals recorded at some stations within 60 km of Goonyella and Peak Downs (Figs. 3a, 4a). However, not all stations within this distance range recorded such arrivals, indicating that the layer has limited extent. A 6.00 km/s layer was reported at a depth of 2.4 km between Comet and Dingo (Robertson, 1965), but does not necessarily occur along the entire refraction traverse. Travel times computed from a model which includes this layer, fit the data from upper crustal layers in the north for northern shots, but are too early

for lower crustal and mantle arrivals at stations in the south. They are also too early for all arrivals from southern shots.

Below this, at a depth of 6.3 km, a 6.39 ± 0.07 km/s layer is well defined from both the northern and southern shots. This is the shallowest layer for which arrivals were recorded from the south (Fig. 3c). Near Dingo, 6.7 km of folded sediments, overlying a basement of igneous rocks or granitised sediments, were found by seismic reflection (Robertson, 1965) and a basement velocity of 6.40 km/s was adopted in that survey.

The model includes a lower crustal layer, with a velocity of 7.07 ± .02 km/s, though this was inferred from the later arrival data only (Fig. 3). The reciprocal time at Moura for these arrivals from the north is 59.08 seconds, and from the south, at Goonyella, is 59.43 seconds. On the basis of similar apparent velocities, intercepts and reciprocal times, these later arrivals were considered to be refracted energy from a relatively thin layer above the Moho. The depth of this layer is 30 km at the centre of the traverse; its thickness increases from 5 km below Peak Downs, to 6 km below Dingo.

The travel-time equation adopted for upper mantle arrivals from shots in the north is

$$T = D/8.07\ (\pm\ 0.09) + 6.86\ (\pm\ 0.33),$$

and from shots in the south is

$$T = D/8.22\ (\pm\ 0.11) + 7.44\ (\pm\ 0.37)$$

where T is the travel time in seconds and D is the shot distance in kilometres.

The depth of the Moho at the centre of the traverse is 36 km, and the mean upper-mantle sub-Moho velocity is 8.13 km/s. Correcting for the earth's curvature (Mereu, 1967) reduces this velocity by about 0.4 percent to 8.10 km/s.

The least squares velocities and intercepts indicate that the Moho dips southwards at 0.7 degrees. However, the apparent velocities are based on limited data (Fig. 3), and they are not significantly different at confidence levels greater than 75 percent. Confirmation of a southward-dipping Moho would require additional, more detailed, field observations.

Strong late arrivals with a velocity of about 4.7 km/s were recorded; this corresponds closely to the velocity expected of upper mantle S-waves.

The crustal model derived here was incorporated in the starting model used by Mills & Fitch (1977) in their surface-wave analysis of the Picton (near Sydney) earthquake of 9 March 1973. The models they finally derived from their analysis gave sub-crustal S-velocities of 4.20-4.32 km/s, which imply unrealistically high Poisson's ratios (0.30-0.32), unless the P-velocity is reduced to 7.6-7.8 km/s. These P-velocities are lower than any found from seismic refraction surveys in eastern Australia. Cleary & Doyle (1962), and Doyle & others (1966) have quoted sub-crustal S-velocities of about 4.7 km/s for southeast Australia; this value agrees with the velocity observed here from the late arrival data, and gives a reasonable value of Poisson's ratio (0.25) for a P-velocity of 8.10 km/s.

Wide-angle reflections were not used in the interpretation because of the difficulty in correlating late arrivals over any appreciable distance. Reflection times calculated from the preferred model could not be matched with any distinct set of recorded arrivals.

Deep vertical reflections were recorded 10 km east of Comet during the Emerald-Duaringa survey (Robertson, 1961, 1965). The arrivals were poor in quality, with two-way travel times between 7.6 and 8.3 seconds. Assuming an average crustal velocity of 6.25 km/s, the depth to the reflector is about 24 to 26 km, which does not correspond to any of the layers derived from the refraction data. The reflections may be from structures associated with the Comet Ridge, and these structures may not extend further east towards the axis of the basin.

Discussion of gravity observations

The observed Bouguer gravity increases along the traverse from an average of $-100\ \mu ms^{-2}$ in the north to about $50\ \mu ms^{-2}$ in the south (Fig. 2). This conflicts with the gravity field computed from the seismic model of Figure 5, for which a southward decrease is expected —up to $700\ \mu ms^{-2}$ if the depths and dips are extrapolated to the ends of the traverse. A possible explanation for this discrepancy is outlined below.

The southern end of the traverse is adjacent to the Auburn Arch, at the eastern edge of the Bowen Basin, where high density rocks may be present at shallower depth. Along the eastern margin of the basin there is an easterly positive gradient of about $220\ \mu ms^{-2}$ per 50 km, which Darby (1966) suggests is due to the hinge line between the Bowen Basin and the axis of central uplift of the Tasman Geosyncline. Superimposed on this regional gradient are the Duaringa gravity highs related to the rise in the pre-Permian basement. The shallowing of basin sediments is also reflected by the interpreted magnetic basement, which rises from deeper than 12 km in the Mimosa Syncline (Fig. 1) to about 4 km along the eastern margin (Wells & Milsom, 1966). Along the traverse, the magnetic basement lies between 6 and 8 km depth below the northern 150 km and between 4 and 5 km beneath the southern 50 km. From well data, the magnetic basement lies at least 1.5 km below the Permo-Triassic sedimentary sequence, and probably represents the Early to Middle Palaeozoic basement. It appears to correspond with the boundary between the 5.33 to 6.39 km/s layer. This is in agreement with the reflection results near Dingo, which give similar depths and velocities to the refraction data. Robertson also recorded a westerly dipping refractor with a velocity of 5.20 km/s at a depth of 0.3 km east of Duaringa, It is therefore apparent, from the magnetic, seismic reflection, and gravity data, that the 5.53 and 6.39 km/s layers shallow in the south, and the dips found from the refraction data should not be extrapolated. Thinning of the sediments could account for the discrepancy between the gravity and seismic refraction data at the southern end of the traverse.

The negative Bouguer gravity in the northern part of the traverse is enhanced by two features described by Darby (1966). The first is the Poitrel gravity low, about 40 km from Goonyella (Fig .2), with an amplitude of about $-200\ \mu ms^{-2}$ which may be due to either an area of increased subsidence, or to a deep-seated low-density plutonic intrusion. However, neither of these explanations is entirely satisfactory; there is seismic reflection evidence against thickening sediments, and it is unusual for large batholiths to occur in areas of subsidence. The second feature, the Mount Roper gravity low, is about 110 km from Goonyella and has an amplitude of about $-50\ \mu ms^{-2}$ where it intersects the traverse. It is possibly due to a pile of acid volcanics north of the Comet Ridge, rather than a thickening of the Permian sediments. Both these features tend

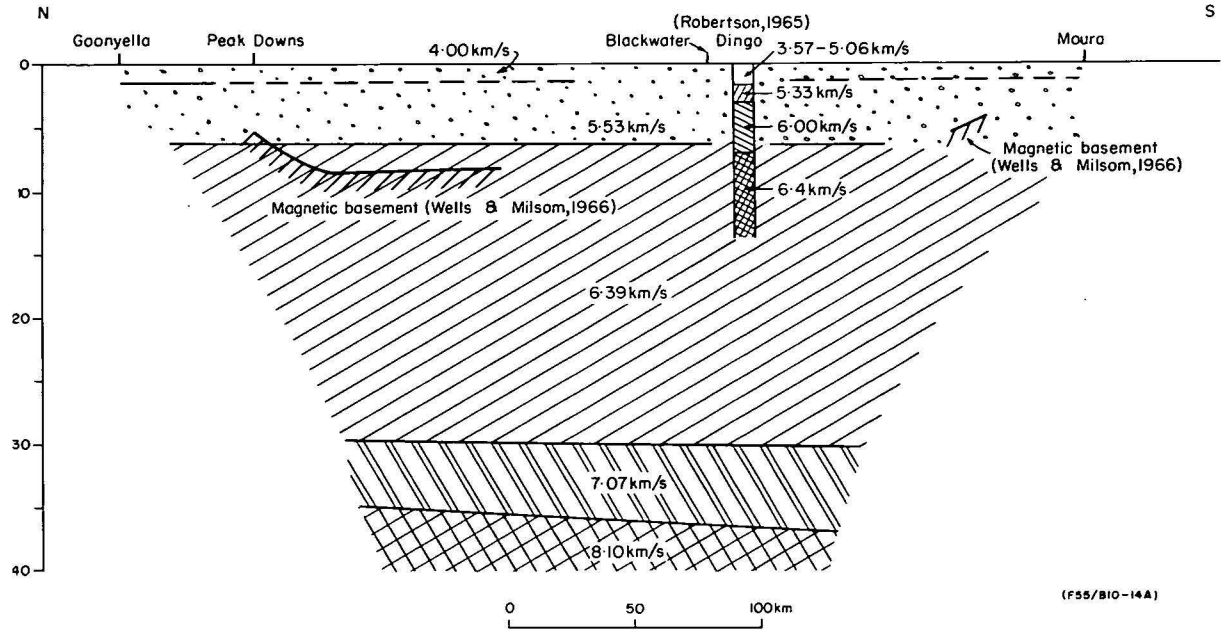

Figure 5. Preferred crustal model of the central Bowen Basin.

to give the observed gravity a negative gradient northwards, which is not caused by a thickening of sediments.

Because of seismic offset distances, the lower crustal and upper mantle interpretation is limited to the central 200 km of the traverse and it may not be valid to extrapolate under the whole traverse length.

Acknowledgements

The author gratefully acknowledges the help and guidance received from J. P. Webb of the University of Queensland who suggested the survey; D. M. Finlayson, J. B. Connelly and B. J. Drummond of the Regional Structural Surveys Group, BMR; and J. W. Cottle (BMR), who assisted with statistical tests. I would also like to thank the management and staff of the Blackwater, Goonyella, Moura, Kianga, and Peak Downs mines for their co-operation, and the many property owners who allowed recording stations to be placed on their properties. The field work for this survey was conducted while the author was a BMR cadet at the University of Queensland. The text figures were drawn by G. Clarke.

References

CLEARY, J. R., & DOYLE, H. A., 1962—Application of a seismograph network and electronic computer in near earthquake studies. *Bulletin of the Seismological Society of America,* **52,** 673-82.

CONNELLY, J. B., & COLLINS, C. D. N., 1973—Bowen Basin Seismic refraction survey, May-June 1973: Operational report. *Bureau of Mineral Resources, Australia—Record* **1973/212** (unpublished).

CULL, J. P., 1973—Seismic ray tracing in a spherical earth using computer models. *Bureau of Mineral Resources, Australia—Record* **1973/122** (unpublished).

CULL, J. P., & RIESZ, E. M., 1972—Deep crustal seismic reflection/refraction survey between Clermont and Charters Towers, Queensland, 1971. *Bureau of Mineral Resources, Australia—Record* **1972/97** (unpublished).

DARBY, F., 1966—North Bowen Basin reconnaissance gravity survey, central Queensland, 1963. *Bureau of Mineral Resources, Australia—Record* **1966/209** (unpublished).

DEPARTMENT OF NATIONAL DEVELOPMENT (CANBERRA), 1966—Geology map sheet and booklet, Fitzroy Region, Queensland. *Resources Series.*

DICKINS, J. M., & MALONE, E. J., 1973—Geology of the Bowen Basin, Queensland. *Bureau of Mineral Resources, Australia—Bulletin* **130.**

DOYLE, H. A., UNDERWOOD, R., & POLAK, E. J., 1966—Seismic velocities from explosions off the Central Coast of New South Wales. *Journal of the Geological Society of Australia,* **13,** 355-72.

FINLAYSON, D. M., 1968—First arrival data from the Carpentaria Region Upper Mantle Project (CRUMP). *Journal of the Geological Society of Australia,* **15,** 33-50.

HAWKINS, L. V., 1961—The reciprocal method of routine shallow seismic refraction investigations. *Geophysics,* **26,** 806-19.

JACK, R. L., 1879—The Bowen River Coalfield. *Publication of the Geological Survey of Queensland,* **4.**

LONSDALE, G. F., 1965—Southern Queensland contract reconnaissance gravity survey using helicopters, 1964. *Bureau of Mineral Resources, Australia—Record* **1965/251** (unpublished).

MEREU, R. F., 1967—Curvature corrections to Upper Mantle Seismic refraction Surveys. *Earth and Planetary Science Letters,* **3,** 469-75.

MILLS, J. M., & FITCH, T. J., 1977—Thrust faulting and crust-upper mantle structure in East Australia. *Geophysical Journal of the Royal Astronomical Society* **48,** 351-84.

ROBERTSON, C. S., 1961—Emerald-Duaringa seismic survey. *Bureau of Mineral Resources, Australia—Record* **1961/150** (unpublished).

ROBERTSON, C. S., 1965—Emerald-Duaringa seismic survey, Queensland, 1960. *Bureau of Mineral Resources, Australia—Record* **1965/2** (unpublished).

SHELL (QLD) DEVELOPMENT PTY LTD, 1952—General report on investigations and operations carried out by the Company in the search for oil in Queensland, 1940-1951. *Geological Survey of Queensland A-P Report* **640** (unpublished).

SMITH, E. R., 1951—Report on seismic refraction traverse at Comet, Queensland. *Bureau of Mineral Resources, Australia—Record* **1951/9** (unpublished).

WELLS, R. R., & MILSOM, J. S., 1966—Bowen Basin aeromagnetic and radiometric survey, Queensland, 1961-1963. *Bureau of Mineral Resources, Australia—Record* **1966/208** (unpublished).

A new nannofossil zone based on the Santonian Gingin Chalk, Perth Basin, Western Australia

Samir Shafik

Studies of the Gingin Chalk have indicated that it is Santonian in age; these studies did not deal with calcareous nannofossils. Santonian biostratigraphy in terms of nannofossils is problematic. The relative ranges of several Upper Cretaceous key nannofossil species, particularly those of the Santonian, are controversial. Precise determination of these ranges hinges on suitable illustration of the species using optical microscopy for successful subsequent identifications.

Light microscopic illustrations of most of the nannofossil species recovered from the Gingin Chalk are presented. Based on several species among the Gingin Chalk assemblages a new Santonian zone, the *Lucianophabdus maleformis* Zone, is proposed. Thus, on the basis of sequential earliest occurrences of several key species, the late Coniacian-early Campanian interval can be subdivided into: the *Marthasterites furcatus*, *Lucianorhabdus maleformis*, and *Broinsonia parca* Zones.

Introduction

The Gingin Chalk (Glauert, 1910) is a lenticular unit of abundantly fossiliferous, fine-grained chalk, less than 20 m thick. It crops out in a series of exposures in the Gingin (Fig. 1) and Dandaragan districts of the Perth Basin in Western Australia.

In the Gingin area, the Gingin Chalk constitutes a middle unit in an apparently paraconformable sequence of three units; the Molecap and Poison Hill Greensands (Fairbridge, 1953) constitute the lower and upper units respectively. Most exposures represent incomplete sections of the Gingin Chalk with the upper and/or lower parts missing; the contacts between the Gingin Chalk and the underlying and overlying units are abrupt (Feldtmann, 1963). However, where the Gingin Chalk is fully represented, the contacts between the chalk, underlying and overlying greensands are gradational, with the basal and upper parts of the Gingin Chalk slightly glauconitic. The sequence has been placed in the Late Cretaceous by many authors (e.g. McWhae & others, 1956).

The Gingin Chalk has attracted a number of Australian workers (e.g. Etheridge, 1913; Chapman, 1917; Withers, 1924, 1926; Spath, 1926; Fedtmann, 1951; Elliott, 1952; Glaessner, 1957; Belford, 1958, 1960; Neale, 1975) with diversified interests. Contributions by these workers are based on a spectrum of fossil groups which does not include calcareous nannofossils, even though Chapman (1917) recorded (in the fine fraction of washed samples) 'flattened shirt-studs', which he referred to as coccoliths.

Two references to the nannofossils of the Gingin Chalk have been noted in the literature: Deflandre (1959) figured a specimen (of *Lucianorhabdus cayeuxi*), and Thierstein (1974, 1976) noted the occurrence of *Kamptnerius magnificus*, *Lucianorhabdus cayeuxi*, *Tetralithus obscurus*, and *T. ovalis* in a sample from the Gingin Chalk.

The main aim of this paper is to assess the biostratigraphy of the Gingin Chalk in terms of nannofossils. This entailed documentation of its nannofossil assemblages, and in the absence of a local nannofossil zonation, a discussion of zonations applicable elsewhere

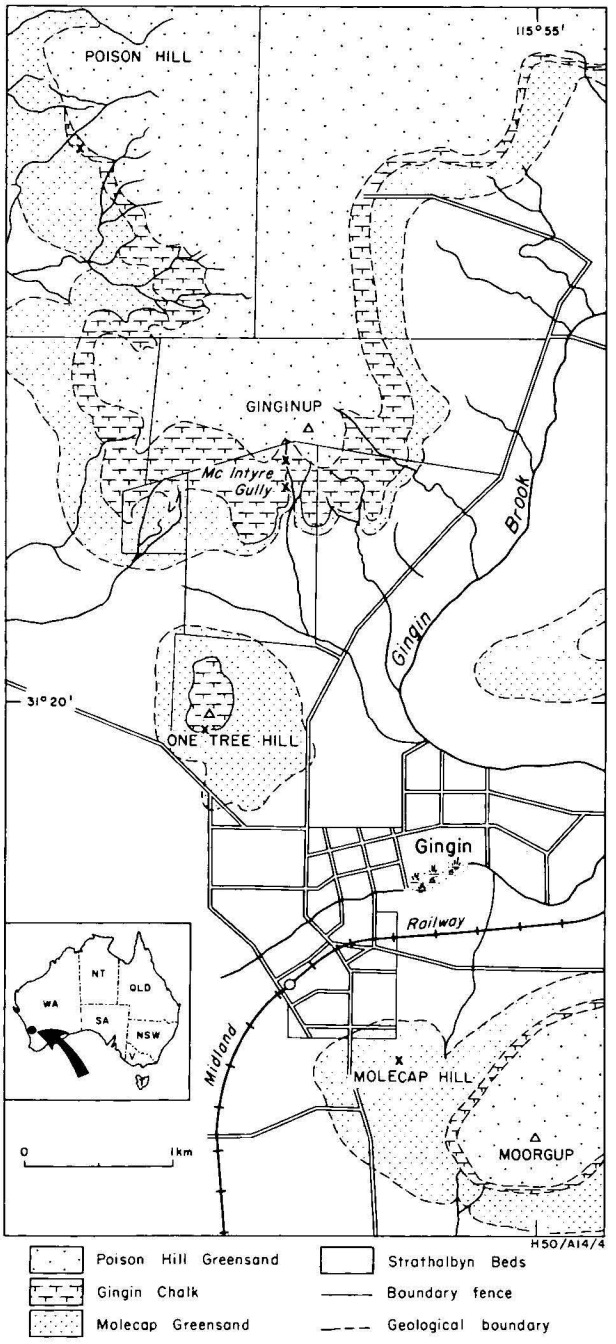

Figure 1. A sketch map of the Gingin area (modified after Feldtmann, 1963); locations of samples are indicated by x.

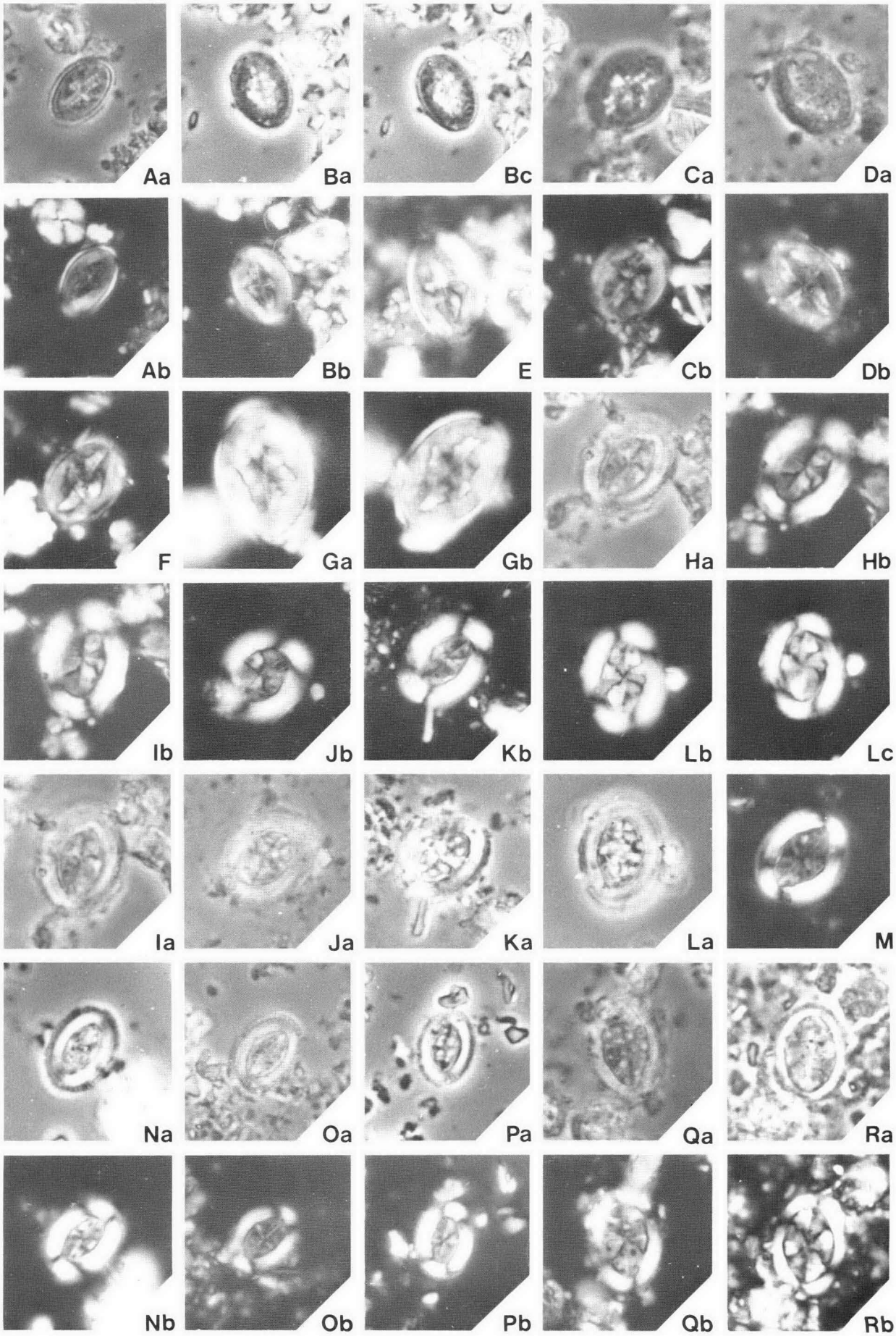
Aa
Ba
Bc
Ca
Da
Ab
Bb
E
Cb
Db
F
Ga
Gb
Ha
Hb
Ib
Jb
Kb
Lb
Lc
Ia
Ja
Ka
La
M
Na
Oa
Pa
Qa
Ra
Nb
Ob
Pb
Qb
Rb

seemed warranted; a new Santonian zone is proposed, and two other (upper Coniacian and lower Campanian) zones are redefined.

Nannofossils of the Gingin Chalk

Material

Material from the Gingin Chalk examined in this study comprises two sets of samples from exposed sections (collected in June, 1971) at Molecap Quarry and a quarry at One Tree Hill, about 100 m SSW of the radio masts; in addition two samples collected from the type section (McIntyre Gully), and one sample from the vicinity of Poison Hill are included in this study. All these localities are in the Gingin area (Fig. 1). Three samples from the underlying Molecap Greensand (at Molecap Quarry) were also available for this study, but they proved to lack calcareous nannofossils.

Nannofossils

Nannofossils are abundant in most of the Gingin Chalk samples. Preservation varies from good to excellent in samples from the Molecap Quarry, and from poor to fair in samples from the quarry at One Tree Hill; preservation generally deteriorates up section at the One Tree Hill Quarry, but a sample from about 10 m above the base of this section yielded nannofossils of excellent preservation. A correlation can be made between the state of preservation of the nannofossils and their diversity in the Gingin Chalk samples. Poor preservation corresponds to less diversified assemblages (e.g. sample at 1.6 m above base of section at One Tree Hill), whereas the highly diversified assemblages (e.g. sample at 1.2 m above base of Gingin Chalk at the Molecap Quarry) are better preserved.

Sixty-five species have been identified using light microscopy, and most of these are illustrated (Figs. 2-7). The distribution of the nannofossil species identified in the material studied is given in Table 1; not included in Table 1 is *Lucianorhabdus arcuatus* Forchheimer, a single specimen of which is found in the sample taken from the creek bed at McIntyre Gully.

The concept adopted herein for *Gartnerago obliquum* (Stradner) (Fig. 2 A-G) is rather wide and includes form referred to several species by other workers (but, see also Roth, 1973, p. 715); this also applies to *Kamptnerius magnificus* Deflandre (Fig. 3 V; Fig. 4 N-R). *Broinsonia enormis* (Shumenko) includes forms with perforated central areas as well as those with imperforate central areas (Fig. 2 H-M). Forms probably referable to *Tranolithus phacelosus* Stover have been included in *Tranolithus exiguus* Stover.

The lower part of the Gingin Chalk (at Molecap Quarry) is characterised by the sporadic occurrence of the cosmopolitan species, *Marthasterites furcatus*, even though the species also occurs at a higher level at One Tree Hill. Many species occur consistently in most (if not all) samples (Table 1). Species which are common to most samples of the Gingin Chalk, also occur in other (coeval) sediments on the western margin of Australia (Toolonga Calcilutite; Shafik, unpublished data). These species include *Ahmuellerella octaradiata, Arkhangelskiella cymbiformis, Biscutum blacki, Broinsonia enormis, B. furtiva, Chiastozygus fessus, Cretarhabdus crenulatus, Cribrosphaera ehrenbergi, Cylindralithus asymmetricus, C. biarcus, C. coronatus, C. serratus, Eiffellithus eximius, E. turriseiffeli, Gartnerago obliquum, Kamptnerius magnificus, Lithraphidites carniolensis, Lucianorhabdus cayeuxi, L. maleformis, Micula staurophora, Prediscosphaera cretacea, P. spinosa, Reinhardtites anthrophorus, R. biperforatus, Tetralithus obscurus, T. ovalis, Vagalapilla imbricata, Watznaueria barnesae* and *Zygodiscus diplogrammus*. Studies by the writer have shown that several of these species are important in the Upper Cretaceous biostratigraphy of the Australian western margin.

The assemblages recovered from the Gingin Chalk (Table 1) resemble in composition those recorded from the Santonian sediments of the nearby Deep Sea Drilling (DSDP) Site 285, Naturaliste Plateau (Thierstein, 1974, Table 6). They differ, however, in the presence of *Braarudosphaera bigelowi, Cribrosphaera ehrenbergi, Lucianorhabdus maleformis, Tetralithus obscurus*, and *T. ovalis* in the Gingin Chalk.

Nannofossil biostratigraphy

In relation to the standard (European) Cretaceous, the age of the Gingin Chalk has long been established as Santonian. This was based on the occurrence of plates of the crinoid genera *Marsupites* and *Uintacrinus* (Withers, 1924, 1926). This early view has been adopted in several subsequent studies (e.g. Feldtmann, 1951; Neale, 1975), and has been supported by other independent evidence. Planktic foraminiferal analyses by Belford (1958, 1960) confirmed the Santonian age for the Gingin Chalk (see also Herb, 1974); neither Belford nor Herb placed the Gingin Chalk in any foraminiferal zonation.

Nannofossil biostratigraphy of the Santonian interval is seemingly difficult; problems are caused primarily by the very small size of most of the forms. This has enticed several workers (e.g., Bukry, 1969) to utilise electron microscopy rather than optical microscopy, even though routine biostratigraphic work is usually carried out by optical methods. Matching species descriptions resulting from the different techniques (i.e., electron and optical microscopies) is, however, difficult (Gartner, 1968), and usually involves some uncertainty. Furthermore, ultrastructures which are important in differentiating various species and subspecies are in most cases discernible only by electron microscopy; these forms may appear similar using light microscopy (Roth & Thierstein, 1972). In addition, a large number of forms are difficult to illustrate using light microscopy; some forms are easier to photograph than others. Most of those species which are difficult to photograph under light microscopy cause problems concerning subsequent identifications by other workers.

These difficulties have hampered establishing precisely the relative ranges of a large number of species.

To date, the few nannofossil studies dealing with the Santonian interval do not permit an adequate under-

Figure 2. (All photographs are x2000.)

As-Gb *Gartnerago obliquum* (Stradner): A = CPC 18224, B = CPC 18225, C = CPC 18226, D = CPC 18227, E = CPC 18228, F = CPC 18229, G = CPC 18230. Ha-M *Broinsonia enormis* (Shumenko); (with central area imperforate in H-I, and perforate in J-M): H = CPC 18231 I = CPC 18232, J = CPC 18233, K = CPC 18234, L = CPC 18235, M = CPC 18236. Na-Pb *Broinsonia furtiva* Bukry: N = CPC 19237, O = CPC 18238, P = CPC 18239. Qa = Rb *Arkhangelskiella cymbiformis* Vekshina: Q = CPC 18240, R = CPC 18241.

Location	Molecap Quarry						Quarry at One-Tree Hill						McIntyre Gully		
Sample level (form base) / Nannofossil species	Base Fm.	0.6 m	1.2 m	1.95 m	2.75 m	3.65 m	Base Section	0.35 m	0.7 m	1.2 m	1.6 m	10.0 m	Creek bed	5.8 m	Poison Hill
Ahmuellerella octaradiata	+	+	+	+	+	+	+	+	+	+		+		+	+
Arkhangelskiella cymbiformis	+	+	+	+	+	+	+		+	+		+	+	+	
Bidiscus cf. *monocavus*				+			+		+	+		+			+
Biscutum blacki	+	+	+	+	+	+	+	+	+	+		+	+	+	+
Biscutum cf. *coronum*	+												+	+	+
Braarudosphaera bigelowi	+	+	+	+			+	+		+				+	
Broinsonia enormis			+		+	+		+		+	+		+	+	+
Broinsonia furtiva	+	+	+	+	+	+		+	+	+			+	+	+
?Broinsonia signata	+	+	+		+	+	+	+	+				+	+	+
Chiastozygus fessus	+	+	+	+	+	+	+	+	+	+		+	+	+	+
Chiastozygus litterarius			+				+			+					
Chiastozygus aff. *litterarius*					+				+					+	+
Chiastozygus plicatus		+	+	+	+	+	+						+	+	
Chiastozygus synquadriperforatus													+	+	
Corollithion achlyosum		+	+				+	+							
Corollithion rombicum												+			
Corollithion signum												+			
Cretarhabdus conicus	+	+	+	+	+		+		+	+		+			
Cretarhabdus crenulatus		+	+	+	+	+	+	+	+	+		+	+	+	
Cribrosphaera ehrenbergi	+	+	+	+	+	+	+	+				+	+	+	+
Cyclagelosphaera margereli													+		
Cylindralithus asymmetricus													+		
Cylindralithus biarcus														+	
Cylindralithus coronatus	+				+		+	+	+						
Cylindralithus serratus	+	+	+	+	+					+					
Eiffellithus eximius	+	+	+	+	+	+	+	+	+	+	+	+	+	+	+
Eiffellithus aff. *eximius*	+	+	+	+	+	+			+	+			+	+	+
Eiffellithus turriseiffeli	+	+	+	+	+	+	+	+	+	+		+	+	+	+
Gartnerago obliquum	+	+	+	+	+	+	+	+	+			+	+	+	+
Kamptnerius magnificus	+	+	+	+	+	+	+	+	+	+	+	+	+	+	+
Lapideacassis mariae			+												
Lithraphidites carniolensis	+	+	+	+	+		+	+	+	+	+	+	+	+	
Lithraphidites helicoides	+	+	+	+	+				+	+	?		+		+
Lithrastrinus floralis					+			+							
Lucianorhabdus cayeuxi	+	+	+	+	+	+	+	+	+	+	+	+	+	+	+
Lucianorhabdus maleformis	+		+	+	+	+	+	+					+		
Manivitella pemmatoidea	+								+						+
Marthasterites furcatus	+	+	+		+				+						
Marthasterites inconspicuus					+	+	+								
Microrhabdulus decoratus	+	+	+		+		+	+	+					+	
Micula staurophora	+	+	+	+	+	+	+	+	+	+		+	+	+	+
Parhabdolithus angustus		+	+	+			+	+		+			+		
Prediscosphaera cretacea	+	+	+	+	+	+	+	+	+	+	+	+	+	+	+
Prediscosphaera spinosa	+	+	+	+	+		+		+	+			+	+	+
Reinhardtites anthrophorus	+	+	+	+	+		+	+	+	+		+	+		
Reinhardtites aff. *anthrophorus*	+	+				+	+		+				+	+	+
Reinhardtites biperforatus	+	+	+	+	+	+	+		+	+			+	+	+
Scapholithus fossilis			+	+		+	+								
Sollasites horticus		+													
Stephanolithion laffittei		+	+	+	+				+				+		
Tetralithus obscurus		+	+	+	+	+	+	+	+	+		+	+		
Tetralithus ovalis		+	+	+	+	+	+	+	+	+			+	+	+
Tetralithus sp. 1		+	+												
Tetralithus sp. 2					+										+
Tranolithus exiguus	+	+	+		+	+	+		+				+	+	+
Tranolithus sp.							+		+						
?Vagalapilla cf. *dorfii*		+	+	+	+		+		+	+			+	+	+
Vagalapilla imbricata		+		+	+	+	+	+	+	+		+	+	+	+
Watznaueria barnesae	+	+	+	+	+	+	+	+	+	+	+	+	+	+	+
Zygodiscus diplogrammus	+	+	+		+		+	+	+			+	+	+	+
Zygodiscus cf. *pseudanthrophorus*	+	+		+	+			+	+				+	+	
Zygodiscus cf. *sigmoides*	+	+	+		+				+	+			+		+
Zygodiscus spiralis	+	+					+	+	+	+			+	+	
Zygodiscus theca					+			+	?						

Table 1. Distribution of calcareous nannofossil species in the Gingin Chalk samples.

standing of the rates of species evolution and extinction during the interval. The effects of selective dissolution and provincialism (e.g. elimination of certain species from a specific area) are, however, better understood.

A brief review of some of the nannofossil biostratigraphic schemes which have been proposed for the Coniacian-Campanian interval may help in evaluating the various points discussed above.

Problems of Coniacian-Campanian nannofossil biostratigraphy

Rates of evolution and extinction

Stradner (1963) recognised several nannofossil associations for the Cretaceous. Although the state of knowledge in the early sixties was rather modest, Stradner's associations can be considered collectively as a good indication of the nannoplankton temporal changes which occurred during the Cretaceous. The Coniacian-Santonian interval could not be characterised by a specific association, in contrast with the Campanian (*Gothicus*-associations) and the Turonian (*Staurophorus*-associations). This suggests lack of profound changes in the large and easily identifiable species by means of light microscopy among the Coniacian-Santonian assemblages, and probable slow rates of evolution and/or extinction for these species during this interval.

Electron vs light microscopic illustrations

Bukry (1969) proposed a zonation, based on species described solely from electron microscopy, for the Santonian-Campanian sequence of Texas. This zonation has only rarely been applied to other sections. Because light microscopy is the most practical means for routine biostratigraphic work, the limited use of Bukry's zonation may be taken as an indication of the difficulties of light microscopic recognition of forms originally described by electron microscopy. Roth & Thierstein (1972) indicated that some Cretaceous forms cannot be differentiated by light microscopy. For example, they considered that the differentiation between *Staurolithites matalosus* (Stover) Čepek & Hay, *Broinsonia signata* (Nöel) Nöel, and *B. dentata* Bukry using light microscopy is impossible; this was substantiated by light and electron microscopic illustrations of the same specimens.

Relative ranges of species

Čepek & Hay (1969) introduced a nannofossil zonation for the Upper Cretaceous sequence of Alabama (USA), and mainly used the species easily identifiable by light microscopy. However, correlations with Upper Cretaceous sections studied by other workers (e.g. Gartner, 1968; Bukry, 1969) indicate that the sequence of events presented by Čepek & Hay is partly out of order; the relative ranges of some of their key species are controversial. According to the correlation made by *Gartner* (*in* Cita & Gartner, 1971) the earliest occurrences of *Marthasterites furcatus, Arkhangelskiella ethmopora, Kamptnerius punctatus,* and *K. magnificus* in the zonation of Čepek & Hay (1969) are of Santonian to Campanian age (see also correlation by Smith, 1975, which suggests a Campanian age for all these events). *K. punctatus* Stradner and *K. magnificus* Deflandre are known to occur in older sediments (Turonian: Stradner, 1963; Manivit, 1968; Bukry, 1969; Čepek, 1970. Coniacian: Gartner, 1968; see also Stover, 1966; discussions by Thierstein, 1971, p. 41; 1974, p. 640. Santonian: Manivit (1971); *K. punctatus* Stradner is regarded, however, as a junior synonym of *K. magnificus* Deflandre in the present study (see also Thierstein, 1974).

In his discussion of the calcareous nannofossil assemblages of the various stages of the Upper Cretaceous of northwest Germany, Čepek (1970) indicated that the upper Coniacian and lower Santonian cannot be differentiated, but pointed out that the upper Santonian is characterised by the occurrence of *Kamptnerius pseudopunctatus* Čepek (= *K. magnificus* Deflandre) and *Discolithus octacentralis* Stover (junior synonym of *Gartnerago obliquum* (Stradner) Reinhardt. However, *K. magnificus* and *G. obliquum* are known to occur in Turonian sediments (see Roth & Thierstein, 1972; and references cited above).

Correlation between the nannofossil and planktic foraminiferal zones recognised in a section of the upper Helvetic nappes of Eastern Switzerland (Thierstein, 1971) indicates that the lowest appearance of *Marthasterites furcatus* is at the base of the upper Santonian or high in the lower Santonian. *M. furcatus* occurs first in Coniacian sediments as has been reported by many authors (e.g. Gartner, 1968; Čepek, 1970; Roth, 1973), though Stradner (1963) regarded the species as ranging from upper Turonian to Campanian.

Provincialism and selective dissolution

Roth (1973) proposed two zones for the Coniacian-Santonian (oceanic) sediments of the central Pacific: the *Marthasterites furcatus,* and the *Gartnerago obliquum* Zones. The latter is a gap zone relying on the absence of two species: *Marthasterites furcatus* (below) and *Broinsonia parca* (above). The lack of biostratigraphic criteria (gap zone) supports an earlier suggestion regarding the rate of evolution and extinction being slow and/or difficult to resolve for the Santonian taxa, particularly those forms which are easily recognisable by light microscopy. The other zone (*M. furcatus* Zone) is defined by the total range of the name species (Roth, 1973). Previously, Čepek & Hay (1969) introduced a zone of the same name for hemipelagic sections in Alabama, but defined it by the interval from the first occurrence of *M. furcatus* (base) to the first occurrence of *Arkhangelskiella ethmopora* Bukry (top). *A. ethmopora* is absent from deep oceanic sediments (Roth, 1973) probably because of either its susceptibility to solution or to unfavourable ecological conditions. Such an interpretation matches the several cases of selective dissolution and provincial distribution among many Upper Cretaceous species which have been recorded by several workers. Species of the genera *Braarudosphaera, Kamptnerius, Lucianorhabdus,* and *Tetralithus* are absent or rarely occur in deep oceanic sediments, but are common in shallow hemipelagic sediments. This is probably because these species are largely susceptible to dissolution in deep water. The relative geographic distribution of *Nephrolithus frequens* Gorka and *Micula mura* (Martini) Bukry in coeval upper Maastrichtian sediments in various parts of the world is a well-quoted example of provincialism among Upper Cretaceous species: *N. frequens* has a bipolar distribution (Worsely & Martini, 1970; Gartner, 1974), and *M. mura* is restricted to low-latitude sediments (Worsely & Martini, 1970; Shafik & Stradner, 1971), but see Perch-Nielsen (1977). In high latitude Upper Cretaceous (including Santonian) sediments, Bukry (1973) pointed out the absence of the usually

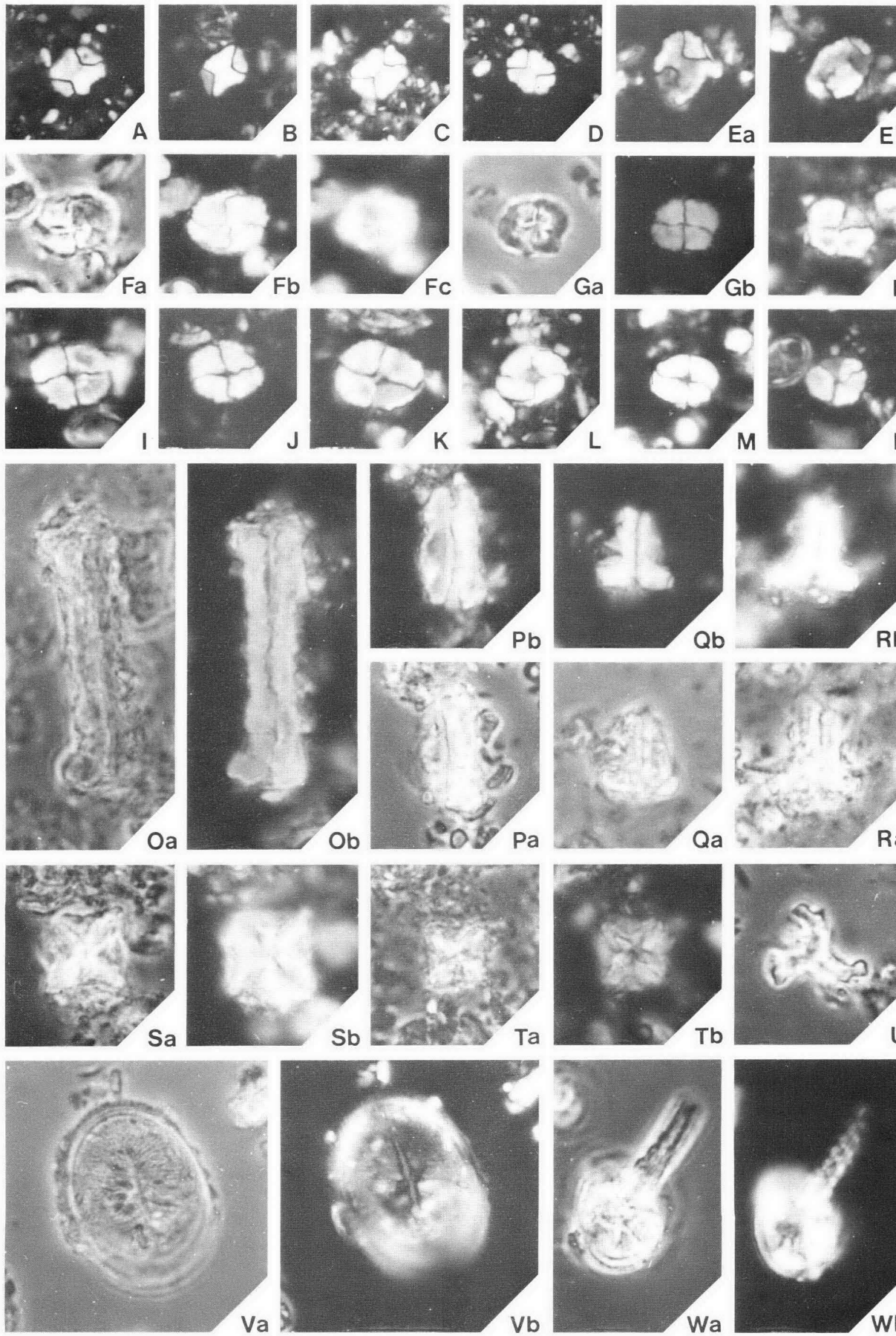
A
B
C
D
Ea
Eb
Fa
Fb
Fc
Ga
Gb
H
I
J
K
L
M
N
Oa
Ob
Pb
Qb
Rb
Pa
Qa
Ra
Sa
Sb
Ta
Tb
U
Va
Vb
Wa
Wb

common, long-ranging *Watznaueria barnesae* (Black) Perch-Nielson. This species is highly resistant to dissolution and strong diagenesis, and its absence from high-latitude sediments must be regarded as an exclusion in response to low temperatures.

Criteria for species recognition

Recently, Lauer (1975) proposed four informal zones for the upper Santonian-upper Campanian Fiqa Formation of Central Oman, southeast Arabia. These zones are based on three separate evolutionary lineages which are manifested by three genera of the family Arkhangelskiellaceae: *Aspidolithus* Noël (junior synonym of *Broinsonia* Bukry), *Arkhangelskiella* Vekshina, and *Gartnerago* Bukry. Lauer claimed that recognition of the several morphotypes constituting the evolutionary lineages is possible by means of optical microscopy, but did not present sufficient criteria for distinguishing his species.

Biostratigraphy of the Gingin Chalk

No local Cretaceous nannofossil zonation has been formalised to date, and zonations currently applied elsewhere seem unsatisfactory. Current Santonian zones either rely on presence of species which possibly range into older sediments (e.g. Čepek & Hay, 1969) or which are difficult to identify using light microscopy (e.g. Bukry, 1969), or are based on negative evidence (e.g. Roth, 1973).

Several workers (e.g. Bukry, 1974; Shafik, 1975) have adopted the two zones which were proposed by Roth (1973) for the Santonian (and Coniacian). As mentioned above, the Santonian *Gartnerago obliquum* Zone (Roth, 1973) is a gap zone, bracketed by the last appearance of *Marthasterites furcatus* (below) and the first appearance of *Broinsonia parca* (above). These species, however, have been found co-occurring in Campanian sediments in Texas (Bukry, 1969) and in the Carnarvon Basin of Western Australia (Shafik, unpublished data). Although such an overlap in their ranges may be local (e.g., resulting from displacement), it is generally accepted that biostratigraphic evidence based on extinction is usually tenuous and often involves some doubt regarding possible reworking: criteria based on earliest occurrences of distinct species are widely considered as more reliable. For this reason, a new zone, the *Lucianorhabdus maleformis* Zone, is proposed herein to substitute the Santonian part of the *Marthasterites furcatus* Zone and *Gartnerago obliquum* Zone (both of Roth, 1973).

Lucianorhabdus maleformis Zone

The base of this zone is defined by the earliest occurrence of *Lucianorhabdus cayeuxi* Deflandre, *L. maleformis* Reinhardt, *Tetralithus obscurus* Deflandre and *T. ovalis* Stradner, and its top is defined by the earliest occurrence of *Broinsonia parca* (Stradner) prior to the earliest occurrence of *Tetralithus aculeus* (Stradner). The age of this zone is Santonian. Sissingh (1977) proposed a zone with the same name for the interval between the first occurrences of *Lucianorhabdus maleformis* (base of the zone) and *Marthasterites funcatus* (top of the zone). He indicated that his zone is late Turonian to early Coniacian in age. Because Sissingh (1977) did not illustrate *Lucianorhabdus maleformis* Reinhardt, his concept of this species could not be tested adequately; his *L. maleformis* Zone cannot be related to the *L. maleformis* Zone of the present study (see also below).

Important species common in the *Lucianorhabdus maleformis* Zone of the present study include *Broinsonia furtiva* Bukry, *B. enormis* (Shumenko), *Cylindralithus asymmetricus* Bukry, *C. biarcus* Bukry, *C. coronatus* Bukry, *C. serratus* Bramlette & Martini, *Kamptnerius magnificus* Deflandre, and *Reinhardtites anthrophorus* (Deflandre). The zone is based essentially on the Gingin Chalk assemblages (Table 1); species employed are either large forms (e.g. *Lucianorhabdus cayeuxi*) or exceptionally distinct small forms (e.g. *Tetralithus obscurus*); all are easily identifiable under light microscopy. These species, however, though common in shelf sediments (Gingin Chalk); Toolonga Calcilutite, see below), are possibly absent or rarely appearing in coeval oceanic sediments. This suggests some limitations on the use of the zone.

Lack of material transitional between the *L. maleformis* Zone of the present study and the subjacent *Marthasterites furcatus* Zone (redefined below) hampers refining the definition of the boundary separating them. Locally, criteria defining this boundary are satisfactory, but elsewhere this may not be the case because it is not expected that the earliest occurrences of several species (*Lucianorhabdus maleformis, L. cayeuxi, Tetralithus obscurus* and *T. ovalis*) will be at the same level particularly in continuous sections with high rates of deposition. Wind (1975, p. 353) demonstrated, however, that *Lucianorhabdus cayeuxi* and *Tetralithus obscurus* or *T. ovalis* are probably end members of 'two continuous and parallel morphological series'. Nevertheless, he placed *Lucianorhabdus maleformis* in synonymy with *L. cayeuxi*. Although Wind (1975) did not allude to it, it seems possible from his paper to conclude that *Lucianorhabdus cayeuxi, L. maleformis, Tetralithus obscurus* and *T. ovalis* are collectively one species; a conclusion which is worth further investigation, but is beyond the scope of the present paper.

Correlation. Calcareous nannofossil assemblages from the lower parts of the Toolonga Calcilutite (in the southern Carnarvon Basin, Western Australia) are identified as belonging to the *Lucianorhabdus maleformis* Zone of the present study (Shafik, unpublished data), and therefore equate with the Gingin Chalk; foraminiferal evidence presented by Belford (1958, 1960) is consistent with this conclusion.

It seems possible that the *Lucianorhabdus maleformis* Zone of the present study can be correlated (though with some reservation; see remarks below) with other nannofossil zones which have been applied to sediments elsewhere (Table 2). The *L. maleformis* Zone of the present study may be correlated tentatively with

Figure 3. (All photographs are x2000.)

A-Eb *Tetralithus obscurus* Deflandre: A = CPC 18242, B = CPC 18243, C = CPC 18244, D = CPC 18245, E = CPC 18246. Fa-M *Tetralithus ovalis* Stradner: F = CPC 18247, G = CPC 18248, H = CPC 18249, I = CPC 18250, J = CPC 18251, K = CPC 18252, L = CPC 18253, M = CPC 18254. N *Tetralithus* sp. 1 CPC 18255. Oa-Pb *Lucianorhabdus caveuxi* Deflandre: O = CPC 18256, P = CPC 18257. Qb-Ra *Lucianorhabdus maleformis* Reinhardt: Q = CPC 18258, R = CPC 18259. Sa-Tb *Micula staurophora* (Gardet): S = CPC 18260, T = CPC 18261. U = *Marthasterites furcatus* (Deflandre) CPC 18262. Va-Vb *Kamptnerius magnificus* Deflandre CPC 18263 (= *K. magnificus sculptus* Bukry). Wa-Wb *Eiffellithus turriseiffeli* (Deflandre) CPC 18264.

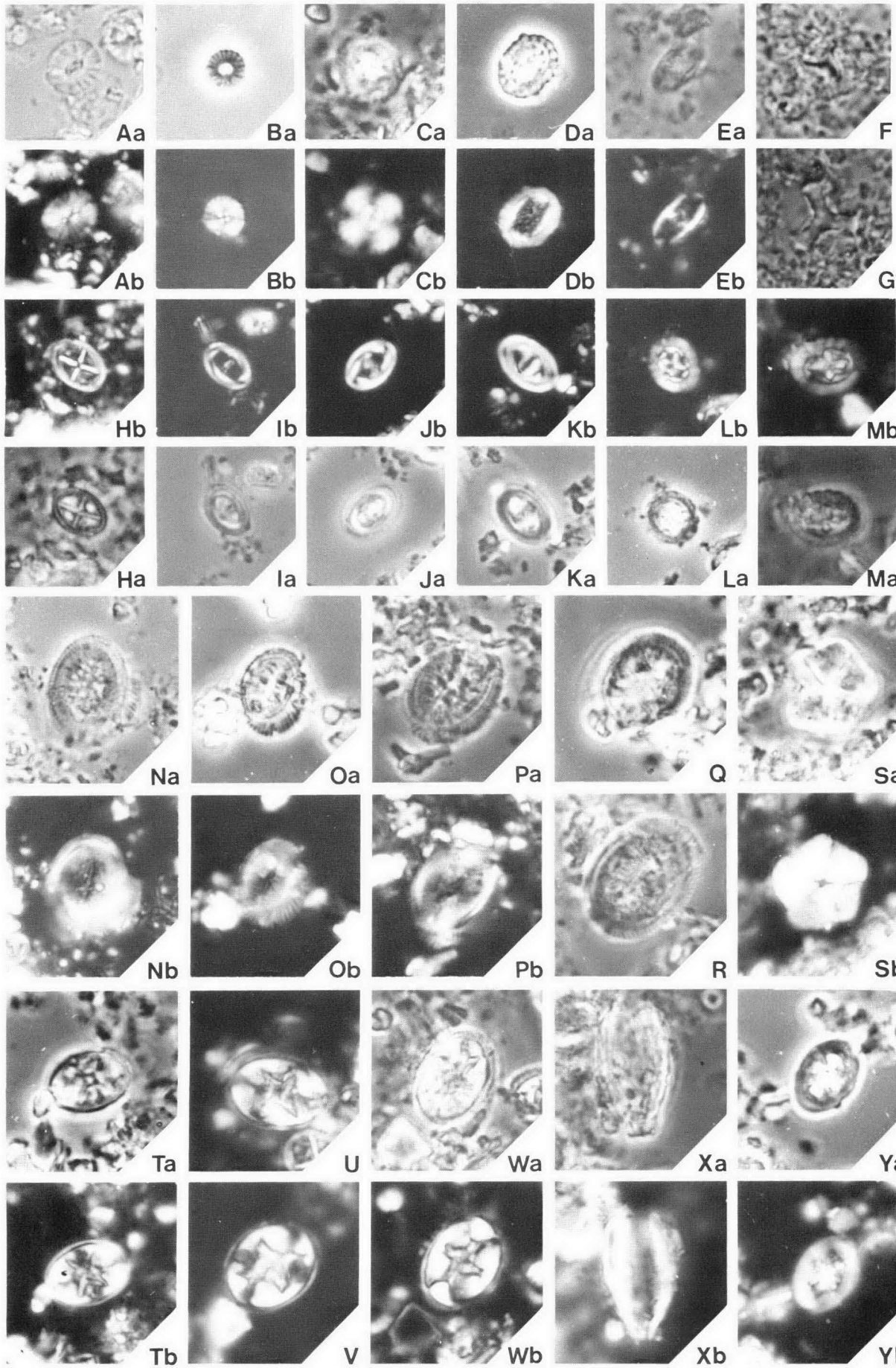
Aa
Ba
Ca
Da
Ea
F
Ab
Bb
Cb
Db
Eb
G
Hb
Ib
Jb
Kb
Lb
Mb
Ha
Ia
Ja
Ka
La
Ma
Na
Oa
Pa
Q
Sa
Nb
Ob
Pb
R
Sb
Ta
U
Wa
Xa
Ya
Tb
V
Wb
Xb
Yb

Zones by / AGE	Shafik, present study	Sissingh, 1977	Roth, 1973	Manivit, 1971	Čepek & Hay, 1969 (F)
CAMPANIAN (in part)	*Broinsonia parca*	*Calculites ovalis* — — — (A) — — — *Aspidolithus parcus*	*Eiffellithus eximius (in part)*	*Arkhangelskiella specillata* — (C) —	
SANTONIAN	*Lucianorhabdus maleformis*	*Calculites obscurus* (B) — — — — — — — — *Lucianorhabdus cayeuxii* — — — — — — — — *Reinhardtites anthrophorus*	*Gartnerago obliquum* — — — (A) — — — *Marthasterites furcatus*	*Kamptnerius magnificus* (D)	*Kamptnerius magnificus* (D)
CONIACIAN (in part)	*Marthasterites furcatus*	*Micula staurophora* — — — — — — — — *Marthasterites furcatus*		*Marthasterites furcatus*	*Kamptnerius punctatus* (E) — — — — — — — — *Arkhangelskiella ethmopora* — — — — — — — — *Marthasterites furcatus*

(A) the boundary is based on extinction of *M. furcatus* (Deflandre) (see text); other boundaries are based on earliest occurrences.

(B) this zone is Campanian in age according to its proposer; its base is tentatively placed.

(C) definitions of base *A. specillata* Zone and top *K. magnificus* Zone are based on different criteria (see Manivit, 1971).

(D) *Tetralithus obscurus* Deflandre occurs in this zone.

(E) these three zones are shown by Čepek & Hay (1969, Fig. 4) to contain *L. cayeuxi* (Deflandre), *Tetralithus ovalis* Stradner and *B. parca* (Stradner) (see text).

(F) according to Smith (1975) zones shown here are Campanian in age.

H50/A14/5

Table 2. Correlation of late Coniacian-early Campanian nannofossil zones. (Solid lines signify good correlation; broken lines suggest tentative correlation; short broken lines indicate very doubtful correlation.)

the *Kamptnerius magnificus* Zone of Čepek & Hay (1969) based on the common occurrence of *Tetralithus obscurus* in both zones. Similarly, it can be correlated with the *Kamptnerius magnificus* Zone of Manivit (1971); both zones contain *Tetralithus obscurus* and lack *Broinsonia parca*. (The upper part of the *Marthasterites furcatus* Zone together with the *Gartnerago obliquum* Zone as proposed by Roth (1973) are equivalent to the *L. maleformis* Zone of the present study.)

Recently, Sissingh (1977) described 26 nannofossil zones spanning the entire Cretaceous. His *Lucianorhabdus cayeuxii* and *Calculites obscurus* Zones (Santonian-Campanian) are bracketed by the first occurrences of *Lucianorhabdus cayeuxi* (at the base of his *L. cayeuxii* Zone) and *Broinsonia parca* (reported as *Aspidolithus parcus*) (above), and accordingly, these two zones combined can be correlated with the *Lucianorhabdus maleformis* Zone of the present study. However, *Reinhardtites anthrophorus* (index species for Sissingh's *Reinhardtites anthrophorus* Zone) appears with *L. cayeuxi* at the base of the Gingin Chalk (Table 1, i.e. *L. maleformis* Zone) and correlation of the *L. maleformis* of the present study may be extended to include the *R. anthrophorus* Zone of Sissingh (1977) (Table 2).

Sissingh (1977) differentiated between his *Lucianorhabdus cayeuxii* and *Calculites obscurus* Zones by the 'regular' occurrence in the latter of *Tetralithus obscurus* (reported as *Calculites obscurus*). *T. obscurus* occurs regularly in the Gingin Chalk, and accordingly, the formation can be placed in the *Calculites obscurus* Zone of Sissingh (1977). This zone is early Campanian in age, according to its proposer, but such an age assignment for the Gingin Chalk is negated by evidence from other fossil groups (crinoids: Withers, 1924, 1926; foraminiferids: Belford, 1958, 1960; Herb, 1974).

Remarks

Čepek & Hay (1969) did not relate their zones to the European stages nor to other biostratigraphic zones,

Figure 4. (All photographs are x2000.)

Aa-Ab *Biscutum blacki* Gartner CPC 18265. Ba-Bb *Bidiscus* sp. cf. *B. monocavus* Bukry CPC 18266. Ca-Cb *Cyclagelosphaera margereli* Noël CPC 18267. Da-Db *Cribrosphaera ehrenbergi* Arkhangelsky CPC 18268. Ea-Eb *Parhabdolithus angustus* (Stradner) CPC 18269. F *Marthasterites inconspicuus* Deflandre CPC 18270. G *Marthasterites furcatus* (Deflandre) CPC 18271. Ha-Hb *?Vagalapilla* sp. cf. *V. dorfii* Bukry CPC 18272. Ib-Ja *Zygodiscus spiralis* Bramlette & Martini: I = CPC 18273, J = CPC 18274. Kb-Ka *Zygodiscus diplogrammus* (Deflandre) CPC 18275. Lb-La *Prediscosphaera cretacea* (Arkhangelsky) CPC 18276. Mb-Ma *Prediscosphaera spinosa* (Bramlette & Martini) CPC 18277. Na-R *Kamptnerius magnificus* Deflandre: N = CPC 18278, O = CPC 18279, P = CPC 18280, Q = CPC 18281, R = CPC 18282. Sa-Sb *Braarudosphaera bigelowi* (Gran & Braarud) CPC 18283. Ta-U *Eiffelithus turriseiffeli* (Deflandre): T = CPC 18284, U = CPC 18285. V *Eiffellithus* sp. aff. *E. eximius* (Stover) CPC 18286. Wa-Wb *Eiffellithus eximius* (Stover) CPC 18287. Xa-Xb *Lapideacassis mariae* Black CPC 18288. Ya-Yb *Chiastozygus fessus* (Stover) CPC 18289.

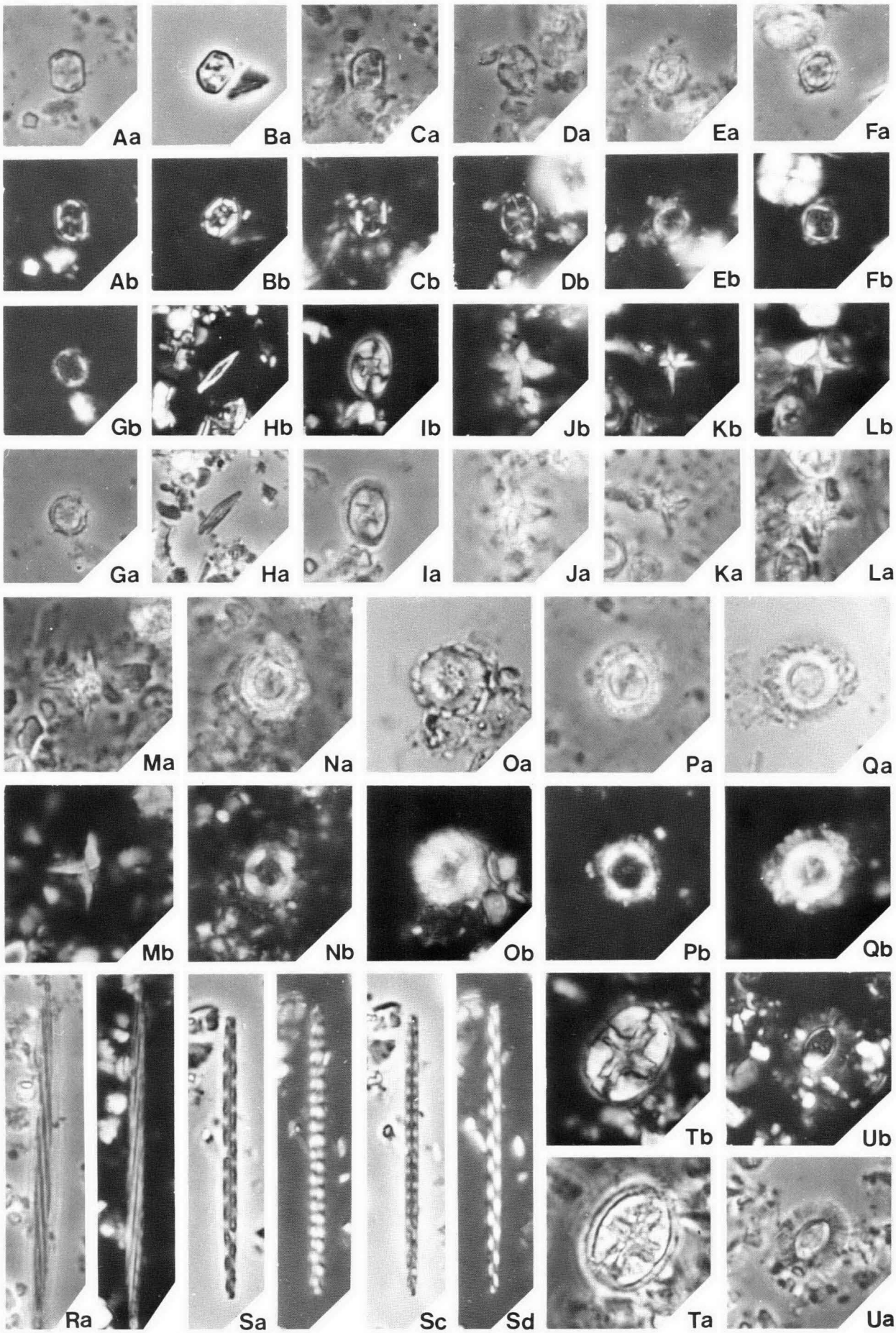
Aa
Ba
Ca
Da
Ea
Fa
Ab
Bb
Cb
Db
Eb
Fb
Gb
Hb
Ib
Jb
Kb
Lb
Ga
Ha
Ia
Ja
Ka
La
Ma
Na
Oa
Pa
Qa
Mb
Nb
Ob
Pb
Qb
Ra
Sa
Sc
Sd
Tb
Ub
Ta
Ua

apart from some references to the zones proposed by Bukry (1969). Gartner (*in* Cita & Gartner, 1971), and Smith (1975) attempted to relate the zones which were proposed by Čepek & Hay (1969) to the European stages: Gartner assigned the lower part of the *Arkhangelskiella ethmopora* Zone and the underlying *Marthasterites furcatus* Zone to the Santonian, whereas Smith advocated a stratigraphic gap, representing the interval from the middle Turonian through to the early Campanian within the *Tetralithus pyramidus* Zone, which underlies the *M. furcatus* Zone in Čepek & Hay's scheme. In the light of the current usages of both *Tetralithus pyramidus* and *Marthasterites furcatus* Zones by several workers, the age assignments made by Gartner for Čepek & Hay's zones seem satisfactory. However, the range given for *Broinsonia parca* (*Arkhangelskiella parca* in Čepek & Hay, 1969, fig. 4, extending down to the upper part of the *T. pyramidus* Zone) supports the argument presented by Smith (1975), that the upper part of *T. pyramidus* Zone (in Čepek & Hay, 1969) is early Campanian in age, because the earliest occurrence of *B. parca* is assigned to the early Campanian by many workers (see also below). Furthermore, some of the species which have been used as biostratigraphic markers for the Santonian (e.g. *Lucianorhabdus cayeuxi, Tetralithus ovalis*) first appear at the same level as *Broinsonia parca* in Figure 4 of Čepek & Hay (1969).

The Santonian *Kamptnerius magnificus* Zone of Manivit (1971) is based on the vertical range of the name species prior to the earliest occurrence of *Broinsonia parca. K. magnificus* Deflandre (considered here to include *K. pseudopunctatus* Čepek, *K. punctatus* Stradner, and *K. magnificus sculptus* Bukry) has been reported occurring in Turonian sediments by several workers (see above). Furthermore, *K. magnificus* is not as common as species of *Lucianorhabdus* and *Tetralithus* in the Santonian sediments of Western Australia, even though it is consistently present in the Gingin Chalk. However, according to Manivit (1971, Tables 8, 9) *Tetralithus obscurus* first appears at the base of the Santonian, her *Kamptnerius magnificus* Zone.

Other than the earliest occurrence of *Lucianorhabdus cayeuxi,* criteria used to define the base of the *Lucianorhabdus maleformis* Zone of the present study have also been used by Sissingh (1977), but at various stratigraphic levels. He used the 'first regular occurrence' of *Tetralithus ovalis* (reported as *Calculites ovalis*) as additional evidence for the recognition of the base of his *Microrhabdus decoratus* Zone which he assigned to the late Cenomanian. The base of his *Lucianorhabdus maleformis* Zone is defined by the first occurrence of the name species, which he regarded as Turonian in age, and the base of his (Campanian) *Calculites obscurus* Zone is defined by the first occurrence of the nominate species (=*Tetralithus obscurus*). Evidence for these data is a section (Dyr el Kef) in Tunisia (Sissingh, 1977, fig. 9). However, other sections studied by Sissingh (1977, fig. 10), which include the stratotypes of the Cenomanian, Turonian and Coniacian, do not contain *Lucianorhabdus maleformis* or *Tetralithus ovalis*—even though these species together with *Tetralithus obscurus* do occur in his younger samples (stratotypes of Santonian and Senonian).

The introduction of the *Lucianorhabdus maleformis* Zone as defined in the present study necessitates redefining the *Marthasterites furcatus* Zone of Roth (1973) and defining an early Campanian zone, the *Broinsonia parca* Zone (Table 2).

Marthasterites furcatus Zone. The base of this zone is defined by the earliest occurrence of *Marthasterites furcatus* (Deflandre), and its top is defined by the earliest occurrence of *Lucianorhabdus cayeuxi* Deflandre, *L. maleformis* Reinhardt, *Tetralithus obscurus* Deflandre and *T. ovalis* Stradner.

The age of the *Marthasterites furcatus* Zone (as redefined here) is considered as late Coniacian. Evidence for this is based on the results of Manivit (1971) who indicated that the earliest occurrence of *M. furcatus* is late Coniacian in age, whereas the age of the earliest occurrence of *Tetralithus obscurus* is Santonian. Assemblages assignable to the *M. furcatus* Zone occur in several subsurface sections in the northern Carnarvon Basin of Western Australia: Rough Range, Giralia Anticline, and Exmouth Gulf areas. Important species of the *M. furcatus* Zone include *Cylindralithus asymmetricus, Eiffellithus eximius, Gartnerago obliquum, Kamptnerius magnificus, Manivitella pemmatoidea, Micula staurophora,* and *Marthasterites furcatus.*

Broinsonia parca Zone. The base of this zone is defined by the earliest occurrence of *Broinsonia parca* (Stradner), and its top is defined by the earliest occurrence of *Tetralithus aculeus* (Stradner).

The age of the *Broinsonia parca* Zone (as defined here) is considered as early Campanian. Evidence indicating that the age of the earliest occurrence of *B. parca* is early Campanian can be found in many publications (e.g. Bukry, 1969; Manivit, 1971); *Tetralithus aculeus* has not been found below the occurrence of *B. parca;* its earliest occurrence is probably mid-Campanian in age. Assemblages that can be assigned to the *B. parca* Zone occur in the Toolonga Calcilutite (particularly in the northern parts of the Carnarvon Basin). Important species of the *B. parca* Zone are those of the *Lucianorhabdus maleformis* Zone plus *Broinsonia parca; Lucianorhabdus maleformis* has not yet been identified among the assemblages of the *B. parca* Zone.

Palaeoenvironment of the Gingin Chalk

The palaeoenvironment of the Gingin Chalk has been discussed recently by Herb (1974), and Neale (1975). Herb (1974) cited foraminiferal evidence as reflecting an extratropical and slightly shallow-water palaeoenvironment. Based on ostracod faunas, Neale (1975) viewed the palaeoenvironment as warm (with minimum

Figure 5. (All photographs are x2000.)

Aa-Cb *Corollithion signum* Stradner: A = CPC 18290, B = CPC 18291, C = CPC 18292. Da-Db *Corollithion rombicum* (Stradner & Adamiker) CPC 18293. Ea-Eb *Corollithion achlyosum* (Stover) CPC 18294. Fa-Ga *Stephanolithion laffittei* Noël: F = CPC 18295, G = CPC 18296. Ha-Hb *Scapholithus fossilis* Deflandre CPC 18297. Ib-Ia *Eiffellithus turrieseiffeli* (Deflandre) CPC 18298. Jb-Mb *Tetralithus* sp.2: J = CPC 18299, K = CPC 18300, L = CPC 18301, M = CPC 18302. Na-Nb *Cylindralithus coronatus* Bukry CPC 18303. Oa-Ob *Cylindralithus serratus* Bramlette & Martini CPC 18304. Pa-Pb *Cylindralithus biarcus* Bukry CPC 18305. Qa-Qb *Cylindralithus asymmetricus* Bukry CPC 18306. Ra-Rb *Lithraphidites helicoides* (Deflandre) CPC 18307. Sa-Sb *Microrhabdulus decoratus* Deflandre CPC 18308. Tb-Ta *Eiffellithus eximius* (Stover) CPC 18309. Ub-Ua *Sollasites horticus* (Stradner, Adamiker & Maresch) CPC 18310.

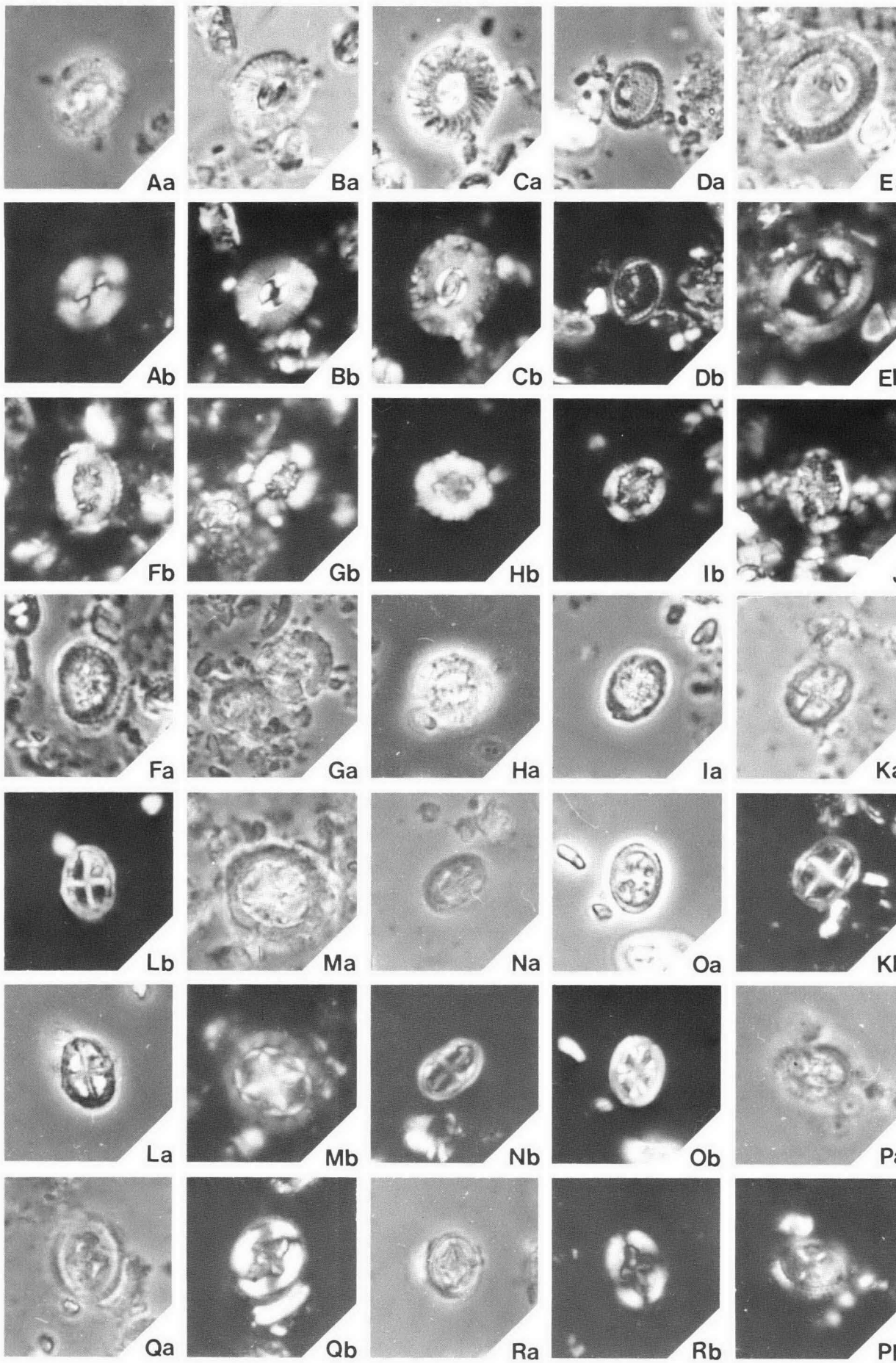
Aa
Ba
Ca
Da
Ea
Ab
Bb
Cb
Db
Eb
Fb
Gb
Hb
Ib
J
Fa
Ga
Ha
Ia
Ka
Lb
Ma
Na
Oa
Kb
La
Mb
Nb
Ob
Pa
Qa
Qb
Ra
Rb
Pb

temperature of about 10°C), euhaline and shallow (with depth being of the order of 100 m) but also suggested some influence by oceanic currents, as his ostracod faunas include endemic as well as cosmopolitan elements. Earlier, Chapman (1917) envisaged that the deposition of the Australian marine Cretaceous occurred in deep gulfs of moderate depth (epicontinental seas); for the Gingin Chalk, he added that warm-temperature conditions prevailed.

Nannofossil evidence supports the conclusion that deposition was in an epicontinental sea which had a good access to open ocean. This is based on the occurrence of *Braarudosphaera bigelowi, Kamptnerius magnificus, Lucianorhabdus cayeuxi, L. maleformis, Tetralithus obscurus, T. ovalis* (Table 1). These species are absent or rarely appear in deep oceanic sediments, but are widely distributed in coeval hemipelagic sediments. Open-marine conditions (which are the basic requirements to the flourishing of most Recent nannoplankton) is suggested by the great abundance and diversity of the nannofossil taxa of the Gingin Chalk.

Provincialism could not be detected among the nannofossil assemblages of the Gingin Chalk, in contrast with its ostracod faunas (Neale, 1975), and with other coeval nannofossil assemblages from the nearby (DSDP) Site 258 (Bukry, 1974): specimens of *Cribrosphaera* are absent from the Santonian sediments of Site 258, whereas *C. ehrenbergi* occurs in the Gingin Chalk (Table 1; illustrated in Figs. 4, 6) and the slightly younger (Campanian) sediments of (DSDP) Site 264 (Bukry, 1975; personal observation) (both sites are on the Naturaliste Plateau, off southwestern Australia).

Evidence suggesting warm-water conditions during the deposition of the Gingin Chalk is tenuous, but includes the occurrence of *Watznaueria barnesae.*

Acknowledgements

I thank both Drs D. J. Belford and G. C. H. Chaproniere, Bureau of Mineral Resources, for supplying the samples and for reading the manuscript. I thank Drs W. Siesser and H. Hekel for their critical comment.

List of calcareous nannofossil species considered in this paper, with two new combinations.

Ahmuellerella octaradiata (Gorka) Reinhardt, 1966.
Arkhangelskiella cymbiformis Vekshina, 1959.
Bidiscus monocavus Bukry, 1969.
Biscutum blacki Gartner, 1968.
Biscutum coronum Wind & Wise, 1976.
Braarudosphaera bigelowi (Gran & Braarud) Deflandre, 1947.
Broinsonia enormis (Shumenko) Manivit, 1971.
Broinsonia furtiva Bukry, 1969.
Broinsonia signata (Noël) Noël, 1970
Broinsonia parca (Stradner) Bukry, 1969.
Chiastozygus fessus (Stover) n. comb. (ex *Discolithus*).
Chiastozygus litterarius (Gorka) Manivit, 1971.
Chiastozygus plicatus Gartner, 1968.
Chiastozygus synquadriperforatus Bukry, 1969.
Corollithion achlyosum (Stover) Thierstien, 1971.
Corollithion rombicum (Stradner & Adamiker) Bukry, 1969.
Corollithion signum Stradner, 1963.
Cretarhabdus conicus Bramlette & Martini, 1964.
Cretarhabdus crenulatus Bramlette & Martini, 1964.
Cribrosphaera ehrenbergi Arkhangelsky, 1912.
Cyclagelosphaera margereli Noël, 1965.
Cylindralithus asymmetricus Bukry, 1969.
Cylindralithus biarcus Bukry, 1969.
Cylindralithus coronatus Bukry, 1969.
Cylindralithus serratus Bramlette & Martini, 1964.
Eiffellithus eximus (Stover) Pecth-Nielsen, 1968.
Eiffellithus turriseiffeli (Deflandre) Reinhardt, 1965.
Gartnerago obliquum (Stradner) Reinhardt, 1970.
Kamptnerius magnificus Deflandre, 1959.
Lapideacassis mariae Black, 1971.
Lithraphidites carniolensis Deflandre, 1963.
Lithraphidites helicoides (Deflandre) Čepek & Hay, 1969.
Lithrastrinus floralis Stradner, 1962.
Lucianorhabdus arcuatus Forchheimer, 1972.
Lucianorhabdus cayeuxi Deflandre, 1959.
Lucianorhabdus maleformis Reinhardt, 1966.
Manivitella pemmatoidea (Deflandre) Thierstein, 1971.
Marthsterites inconspicuus Deflandre, 1959.
Marthasterites furcatus (Deflandre) Deflandre, 1959.
Microrhabdulus decoratus Deflandre, 1959.
Micula staurophora (Gardet) Stradner, 1963.
Parhabdolithus angustus (Stradner) Stradner, Adamiker & Maresch, 1968.
Prediscosphaera cretacea (Arkhangelsky) Gartner, 1968.
Prediscosphaera spinosa (Bramlette & Martini) Gartner, 1968.
Reinhardtites anthrophorus (Deflandre) Perch-Nielsen, 1968.
Reinhardtites biperforatus (Gartner) n. comb. (ex *Zygodiscus*).
Scapholithus fossilis Deflandre, 1954.
Sollasites horticus (Stradner, Adamiker & Maresch) Čepek & Hay, 1969.
Stephanolithion laffittei Noël, 1956.
Tetralithus aculeus (Stradner) Gartner, 1968.
Tetralithus obscurus Deflandre, 1959.
Tetralithus ovalis Stradner, 1963.
Tranolithus exiguus Stover, 1966.
Vagalapilla dorfii Bukry, 1969.
Vagalapilla imbricata (Gartner) Bukry, 1969.
Watznaueria barnesae (Black) Perch-Nielsen, 1968.
Zygodiscus diplogrammus (Deflandre) Gartner, 1968.
Zygodiscus pseudoanthrophorus Bramlette & Martini, 1964.
Zygodiscus sigmoides Bramlette & Sullivan, 1961.
Zygodiscus spiralis Bramlette & Martini, 1964.
Zygodiscus theca (Black) Bukry, 1969.

Negatives of all figured specimens and their permanent mounts are deposited in the Commonwealth Palaeontological Collection in the Bureau of Mineral Resources, Canberra; their numbers are prefixed by CPC.

Figure 6. (All photographs are x2000.)

Aa-Ab *Watznaueria barnesae* (Black) CPC 18311. Ba-Bd *Biscutum blacki* Gartner CPC 18312. Ca-Cb *Biscutum* sp. cf. *B. coronum* Wind & Wise CPC 18313. Da-Db *Cribrosphaera ehrenbergi* Arkhangelsky CPC 18314. Ea-Eb *Manivitella pemmatoidea* (Deflandre) CPC 18315. Fb-Ha *Cretarhabdus crenulatus* Bramlette & Martini: F = CPC 18316, G = CPC 18317, G (bottom left corner *Prediscosphaera cretacea* (Arkhangelsky) CPC 18318); H = CPC 18319. Ib-J *Cretarhabdus conicus* Bramlette & Martini: I = CPC 18320, J = CPC 18321. Ka-La *Prediscosphaera spinosa* (Bramlette Martin): K = CPC 18322, L = CPC 18323. Ma-Mb *Prediscosphaera cretacea* (Arkhangelsky) CPC 18324. Na-Nb *Vagalapilla imbricata* (Gartner) CPC 18325. Oa-Ob *Ahmuellerella octaradiata* (Gorka) CPC 18326. Pa-Pb *Microrhabdulus decoratus* Deflandre CPC 18327. Qa-Rb *?Broinsonia signata* (Noël): Q = CPC 18328, R = CPC 18329.

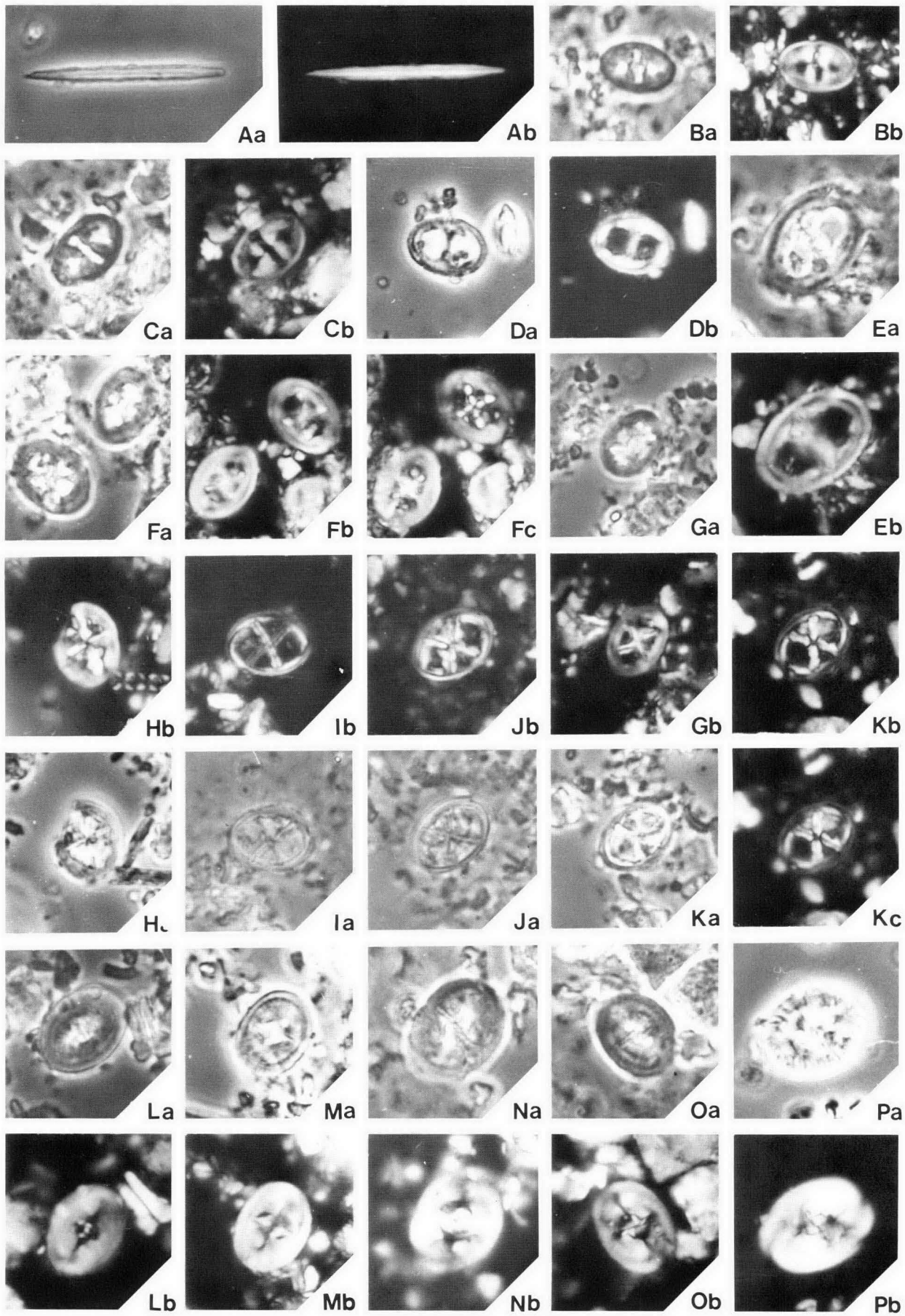
Aa
Ab
Ba
Bb
Ca
Cb
Da
Db
Ea
Fa
Fb
Fc
Ga
Eb
Hb
Ib
Jb
Gb
Kb
Ia
Ja
Ka
Kc
La
Ma
Na
Oa
Pa
Lb
Mb
Nb
Ob
Pb

References

BELFORD, D. J., 1958—Stratigraphy and micropalaeontology of the Cretaceous of Western Australia. *Geologische Rundschau,* **47**, 629-47.

BELFORD, D. J., 1960—Upper Cretaceous foraminifera from the Toolonga Calcilutite and Gingin Chalk, Western Australia. *Bureau of Mineral Resources, Bulletin* **57**, 1-198.

BUKRY, DAVID, 1969—Upper Cretaceous coccoliths from Texas and Europe. *Kansas University Paleontological Contributions,* **51** (Protista 2), 1-79, 40 pl.

BUKRY, DAVID, 1973—Coccolith and silicoflagellate stratigraphy, Tasman Sea and Southwestern Pacific Ocean, Deep Sea Drilling Project Leg 21. *In* BURNS, R. E., ANDREWS, J. E., & others, INITIAL REPORTS OF THE DEEP SEA DRILLING PROJECT. *U.S. Government Printing Office, Washington,* **21**, 885-93.

BUKRY, DAVID, 1974—Cretaceous and Paleogene coccolith stratigraphy, Deep Sea Drilling Project. *In* DAVIES, T. A., LUYENDKY, T. A., & others, INITIAL REPORTS OF THE DEEP SEA DRILLING PROJECT. *US Government Printing Office, Washington,* **26**, 669-73.

BUKRY, DAVID, 1975—Coccolith and silicoflagellate stratigraphy near Antarctica, Deep Sea Drilling Project, Leg 28. *In* HAYES, D. E., FRAKES, L. A., & others, INITIAL REPORTS OF THE DEEP SEA DRILLING PROJECT. *US Government Printing Office, Washington,* **28**, 709-23.

ČEPEK, PAVEL, 1970—Zur Vertikalverbreitung von Coccolithen-Arten in der Oberkreide NW-Deutschlands. *Geologische Jahrbuch,* **88**, 235-64.

ČEPEK, PAVEL, & HAY, WILLIAM W., 1969—Calcareous nannoplankton and biostratigraphic subdivision of the Upper Cretaceous. *Transactions of Gulf Coast Association of Geological Societies,* **29**, 323-36.

CHAPMAN, F., 1917—Monograph of the foraminifera and ostracoda of the Gingin Chalk. *Geological Survey of Western Australia, Bulletin* **72**, 9-87.

CITA, M. B., & GARTNER, S., 1971—Deep Sea Upper Cretaceous from the western North Atlantic. *In* FARINACCI, A. (Editor), PROCEEDINGS OF THE II PLANKTONIC CONFERENCE ROME 1970. *Edizioni Tecnoscienza,* **1**, 287-319.

DEFLANDRE, G., 1959—Sur les nannofossils calcaires et leur systématique. *Revue de Micropaléontologie,* **2**, 127-52.

ELLIOTT, G. F., 1952—The internal structure of West Australian Cretaceous Brachiopods. *Journal of the Royal Society of Western Australia,* **36**, 1-21.

ETHERIDGE, R., 1913—The Cretaceous fossils of the Gingin Chalk. *Geological Survey of Western Australia, Bulletin* **55**, 9-31.

FAIRBRIDGE, R. W., 1953—Australian Stratigraphy. *University of Western Australia, Text Books Board.*

FELDTMANN, F. R., 1951—Pectens of the Gingin Chalk. *Journal of the Royal Society of Western Australia,* **35**, 9-29.

FELDTMANN, F. R., 1963—Some pelecypods from the Cretaceous Gingin Chalk, Western Australia, together with descriptions of the principal chalk exposures. *Journal of the Royal Society of Western Australia,* **46**, 101-25.

GARTNER, STEFAN, Jr, 1968—Coccoliths and related calcareous nannofossils from Upper Cretaceous deposits of Texas and Arkansas. *Kansas University Paleontological Contributions* **48** (Protista 1), 1-56, 28 pl.

GARTNER, STEFAN, Jr, 1974—Nannofossil biostratigraphy, Leg 22, Deep Sea Drilling Project. *In* VON DER BORCH, CHRISTOPHER, C. SCLATER, JOHN, G., & others, INITIAL REPORTS OF DEEP SEA DRILLING PROJECT. *US Government Printing Office, Washington,* **21**, 577-97.

GLAESSNER, M. F., 1957—Crustacea from the Cretaceous and Eocene of Western Australia. *Journal of the Royal Society of Western Australia,* **40**, 33-35.

GLAUERT, L., 1910—The geological age and organic remains of the Gingin Chalk. *Geological Survey of Western Australia, Bulletin* **36**, 115-127.

HERB, R., 1974—Cretaceous planktonic foraminifera from the Eastern Indian Ocean. *In* DAVIES, T. A., LUYENDYK, B. P., & others, INITIAL REPORTS OF DEEP SEA DRILLING PROJECT. *US Government Printing Office, Washington,* **26**, 745-69.

LAUER, G., 1975—Evolutionary trends in the Arkhangelskiellaceae (calcareous nannoplankton) of the Upper Cretaceous of Central Oman, SE Arabia. *In* NÖEL, DENISE, & PERCH-NIELSEN, KATHARINA (Editors), REPORT ON THE CONSULTANT GROUP OF CALCAREOUS NANNOPLANKTON, KIEL, SEPTEMBER, 1974. *Archives des Sciences Geneve,* **28**, 259-62.

MCWHAE, J. R. H., PLAYFORD, P. E., LINDNER, A. W., GLENISTER, B. F., & BALME, B. E., 1958—The stratigraphy of Western Australia. *Journal of the Geological Society of Australia,* **4**.

MANIVIT, HELENE, 1968—Nannofossiles calcaires du Turonien et du Sénonien. *Revue de Micropaléontologie,* **10**, 277-86.

MANIVIT, HELENE, 1971—Nannofossiles calcaires du Crétacé Français (Aptian-Maestrichtian): Essai de biozonation appuyée sur les stratotypes. *Thèse Doctorate d'Etat, Institut de Geologie de la Faculte des Sciences d'Orsay,* Hayet, 187 pp., 32 pl.

NEALE, J. W., 1975—The ostracod fauna from the Santonian Chalk (Upper Cretaceous) of Gingin, Western Australia. *Palaeontological Association, Special papers in Palaeontology,* **16**, 1-81.

PERCH-NIELSEN, K., 1977—Albian to Pleistocene calcareous nannofossils from the western south Atlantic, DSDP Leg 39. *In* SUPKO, P. R., PERCH-NIELSEN, K., & others, INITIAL REPORTS OF THE DEEP SEA DRILLING PROJECT. *US Government Printing Office, Washington,* **39**, 699-823.

ROTH, PETER H., 1973—Calcareous nannofossils—Leg 17, Deep Sea Drilling Project. *In* WINTERER, E. L., EWING, J. L., & others, INITIAL REPORTS OF THE DEEP SEA DRILLING PROJECT. *US Government Prining Office, Washington,* **17**, 695-795.

ROTH, PETER H., & THIERSTEIN, HANS, 1972—Calcareous nannoplankton—Leg 14 of the Deep Sea Drilling Project. *In* HAYES, D. E., PIMM, A. C., & others. INITIAL REPORTS OF THE DEEP SEA DRILLING PROJECT. *US Government Printing Office, Washington,* **14**, 421-85.

SHAFIK, SAMIR, 1975—Nannofossil biostratigraphy of the Southwest Pacific Deep Sea Drilling Project, Leg 30. *In* ANDREWS, J. E., PACKHAM, G., & others, INITIAL REPORTS OF THE DEEP SEA DRILLING PROJECT. *US Government Printing Office, Washington,* **30**, 549-98.

SHAFIK, SAMIR, & STRADNER, HERBERT, 1971—Nannofossils from the Eastern Desert, Egypt with reference to Maaistrichtian nannofossils from the USSR. *Jahrbuch der Geologischen Bundesanstalt (Wien),* **17**, 69-104.

SMITH, C. C., 1975—Upper Cretaceous calcareous nannoplankton zonation and stage boundaries. *Transactions of the Gulf Coast Association of Geological Societies,* **25**, 263-78.

Figure 7. (All photographs are x2000.)

Aa-Ab *Lithraphidites carniolensis* Deflandre CPC 18330. Ba-Bb *Tranolithus exiguus* Stover CPC 18331. Ca-Cb *Tranolithus* sp. CPC 18332. D *Zygodiscus theca* (Black) CPC 18333. E *Zygodiscus* sp. cf. *Z. pseudanthophorus* Bramlette & Martini CPC 18334. F *Chiastozygus fessus* (Stover): left specimen = CPC 18335, right specimen = CPC 18336. G *Chiastozygus plicatus* Gartner CPC 18337. H *Chiastozygus synquadriperforatus* Bukry CPC 18338. I *Chiastozygus* sp. aff. *C. litterarius* (Gorka) CPC 18339. J-K *Chiastozygus litteraruis* (Gorka): J = CPC 18340, K = CPC 18341. L *Reinhardtites biperforatus* (Gartner) CPC 18342. M-O *Reinhardtites* sp. aff. *R. anthrophorus* (Deflandre): M = CPC 18343, N = CPC 18344, O = CPC 18345. P *Reinhardtites anthrophorus* (Deflandre) CPC 18346.

SPATH, L. F., 1926—Note on two Ammonites from the Gingin Chalk. *Journal of the Royal Society of Western Australia,* **12**, 53-5.

SISSINGH, W., 1977—Biostratigraphy of Cretaceous calcareous nannoplankton. *Geologie en Mijnbouw,* **56**, 37-65.

STOVER, L. E., 1966—Cretaceous coccoliths and associated nannofossils from France and the Netherlands. *Micropalaeontology,* **12**, 133-67.

STRADNER, HERBERT, 1963—New contributions to Mesozoic stratigraphy by means of nannofossils. *Proceedings of the 6th World Petroleum Congress,* **1**, 1-16.

THIERSTEIN, HANS, 1971—Foraminiferen und Nannoplankton aus einem Profil durch santone Amdenerschicten in den östlichen Churfirsten. *Ecolgae Geologicae Helvetiae,* **64**, 29-45.

THIERSTEIN, HANS, 1974—Calcareous nannoplankton—Leg 26, Deep Sea Drilling Project. *In* DAVIES, T. A., LUYENDYK, B. P., & others, INITIAL REPORTS OF THE DEEP SEA DRILLING PROJECT. *US Government Printing Office, Washington,* **26**, 619-67.

THIERSTEIN, HANS, 1976—Mesozoic calcareous nannoplankton biostratigraphy of marine sediments. *Marine Micropaleontology,* **1**, 325-62.

WIND, F. H., 1975—Affinity of *Lucianorhabdus* and species of *Tetralithus* in Late Cretaceous Gulf Coast samples. *Transactions of the Gulf Coast Association of Geological Societies,* **25**, 350-61.

WITHERS, T. H., 1924—The occurrence of the crinoid *Uintacrinus* in Australia. *Journal of the Royal Society of Western Australia,* **11**, 15-18.

WITHERS, T. H., 1926—The crinoid *Marsupites* in the Upper Cretaceous of Western Australia. *Journal of the Royal Society of Western Australia,* **12**, 97-100.

WORSLEY, T. R., & MARTINI, E., 1970—Late Maastrichtian nannoplankton provinces. *Nature,* **225**, 1242-3.

The age of the Mud Tank Carbonatite, Strangways Range, Northern Territory

L. P. Black and B. L. Gulson[1]

Dates of 732 ± 5 m.y. (U-Pb zircon) and 735 ± 75 m.y. (Rb-Sr total rock) define the crystallisation age, and possibly also the emplacement age, of the Mud Tank Carbonatite. Deformation structures in the carbonatite probably formed during resetting of Rb-Sr biotite ages at about 320 m.y. by reactivated fault movement. Feldspathic carbonatite apparently formed by country rock contamination. The Mud Tank Carbonatite differs markedly, both in age and initial Sr^{87}/Sr^{86} ratio, from the ultrapotassic Mordor Igneous Complex 50 km to the south. The age of the carbonatite does not correspond to any known event in the Arunta Block.

Introduction

The best studied of Australia's few known carbonatites is the Mud Tank Carbonatite in the Strangways Range of the Northern Territory. Although described by several authors, there is no reliable estimate of its time of crystallisation. Bhandari & others (1971) published a fission track age of 1050 m.y. on apatite from the carbonatite. Moore & Gray (1973), and Moore (1973) estimated an age of 2000 m.y. from structural considerations and tentative age data from granite and gneiss in the eastern part of the Arunta Block. The present article seeks to provide additional quantitative data on its age.

Geological setting

The geology of the area has been described by Shaw & Stewart (1975), and Stewart & Warren (1977). The Arunta Block occupies about 300 000 sq. km in the southern part of the Northern Territory. It consists of multiply deformed and polymetamorphosed Precambrian rocks, which are extensively intruded by granite ranging in age from 1800 to 1000 m.y. (Black, 1975, and unpublished analyses). The Mud Tank Carbonatite intrudes a probable correlative of the Strangways Metamorphic Complex (metamorphosed at about 1800 m.y.—Marjoribanks & Black, 1974; Black, 1975), which is thought to include the oldest of the metamorphic rocks in the Arunta Block. In the vicinity of the carbonatite the Strangways Metamorphic complex consists mainly of semi-pelitic quartz-biotite-muscovite schist, phyllonite, and mylonite.

The basement rocks are cut by numerous faults, and a major gravity structure, the Woolanga Lineament, which trends west-northwest for 300 km in the eastern half of the Block (Anfiloff & Shaw, 1973). Many major faults coincide with, or diverge from, this lineament. The Mud Tank Carbonatite occurs in one such splay off the Woolanga Lineament.

Both basement, and the cover rocks forming the Amadeus Basin to the south, were affected by widespread thrust faulting and associated retrogressive metamorphism during the late Palaeozoic Alice Springs Orogeny.

The Mud Tank Carbonatite

The Mud Tank Carbonatite has been described in detail by Crohn & Gellatly (1968), Gellatly (1969, 1972), Crohn (1971), Moore (1973), and Moore & Gray (1973). It comprises four separate lenses (Fig. 1) of crystalline calcitic and dolomitic rocks, and schistose biotite-bearing carbonate rocks which crop out in a northeast-trending zone 4 km long. Most of the carbonatite is considerably altered and partly ferruginised at the surface, and was originally detected by the large detrital concentrations of coarse apatite, magnetite, and zircon. In places the country rocks occurs within 20 m of the carbonates, but the contacts are not exposed.

The carbonatite is composed of three major rock groups whose age relations are not clear. The first group comprises **crystalline carbonate rocks** in which carbonates dominate all other minerals; apatite, magnetite, phlogopite (which locally shows reverse pleochroism), chlorite, soda-amphibole, pyrite, and zircon are subordinate. Schistosity may or may not be developed. The proportions of calcite to dolomite differ widely.

Foliated micaceous carbonate rocks form the second and most abundant group observed in drill core. They consist of carbonates, pale brown biotite, and subordinate soda-amphibole. Minor amounts of apatite and magnetite are commonly present. These rocks have gradational contacts with the crystalline carbonate rocks, with which they are locally interlayered.

The third group are **feldspathic carbonate rocks,** which form a series from carbonate-free silicate rocks towards typical carbonatite. These rocks are basically of two varieties: acid rocks characterised by aegirine and soda-amphibole, and aegirine-free hastingsite-bearing amphibolite. Both are thought to represent contaminated phases of the carbonatite magma (see later).

Small bodies of basic rock and pegmatite occur in the carbonatites, though once again contacts are not exposed. The pegmatite, which contains coarse sodic plagioclase, soda amphibole, biotite, apatite, and minor aegirine-augite, and is locally veined by carbonate, forms veins and lenses in the carbonatite.

U-Pb zircon dating

Analytical techniques

Zircon from the Mud Tank Carbonatite is coarse grained and euhedral to anhedral. The Mud Tank zircon sample obtained from the Australian Museum for use as a standard (STD, Table 1) measured 4 cm across. In an attempt to obtain a suite of samples with different U contents, detrital zircon grains with a range of fluorescent colours were selected. These were washed in cold 6N HCl for 15 minutes, crushed to −200 mesh, and successively washed in 7N HNO_3, H_2O, 6N HCl, and

1. Mineral Research Laboratories, CSIRO, P.O. Box 136, North Ryde, N.S.W. 2113.

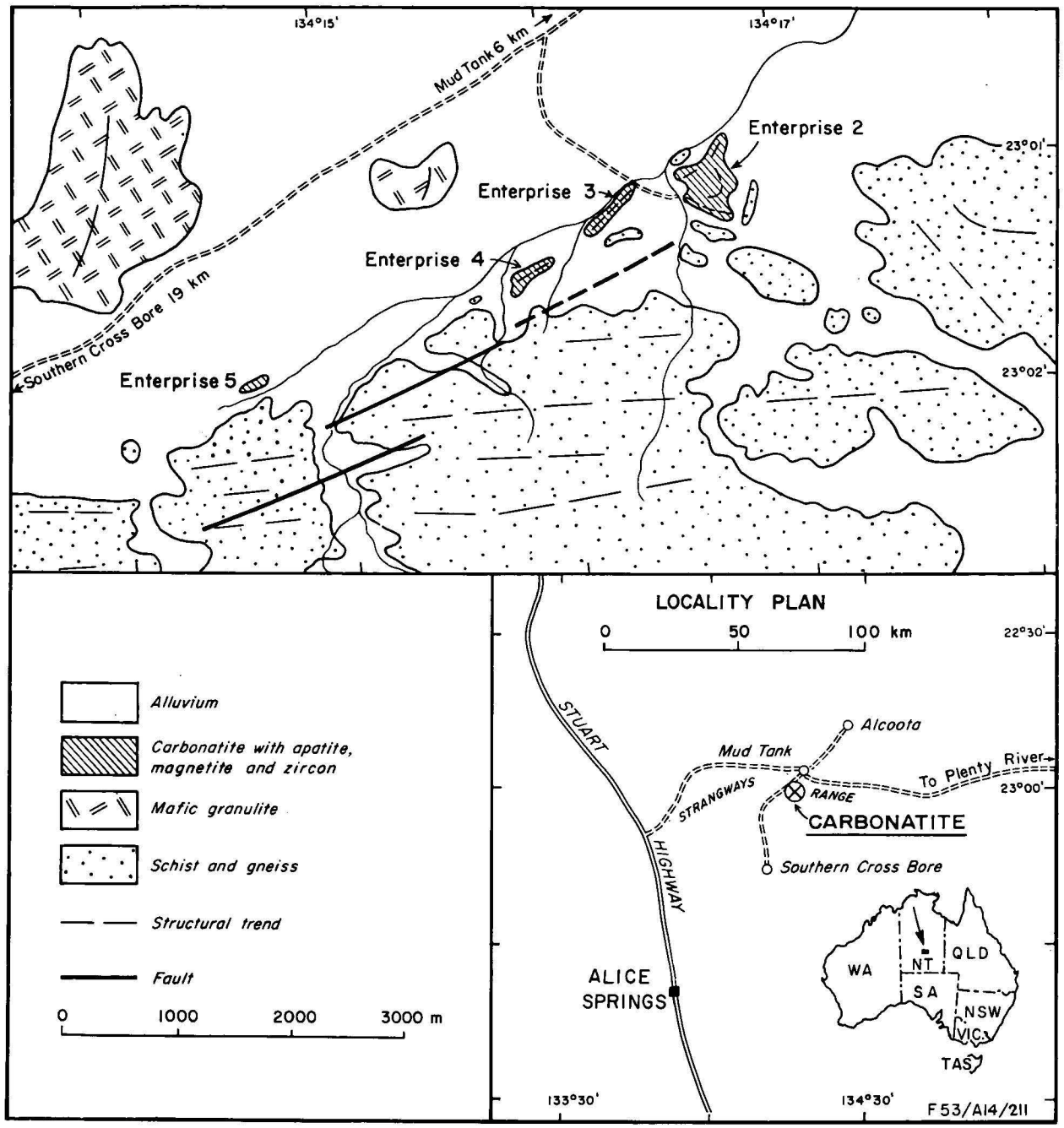

Figure 1. Locality map of the Mud Tank Carbonatite (after Crohn & Gellatly, 1968).

H_2O. Because of the low Pb concentrations, 80 to 200 mg of zircon was treated according to the Krogh hydrothermal method (1973). Analysis for U and Pb was carried out on the high ion beam transmission mass spectrometer in the Research School of Earth Sciences, ANU. 'Within-run' precision for a set of twelve Pb^{207}/Pb^{206} ratios ranged from 0.06 to 0.12 percent (1 δ); an estimate of reproducibility can be gained from the agreement of the Pb^{207}/Pb^{206} data in Table 1. Unit-cell dimensions were obtained by the method of Holland & Gottfried (1955).

Analytical data

Analytical data are presented in Table 1 and Figure 2. The unusual feature of the zircon is its very low content of U, which ranges from 6.1 to 36.5 μg/g. Low U concentrations in zircon from mafic and ultramafic rocks, particularly kimberlite, are well known (e.g. Silver, 1969; Gulson & Krogh, 1975; Kresten & others, 1975; Ahrens & others, 1967; Davis, 1976), but that of 6.1 μg/g is one of the lowest values known to us. There does not appear to be any obvious correlation of fluorescence with U concentration.

Deletion of the poor quality mass-spectrometric data of M1 FB yields a range in Tilton diffusion ages of 727-737 m.y. for the other five samples. Thus the age of the carbonatite on the basis of the zircon data is 732 $\pm$ 5 m.y. Because of the concordant data (i.e., the short extrapolation of any chord drawn through the data to meet the upper concordia), the age can be viewed with a high degree of confidence. Apatite from the carbonatite plots at the lower end of the zircon line on a $Pb^{207}/$

Sample No.	A	B	C	D	Atomic abundances relative to 206 = 100 204	207	208	E	F	G	H	Colour	Fluorescence
STANDARD (STD)	1.99	16.65	0.02	887	0.0208	6.661	14.789	0.1157 (705)	1.0137 (711)	0.06355 (727)	730	Brownish	Yellow
M1FB*	0.73	6.11	0.05	401	0.1118	8.079	14.947	0.1185 (722)	1.0560 (732)	0.06464 (763)	768	Clear	65% Bluish purple 35% No fluorescence
M2NF	2.27	19.67	0.64	209	0.4283	12.543	25.298	0.1149 (701)	1.0061 (703)	0.06350 (725)	729	Clear	45% Bluish purple 10% Yellow 45% No fluorescence
M2FB	2.51	20.62	0.02	3200	0.0108	6.507	13.329	0.1181 (719)	1.0338 (721)	0.06351 (725)	727	Clear	Blue
M2FY-1	2.51	34.74	0.04	1054	0.0325	6.747	13.733	0.0705 (439)	0.6104 (484)	0.06277 (700)	737	Brown	60% Yellow 40% Blue
M2FY-2	4.39	36.48	0.02	2031	0.0058	6.452	12.954	0.1173 (715)	1.0300 (719)	0.06368 (731)	734	Clear	60% Yellow 40% Blue

APATITE	Pb^{208}/Pb^{206} 2.1026	Pb^{207}/Pb^{206} 0.7075	Pb^{206}/Pb^{204} 22.34		
Blank lead	Pb^{206}/Pb^{204} 16.9	Pb^{207}/Pb^{204} 15.5	Pb^{208}/Pb^{204} 36.3	0.52×10^{-12} moles^{204}	
Common lead correction	Pb^{206}/Pb^{204} 17.00	Pb^{207}/Pb^{204} 15.54	Pb^{208}/Pb^{204} 36.80	+ Poor quality i.c. data	

U^{238} 0.15513×10^{-9}/yr U^{235} 0.98485×10^{-9}/yr (Jaffey & others, 1971) $\frac{U^{238}}{U^{235}} = 137.88$ (Shields, 1974)

A Radiogenic Pb (μg/g).
B U (μg/g).
C Common Pb (μg/).
D Raw Pb^{206}/Pb^{204}.
E Pb^{206}/U^{238} (age).
F Pb^{207}/U^{235} (age).
G Pb^{207}/Pb^{206} (age).
H Tilton Diffusion age (m.y.).

Table 1. Analyses of zircons from the Mud Tank Carbonatite.

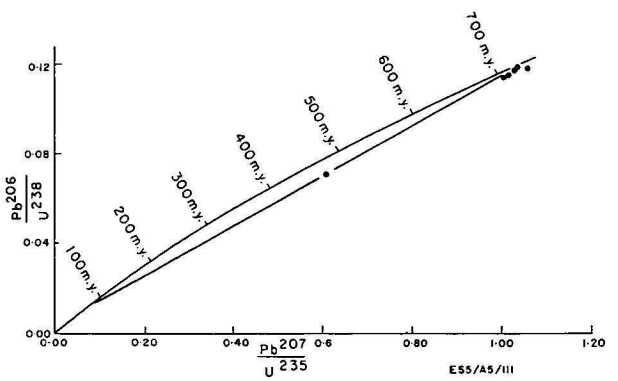

Figure 2. Pb^{206}/U^{238} vs $Pb^{207}/^{235}$ concordia diagram for zircons from the Mud Tank Carbonatite.

Pb^{204} vs Pb^{206}/Pb^{204} plot (not shown). The line has a slope of 0.06376, equivalent to an age of 734 m.y., and thus indicates a similar age for the zircon and apatite.

Comparison of unit-cell dimensions (Table 2) with the data for an undamaged gem zircon from Sri Lanka (Holland & Gottfried, 1955) shows that the Mud Tank Zircon is also undamaged. This might have been expected from their low U contents and concordant position (except for M2 FY-1) on the concordia plot.

Rb-Sr dating

Analytical techniques

All samples were obtained from diamond-drill core (DDH's A and D in Enterprise 3, and DDH B in Enterprise 2—Fig. 1) sited by the Northern Territory Geological Survey. Chemical procedures are outlined in Page & others (1976), and Williams & others (1976). Blank corrections of 6 ng for both Rb and Sr have been made where appropriate. Regression of the analyses was done by the method of McIntyre & others (1966). Relative deviations of 0.5 percent for Rb^{87}/Sr^{86}, and a standard deviation of 1×10^{-4} for Sr^{87}/Sr^{86}, have been used. Uncertainty limits are expressed at the 95 percent confidence level. The value $1.42 \times 10^{-11}y^{-1}$ (Steiger & Jäger, 1977) has been used for the decay constant of Rb^{87}.

Analytical data

Both total rocks and minerals have been isotopically analysed for Rb and Sr (Table 3). Total-rock data are plotted on the conventional isochron diagram (Fig. 3), and show a marked scatter from ideal isochron conditions. There are, however, petrographic features which correlate with the most divergent analyses. For example, 75913025 and 75913026, which plot above the other points, are the only two samples which contain feldspar (in this case, plagioclase). All four of Moore and Gray's (1973) analyses for the Mud Tank Carbonatite would also plot above the isochron, though their samples and 4 are close to it. Their analyses, which were used only for initial Sr^{87}/Sr^{86} estimates, and which are consequently not as precise as those of this study, are excluded from the present isochron. Moore & Gray's (1973) sample 3 plots well above the isochron; it contains 45 percent plagioclase. This correlation with discrepant Rb-Sr analyses suggests that the plagioclase represents a contaminant, presumably of country-rock derivation. No analyses of nearby country rock are available, but all other currently analysed Precambrian rocks from the Arunta Block (Black, 1975, and unpublished analyses), including the Strangways Metamorphic Complex, have suitable isotopic compositions to provide plagioclase with the requisite high Sr^{87}/Sr^{86} ratios.

Sample 75913027, which is composed entirely of biotite and amphibole, is by far the most enriched in Rb^{87} relative to Sr^{86}. As such, it strongly controls the age given by any regression through it. It plots below the regression line through the remaining points, presumably because of its unique composition. This rock type is rare, and occurs over 2.4 m in only one drill core (B). The pleochroism of the amphibole suggests it is hornblende rather than the soda-amphibole of the carbonate-bearing rocks. Crohn (1971) suggested that it

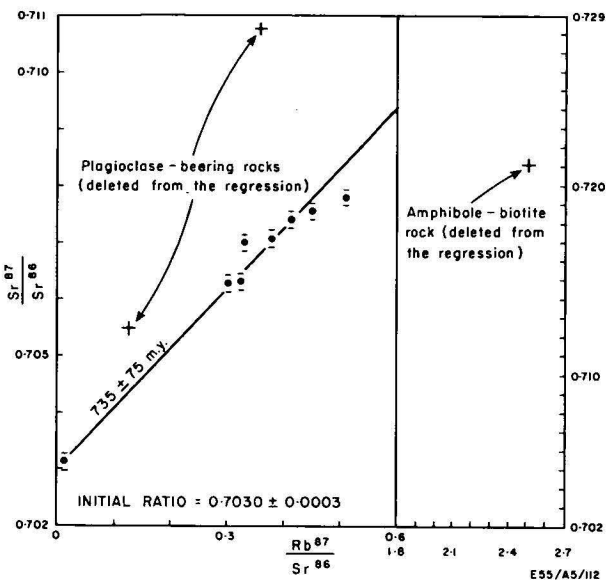

Figure 3. Rb-Sr isochron diagram for total-rock samples from the Mud Tank Carbonatite.

Sample	a_0 (A°)	c_0 (A°)	*U* (μg/g)
M1 FB	6.609	5.957	6.11
Standard	6.603	5.980	16.65
M2 NF-1	6.603	5.980	19.67
-2	6.605	5.960	
M2 FB-1	6.603	6.017	20.62
-2	6.603	5.962	
M2 FY-1	6.603	5.980	34.74
-2	6.605	5.978	36.48
*Undamaged zircon**	6.603	5.98	

* Holland & Gottfried, 1955.

Table 2. Unit-cell measurements on zircons from Mud Tank Carbonatite.

may have formed by local segregation from the amphibole or pyroxene-bearing feldspar-carbonate rocks which enclose it. The isotopic data also suggest that it may be younger than the carbonate-bearing rocks. A younger limit is provided by the biotite ages given below. Comparably young Rb-Sr total-rock ages in the Arunta Block have only been obtained from small pegmatite and aplitic bodies in the Huckitta Dome, 110 km to the east (Black, 1975). A possible alternative explanation for the relatively low position of the amphibole-biotite rock on the isochron diagram is that its constituent minerals were isotopically reset during this later event. Radiogenic Sr released from the biotite may not have been sufficiently strongly fixed in these carbonate and feldspar-free rocks, and some may have been lost from the total-rock system.

Deletion of the two feldspar-bearing rocks and the possibly younger amphibole-biotite rock from the regression produces a model 2 isochron (mean square of weighted deviates = 10), yielding an age of 735 ± 75 m.y. and an initial ratio of 0.7030 ± 0.0003.

Biotite separates from samples 75913024, 75913026, and 75913033 yielded ages of 319, 349, and 329 m.y., respectively. The three are probably recording the same event to which the first biotite has equilibrated more fully. Results from other minerals from the same rocks (Table 3) indicate that total inter-mineral Sr-isotopic equilibration was not achieved at this time. Carbonate and plagioclase have relatively high Sr^{87}/Sr^{86} ratios, as is to be expected from their ability to fix radiogenic Sr.

Discussion

The close similarity between total-rock Rb-Sr (735 ± 75 m.y.) and zircon U-Pb (732 ± 5 m.y.) ages is strong evidence that this is the crystallisation age of the Mud Tank Carbonatite. Further support is provided by the highly concordant nature of the zircon results. The low initial Sr^{87}/Sr^{86} ratio (0.7030 ± 0.0003) militates against this being a reset age. It also provides more definitive isotopic evidence (especially with the significantly younger age derived in this work) than given by Moore (1973), and Moore & Gray (1973), that the rocks are carbonatite rather than marble.

The feldspar-bearing carbonate rocks were considered by Crohn (1971) as products of crystallisation from a magma undergoing continuous modification, possibly by assimilation of pre-existing rocks (country rock of the Arunta Block or earlier carbonatite). Gellatly regards them as metasomatised country rock. Sr-isotopic data also indicate a contamination origin for the feldspar-bearing carbonate rocks, but cannot distinguish between the merits of these two hypotheses.

The youngest biotite ages of this study correspond with the youngest K-Ar ages reported by Stewart (1971) as an estimate of the time of the Alice Springs Orogeny. Thus, in common with many other rocks in the southern part of the Arunta Block, the Mud Tank Carbonatite also appears to have been affected by this event. Indeed, the distinct layering and preferred mineral orientation observed in much of the carbonatite probably formed at this time during renewed movement along the splay fault off the Woolanga Lineament. Reactivation of faults and deformed zones at this time has been postulated for other parts of the Arunta Block (Marjoribanks & Black, 1974). Because of its relative youth, the Mud Tank Carbonatite cannot have been involved in the main metamorphism of the country rock, as was implied by Moore & Gray (1973).

It cannot be entirely ruled out that the carbonatite originally crystallised at about 730 m.y. and was subsequently remobilised to its present setting by forceful intrusion at a later date—for example, during the Alice Springs Orogeny. Such a process might be expected to have affected the U-Pb systematics of the zircons at this time. The discordia of Figure 2, which does, however, rely entirely on the analytical results for M2 FY-1, shows no such trend, suggesting that crystallisation of the carbonatite was contemporaneous with its final emplacement. It must be emphasised, however, that the U-Pb systematics of zircon are not well understood and it is conceivable that the low-uranium zircon of this study might be isotopically insensitive to solid-state emplacement.

Fifty kilometres south-southeast of the Mud Tank Carbonatite, and also adjacent to the Woolanga Lineament, is the Mordor Complex (Langworthy & Black, in press). This is a potassic ultrabasic to basic composite intrusion ranging in composition from phlogopite dunite through phlogopite-rich wehrlite, lherzolite, shonkinite, pyroxenite, and melamonzonite, to syenite. Many alkalic igneous rocks elsewhere appear to be genetically related to spatially associated carbonatites (see Faure & Powell, 1972, p. 56). Indeed, in addition to its proximity to the Mud Tank Carbonatite, veinlets, plugs, and dykes of carbonate-rich material occur in the Mordor Complex itself. However, trace-element contents (Gellatly, 1969;

Sample no.	DDH	Depth in metres	Principal minerals (in decreasing abundance)	Rb (μg/g)	Sr (μg/g)	Sr^{87}/Sr^{86}	Rb^{87}/Sr^{86}	Age (m.y.)
75913023 total rock	A	84.7	Carbonates	12.48	3533	0.70312	0.0102	
75913024 total rock	A	132.0	Carbonates-amphibole-biotite	174.3	1690	0.70628	0.2977	
amphibole				1.580	60.53	0.70513	0.0753	
carbonate				0.3273	5506	0.70645	0.000172	
biotite				302.8	7.6179	1.2546	120.9	319
75913025 total rock	B	115.2	Biotite-carbonates-apatite-opaques-amphibole-plagioclase	111.6	2569	0.70548	0.1253	
75913026 total rock	B	136.2	Biotite-carbonates-pyroxene-plagioclase	46.43	377.4	0.71076	0.3553	
plagioclase				1.237	632.1	0.70943	0.00565	
pyroxene				1.958	43.88	0.70831	0.1288	
biotite				344.0	3.098	2.5955	379.8	349
75913027 total rock	B	142.6	Amphibole-biotite	61.61	71.09	0.72117	2.506	
75913028 total rock	D	124.5	Carbonates-apatite-phlogopite-opaques	199.1	1776	0.70630	0.3235	
75913029 total rock	D	132.8	Biotite-carbonates-apatite-opaques-amphibole	236.4	1801	0.70708	0.3790	
75913030 total rock	D	137.8	Biotite-carbonates-amphibole-opaques	236.6	1334	0.70778	0.5107	
75913031 total rock	D	143.6	Biotite-carbonates-apatite-opaques-amphibole	211.3	1856	0.70700	0.3288	
75913032 total rock	D	149.7	Biotite-carbonates-amphibole-apatite-opaques	239.5	1680	0.70740	0.4116	
75913033 total rock	D	153.9	Biotite-carbonate-amphibole-opaques	234.4	1501	0.70756	0.4511	
biotite				314.2	8.022	1.2634	119.2	329
carbonate				0.620	6424	0.70569	0.000279	

Table 3. Rb-Sr isotopic composition of Mud Tank Carbonatite samples.

Moore, 1973; Langworthy & Black, in press) show that the carbonate rocks at Mordor are of different origin to those at Mud Tank. This is further supported by the low initial Sr^{87}/Sr^{86} ratio of the Mud Tank Carbonatite (0.703) as compared with values of 0.716 to 0.721 for the Mordor carbonates. In common with the alkalic rocks of the African Rift Valleys (Bell & Powell, 1969, 1970), the Mud Tank Carbonatite has a significantly lower initial Sr^{87}/Sr^{86} ratio than the alkalic rocks of the Mordor Complex (0.711). The ages of the two—730 m.y. for the Mud Tank Carbonatite and about 1200 m.y. for the Mordor Complex—are also clearly different. Indeed, the 730 m.y. age for the Mud Tank Carbonatite is not associated with any other known event in the Arunta Block.

MacIntyre (1971, 1977) has suggested that in Canada, and perhaps elsewhere in the world as well, carbonatite emplacement has been at regular intervals about 230 m.y. apart until 130 m.y. ago. Certain exceptions were also reported. The present data show that the Mud Tank Carbonatite is also an exception to this theory.

Acknowledgements

The diamond-drill core samples were supplied by O. G. Fruzzetti of the Northern Territory Geological Survey, and the standard zircon sample by L. Sutherland of the Australian Museum. We express our thanks to D. C. Gellatly, R. W. Page, J. Ferguson, W. B. Dallwitz, A. P. Langworthy, R. D. Shaw, A. J. Stewart, and R. G. Warren for constructive criticism of the manuscript. M. W. Mahon, T. K. Zapasnik, and J. L. Duggan provided technical assistance in sample preparation and processing. A. Horne obtained the unit-cell dimensions. The figures were prepared by Rosa Fabbo of the BMR Drawing Office. The zircon analyses were done by B. L. G. whilst a visiting fellow at RSES, Australian National University, Canberra.

References

AHRENS, L. H., CHERRY, R. D., & ERLANK, A. J., 1967—Observations on the Th-U relationship in zircons from granitic rocks and from kimberlites. *Geochimica et Cosmochimica Acta*, **31**, 2379-87.

ANFILOFF, W., & SHAW, R. D., 1973—The gravity effects of three large uplifted granulite blocks in separate Australian shield areas. *Proceedings of the Symposium on Earth's Gravitational Field and Secular Variation in Position, Sydney* (1973), 273-8.

BELL, K., & POWELL, J. L., 1969—Strontium isotopic studies of alkalic rocks: the potassium-rich lavas of the Birunga and Toro-Ankole regions, East and Central Equatorial Africa. *Journal of Petrology*, **10**, 536-72.

BELL, K., & POWELL, J. L., 1970—Strontium isotopic studies of alkalic rocks: the alkali complexes of Eastern Uganda. *Bulletin of the Geological Society of America*, **81**, 3481-90.

BHANDARI, N., BHAT, S. G., LAL, D., RAJAGOPALAN, G., TAMHANE, A. S., & VENKATAVARADAN, V. S., 1971—Fission fragment tracks in apatite: Recordable track lengths. *Earth and Planetary Science Letters*, **13**, 191-9.

BLACK, L. P., 1975—Present status of geochronological research in the Arunta Block, N.T. *First Australian Geological Convention—Proterozoic Geology, Geological Society of Australia*, Adelaide, May 1975—Abstracts, 37.

CROHN, P. W., 1971—Investigations at the Strangways Range carbonatite locality, N.T. *Geological Survey of the Northern Territory—Record* **G.S. 71/1** (unpublished).

CROHN, P. W., & GELLATLY, D. C., 1968—Probable carbonatites in the Strangways Range area, central Australia. *Bureau of Mineral Resources, Australia—Record* **1968/114** (unpublished).

DAVIS, G. L., 1977—The ages and uranium contents of zircons from kimberlites and associated rocks. *Annual Report of the Geophysical Laboratory, Carnegie Institution of Washington Yearbook*, **76**, 631-5.

FAURE, G., & POWELL, J. L., 1972—STRONTIUM ISOTOPE GEOLOGY. *Springer-Verlag, Berlin.*

GELLATLY, D. C., 1969—Probable carbonatites in the Strangways Range area, Alice Springs 1:250 000 Sheet area SF53/14: Petrography and Geochemistry. *Bureau of Mineral Resources, Australia—Record* **1969/77** (unpublished).

GELLATLY, D. C., 1972—The petrology of the Strangways Range carbonatite. *Specialists Group Meetings—Geological Society of Australia,* Canberra, February 1972—Abstracts, J10.

GULSON, B. L., & KROGH, T. E., 1975—Evidence of multiple intrusion, possible resetting of U-Pb ages, and new crystallization of zircons in the post-tectonic intrusions ('Rapakivi granites') and gneisses from South Greenland. *Geochimica et Cosmochimica Acta,* **39**, 65-82.

HOLLAND, H. D., & GOTTFRIED, D., 1955—The effect of nuclear radiation on the structure of zircon. *Acta Crystallographica,* **8**, 291-300.

JAFFEY, A. H., FLYNN, K. F., GLENDENIN, L. E., BENTLEY, W. C., & ESSLING, A. M., 1971—Precision measurement of half-lives and specific activities of ^{235}U and ^{238}U. *Physical Review,* **C4**, 1889-906.

KRESTEN, P., FELS, P., & BERGGREN, G., 1975—Kimberlitic zircons—a possible aid in prospecting for kimberlites. *Mineralium Deposita,* **10**, 47-56.

KROGH, T. E., 1973—A low contamination method for decomposition of zircon and extraction of U and Pb for isotopic age determinations. *Geochimica et Cosmochimica Acta,* **37**, 485-94.

LANGWORTHY, A. P., & BLACK, L. P., in press—The Mordor Complex: a highly differentiated potassic intrusion with kimberlitic affinities in central Australia. *Contributions to Mineralogy & Petrology.*

MACINTYRE, R. M., 1971—Carbonatites—apparent periodicity of emplacement in Canada. *Nature Physical Science,* **230**, 79-81.

MACINTYRE, R. M., 1977—Anorogenic magmatism, plate motion and Atlantic evolution. *Journal of the Geological Society of London,* **133**, 375-84.

MCINTYRE, G. A., BROOKS, C., COMPSTON, W., & TUREK, A., 1966—The statistical assessment of Rb-Sr isochrons. *Journal of Geophysical Research,* **71**, 5459-68.

MARJORIBANKS, R. W., & BLACK, L. P., 1974—Geology and geochronology of the Arunta Complex, north of Ormiston Gorge, central Australia. *Journal of the Geological Society of Australia,* **21**, 291-300.

MOORE, A. C., 1973—Carbonatites and kimberlites in Australia: A review of the evidence. *Minerals Science and Engineering,* **5**, 81-91.

MOORE, A. C., & GRAY, C. M., 1973—Carbonatites of the Strangways Range, central Australia: Evidence from strontium isotopes. *Journal of the Geological Society of Australia,* **20**, 71-3.

PAGE, R. W., BLAKE, D. H., & MAHON, M. W., 1976—Geochronology and related aspects of acid volcanics, associated granites, and other Proterozoic rocks in The Granites-Tanami region, northwestern Australia. *BMR Journal of Australian Geology and Geophysics,* **1**, 1-13.

SHAW, R. D., & STEWART, A. J., 1975—Arunta Block—regional geology; *in* KNIGHT, C. L. (Editor), ECONOMIC GEOLOGY OF AUSTRALIA AND PAPUA NEW GUINEA: 1. METALS. *Australasian Institute of Mining and Metallurgy —Monograph Series,* **5**, 437-42.

SHIELDS, W. R., 1974; *in* WEAST, R. C., & SELBY, S. M. (Editors), HANDBOOK OF CHEMISTRY AND PHYSICS. *Chemical Rubber Company, Cleveland,* 1974 Edition.

SILVER, L. T., 1969—A geochronologic investigation of the Anorthosite complex, Adirondack mountains, New York; *in* ISACHSEN, Y. W. (Editor), ORIGIN OF ANORTHOSITE AND RELATED ROCKS. *New York State Museum and Science Service—Memoir* **18**, 233-51.

STEIGER, R. H., & JÄGER, E., 1977—Subcommission on geochronology: Convention on the use of decay constants in geo- and cosmochronology. *Earth and Planetary Science Letters,* **36**, 359-62.

STEWART, A. J., 1971—Potassium-argon dates from the Arltunga Nappe Complex, Northern Territory. *Journal of the Geological Society of Australia,* **17**, 205-11.

STEWART, A. J., & WARREN, R. G., 1977—The mineral potential of the Arunta Block, central Australia. *BMR Journal of Australian Geology and Geophysics,* **2**, 21-34.

WILLIAMS, I. S., COMPSTON, W., CHAPPELL, B. W., & SHIRAHASE, T., 1976—Rubidium-strontium age determinations on micas from a geologically controlled, composite batholith. *Journal of the Geological Society of Australia,* **22**, 497-506.

Stable isotope and chemical studies of volcanic exhalations and thermal waters, Rabaul caldera, New Britain, Papua New Guinea

D. C. Green[1], J. R. Hulston[2], & I. H. Crick

Thermal waters in Matupi Harbour and Sulphur Creek, Rabaul caldera have D/H and O^{18}/O^{16} ratios that are indicative of a mixed source. They are the result of mixing of local meteoric waters with hot water of marine origin. The stable isotope data are grouped into distinct areas close to the meteoric water line. They suggest that the thermal systems away from the shoreline are dominated by meteoric water and that warmed sea water only enters the springs at the shoreline. Low temperature (100°C) fumarolic exhalations from Tavurvur and Rabalankaia volcanoes consist largely of recycled meteoric water. These conclusions conflict in part with those drawn from anion ratio and trace metal contents which were inferred by previous authors to be consistent with an hypothesis of modified sea water origin. We suggest that the chemistry of these acid, mineralised geothermal waters is a reflection of their later, near surface, history and does not necessarily give a correct picture of their ultimate origin. The enhanced Fe, Mn, and Zn values of the Matupi springs are a function of the leaching potential of geothermal fluids at elevated temperatures, and of the chemistry of the porous and chemically reactive rocks through which they pass.

Introduction

Thermal water issuing from springs on the eastern and northern shores of Matupi harbour, New Britain (Fig. 1) have been proposed as the source of significant enrichments in iron, manganese, and zinc contents of silt-grade sediments in the harbour (Ferguson & Lambert, 1972). Stable isotope and chemical studies give important clues to the origin of the waters forming these springs and the associated fumaroles.

The area is composed of Quaternary calc-alkaline pyroclastics and minor flows forming the largely drowned Rabaul caldera (Heming, 1974; Fisher, 1976). Recent volcanic activity in the area culminated in the major eruption of Tavurvur between June 1941 and March 1942. Since that time, Tavurvur has returned to a quiet solfataric condition. Rabalanakaia has not erupted since observations commenced in about 1850. Preliminary studies of the geothermal areas on the north shore of Matupi harbour (Studt, 1961; Fooks, 1961) suggested that sea water plays a large part in the hydrothermal systems.

This study extends the investigation of Ferguson & Lambert (1972) into the volcano-exhalative-sedimentary environment in Matupi harbour. Spooner (1974) quotes the results of Ferguson & Lambert (1972) in support of a proposal that the metal-enriched brines are of sea-water origin, and were generated in sub-sea floor geothermal systems by a high-temperature leaching process such as that proposed by Spooner & Fyfe (1973).

Sakai & Matsubaya (1974) draw a comparison between the thermal water systems on the Japanese coast and those of Matupi harbour. However, there remain significant differences in chemistry between the two systems, particularly in terms of the anion ratios and sulphate contents.

The regional setting and details of the springs and fumaroles are described in Ferguson & Lambert (1972). Where possible, sample sites are as close as possible to those described in that paper; additional information is also provided on Sulphur Creek springs, on the west flank of Rabalankaia.

Experimental techniques

Representative spring-water samples were collected in clean glass containers, temperature, and pH measurements made in situ, and the remaining chemical analyses performed in one of two laboratories listed below. Fumarole gas condensates were collected with a simple vacuum-pump system. It is likely that some variability in samples (Table 1) from individual fumaroles is the result of differences in obtaining a quantitative collection of condensate.

Gas condensate samples TAV 66, 68, 69, and RAB 63, 64 were chemically analysed by the Mines Division Laboratory, Departments of Lands, Surveys and Mines,

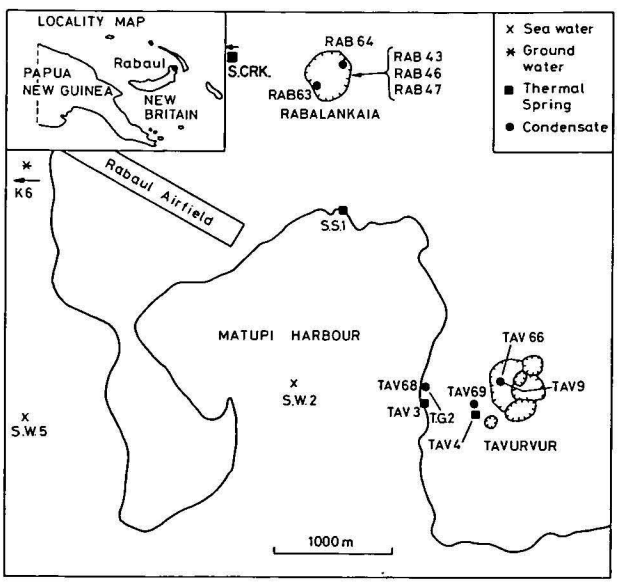

Fig. 1. Locality map. K6 (sea water) was collected approximately 4 km offshore in Rabaul harbour, and Sulphur Creek spring (Sul. Crk.) is located just to the west of the plotted position.

1. Formerly Department of Geology and Mineralogy, University of Queensland, St. Lucia, Brisbane, Queensland, Australia, now Department of Mines, G.P.O. Box 124B, Hobart, Tasmania 7001.

2. Institute of Nuclear Sciences, DSIR, Lower Hutt, New Zealand. INS Contribution no. 811.

PNG (Chief Chemist: G. Gardiner) and all others by the Australian Mineral Development Laboratories, Adelaide (Officer-in-Charge: D. K. Rowley) . Ca^{2+}, Mg^{2+}, Na^{+}, K^{+}, Al^{3+}, and Li^{+} were determined by atomic absorption spectroscopy with accuracies of better than ± 1 ppm, SO_4^{2-} by gravimetric analysis (± 5 ppm), Cl^- by titrimetric methods (± 1 ppm), NO_3^- and silica (± 1 ppm) and boron (± 0.02 ppm) by spectrophotometer, F^- by specific ion electrode (± 0.05 ppm), and Br^- by X-ray fluorescence spectroscopy (± 1 ppm).

All heavy metal analyses were done by the Australian Mineral Development Laboratories using an atomic absorption spectrometer. The detection limits quoted are: Cu, 0.04 ppm; Fe, 0.05 ppm; Mn, 0.02 ppm; Pb, 0.01 ppm and Zn, 0.01 ppm. When values are significantly above the detection limit the accuracy is, in general, ± 2%.

Stable isotope analyses were carried out at the Institute of Nuclear Sciences, DSIR, New Zealand. δD values on water samples were measured on a Micromass 602C mass spectrometer after conversion to hydrogen by passage over hot zinc at 395°C. δO^{18} values are found by measuring the $^{18}O/^{16}O$ ratios of CO_2 in equilibrium with the water sample at 30°C, using a procedure similar to that of Epstein & Mayeda (1953). Overall errors are estimated to be no greater than ± 2% in δD, and ± 0.1% in δO^{18}. $\delta^{18}O_{SO_4}$ and $\delta^{34}S_{SO_4}$ measurements were made on samples of high (1000 ppm) SO_4^{2-} content. The standard for oxygen and hydrogen isotope measurements is I.A.E.A. SMOW; for sulphur, the troilite of the Canön Diablo meteorite is used.

Stable isotope and chemical data are presented in a series of tables (Tables 1 to 5) and the location of samples is found in Figure 1.

δO^{18} results in Table 1 have been corrected for a zero shift of −0.44‰ in samples measured after 1975 using the INS-3 standard, and for scale contraction factors of −0.8% for samples measured prior to 1974 and −0.3% for samples measured after 1975. This minor change of between −0.2 and −0.4‰ relates the δO^{18} values of these samples to the 'normalised' δ scale relative to V-SMOW and SLAP (INS, 1977). The revised meteoric water line now is expressed as approximately $\delta D = 8\ \delta^{18}O + 13$.

Figs. 2, 3, 4 and 5 were drawn and photographed prior to this correction. Since the corrections do not affect the details of the discussion, these figures have not been redrawn. A revised version of the diagrams is available on request from D.C.G.

Results and discussion

Thermal springs

Figure 2 illustrates the D/H and O^{18}/O^{16} data from the warm thermal waters. From this diagram alone there is strong support for a mixing model involving warmed sea water and relatively cool meteoric water. It is considered that the groundwater sample (K6) is more representative of the meteoric water entering the thermal system than a single sample of rainwater (R7) collected at the Rabaul observatory. To support this argument, the river, mine, and surface waters at Bougainville (Ford & Green, 1977) exhibit remarkably uniform, although depleted, δO^{18} and δD values. On

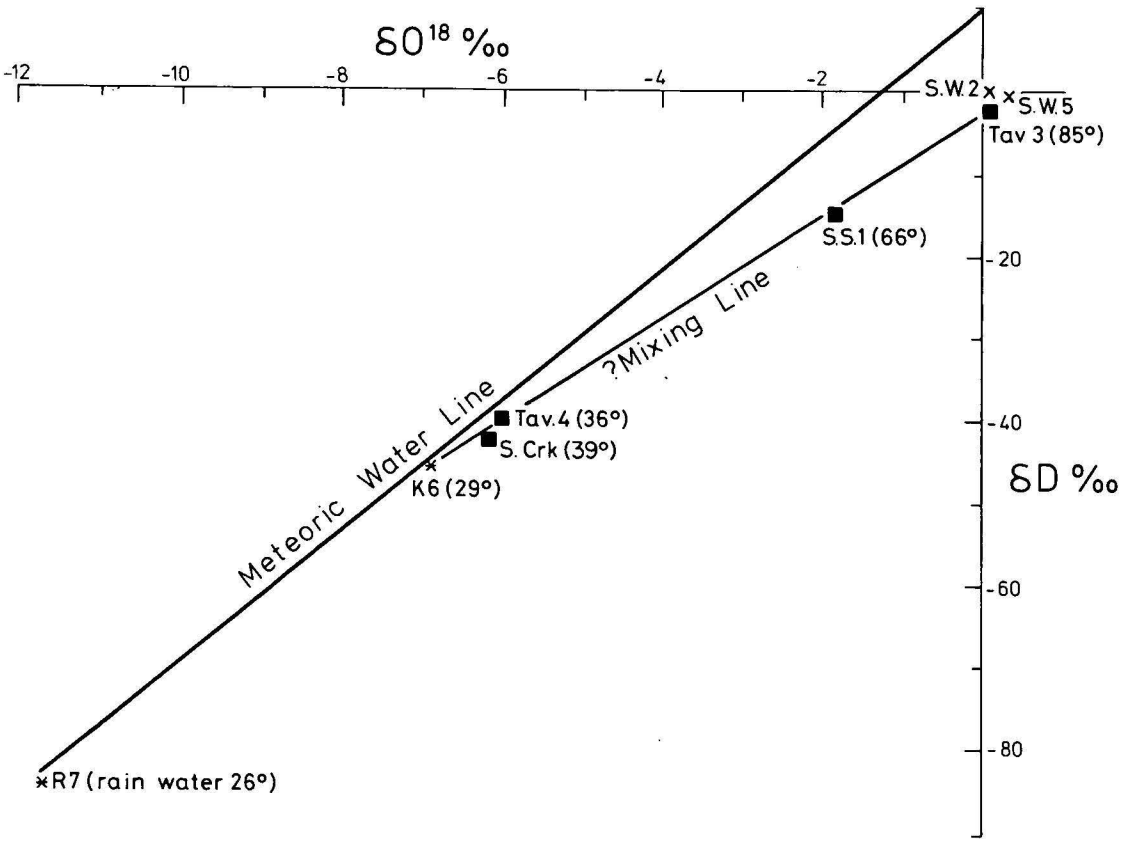

Fig. 2. δO^{18}-δD plot of thermal waters, sea water, and meteoric water samples, Matupi harbour and environs.

Sample	Location	δO^{18}_{SMOW}	δD_{SMOW}	$\delta O^{18}_{SO_4}$ SMOW	$\delta S^{34}_{SO_4}$ CDT	Date collected
Thermal spring waters		‰	‰	‰	‰	
Sul. Crk. (8)	54	−6.5	−42.8	+11.0	n.d.	14/3/75
SSI	34	−2.3	−15.0	+12.5	+18.4	14/3/75
TAV 3	176	−0.3	−0.9	+12.5	+16.9	14/3/75
TAV 4	(upper gully)	−6.3	−40.5	+5.5	+4.9	14/3/75
Sea waters						
SW 2	Matupi harbour	+0.1	−1.4	+10.6	+19.8	4/4/75
SW 5	Rabaul harbour	+0.4	+0.3	+9.5	+20.7	14/3/75
Ground and rain waters						
K 6	Non-thermal stream	−7.3	−46.0			14/3/75
R 7	Rabaul Observatory	−11.9	−85.2			14-16/2/75
Fumaroles						
Tavurvur						
TG 2	18	−10.3	−64.3			14/3/75
TAV 22	18	n.d.	−55.0			4/10/72
TAV 68	18	−9.25	−61.0			31/8/73
TAV 9	6	−8.5	−56.6			4/4/75
TAV 23B	15	n.d.	−18.0			6/10/72
TAV 66	6	−6.73	−46.3			30/8/73
TAV 23A	15	n.d.	−35.0			4/10/72
TAV 69	15	−6.75	−38.4			31/8/73
Rabalankaia						
RAB 43	43	−6.0	−38.3			14/3/75
RAB 63	43	−7.94	−55.5			23/8/73
RAB 46	46	−2.3	−11.9			19/3/75
RAB 47	47	−4.6	−31.0			19/3/75
RAB 64	47	+0.14	−14.1			23/8/73
RAB 27	47	n.d.	−23.0			31/10/72

Table 1. Stable isotope data of thermal, rain, ground and sea water samples from the Rabaul caldera.

the other hand, rainwaters in the tropics commonly exhibit very variable isotopic compositions—because of sharp temperature contrasts between the sea and cloud formations (Dansgaard, 1964).

A good linear correlation exists between temperature and O^{18} (and D), but the Cl^- contents predicted on a simple sea-water mixing model depart considerably from those measured. In contrast, the relationship between Cl^- content and δO^{18} (and δD) is logarithmic in nature (Fig. 3). This suggests that mixing of the water phase is taking place, but that there has been some modification during the mixing process to the chemical components. The reason for this chemical modification is not known but micropore filtration and density stratification are possibilities. However, there is no visible evidence of density of ionic stratification such as encountered in the Red Sea brines. The logarithmic relationship obtained for the chloride content suggests that mixing takes place without excessive convection, while the linear relationship between the surface temperature and the $\delta^{18}O$ value suggests that there has not been excessive loss of heat from the water phase to the surrounding rocks.

The δO^{18} and δS^{34} results from sulphate extracted from sea water and thermal spring waters are listed in Table 1. As expected, the sea water samples fall close to the normal values. The higher temperature spring waters, e.g. TAV3, have similar δO^{18} and δS^{34} values of $\sim$ + 12‰ and 18‰ respectively.

The values could be explained by the subsurface addition of sulphate of $\delta O^{18} \sim +$ 13‰ and $\delta S^{34} \sim +$ 15‰ to sea water followed by dilution (in the case of SSI) with cold surface water of low sulphate content. In contrast, TAV4 appears to have isotopically light (?volcanic) sulphate added, probably after dilution. This sample is of relatively low chloride content (Cl^- = 575 ppm) but contains a substantial sulphate content (SO_4^{2-} = 4454 ppm). From these results, it is likely that the sulphate is derived from a source other than sea water.

If it is assumed that there is equilibrium between $\delta^{18}O_{H_2O}$ and $\delta^{18}O_{SO_4}$ in TAV3, SSI, and possibly TAV4, the application of the sulphate geothermometer of Mizutani & Rafter (1969) yields below ground temperatures of 125-165°C. This approach is an oversimplification; the temperatures may be misleading, as exchange equilibrium between the oxygen-bearing phases is not demonstrated. Cation (Na:K, and Na:K:Ca) and SiO_2 geothermometers may also give misleading results for one of several reasons: either (a) amorphous silica saturation, (b) acid solutions, (c) sea water involvement (cf. Truesdell, 1975). An analysis of the chemical data by Dr C. Downes shows that all spring samples are supersaturated in amorphous silica (Table 5, ΔG + ve), and hence the normal silica geothermometer (Fournier & Rowe, 1966) is

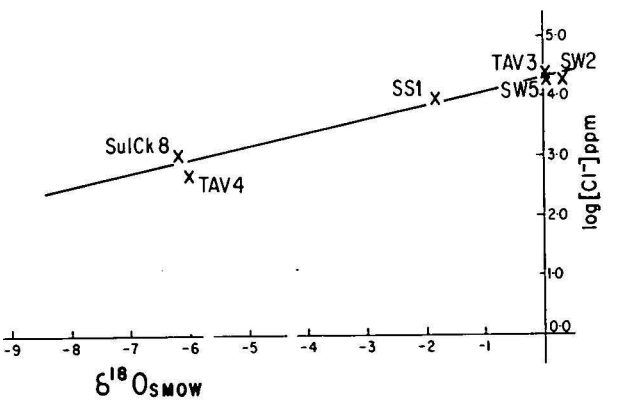

Fig. 3. δO^{18}_{SMOW}-log (Cl^-) plot of thermal waters studied. An approximate linear relationship between some spring samples and sea water is indicated by a solid line.

Field No.	*R7*	*K6**	*SW5†*	*SW2†*	*TAV3‡*	*TAV4‡*	*SSl‡*	*Sul. Crk. 8‡*
Temp. C°	24	29	27	—	85	36	66	39
pH (20°C)	4.8	8.4	7.8	8.3	3.1	3.5	7.9	8.1
Ca	1	15	382	398	426	400	229	68
Mg	1	8	1 300	1 280	1 740	490	550	60
Na	1	119	10 760	11 000	13 260	1 000	5 250	660
K	1	5	331	325	781	78	223	38
Li	—	1	1	1	1	1	1	1
B	—	0.06	4.25	4.25	15.50	2.00	3.15	0.75
Al	—	0.05	0.05	0.05	1.25	0.50	0.05	0.05
Br	—	1	58	60	70	1	30	3
Cl	2	60	19 171	19 351	22 860	575	9 264	1 028
F	—	0.80	0.95	1.00	0.85	1.40	1.05	2.75
HCO_3	5	207	147	140	5	5	247	207
SO_4	5	48	2 683	2 700	6 367	4 454	1 420	237
NO_3	1	1	4	1	42	1	1	1
SiO_2	—	86	2	2	274	138	164	104

* = ground water, R7 = rain (Rabaul Observatory), † = sea water, ‡ = thermal spring.

Table 2. Chemistry of thermal, rain, ground, and sea water samples from the Rabaul caldera. All elements in ppm.

Field No.	*K6**	*SW5†*	*SW2†*	*TAV3‡*	*TAV3‡ (acidified)*	*TAV4‡*	*TAV4‡ (acidified)*	*SSl‡*	*Sul. Crk. 8‡*
Cu	0.04	0.04	0.04	0.04	0.08	0.04	0.04	0.04	0.04
Fe	0.05	0.05	0.05	48.6	52.5	1.48	41.8	0.05	0.05
Mn	0.04	0.02	0.02	106	100	11.3	11	0.6	0.02
Pb	0.01	0.01	0.01	0.01	0.01	0.01	0.01	0.01	0.01
Zn	0.01	0.02	0.01	0.76	0.76	0.30	0.29	0.02	0.02
As	0.015	0.005	0.005	0.04	0.055	0.005	0.005	0.025	0.025

* = ground water, † = sea water, ‡ = thermal spring.

Table 3. Heavy metal ion composition of thermal, rain, ground, and sea water samples from the Rabaul caldera. All elements in ppm.

Field No.	*K6**	*SW5†*	*SW2†*	*TAV3‡*	*TAV4‡*	*SSl‡*	*Sul. Crk. 8‡*
Na/Cl	1.98	0.56	0.57	0.58	1.74	0.57	0.64
K/Cl	0.083	0.017	0.017	0.034	0.136	0.024	0.037
Ca/Cl	0.250	0.020	0.021	0.019	0.696	0.025	0.066
Mg/Cl	0.133	0.068	0.066	0.076	0.852	0.059	0.058
Br/Cl		3.0 x 10–4	3.1 x 10–3	3.1 x 10–3	1.7 x 10–3	3.2 x 10–3	2.9 x 10–3
B/Cl	10 x 10–4	2.2 x 10–4	2.2 x 10–4	6.8 x 10–4	3.5 x 10–4	3.4 x 10–4	7.3 x 10–4
SO_4/Cl	0.80	0.14	0.14	0.28	7.75	0.15	0.23
HCO_3/Cl	3.45	0.01	0.01	—	—	0.03	0.20

* = groundwater, † = sea water, ‡ = thermal spring.

Table 4. Ion ratios of thermal springs, ground, and sea waters, Rabaul caldera.

not applicable. Although White (1970) suggests that the SiO_2 geothermometer not be used for waters with an acid pH and low Cl^- concentration when below 100° because of amorphous silica saturation, it is possible to obtain equilibrium estimates of temperature (within 5°C) from TAV3 and TAV4 using amorphous quartz solubility data (cf. Table 5). The three alkaline samples (SSl, Sul. Crk., and K6) are slightly supersaturated with respect to calcium carbonate polymorphs and thus the Na-K-Ca geothermometer is invalid at these temperatures (cf. Paces, 1975). For these reasons, it is considered inadvisable to give an estimate of underground temperatures and an exploratory drill hole is strongly recommended.

The major ion chemistry of the thermal springs does not differ significantly from the results of Ferguson & Lambert (1972), with the exception of the Tavurvur gully springs. In this study, water from these springs (TAV4, see Fig. 2) is distinctly different from sea water in Br/Cl and B/Cl ratios. Heavy metal contents (Table 4) are comparable with those of Ferguson & Lambert (1972), particularly in Mn and Fe. Cu and Zn values reported here are somewhat below those quoted in that paper. The rate of flow of these springs is less than 0.1 l/sec and they commonly stop flowing during the May-August dry season. Heavy metal enrichments and variable chloride contents of the springs may imply considerable interaction with the wall rocks, possibly by some process of micropore filtration. There is, however, no evidence in the spring waters of the positive oxygen isotope shift which usually characterises this interaction if it occurs at elevated temperatures.

The chemistry of the spring waters differs from the coastal thermal waters of Japan described by Sakai & Matsubaya (1974), in that SO_4^{2-} remains at a relatively high concentration (see SO_4/Cl ratios) as does Mg^{2+}, an indication that precipitation of anhydrite is not common. Beevers (1965) reports some gypsum in fumarolic products from Tavurvur and Rabalankaia. The SO_4^{2-}/Cl^- ratios are in accord with a mixing model, with the exception of TAV4 (Tavurvur upper gully spring) which, as discussed earlier, shows S iso-

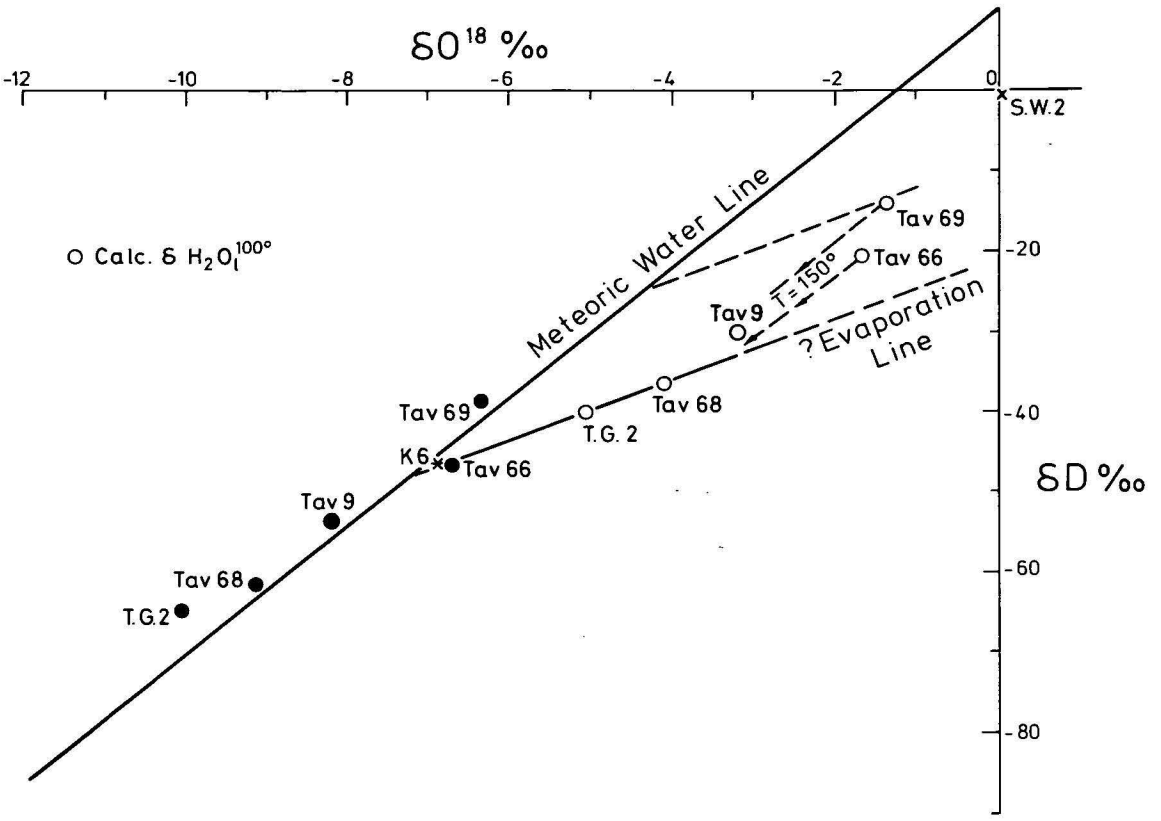

Fig. 4. δO^{18}-δD plot of fumaroles from Tavurvur crater and western slopes to sea level. Calculated $\delta H_2O_\ell^{100°C}$ values are shown as open circles. Possible evaporation paths are indicated as dashed lines of slope 3.75.

tope evidence for the late addition of light sulphur. The analysis of the chemical data by Dr C. Downes shows that TAV4 is the only spring water sample to exhibit supersaturation in gypsum and anhydrite.

Ferguson & Lambert (1972, p. 33) contend that the enhanced total dissolved solids and chloride content of the Tavurvur shore springs are probably due to boiling off of fumarolic vapours during ascent of the heated water column. It is shown in the following section that all the fumaroles on Tavurvur have a very substantial meteoric water component. A common origin is unlikely if the chemical evidence of essentially unmodified sea water for TAV3 is accepted. The Tavurvur shore springs have Br/Cl, Na/Cl, Ca/Cl, and Mg/Cl ratios that are almost identical to sea water, but K/Cl, B/Cl and SO_4/Cl ratios are higher.

It has been shown that water from the spring located in the upper part of the prominent gully on the west flank of Tavurvur is distinctly different from the other thermal springs. Chemical data (TAV4, Tables 2, 3, 4) confirm the suggestion of Ferguson & Lambert (1972) that the enhanced heavy metal content of this spring water is a function of the relatively slow passage of these cool, acid waters through the surrounding rocks.

Fumaroles

Tavurvur

The stable isotope data from the fumaroles at the shoreline, in the upper Tavurvur gully, and in the crater are listed in Table 1; the data are plotted on Figure 4, together with the calculated liquid water phase compositions at 100°C using the fractionation data of Bottinga & Craig (1968). Two calculated $\delta H_2O_\ell^{100°}$ values fall on a line, which if projected, cuts the average meteoric water line (approximately $\delta D = 8 \times \delta O^{18} + 13$) at about the composition of the non-thermal groundwater sample K6. The slope of this line (3.75) is approximately that of a kinetic evaporation line (cf. Craig, 1963; Craig & others, 1963). The remaining three results, TAV9, TAV66, and TAV69 would also fall close to this line if temperatures of vapour phase separation of 150-200°C were assumed. However, it is evident from Table 1 that there is considerable variation in δD and δO^{18} values in condensate samples from an individual fumarole, collected at different times. It is suggested that these may be seasonal variations (Perry & Crick, 1976), but further work is necessary to exclude variations arising from collection methods. It is recognised that the calculated $H_2O_\ell^{100°}$ values represent likely maximum heavy isotopic enrichments of the liquid phase. Truesdell & others (1976) examines this question in much greater detail.

The chemistry of the gas condensates from the fumaroles is similar to that presented by Ferguson & Lambert (1972). All contain low amounts of major ions and are acidic. The slightly enhanced SO_4^{2-} content in most samples and the low pH values are probably due to dissolved oxy-sulphur gases resulting from oxidation of H_2S. In coastal areas the effect of cyclic chlorides must also be considered. Hutton (1976) states that the chloride content may reach 35 ppm in rainwater collected in temperate zones on the Australian coast. A similar effect is likely in tropical areas where onshore winds are common. This factor may assist to explain a slight difference in average Cl^- values from Tavurvur (3.8 ppm) and Rabalankaia (2.6 ppm)

Sample	pH	Surface T°C	Silica T°C	Am Si T°C	G (Am Si)	Ca/Na	Na/K T°C	Na/K/Ca T°C	$p(CO_2)$ atm.2	Q*
TAV 3	3.1	85	206	80.3	+—.39	1/30	129	205	—	1.208
SSI	7.9	66	163	37.9	+0.10	1/25	102	175	0.0024	1.441
TAV 4	3.5	36	156	32.0	+0.40	1/2½	156	172	—	1.458
Sul. Crk.	8.1	39	136	13.4	+0.13	1/10	127	165	0.0017	1.523
K 6	8.4	29	125	3.3	+0.14	1/8	101	85	0.0008	1.798

$^*Q = \log \frac{Na+}{K+} + \frac{1}{3} \log \frac{Ca^{2}+}{Na+}$, Am Si = Amorphous silica.

Table 5. Rabaul spring samples—summary of temperature estimates from chemical models and cation ratios.

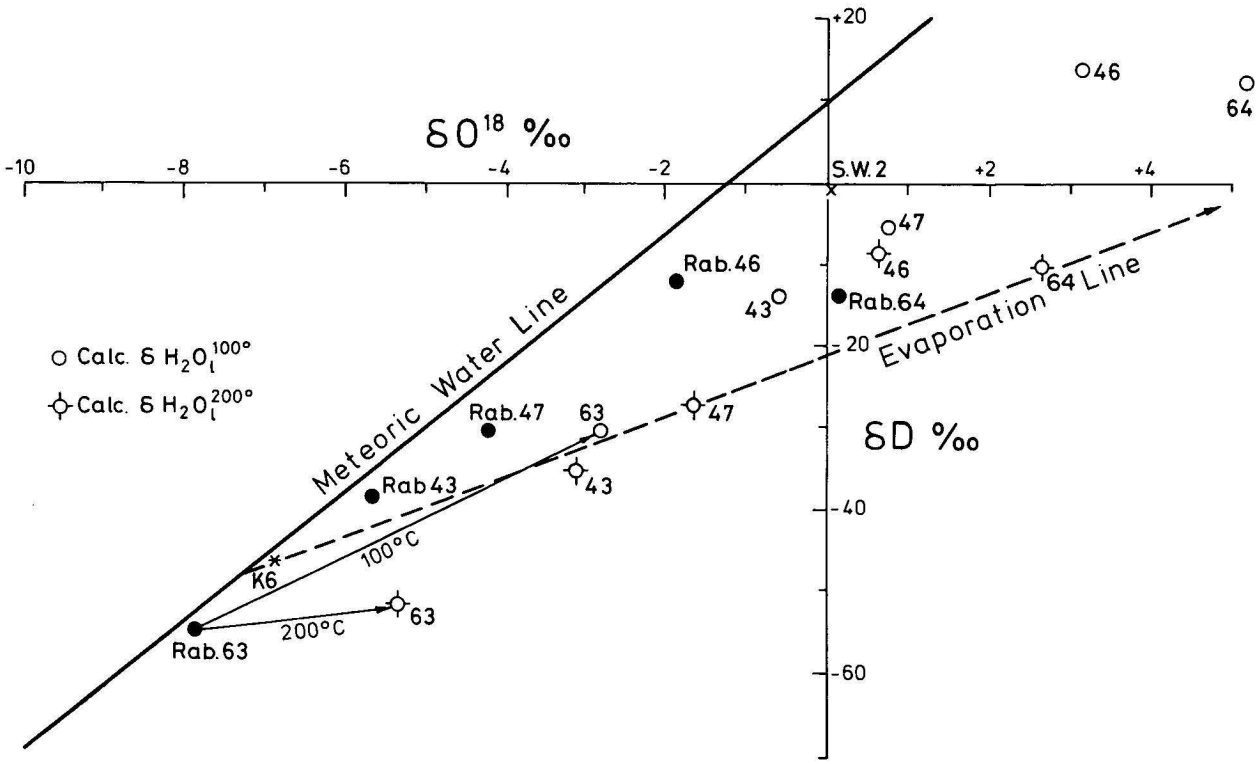

Fig. 5. δO^{18}-δD plot of fumaroles from the Rabalankaia crater. Calculated $\delta H_2O_t^{100°C}$ and $\delta H_2O_t^{200°C}$ values are shown as open circles. The suggested evaporation line in Figure 3 is reproduced for comparative purposes.

fumaroles. Rainwater sample R7, collected at the Rabaul Volcanological Observatory, 150 m above sea level and 1.5 km inland, contained only 2 ppm chloride.

Rabalankaia

In the Rabalankaia crater the weak fumarolic activity is not associated with springs, but with areas of heated ground readily identified by I.R. imagery (Perry & Crick, 1976). Springs only occur on the lower flanks at Sulphur Creek (Sul. Crk) and Sulphur Springs (SSI). There is considerable variation in values of δO^{18} and δD with date of collection (Table 1, Fig. 5). For example, RAB63 was collected from the same site as RAB43, and RAB64 from the same site as RAB47.

It is possible that the outer fumarole ring is associated with a shallower, essentially meteoric water circulation related to ring fractures. Samples RAB47 and RAB64 may be related by an evaporative process such as that suggested for the Tavurvur fumaroles.

In Figure 5, calculated $\delta H_2O_t^{100°}$ and $\delta H_2O_t^{200°}$ values are shown in an attempt to suggest limiting conditions, but it also is possible that the range of Rabalankaia results may be explained on the basis of variable recharge or permeability. Emeleus (1977) suggests that the 'high rainfall and absence of surface drainage ensure a large groundwater supply . . . sufficient to regulate the gas temperature to its observed value of close to 100°C'. On the basis of total magnetic field measurements, Emeleus (fig. 6) postulates the existence of a basalt plug about 72 m in diameter, located just outside the inner fumarole ring in the northwest quadrant of the crater. It is doubtful that an entirely steady state will exist in a relatively shallow natural geothermal system, and seasonal variations are likely.

Conclusions

The warm springs around the Tavurvur and Rabalankaia craters adjacent to Matupi harbour show evidence of variable, possibly seasonal, incorporation of local meteoric waters into the geothermal systems. The isotopic composition of waters such as TAV3 suggests that heating of sea water by conduction is largely responsible for the formation of the shoreline springs.

The weak fumarolic activity is dominated by local meteoric waters that are modified by evaporation. The remarkable enrichment of some of the thermal waters in heavy metals, particularly Mn, Fe, and Zn, is seen not as the result of high temperature sub-sea-floor hydrothermal leaching by heated sea water, but rather as the result of relatively shallow, but extensive, interaction of the acidic, warmed waters with the loosely consolidated Quaternary basalt-andesite pyroclastic rocks.

It is tempting to consider mixing models such as those developed by Fournier & Truesdell (1974), but neither model (p. 264, fig. 1) is entirely suitable. A modification to allow access of meteoric water in varying amounts into the area in which heat is supplied (and prior to steam separation) is necessary—if the fumaroles and springs are to have a common origin, and if the isotopic evidence of essentially meteoric origin for the gas phase in the fumaroles is accepted.

Acknowledgements

The considerable assistance and patience of Mr D. A. Wallace of the Papua New Guinea Geological Society in collection of samples is greatly appreciated. We also acknowledge the help of Dr T. A. Rafter and the staff of the Institute of Nuclear Sciences, Lower Hutt, in particular Mrs M. A. Cox, in laboratory procedures and mass spectrometry. Stimulating discussions with Dr S. M. F. Sheppard at the Scottish Universities Research and Reactor Centre, East Kilbride, Scotland, Drs M. K. Stewart, B. W. Robinson, and G. Lyon at I.N.S., and Mr J. H. Ford (University of Queensland) during the preparation of this paper are also acknowledged. The assistance of Dr Colin Downes (Chemistry Division, DSIR, New Zealand), in analysing the chemical data is gratefully acknowledged.

D. C. Green publishes with the permission of Mr J. G. Symons, Director of Mines, Tasmania.

References

BEEVERS, J. R., 1965—Identification and chemical analysis of some volcanic samples from New Guinea. *Bureau of Mineral Resources, Australia, Record* **1965/209**.

BOTTINGA, Y., & CRAIG, H., 1968—Liquid-vapour fractionation factors for H_2O-HDO-H_2O^{18} in the temperature range 100-340°C. *Transaction of the American Geophysical Union,* **49**, 356-7 (Abstract).

CRAIG, H., 1963—The isotopic geochemistry of water and carbon in geothermal areas. *In* TONGIORGI, T. (Editor), NUCLEAR GEOLOGY IN GEOTHERMAL AREAS, 17-53. *Consiglio Nazionale delle Ricerche, Pisa.*

CRAIG, H., GORDON, L. I., & HORIBE, Y., 1963—Isotopic Exchange Effects in the Evaporation of Water: 1. Low-Temperature Experimental Results. *Journal of Geophysical Research,* **68**, 5079-86.

DANSGAARD, W., 1964—Stable isotopes in precipitation. *Tellus,* **16**, 436-68.

EPSTEIN, S., & MAYEDA, T., 1953—Variation of ^{18}O content of waters from natural sources. *Geochimica et Cosmochimica Acta,* **4**, 213-24.

EMELEUS, T. G., 1977—Thermo-magnetic measurements as a possible tool in the prediction of volcanic activity in the volcanoes of the Rabaul caldera, Papua New Guinea. *Journal of Volcanology and Geothermal Research,* **2**, 343-59.

FERGUSON, J., & LAMBERT, I. B., 1972—Volcanic exhalations and metal enrichments at Matupi harbour, New Britain, TPNG. *Economic Geology,* **67**, 25-37.

FISHER, N. H., 1976—1941-42 eruption of Tavurvur volcano, Rabaul, Papua New Guinea. *In* JOHNSON, R. W. (Editor), VOLCANISM IN AUSTRALASIA. *Elsevier, Amsterdam,* 201-10.

FOOKS, A. C. L., 1961—Preliminary investigation of the Rabaul geothermal area for the production of electric power. New Sources of Energy—Proceedings of the Conference (Rome) 21-31 August, 1961, Volume 2.

FORD, J. H., & GREEN, D. C., 1977—A light stable isotope study of the Panguna porphyry copper deposit, Bougainville. *Journal of the Geological Society of Australia,* **24**, 63-80.

FOURNIER, R. O., & ROWE, J. J., 1966—Estimation of underground temperatures from the silica content of water from hot springs and wet-stream wells. *American Journal of Science,* **264**, 685-97.

FOURNIER, R. O., & TRUESDELL, A. H., 1974—Geochemical indicators of subsurface temperature: 2, estimation of temperature and fraction of hot water mixed with cold water. *US Geological Survey Journal of Research,* **2**, 253-70.

HEMING, R. F., 1974—Geology and petrology of Rabaul caldera, Papua New Guinea. *Bulletin of the Geological Society of America,* **85**, 1253-64.

HUTTON, J. T., 1976—Chloride in rainwater in relation to distance from ocean. *Search,* **7**, 207-8.

INS, 1977—Institute of Nuclear Sciences, DSIR, Lower Hutt, NZ. Progress Report 28.

MIZUTANI, Y., & RAFTER, T. A., 1969—Oxygen isotopic composition of sulphates. 3. Oxygen isotopic fractionation in the bisulphate ion-water system. *New Zealand Journal of Science,* **12**, 54-9.

PACES, T., 1975—A systematic deviation from Na-K-Ca geothermometer below 75°C and above 10^{-4} atm P_{CO_2}. *Geochimica et Cosmochimica Acta,* **39**, 541-4.

PERRY, W. J., & CRICK, I. H., 1976—Aerial thermal infrared survey, Rabaul area, Papua New Guinea, 1973. *In* JOHNSON, R. W. (Editor), VOLCANISM IN AUSTRALASIA. *Elsevier, Amsterdam,* 211-19.

SAKAI, H., & MATSUBAYA, O., 1974—Isotopic geochemistry of the thermal waters of Japan and its bearing on the Kuroko ore solutions. *Economic Geology,* **69**, 974-91.

SPOONER, E. T., 1974—Sub-sea-floor metamorphism, heat and mass transfer; an additional comment. *Contributions to Mineralogy and Petrology,* **45**, 169-73.

SPOONER, E. T., & FYFE, W. A., 1973—Sub-sea floor metamorphism, heat and mass transfer. *Contributions to Mineralogy and Petrology,* **42**, 287-304.

STUDT, F. E., 1961—Preliminary survey of the hydrothermal field at Rabaul, New Britain. *New Zealand Journal of Geology and Geophysics,* **4**, 274-82.

TRUESDELL, A. H., 1975—Summary report, Section III, Geothermometers. *Proceedings 2nd UN Symposium on the Development and Use of Geothermal Resources, San Francisco, California, USA,* 20-29 May, 1975.

TRUESDELL, A. H., NATHENSON, M., & RYE, R. O., 1976—The effects of subsurface boiling and dilution on the isotopic compositions of thermal waters. *International Conference on Stable Isotopes, INS, DSIR, Lower Hutt, New Zealand,* August, 1976 (Abstract).

WHITE, D., 1970—Geochemistry applied to the discovery, evaluation and exploitation of geothermal energy resources. *Geothermics, Special Issue,* **2**, 58-80.

Early geophysical practice — the BMR instrument collection

P. H. Sydenham[1]

The Bureau of Mineral Resources, Geology and Geophysics was formed in 1946. It replaced the Mineral Resources Survey (1942-46) whose forerunners were the Aerial Geological and Geophysical Survey of Northern Australia (AGGSNA) (1934-1941) and the earlier Imperial Geophysical Experimental Survey (IGES) (1928-30). The notably large BMR geophysical achievement has used a wide variety of geophysical and allied measuring apparatus, much of which was placed in storage as its effectiveness declined. The collection has been further enhanced by direct donation from exploration companies and joint international programs.

One hundred and ten artefacts from the collection were recorded, along with details of origin and use where known. Reference is made to early literature describing many of the objects.

This account provides a general overview of the collection.

Introduction

This account summarises a collection of 19th and 20th century geophysical instruments that has been assembled in Australia during the past eighty years or so. This collection has resulted from the wide range of geophysical programs conducted by the Bureau of Mineral Resources, Geology and Geophysics (BMR) since 1946. The holdings have been extended by the addition of equipment presented to the Bureau by exploration companies and by overseas co-operative agencies. Additional sources such as these have provided the collection with equipment of much earlier origin than the 1940s. The collection is a significant part of Australia's technological heritage.

It is BMR policy to add outdated equipment to the collection which is housed in warehouse storage at the Commonwealth Government Store, Oaklands, NSW. This particular location is excellent for storage—industrial pollutants are absent and the stores are well managed and supervised at all times.

In May 1977 the bulk of the collection was studied and recorded by some members of the Department of Geophysics, University of New England under guidance of the author who represented the National Sub-Committee for Engineering Heritage of the Institution of Engineers, Australia, and who was at that time a member of that Department.

One hundred and ten items, or sets of items, were uncrated, examined, photographed, and recorded on cards for purposes of further study and research. Recording procedures used were in line with those considered for adoption for moveable artefacts by the I E Aust Engineering Heritage Sub-Committee.

Following the initial cataloguing process some preliminary research was conducted on the artefacts by the author, being confined to general comment rather than of any specific relevance to past BMR programs. The original set of cards is held by the author; a copy being provided for use by BMR staff.

At the time of preparation of this summary members, present and past, of the BMR had begun research on the relevance of the artefacts to BMR history. The detailed and more complex description of the collection will eventually be published as a BMR Record under the title 'The BMR Historic Geophysical Apparatus Collection'. Table 1 summarises the collection holdings.

1. School of Natural Resources, University of New England, Armidale, N.S.W. 2351, Australia.

Literature on history of earth sciences

Many of the artefacts have origins in other countries of the world. Appreciation and understanding of the collection, therefore, must be gained by study of global literature.

Geophysics is itself a multi-disciplinary subject; the BMR collection reflects certain facets. In reviewing the literature the terms of reference were kept broad so as not to lose perspective.

Early texts of direct relevance are rare, most 19th century and early 20th century earth-science work being discussed instead in books on natural philosophy, electrical engineering and the like. Walker (1913), however, reviewed the latest in seismological technique at the time when Milne died. The life and work of Milne on the Isle of Wight, England is the subject of a small study by Herbert-Gistar & Nott (1974). Early use of the pendulum in determination of gravity force is the topic of a detailed history by Lenzen & Multhauf (1965).

Wartnaby (1957) published a brief historical survey and catalogue of exhibits in the then existing Seismological section of the Science Museum, London. (This section has now been incorporated into an extensive new gallery of Geophysics and Oceanography opened February, 1977.) This study includes a 51-entry bibliography on seismology from 1702-1954 along with descriptions of 45 sets of equipment held by the Museum. Wartnaby (1972) has studied the works of John Milne and Robert Mallet for a doctoral thesis, this following his previous M.Sc. thesis on the only work of Milne. Descriptions of the new Science Museum, London gallery (which includes material relevant to Australian history) are available in McConnel (1976, 1977).

A commemorative issue of 'Timebreak' (Geo. Space Corp., 1971) explored the development of reflection seismology in exploration. The history of early seismic exploration method was published by Mintrop (1930). Dobrin (1960) includes a brief history of geophysical method, as does Jakosky (1950).

Other early texts on geophysics include Davison (1921), Davison (1927), Ambronn (1928), Gutenberg (1929), Rothe (1930), Wien & Harms (1930), Shaw (1931), Imamaru (1937), Leet (1938), Heiland

(1940), Nettleton (1940), Byerly (1942), Rayleigh (1945), Dix (1952), Landsberg (1952), and Eve & Keys (1956).

Specific histories compiled include Weatherby (1940) on seismic prospecting, Eckhardt (1940) on gravity method for oil search, and Rust (1938) on electrical methods.

The Royal Society arranged a London exhibition in 1925. Its report, Royal Society (1925) includes descriptions of geophysical demonstrations by Sir Napier Shaw, FRS (Solar and Terrestrial Radiation and Meteorology), Capt. C. J. P. Cave (Cloud photographs), C. Chree, FRS and C. S. Wright (Terrestrial Magnetism and Atmospheric Electricity), and H. H. Turner, FRS and J. J. Shaw (Seismology).

Turning to works more specific to Australian history it will be found that little exists. History of Australian science studies are embryonic, there being no definitive work yet completed. Hoare (1975) provided a brief account of science since Cook's first voyage to Australia in the 1760s. A little depth into geophysical endeavours in meteorology and astronomy of the 1800s is available in the published correspondence compiled as a chapter of a work by Mozley-Moyal (1976). Introductory sections on meteorology and astronomy give some useful information on magnetic data and observatory programs. Source documents held in libraries throughout Australia can be located using a guide to manuscripts by Mozley (1966). The Adolph Basser Library of the History of Australian Science, Academy of Sciences Building, Canberra holds extensive historical science material.

Wood (1966) reviewed the early weather and astronomical observatories of Sydney, Melbourne, Adelaide, Perth, Riverview College, and Mount Stromlo, and describes past events of Government and University groups since settlement—1780s up to 1966. Wood begins his account with the comment that James Cook came to the then vaguely known Australasian region to observe a transit of Venus at Tahiti in 1769. Cook also performer valuable magnetic and marine charting at such a standard of precision that many of his charts were not bettered for nearly two centuries. Cook's voyages are described in a popular style by R. and T. Rienits (1968). Day (1966) reviews the development of Australian geophysics since the earliest settlement to about 1950.

An historic sea voyage made a century later, that of the *Challenger* of 1872-1876 (Linklater, 1972), also provided some geophysical measurements in the Australasian region. The emphasis, however, was mainly on exploration of the depths of the oceans. In 1914 the annual meeting of the British Association was held in Australia. Howarth (1931) provided a brief report of visitors' activities. A more detailed account was published in the Report of the British Association for 1914, p. 679.

Cooks' magnetic measurements had been preceded by those of Bligh and Hunter in 1787-1789, and earlier still by Tasman in 1642. Green (1972) provides a short account of magnetic measurements of the 1840s, including the operations of the short-lived magnetic program of the Rossbank Magnetic Observatory of Hobart Town.

Early accounts of geophysical method being used in exploration for minerals, water, and oil include Aplin (1926), and Hautpick (1928)—who discussed the methods being adopted at that time, suggesting their

GRAVITY

—Askania, Oertling, torsion balances 1920
—Thyssen gravimeter 1920
—Holweck-Lejay inverted pendulums 1955
—North American marine set 1955

MAGNETISM

—Kew-pattern dip circles 1920
—Sharpe low-precision dip circle 1955
—Kew-pattern magnetometers of British, German, US origin 1910
—Sharp personal torsion magnetometer 1965
—Earth-inductors of German origin 1920-50
—Vertical and horizontal force variometers of British and German design 1930-50
—Proton precession magnetometer 1950
—Magnetometer calibrators 1930-50

RADIOACTIVITY

—Portable geiger counters of Australian, Dutch, Canadian, British and U.S. design 1955
—Portable scintillometers of Canadian, U.S. design 1955
—Electronic scaling units and amplifiers of British, Australian design 1955
—Airborne scintillometers of Canadian, British design 1955
—Borehole logging set 1955
—Sample assay units 1955

SEISMIC

—Cambridge Inst. Soundranging set with telephones 1920
—BMR long-period seismographs 1960
—Mid western reflection set for marine use 1955

POSITION

—Aneroid altimeter 1950
—Observers magnetic compasses 1935
—NML Straight line flight indicator 1950
—Theodolites 1930-40

TIME INTERVAL

—Landis observatory master clock
—Synchronome slave clocks 1910-50
—Chronometers in gymbals 1880-1960

ATMOSPHERIC PARAMETERS

—Dust samplers and observing kit 1920-1955
—Recording barograph 1900

SOLAR RADIATION

—Spectro-helioscope (part only) 1950
—Jordan sunshine recorder 1900

ELECTRICAL INSTRUMENTS

—Toepfer, Askania, Cambridge optical-lever galvanometers 1910-30
—Quadrant mirror electrometers 1900
—Weston voltmeter and ampmeter 1905, 1930
—Weston multimeter
—Ionisation tester
—Sullivan-Griffith bridge 1950
—L and N potentiometer 1950

RECORDERS

—Light spot photographic 1930, 1960
—Cambridge Vibrograph 1940

PROSPECTING EQUIPMENT

—EM Compensator 1950
—Ratiometer 1950
—ABEM Slingram & Turam 1955
—SP Voltmeters 1950

Table 1. Summary of the collection.
(Dates given indicate approximate decade only)

increased use in Australia as a means to boost the then ailing mining industry.

The definitive early work on the relevance and application of geophysical method in Australia was that of the Imperial Geophysical Experimental Survey. This study (Broughton-Edge & Laby, 1931), was made to establish the value of geophysical methods in Australian conditions, not to discover profitable geological materials. This survey was a prime factor in the later creation of the BMR in 1946.

The Bureau of Mineral Resources today maintains five geophysical observatories in which geomagnetic and seismic equipment are operated; Dooley (1958) has compiled an account of the history of the Toolangi (Victoria) observatory.

Gravity measurements have been made since the 17th century, so it is not surprising that they were made in Australia from its earliest settlement. Dooley & Barlow (1976) have published an extensive account of gravity measurements made in Australia since 1819, providing details of instrumentation through the many references cited. Figure 1 shows an early Oertling gravity torsion balance of the collection.

Figure 1. Oertling torsion balance, c 1915.

Assessment of the collection

Australian professional science in the 19th century follows a pattern more like that of the USA for, compared with Europe, very little physical science was practised. Records reveal that some scientific instruments were in use throughout the land, but it seems little has survived from the 19th century.

Prior to the structured work of government agencies, which began in the 1930s, geophysical work was scattered, uncoordinated and poorly documented. As a consequence historians must re-discover the past.

The BMR Collection is the most extensive assembly of historic geophysical apparatus in Australia. All other national sources combined would add little more to its scope. It is hoped that the collection will be made more available to the public, for it presents a significant amount of national activity in the more modern era of earth sciences.

The collection is lacking in originals and replicas of epoch-making designs of overseas and to a lesser extent local origin. A balanced collection would need items that represent the earlier works of such people as Tasman, Cook, the Challenger Expedition and the Threlfall gravity meter. The collection is a most worthy basis for expansion, if acquisition becomes possible.

Notable artefacts from the Australian viewpoint include several Australian-made equipments, the range of radioactivity measuring sets, and several pieces that have important associations with early scientists in the region. Figure 2 is an early etching of the dip needle design commonly known as the Kew pattern.

The collection appears to possess little of global importance. Much of what is held is similar to holdings of the larger Northern Hemisphere science museums (Sydenham, 1977). It is, however, important to realise that this collection is as valuable to the nation of the future as it is to us immediately.

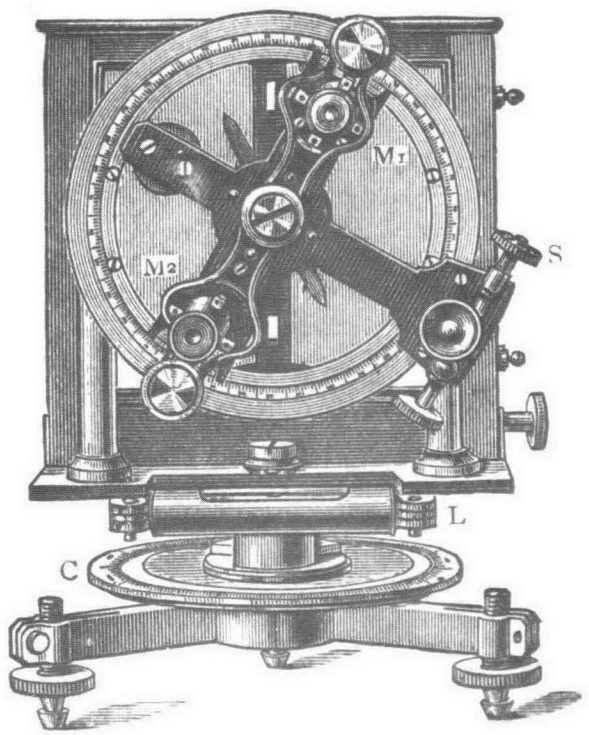

Figure 2. Kew-pattern dip-circle (Mullineux-Walmsley, 1910).

Historical geophysical instruments elsewhere in Australia

A small number of early geophysical instruments are extant in other Australian collections. More research

is needed to provide an exhaustive list; the following provides an indication.

The Science Museum of Victoria, Melbourne, has some of the instruments used in the original Melbourne Observatory. These include galvanometers from the 1840s, a sunshine recorder, and an 1880s three-component seismograph.

The Department of Geology, Melbourne University, is to donate a small collection of exploration apparatus (including an early gravity meter) to the BMR holdings.

The Basser Library of Australian Science, Canberra has custody of radio apparatus used in early Antarctica magnetosphere research.

Relics from the Sydney Observatory, the Bureau of Meteorology, and the Department of Health were presented to the Museum of Applied Arts and Sciences, Sydney. These include meteorological instruments, galvanometers and recording barographs and thermographs of the 1900 era.

Another source of early equipment is University Departments concerned with Physics, Earth Sciences, and Engineering. These have yet to be studied, but it is apparent that a considerable amount of obsolete field equipment has gone to these institutions from commercial companies who no longer had use for it.

General comment on instruments of the collection

An IEAust. code number was assigned to each article, a label being attached to items recorded. Most items also possess a BMR vocabulary code that shows their relationship to the general inventory. A card was completed for each item. These were then sorted in groups on the basis of the physical variable that the apparatus measured. Table 1 summarises the collection and should be consulted when reading the following comments.

Gravity force

Torsion balances. Torsion balances originated and were used in the 1900-1930 period following the success of the Eotvos balance (designed in the late 1890s) in geophysical exploration for oil. Their relative fragility, sheer size, and slow operation eventually led to a decline in use. They were used to determine gravity gradients and curvatures of equipotential surfaces, not the absolute value at a station, and were capable of detecting 10^{-13} gm force differences. They made use of opto-mechanical transducer principles.

The collection contains Askania and Oertling torsion balances, and a Thyssen gravimeter known to have been used in oil search in Australia and Indonesia.

Pendulums. The development of pendulum measurements of gravity began in the 1600s. By the 19th century absolute measurements were made by this method. Early in the 20th century the nominal 0.5 m (and shorter) pendulum apparatus was introduced into exploration geophysics. This development has been researched in depth by Lenzen & Multhauf (1965), who reported the progress to about 1920. Dooley & Barlow (1976) have published an account containing the pendulum measurements made in Australia. The most recent use in Australia was with the multiple instrument systems of the Russians in 1974. Pendulum absolute gravity measurements are rapidly being displaced by the thrown-mass laser interferometer of absolute determination, the grid being filled in by relative measurements made with spring-mass instruments.

The collection contains a complete field system for using the inverted pendulum of Holweck-Lejay design. This system was used by Shell (Queensland) Development Pty Ltd in southern Queensland in 1940-42 (Dooley & Barlow, 1976).

Marine gravity. The BMR, in 1957, purchased a complete North American system for conducting gravity surveys in coastal areas. A deck-mounted hoist unit is used to lower an assembly to the sea-floor. This latter unit houses a spring-mass gravimeter, and can be levelled and read from aboard ship. The gravimeter itself was not recorded, not being in the store inventory. The Bureau possesses a number of spring-mass gravimeters.

Earth's magnetic field

Dip needles. The dip of a compass needle was noticed in earliest times. By the time James Cook made his Australian voyages in the 1760s dip-needle devices had become quite sophisticated. The Kew (Observatory) pattern originated in England. It incorporated opposing optical viewers for precise reading of the vertical angle, and was in common use at the end of the 19th century. Mullineux-Walmsley (1910) gives a description of its use and a fine etching of a unit similar to those of this collection. Dip circles are still used for low precision surveys, the Sharpe instrument of the collection being a relatively modern example.

One of the dip circles was previously owned by Sir Douglas Mawson.

Absolute magnetometers. Commonly known as theodolite magnetometers, these were used to determine declination D and horizontal force H, and—depending

Figure 3. Carnegie Institution of Washington magnetometer equipment, c 1900.

on accessories, inclination I by the earth induction principle. H was determined by the very tedious method of oscillations and deflections. Gauss, in 1832, appears to have been the first to use the dynamic method for H determination.

Mullineux-Walmsley (1910), and Glazebrook (1922, p. 533) provide etchings and lengthy descriptions of the use of the Kew pattern (Elliot) magnetometer systems.

The DTMCIW—illustrated in Figure 3—and Bausch units are American equivalents. These instrument systems provide magnificent examples of the skill of mechanical and optical instrument-makers in the 1900 period.

The equipment sets in the collection were used at Watheroo Magnetic Observatory, and for field observations throughout Australia, SE Asia and SW Pacific. They were passed to BMR when the Watheroo Magnetic Observatory was transferred from the Carnegie Institution of Washington to the Commonwealth in 1947.

Earth inductors. In 1831 Faraday, after many years of experimental frustration, observed and identified the conditions wherein electricity is generated by interaction with magnetic field. Within days he demonstrated that a loop rotated in free space generates a voltage potential because of the existence of the earth's field. In 1853 Weber used this principle quantitatively to determine the absolute value of the earth's field.

Earth inductors were in common use by 1900; the Askania unit of the collection was still marketed in 1969, for complementing total intensity proton-magnetometer measurements by the determination of inclination to $\pm$ 0.3 arc minutes.

A trial, made in Europe by Logachev in 1936, sought to use the earth inductor as magnetometer for airborne surveys. The sensitivity of 1000 gamma available to him was, however, far from adequate for such purposes.

Variometers. The instruments of the collection are commercial forms of Schmidt's 1915 magnetic field balance. An H form magnet is balanced on knife edges, and is read by visual observation of an optical lever. The instrument principle can be arranged to measure either the vertical or the horizontal component of the earth field. An adjustment exists that enables the absolute field at a station to be balanced, so that variations from station to station can be determined. Telford & others (1976) describe the operation and theory of the balance: instrument orientation with respect to the field components being measured is a critical parameter and so these instruments are supplied wtih magnetic compasses. They are inexpensive and reliable, and can provide a resolution of 10 gamma. Operation, however, is tedious, attributing to their eventual decline in usage, especially for horizontal component determination. Hilger and Watts, for example, discontinued sales of new instruments (models SGI, SG2) before 1960.

The age of the variometers held ranges from 1935 to 1955.

Proton or nuclear precession. The phenomenon of nuclear magnetic resonance was quantified around 1945. The principle enabled magnetic field strength to be measured by a new procedure. Varian and Packard, in 1954, developed a new form of total field instrument which became known as the proton precession magnetometer. Advantages were that it was little more than a bottle of water, a coil and electronic circuitry; sensitive; self-calibrated, with absolute measurement to within 1 gamma; and that it did not need specific orientation or stationary working. It did, however, require a ls integrating time between observations.

The Bureau, realising the potential of this new device, decided to construct units for its own use. This was prior to commercial sale of satisfactory field devices. Two units, now without sensors, exist in this collection, along with the airborne towing bird.

Calibrators. Magnetometers can be calibrated either by placing them in a uniform magnetic field of known value, or by observing their response to suitably placed permanent magnets. The former method is precise when the field is produced by electrical current in coils placed in the Helmholtz arrangement.

This collection includes a coil and current source combined, a current calibrating bridge, and a unit made for, or with, a flux-gate magnetometer.

Radioactivity

In 1896 Bequerel reported the existence of radioactive emanations from uranium compounds. Two years later Villard identified the more penetrating gamma rays. Interest in radioactive materials became of fundamental importance to modern science in general, but the demand for radioactive materials was not great until the 1940s when war and then the peaceful uses of radioactivity provided a demand for ores.

First detectors were leaf electroscopes and visually observed scintillation setups. In 1908 Geiger, working with Rutherford, devised an ionisation chamber detector which was later improved by Müller in 1928. Availability of the vacuum tube amplifier enabled sensitive detectors of radioactivity to be devised. By the late 1940s large-scale interest existed in inexpensive portable prospecting Geiger-Müller tube devices. The development of the photo-multiplier in the late 1930s enabled more sensitive measurements to be made by the scintillation method. Thus by the time that the boom in demand for radioactive ores arose around 1950, adequate technology existed for its rapid detection. Survey was either by hand-held ratemeter (using Geiger or scintillation detectors), airborne detector (only scintillometers sufficed), or by well-logging.

The Bureau was heavily committed in the 1950s with this form of search. To assist the program a wide range of equipment was purchased from Australia, UK (mainly through contractors to AERA, Harwell), Holland, Canada and the USA. A geiger counter, manufactured in Melbourne, is shown in Figure 4.

Radioactivity measuring instruments make use of counting of electrical impulses generated by the discrete nuclear process. The time-rate of counts generated is a measure of radioactivity strength. Thus, many units are termed ratemeters.

The collection strongly reflects the derivative nature of Australian technology, and the range of countries from which detection equipment was obtained for use in simple prospecting, in sample assay, and in airborne survey.

Seismic method

Laboratory seismic recording of earthquake activity began with mechanical recording methods, such as Milne's of around 1895. In 1904 Galitzin added electromagnetic transduction, thereby obtaining greatly increased gain and avoiding the restriction for recording from the energy available in the signal. In 1917 Mintrop's mechanical seismic recorder was applied to exploration needs, and by 1921 reflection seismic pros-

Figure 4. Austronic, Melbourne, geiger counter c 1952.

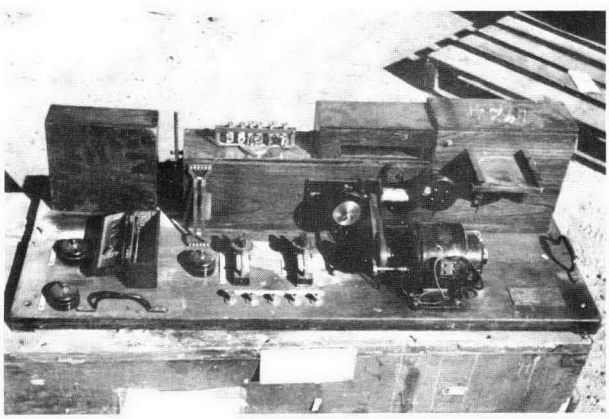

Figure 5. Recording and developing unit of Cambridge Instrument Co., sound-ranging equipment, c 1920

pecting was being used with great effect. Around this time military research was interested in the problem of ranging in on hostile big guns. Research into acoustic location was conducted from the 1914 period onward. An account of the techniques is given in Glazebrook (1923, p. 733). An internal publication of Cambridge Inst. Co. (1956) provides a photograph and brief description of the camera of the system. Figure 5 is a photograph of the camera and developing unit from the collection; this research significantly influenced early workers involved in the introduction of seismic exploration technique. The requirement for microphones with an unusually low and narrow band frequency acceptance response highlighted the need for geophones and galvanometers to be carefully matched.

The BMR Collection contains a virtually complete sound-ranging system dating from around 1916. The system was used in Australia by the Imperial Geophysical Experimental Survey (Broughton-Edge & Laby, 1931). It was reworked in 1941 with additions and alterations being made. Historically this is an important assembly, for it demonstrates one of the earliest uses of geophones, contains an example of the first-ever automatically developed photographic filmstrip recording system, and contains such items of historic interest as an Einthoven string recorder, a tuning fork synchroniser, and a mercury-wetted relay.

In more recent times the BMR constructed observatory vertical seismographs. Two of these exist in the collection.

A complete marine seismic system has been preserved from the 1960 era. Only certain items of this were recorded here.

Related variables

Position location and control. Barometric pressure altimeters and magnetic compasses of flight origin exist in the collection. Especially interesting are straight-line flight indicators using electromechanical computing devices. These were produced at the National Standards Laboratory (now National Measurement Laboratory), Sydney around 1952. A unit is illustrated in Figure 6.

Time interval. A range of chronometers and a system of slave-master electric time keeping has come into the collection. Most of the items are from the Watheroo Magnetic Observatory. None are particularly important but the range covers a wide period of manufacture.

Atmospheric dust. Three items, two from the 1920 period, exist that enable samples to be taken and observed.

Atmospheric pressure. The recording barograph initialled R.F. (Richard Freres) is an interesting example because of the individually sealed capsules, and the use of a considerable tensioning mass that is applied to the aneroid capsule stack.

Solar radiation. The Jordan style sunshine recorder is identical with illustrations of 1888 models.

Electrical indicating instruments. Optical lever galvanometers used in conjunction with earth inductors exist. The quadrant mirror electrometers are typical of 1900 designs. These were used in the atmospheric electricity program at Watheroo from 1922 to the early 1950s. Various single and multi-purpose meters illus-

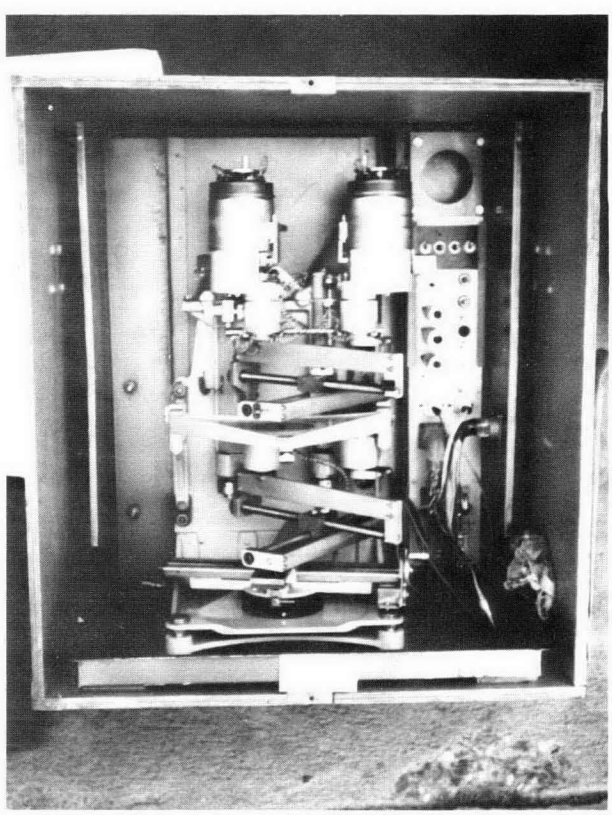

Figure 6. Straight-line flight indicator Mk 2, designed and constructed by the CSIRO Division of Electrotechnology, c 1950 (now NML).

trate the evolution of indicating instruments from pre-1900 to the 1950s.

Bridges. The units are relatively modern, dating from the 1950 period.

Recorders. Various kinds of signal recorder are represented.

The collection contains mechanically driven systems, for use with optical-lever devices requiring photographic recording.

The Cambridge Universal Vibrograph recorder, manufactured in 1944, and of design originating in 1925, records ground vibrations by means of a stylus that presses on celluloid film.

Prospecting equipment

At the time of the visit to the Oaklands store in May 1977, the collection did not include any items of electrical or electromagnetic prospecting equipment. Several such items have since been added. They include an early ratiometer (used in the potential drop ratio method) and EM compensator system, built by BMR to the basic design of original instrumentation used by the Aerial Geological and Geophysical Survey of Northern Australia; several early sets of Slingram and Turam equipment manufactured by the Electrical Prospecting Company of Sweden (ABEM); and various voltmeters used for self-potential surveys.

Acknowledgements

This work was undertaken on behalf of the Bureau of Mineral Resources, Geology and Geophysics. The collection was recorded with help from A. Spence (BMR), A. Hugill and N. Tanim (University of New England) and officers of the Department of National Development Supply Section. A University of New England research grant provided costs of visiting Oaklands. The author wishes to express appreciation for this support and also his gratitude to the Assistant Director, Geophysics (N. G. Chamberlain) and other officers of the BMR who have had the foresight to store historic instruments for eventual display and study.

References

AMBRONN, R., 1928—ELEMENTS OF GEOPHYSICS. *McGraw-Hill, New York.*

APLIN, W., 1926—Scientific prospecting. Lecture delivered at Mount Morgan Technical College, May, 1926. (Copy available Department of Geology Library, University of New England, NSW.)

BROUGHTON-EDGE, A. B., & LABY, T. H., 1931—THE PRINCIPLES AND PRACTICE OF GEOPHYSICAL PROSPECTING. *Cambridge University Press, Cambridge.*

BYERLY, P., 1942—SEISMOLOGY. *Prentice-Hall, New York.*

CAMBRIDGE INSTRUMENT CO., 1956—'75 years'. Cambridge Instrument Co., Internal Publication, Cambridge, England.

DAVISON, C., 1921—A MANUAL OF SEISMOLOGY. *Cambridge University Press, Cambridge.*

DAVISON, C., 1927—THE FOUNDERS OF SEISMOLOGY. *Cambridge University Press, Cambridge.*

DAY, A. A., 1966—The development of geophysics in Australia. *Journal and Proceedings of the Royal Society of NSW*, **100**, 33-60.

DIX, C. H., 1952—SEISMIC PROSPECTING FOR OIL. *Harper, New York.*

DOBRIN, M. B., 1960—GEOPHYSICAL PROSPECTING. *McGraw-Hill, New York.*

DOOLEY, J. C., 1958—Centenary of Melbourne–Toolangi Magnetic Observatory. *Journal of Geophysical Research*, **63**, 731.

DOOLEY, J. C., & BARLOW, B. C., 1976—Gravimetry in Australia, 1819-1976. *BMR Journal of Australian Geology and Geophysics*, **1**, 261-71.

ECKHARDT, E. A., 1940—A brief history of the gravity method of prospecting for oil. *Geophysics*, **5**, 231-42.

EVE, A. S., & KEYS, D. A., 1956—APPLIED GEOPHICS. *Cambridge University Press, London.*

GEO SPACE CORPORATION, 1971—Various short articles and illustrations. *Time Break*, **9**, 49.

GLAZEBROOK, R. (Editor), 1922—DICTIONARY OF APPLIED PHYSICS, **2**. *Macmillan, London.*

GLAZEBROOK, R. (Editor), 1923—DICTIONARY OF APPLIED PHYSICS, **4**. *Macmillan, London.*

GREEN, R., 1972—Sponsored research in geomagnetism 130 years ago. *EOS*, **53**, R, 778-79.

GUTENBERG, B., 1929—LEHRBUCH DER GEOPHYSIK. *Gebruder Borntraeger, Berlin.*

HAUTPICK, E. DE, 1928—GEOPHYSICS IN MINING. *Elphick, Dennis & Co., South Australia.* (Copy available, Department of Geology Library, University of New England, NSW.)

HEILAND, C. A., 1940—GEOPHYSICAL EXPLORATION. *Prentice Hall, New York.*

HERBERT-GUSTAR, L., & NOTT, P. A., 1974—EARTHQUAKE MILNE AND THE ISLE OF WIGHT. *Vectis Biographies, Isle of Wight, England.*

HOARE, M. E., 1975—Light in our past: Australian science in perspective. *Search*, **6**, 285-90.

HOWARTH, O. J. R., 1931—The British Association for the Advancement of Science: A Retrospect 1831-1931. *British Association, London*, 134-40.

IMAMARA, A., 1937—THEORETICAL AND APPLIED SEISMOLOGY. *Maruzen, Tokyo.*

JAKOSKY, J. J., 1950—EXPLORATION GEOPHYSICS, *Trija Publishing Co., Los Angeles.*

LANDSBERG, H. E., 1952—ADVANCES IN GEOPHYSICS, *Academic Press, New York.*

LEET, L. D., 1938—PRACTICAL SEISMOLOGY AND SEISMIC PROSPECTING. *Appleton-Century, London.*

LENZEN, V. F., & MULTHAUF, R. P., 1965—Development of gravity pendulums in the 19th century. *United States National Museum Bulletin*, **240**. Paper **44**, 301-48.

LINKLATER, E., 1972—THE VOYAGE OF THE CHALLENGER. *John Murray, London.*

MINTROP, L., 1930—ON THE HISTORY OF THE SEISMIC METHOD FOR THE INVESTIGATION OF UNDERGROUND FORMATIONS AND MINERAL DEPOSITS. *Seismos, Hannover.*

MCCONNEL, A., 1976—A new display of historical instruments used for geographical research and exploration on view at the Science Museum, London. *Geographical Journal*, **142**, 560-2.

MCCONNEL, A., 1977—A new geophysical and oceanography gallery at the Science Museum, London. *Hydrographic Journal*, **3**, 30-4.

MOZLEY, A., 1966—A GUIDE TO THE MANUSCRIPT RECORDS OF AUSTRALIAN SCIENCE (Australian Academy of Science). *Australian National University Press, Canberra.*

MOZLEY-MOYAL, A., 1976—SCIENTISTS IN NINETEENTH CENTURY AUSTRALIA. *Cassell Australia, Stanmore, NSW*, 152-71.

MULLINEUX-WALMSLEY, R., 1910—ELECTRICITY IN THE SERVICE OF MAN, **1**. *Cassell, London.*

NETTLETON, L. L., 1940—GEOPHYSICAL PROSPECTING FOR OIL. *McGraw-Hill, New York.*

RAYLEIGH, J. W. S., 1945—THE THEORY OF SOUND, 2 volumes. *Dover, New York.*

RIENITS, R., & T., 1968—THE VOYAGES OF CAPTAIN COOK. *Hamlyn, London.*

ROTHE, E., 1930—LES METHODES DE PROSPECTION DU SOUS-SOL. *Gauthier-Villers, Paris.*

ROYAL SOCIETY, 1925—PHASES OF MODERN SCIENCE. *A. and F. Denny, London.*

RUST, W. M., Jr, 1938—A historical review of electrical prospecting methods. *Geophysics*, **3**, 1-6.

SHAW, H., 1931—APPLIED GEOPHYSICS. *HMSO, London.*

SYDENHAM, P. H., 1977—Source guide to history of measurement technology material. Pt 1. *Measurement and Control*, **10**, 257-65.

TELFORD, W. M., GELART, L. P., SHERIFF, R. E., & KEYS, D. A., 1976—APPLIED GEOPHYSICS. *Cambridge University Press, London.*

WALKER, G. W., 1913—MODERN SEISMOLOGY. *Longmans Green, London.*

WARD, F. A. B., 1970—TIME MEASUREMENT. *HMSO, London.*

WARTNABY, J., 1957—SEISMOLOGY. *HMSO, London.*

WARTNABY, J., 1972—Seismological investigations in the nineteenth century. Ph.D. thesis, University of London (unpublished).

WEATHERBY, B. B., 1940—The history and development of seismic prospecting. *Geophysics*, **5**, 215-30.

WIEN, W., & HARMS, F. (Editors), 1930—HANDBUCHER EXPERIMENTAL-PHYSIC, 25, GEOPHYSIK: *Akademische Verlagsgeselschaft, Liepzig.*

WOOD, H., 1966—The sky and the weather *in* A CENTURY OF SCIENTIFIC PROGRESS. *Royal Society of NSW, Sydney*, 379-430.

BMR Journal of Australian Geology & Geophysics, 3, 1978, 248-253

Storage and retrieval systems for the Reference Minerals Collection and the Georgina Basin Project

Eugene L. Smith

Introduction

Two major information storage and retrieval systems now in operation at the Bureau of Mineral Resources —the Reference Minerals Collection Index and the Georgina Basin Project Data Base—are based on INFOL. The first system, used in progressively indexing mineral specimens in the BMR Museum, has been in operation 5 years and will continue indefinitely. The second system, designed for a specific field project, has been in operation for 4 years and has a finite life. The systems are run through CSIRONET on the Cyber 76 computer.

INFOL (described in detail in CSIRO Division of Computing Research Manuals) is a generalised information storage and retrieval system designed to create, maintain, and interrogate a file of information. Basically, it is a free-field language which allows items of information of variable length to be written in plain English. It does not require the use of 80-column coding forms; data are stored in a compressed form—blank fields and non-significant blanks in the data do not take up storage space; complex search strategies are possible; and the report generators are flexible. Output may be obtained as a written report on visual display units, paper or microform, or as input for other computer applications.

The major phases of an INFOL system are ESTABLISHMENT, INTERROGATION, UPDATE, and BOOKKEEPING. During the ESTABLISHMENT phase a *file* (i.e., a list) of *elements* (e.g., mineral specimens) consisting of a number of *items* (identification and descriptive information) is created. The file can then be interrogated or updated. Retrieval criteria can apply to items or sub-items—testing for the existence or non-existence of data, or testing relational criteria. The file may be updated by adding new elements; removing existing elements; adding, removing or changing items; or adding or changing sub-items. BOOKKEEPING occurs automatically at certain stages of INFOL operations. It gives information essential for specifying report formats.

The Reference Minerals Collection index

The Reference Minerals Collection housed in the Bureau of Mineral Resources Museum contains over 20 000 mineral specimens and has a growth rate of about 1000 specimens per year. Approximately half of the specimens are from private collections purchased by the Australian Government. The collection contains about half the known mineral species, and is maintained as a reference for BMR personnel and other research workers. It also provides specimens for display.

Because of the size, growth rate, value, and uses of the collection, a computer system to facilitate its effective management and accessibility was started in 1973. It now contains information on 6953 mineral specimens.

Figure 1 is an example of a completed coding sheet. Each element (in this case, mineral specimen) on the file contains up to 24 items of identification and descriptive information. The first item is a unique integer used to identify and index each element. In the case of the Minerals Index, it is the registered number of the mineral specimen.

Item		No	Information
Reg. Number (R-)		*1*	27057
Mineral species		*2*	STIBNITE
Dana Number	m	*3*	2*8*2*1*
Variety Name		*4*	
Colour	m	*5*	GREY *
Habit	m	*6*	XD *
Lustre	m	*7*	MT *
Other	m	*8*	
Associated Minerals	m	*9*	
Composition - anions	m	*10*	SFI *
Composition - cations	m	*11*	SB *
Identification	m	*12*	VIS *
Continent		*13*	AU
Country		*14*	AUSTRALIA
State		*15*	NEW SØUTH WALES
Region		*16*	
Map Sheet		*17*	
Grid Reference		*18*	
Origin	m	*19*	CHI *
Date acquired		*20*	
Receptacle		*21*	88114
Other location data		*22*	HILLGRØVE
Size	m	*23*	8*1*
Value		*24*	20*

G465-57A

Figure 1. Mineral collection coding sheet.

The standard reference for determining the species and varietal names (items 2 and 4) of mineral specimens is the 1972 edition of *Glossary of Mineral Species* by Michael Fleischer. The standard reference for determining the Dana number and the cationic and anionic composition (items 3, 10, and 11) of mineral specimens is the 7th edition of *The Dana System of Mineralogy*. The colour, habit, lustre, other distinctive properties and associated minerals (items 5, 6, 7, 8 and 9) are determined by observation. The remainder of the information is obtained from the master catalogue or from the specimen label. The value of the specimen (item 24) is subject to periodic review.

Items 6, 7, 8, 10, 12, 13, 16, and 19 are coded items. That is, each of these items consists of a finite set of possible descriptive terms, each of which has been defined and given a mnemonic code. In Figure 1, item 6, XD is the code for crystallised. MT is the code for metallic; SFI, sulphides; VIS, sight identification; AU, Australia; and CHI is the code for a specific collection. All data for coded items is prepared in the coded form. However, reports may contain either the coded forms or the decoded descriptive terms.

The simplest and most often used form of file updating is the addition of new elements to the file. The data may be coded on the coding sheets, or data preparation operators may work directly from the master catalogue.

The main use of the interrogation phase is in file management and data editing. The value of ad hoc interrogations and production of catalogues remains limited, as less than a third of the specimens have been indexed.

File interrogation can be formulated to produce an almost limitless variety of reports. One type of report used for file management is a list of all registered numbers on the file. A second type of report, a replica of the master catalogue, is useful in checking that the basic information in the master catalogue has been correctly transferred to the file. A third type of report gives a complete listing of all information held on the file. An alphabetical listing of all mineral specimens is produced periodically. It is used to edit data as well as to provide information on the number of specimens from various localities held by the Museum.

Two small special-purpose programs have been written to operate on output from retrieval reports. One calculates the total value of indexed specimens. The other produces an alphabetical list of mineral species and the total number of each species indexed.

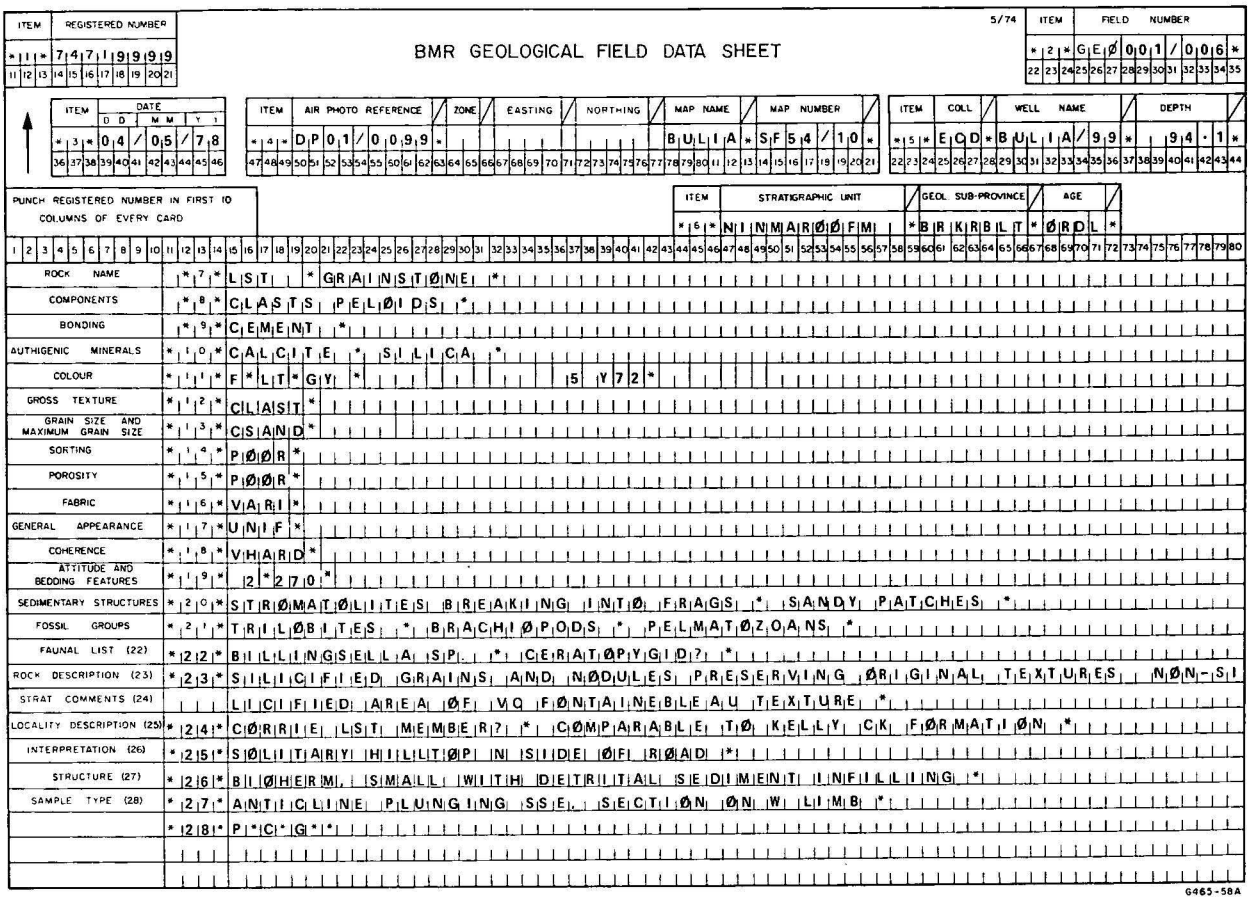

Figure 2. Geological field data sheet.

The Georgina Basin Project data base

The Georgina Basin consists mainly of Cambrian and Early Ordovician marine rocks covering an area of about 325 000 square kilometres in western Queensland and the Northern Territory. Limestone deposition was continuous and widespread in various sedimentary environments. The rocks are structurally uncomplicated and contain abundant fossils.

The project to study the Georgina Basin was started in 1974 and is scheduled to run for 7 years. The aim is to produce a regional biostratigraphic and environmental framework that will also aid in interpreting more structurally complex basins, such as the Amadeus, Wiso, and Daly River.

The Georgina Basin Project storage and retrieval system was started in April 1974 as a pilot study into the possibility of automated storage, retrieval, and processing of geological field data in BMR. The file now comprises 3664 sets of field observations and related data. In addition to the field observations, 791 whole-rock analyses, 194 sets of faunal determinations, 149 detailed carbonate petrographic reports and 90 biostratigraphic analyses are available.

Each element (in this case a field locality, or rock, drillcore or cutting sample) on the file contains up to 41 items of identification and descriptive and interpretive information. Up to 28 items of information are entered from the Field Data sheet (Fig. 2), 8 additional items may be entered from the Carbonate Petrographic Sheet (Fig. 3), and the 5 remaining items may be entered by coding on traditional 80-column coding forms.

In the body of the Field Data sheet and the Carbonate Petrographic sheet, abbreviated words come either from lists prepared for use with the data base, or from the list of abbreviations used by BMR in map compilation. The number of abbreviations used exceeds INFOL's limit for coded items.

In the example of a completed Field Data sheet (Fig. 2), item 1 is the registered number, item 2 the field number. Item 11 allows for subjective descriptions of primary and secondary colours of fresh and weathered surfaces as well as the GSA rock colour code. Item 19 contains the dip and dip direction of an outcrop, and any distinctive bedding features. In item 28 the letter codes indicate that the sample was taken for petrographic, conodont, and geochemical study: The form is large enough for most requirements, but detailed descriptions, with a limitation of 1100 characters per item, may be appended to the sheet.

Figure 3 is an example of a completed Carbonate Petrographic Information Sheet. It was designed as a laboratory work sheet, providing information additional to field data and is usually completed well after the field season. It therefore contains INFOL update control words as part of the pre-printed data. All pre-printed data within the ruled boxes is punched where there is handwritten data.

Examples are given below of some uses of the system. They include collated data reports, project management reports, hypothesis testing and report writing.

Table 1 is an example of the detailed synthesis of field and laboratory data which can be achieved with this system. This type of report has proved especially valuable when geoscientists have been assigned areas for detailed study which were previously covered by several other persons. Printouts on selected areas can be taken into the field without risking the loss of the original Field Data Sheets or laboratory reports. A management report could, for example, be generated to help prepare a budget. We could ask, 'How many samples which were collected for geochemical analysis have not yet been done?', and get a single number answer. If we wished to identify the samples, we could obtain a list of registered numbers in numerical order.

Given in Table 2 is an example of how the system can be used in hypothesis testing. We have asked, 'In the Ninmaroo Formation are copper, lead, or zinc values over 50 ppm associated with high silica or organic carbon values; and on what airphotos do these values occur?' It is then possible, say, to consider the variable silica values of the tabulation, or by studying the relevant airphotos see whether the high metal values are associated with any particular structural feature.

Registered number:
74719999

Field number:
GEO001/006

Date:
4/May/1978

Air photo and map reference:
Digby Peaks 01/0099, Boulia, SF54/10.

Sample source:
E. C. Druce, Boulia/99, 94.1, 94.3

Geologic identification:
Ninmaroo Formation, Burke River structural belt, Lower Ordovician

Rock name:
Limestone, Grainstone

Components:
Clasts peloids

Bonding:
Cement

Authigenic minerals:
Calcite, silica

Colour:
F, Lt, Gy, 5 Y72

Gross texture
Clastic

Grain size and maximum grain size:
Coarse sand

Sorting:
Poor

Porosity:
Poor

Fabric:
Variable

General appearance:
Uniform

Coherence:
Very hard

Attitude and bedding features:
2, 270

Sedimentary structures:
Stromatolites breaking into frags., sandy patches

Fossil groups:
Trilobites, brachiopods, pelmatozoans

Faunal list:
Billingsella sp., Ceratopygid?

Rock description:
Silicified grains and nodules preserving original textures, non-silicified area of VC Fontainebleau texture

Stratigraphic comments:
Corrie Lst Member?, comparable to Kelly Ck Formation

Locality description:
Solitary hilltop N side of road

Interpretation:
Bioherm, small with detrital sediment infilling

Structure:
Anticline plunging SSE, section on W limb

Sample type:
P, C, G

Biostratigraphic analysis:
Cordylodus intermedius, Cordylodus prion, Scolopodus bassleri, Scolopodus iowensis, Oneotodus gracilis, Scolopodus transitans, Oneotodus erectus

Petrologist:
J. Kennard

Date
4/May/1978

Material type:
Thin section, 2 peels, polished section

Rock fabric and sedimentary structure:
Essentially homogeneous, skeletal material; concentrated in layers

Diagenesis:
Recrystallization: common-minor microspar pel
Dolomitization: common .02-.03 mm in grnst.; abundant .01 mm in micritic dol.
Other authigenics: common-minor dissem. pyrite in grnst., rare in micritic dol.
Porosity: 5% common sms. interpart vugs in slt. pel. grnst., up 15% in more slt. lam., partially interconnected

Primary features:
Peloids/pellets: abundant .03-.04 mm diffuse ghosts to mod. well defined, rndd.-ellip.
Clasts: rare 2 mm sl. rndd. lath., microdol.
Siliciclastics: 10-15% c. sand., qtz., feld., musc., tour.; 10% musc., m. slt. qtz. in sh. pel. grnst.

Comments:
Late compaction: solution of skeletal grains particularly at qtz. sand contacts

Rock name:
Cross-laminated c. silt., cs. pel. (clast), dol. (ms.), grnst. with wispy lam. and intlamd micaceous pel. grnst and intlamd (micritic) dol. (fs.)

Longitude and latitude:
140252411, 22283620, 422989, 7535525

Geochemical elements and units:
Ca %, Mg %, acid insol. %, Sr %, Fe %, Mn %, P ppm, Cu ppm, Pb ppm, Zn ppm, V ppm, Ba ppm, F %, org c %, Ca/Mg, Sr/Ca, Fe/Mn, Pb/Zn, Zn/Mg, Pb/Mg

Geochemical analyses:
36, .23, 6.10, .037, .028, .010, 50, 1, 15, 3, 10, 50, .005, .05, 156.52, .00, 2.8, 5, 13.04, 65.22

Heavy residue:
Rk. frags., limonite, ilmenite, zircon, tourmaline, fluorite (purple)

Table 1. An example of a synthesis of field and laboratory data (original as computer printout).

Regd. No.	Petrologist	Date	Material Type
*1*7471 9999	*30*INSERT J. KENNARD	*31*INSERT 4/5/78	*32*INSERT THIN SECTIØN * 2 PEELS * PØLISHED SECTIØN *

Rock Fabric and Sedimentary Structures	Sketch of Rock Fabric
*33*INSERT ESSENTIALLY HØMØGENEØUS, SKELETAL MATERIAL CØNCENTRATED IN LAYERS	

Diagenesis	Abundance Distribution Comment
*34*INSERT	
EARLY COMPACTION:	*
LATE COMPACTION:	*
SOLUTION:	*
CEMENT:	*
RECRYSTALLISATION:	CØMMØN – MINØR MICRØSPAR PEL *
SILICIFICATION:	*
DOLOMITISATION:	CØMMØN 0.02 – 0.03 MM IN GRNST; ABUNDANT 0.01 MM IN MICRITIC DØL *
OTHER AUTHIGENICS:	CØMMØN – MINØR DISSEM PYRITE IN GRNST; RARE IN MICRITIC DØL *
POROSITY: 5 %	CØMMØN SMS INTERPART VUGS IN SLT PEL GRNST; UP TØ 15% IN MØRE SLT LAM, PARTIALLY INTERCØNNECTED *

Primary Features	Abundance Comment
*35*INSERT	
PELOIDS / PELLETS:	ABUNDANT 0.03–0.04 MM DIFFUSE GHØSTS TØ MØD WELL DEFINED, RNDD ELLIP *
OOIDS:	*
CLASTS:	RARE 2 MM SL RNDD LATH, MICRØDØL *
BRACHIOPODS:	*
BIVALVES:	*
GASTROPODS:	*
NAUTILOIDS:	*
PELMATOZOANS:	*
OSTRACODS:	*
TRILOBITES:	*
SPONGE:	*
NON–SKELETAL ALGAE:	*
SKELETAL ALGAE:	*
OTHER:	*
SILICICLASTICS:	10–15% C SAND, QTZ, FELD, MUSC, TØUR; 10% MUSC, M SLT QTZ IN SH PEL GRNST *

Comments

*36*INSERT	LATE CØMPACTIØN: SØLUTIØN ØF SKELETAL GRAINS PARTICULARLY AT QTZ SAND CØNTACTS

Rock Name

*37*INSERT	XLAMD C SLT, CS PEL, [CLAST] DØL [MS] GRNST WITH WISPY LAM & INTLAMD MICA PEL GRNST & INTLAMD [MICRITIC] DØL [FS] *

G465-59A

Figure 3. Carbonate petrographic information—Georgina Basin project.

Airphoto reference	*Reg'd No.*	*Acid insol. %*	*Organic C %*
Digby Peaks 01/0010	74710001	7.80	.32
Digby Peaks 01/0010	74710003	4.55	.09
Digby Peaks 01/0010	74710005	6.40	.06
Digby Peaks 04/0048	74710162	2.45	.09
Digby Peaks 04/0048	74710179	3.50	.05
Digby Peaks 03/0066	74711048	7.20	.03
Digby Peaks 03/0066	74711050	5.65	.03
Digby Peaks 02/0119	74711063	8.70	.04
Toko 13/0022	74711157	6.4	.05
Toko 13/0022	74711158	7.6	.05
Neeyamba Hills 08/0020	74711410	20.2	.05
RC05/0076	74712040	4.30	.03
Digby Peaks 02/0107	74712116	5.50	.05
LK06/0766	74712342	86.7	.07
Glenormiston 11/0262	74712347	83.40	.07
Abudda Lakes 07/0150	74712466	84.80	.10
Mount Whelan 07/0122	74712497	87.50	.10
Neeyamba Hills 12/0032	74712552	7.30	.03
Glenormiston 12/0016	74712591	3.00	.03

Table 2. An example of hypothesis testing (original as computer printout).

Given in Table 3 is an example of using the system to aid in the production of written reports. Certain specific information on the file has been expressed in the format in which it would be directly incorporated into a report or BMR Record.

GEO/K103—Black Mountain 2 m from base section Shergold 1975
Chatsworth Limestone
A layer 7.5-15 cm thick of light purplish to olive grey, coarse-grained bituminous biosparite (shelly calcarenite), grain supported, with fine sparite settling out on upper surfaces of trilobite and pelmatozoan fragments. This limestone appears to be well washed and contains little mud, and there are few signs of the continued abrasion of fragments.
Fauna: *Pseudagnostus clarki patulus, Pseudagnostus elix, Pseudagnostus* sp. A.; *Caznaia squamosa, Euloma (plecteuloma) strix, Hapsidocare chydaeum, Koldinioidia* cf. *cylindrica, Sigmakainella primaeva, Wuhuia* cf. *Wuhuia dryope.*

GEO/K106—Black Mountain 51 m from base section Shergold 1975
Chatsworth Limestone
A 15 cm layer of very coarse biosparite (shelly calcarenite), grain supported, containing infiltered sand and silt grade sediment, and trilobite and pelmatozoan fragments showing few signs of continued abrasion.
Fauna: *Pseudagnostus clarki patulus, Pseudagnostus* sp. B, *Pseudagnostus coronatus; Caznaia squamosa, Ceronocare* sp., *Euloma (Plecteuloma) strix, Hapsidocare chydaeum, Koldinioidia* cf. *cylindrica, Mendosina* sp., *Pagodia (Pagodia)* sp., *Sigmakainella primaeva.*

GEO/K107—Black Mountain 68 m from base Shergold 1975
Chatsworth Limestone
A layer 7.5 cm thick splitting into two leaves and increasing in thickness to 15 cm, of light to medium grey biopelsparite containing abundant fine peloids, and trilobite fragments with geopetal structures.
Fauna: *Pseudagnostus clarki patulus; Caznaia squamosa, Caznaia sectatrix, Atopasaphus stenocanthus, Koldinioidia* cf. *cylindrica, Prosaukia* sp. A.

Table 3. An example illustrating the application for report writing (original as computer printout).

Selection and formatting of geochemical data as input for various statistical analysis programs has been much simplified by using the system. Procedures have been established for obtaining relatively simplistic plots from the system, using library programs. Further development of the system will probably be in this area.

BMR Journal of Australian Geology & Geophysics, 3, 1978, 254-256

Can rank-size 'laws' be used for undiscovered petroleum and mineral assessments?

E. J. Riesz

A number of empirical laws which state that a simple relationship exists between the size and ranking of objects have been used in assessing undiscovered petroleum and minerals resources. The most well known of these, the log-log and log-linear laws, are described and compared with log-normally distributed statistics which I have assumed give a good description of sizes of petroleum and mineral deposits.

The log-log law, which states that the log of size of a mineral deposit plots as a straight line against the log of the rank of the deposit sizes, was found to give a fair fit for the bigger deposit sizes, but the smaller sizes would be over-estimated. The log-linear law which states that the log of size of a deposit plots as a straight line against the rank of the deposit sizes was found to give a poor fit for both the big and small sizes.

The log-log law may be useful for assessing undiscovered resources where geological analogues exist and the largest deposit can be assessed by other means.

Introduction

Simple relationships between the size of a mineral or petroleum deposit within a province and its rank relative to other deposits within the province have been used to assess undiscovered resources. The most well known of these is Zipf's Law, which states the biggest value is twice as big as number two, three times as big as number three and so on, was formulated by Zipf (1949) for use in modelling aspects of human beha-

viour. More recently this law and variants of it have been used in methods of assessing undiscovered mineral resources. Rowlands & Sampey (1977) used Zipf's Law to estimate the undiscovered gold resources of the Western Australian shield, and predicted that large undiscovered gold resources exist in the area.

Zipf's law is a special case of a more general empirical relationship, which states that the log of size (of deposit in the case of minerals) plots as a straight line against the log of the rank of the individual objects (deposit sizes). Zipf's law is the special case where the slope of the line is 45 degrees. I will refer to this generalised relationship as the 'log-log law'. Ivanhoe (1976) has used the law to develop a method to estimate the remaining undiscovered petroleum resources in partially explored areas.

Jeffries (1975) has used a different empirical relationship, that the log of size plots as a straight line against the rank of the individual deposit, to compare the oil fields of the Gippsland Basin, and the Lower Texas Gulf coast, USA. I will refer to this relationship as the 'log-linear law'.

Kaufman & others (1975) have concluded that petroleum field sizes are well described by a log-normal distribution. Krige (1978) shows how a de Wijsian model of mineral concentration will produce a log-normal distribution of ore grades. I have thus come to the conclusion that undiscovered petroleum or mineral deposit sizes do fit a log-normal distribution. Therefore, I have tried to discover what, if any, relationship exists between either the log-log or log-linear laws and the log-normal distribution to determine if they have any validity for undiscovered resource assessment.

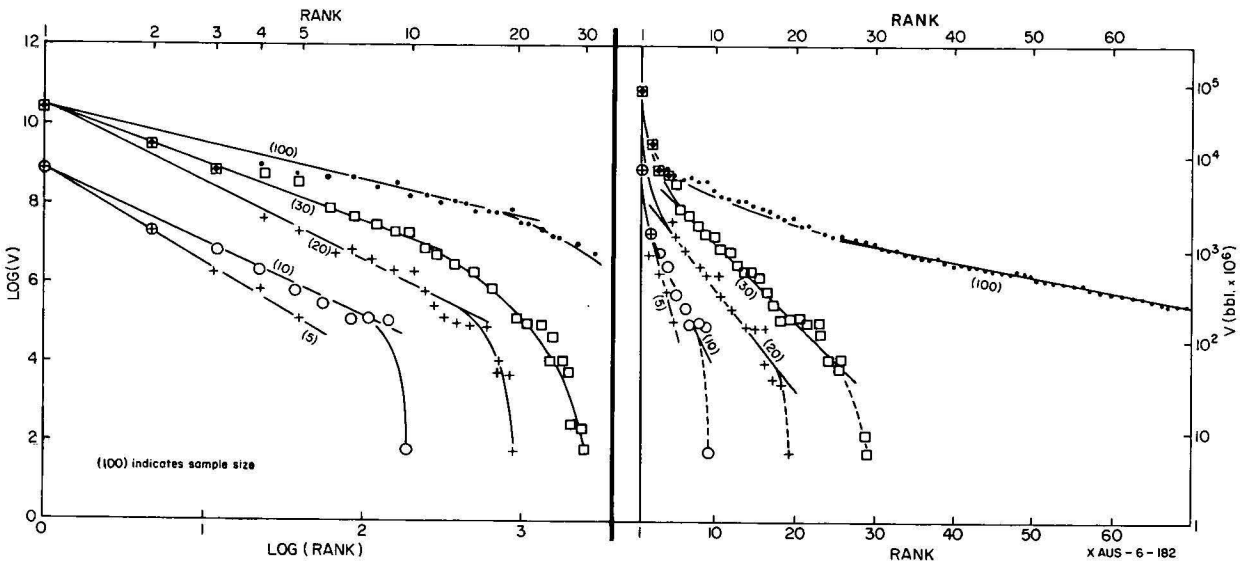

Fig. 1. Fit of log-normal data to empirical laws.

Log-normal fit to empirical laws

I chose a log-normal distribution with a logarithmic standard deviation (σ) of 1.7, similar to that used by Kaufman & others (1975, p. 131) to describe the major Alberta Oil field-size distribution, to produce statistics to test the laws.

The log-normal distribution used was truncated at both ends, with values less than one thousandth or greater than twenty times the size of the mean value of exp ($\mu + \frac{1}{2}\sigma^2$) ignored because of computational restraints. The effect on the values chosen was slight, as the chance that values from a small sample would be selected from these ends is very small.

Samples of between 5 and 100 values were chosen at random, using Monte Carlo simulation and plotted according to both the laws (Fig. 1). For the largest number of samples (100) the computational restraints referred to above affected the size of the biggest value selected; in most cases the minimum value selected by the computer was also constrained. In the measurement of actual deposit sizes very small sizes tend to be either undetected or ignored because of their lack of economic significance, so the effect of the minimum constraint should not be important.

Most of the values selected visually fit the log-log law well, with the exception of the smaller sizes, which (as mentioned above), tend to be insignificant in practice. The bulk of the data fit the log-linear law reasonably well, but high values tend above the line, and low values below. Both laws fit small samples reasonably well.

Sarhan & Greenberg (1962) have computed means and standard deviations for each of up to 20 samples chosen from a normal distribution. The expected values with ranges of plus and minus one standard deviation can be plotted on a logarithmic scale to give results consistent with Figure 1 (G. Hill, CSIRO, personal communication, April 1978).

Probability distributions to fit empirical 'laws'

I have derived continuous frequency distributions, from which, randomly selected values give a good visual fit to the log-log and log-linear laws respectively.

Log-Log law

The frequency distribution is given by:

$$f(v) = \begin{cases} K_2 V^{-1-K_1}, & Z_1 > \log V > Z_N \\ O, & \log V > Z_1,\ Z_N > \log V \end{cases}$$

(derived in following section) where:

K_1 determines the ratio of field sizes ($K_1 = 1$ for Zipf's Law),

K_2 is the normalising constant,

$Z_1 = \log$ (maximum field size), $Z_N = \log$ (minimum field size),

V is field size.

Thirty values were chosen at random from the distribution and plotted according to both empirical laws (Fig. 2). The data only gives a good visual fit to the log-log law. 0.5 was chosen for K_1 which gave a variance close to that used for the log-normal distribution in the previous section.

Log-linear law

The frequency distribution is given by:

$$f(v) = \begin{cases} K_2/V, & Z_1 \geqslant \log V \geqslant Z_N \\ O, & \log V > Z_1,\ Z_N > \log V \end{cases}$$

(derived in following section) where the terms have the same meaning as in A.

Thirty sample values were chosen at random as above, and plotted according to both laws (Fig. 2). In this case, the reverse was true, the data only give a good visual fit to the log-linear law.

Mathematical formulation

Log-log law

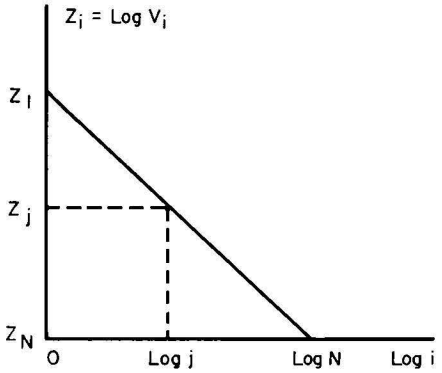

$$\log j = \frac{Zj - Z_1}{Z_2 - Z_1} \times \log 2$$

$$= \frac{Z_1 - Z_j}{m} \quad \text{where } m = \frac{-\log (V_2/V_1)}{\log 2}$$

$$\therefore j = e^{Z_1/m} \times e^{-Zj/m}$$

$$\text{Prob.}\{Z \leqslant Zj\} = \frac{N-j}{N-1}$$

$$= \frac{e^{Z_1/m}\, e^{-Z_N/m} - e^{Z_1/m}\, e^{-Zj/m}}{e^{Z_1/m}\, e^{-Z_N/m} - 1}$$

$$= \frac{e^{-Z_N/m} - e^{-Zj/m}}{e^{-Z_N/m} - e^{-Z_1/m}}$$

Assume the probability distribution is continuous (i.e., values of V between the discrete ones Vi are allowable)

i.e. Cumulative distribution

$$F_1(Z) = \frac{e^{-Z/m} - e^{-Z_N/m}}{e^{-Z_1/m} \quad e^{-Z_N/m}} \qquad (Z_1 \geqslant Z \geqslant Zn)$$

$\therefore$ Frequency distribution

$$f_1(Z) = \frac{-1}{m} \frac{e^{-Z/m}}{e^{-Z/_1 m} - e^{-Z_N/m}} \quad \text{(obtained by } \frac{d}{dZ}\text{)}$$

i.e. $f(V) = \text{constant} \times V^{-1-1/m}$ (by substitution)

$$= \frac{V^{-1-1/m}}{m\,(V_N^{-1/m} - V_1^{-1/m})}$$

$$= K_2 V^{-1-K_1} \qquad (Z_1 \geqslant \log V \geqslant Z_N)$$

Where $K_1 = +1/m$

$$= \frac{\log 2}{\log V_1/V_2}$$

$$K_2 = -K_1 (V_1^{-K_1} - V_N^{-K_1})^{-1}$$

Log-linear law

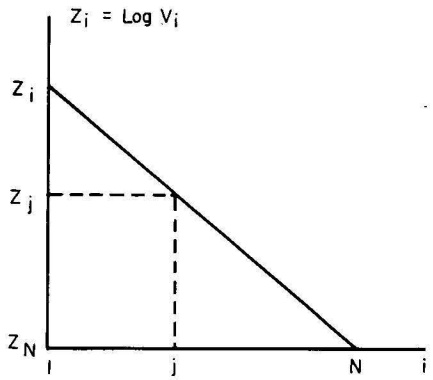

$$j = \frac{Zj + Z^2 - 2Z_1}{Z_2 - Z_1}$$

$$\text{Prob.}\{Z \leqslant Zj\} = \frac{N-j}{N-1}$$

$$= \frac{Zj - Zn}{Z1 - Zn}$$

As for the log-log law, assume the cumulative probability distribution is continuous.

$$\text{i.e. } F_1(Z) = \frac{Z - Zn}{Z_1 - Zn} \qquad (Z_1 \geqslant Z \geqslant Zn)$$

$$\therefore f_1(Z) = \frac{\text{constant}}{Z_1 - Zn} \qquad (\frac{d}{dZ})$$

$$\therefore f(V) = \frac{\text{constant}}{V} \quad (Z_1 \geqslant \log V \geqslant Zn) \quad \text{(by substitution)}$$

$$= (\log V_1/V_N)^{-1} \times V^{-1} \text{ (normalising condition)}$$

Conclusions

If the assumption that undiscovered mineral deposits (oil fields or ore bodies) are log-normally distributed is correct, then neither of the so-called laws (log-log or log-linear) are strictly correct.

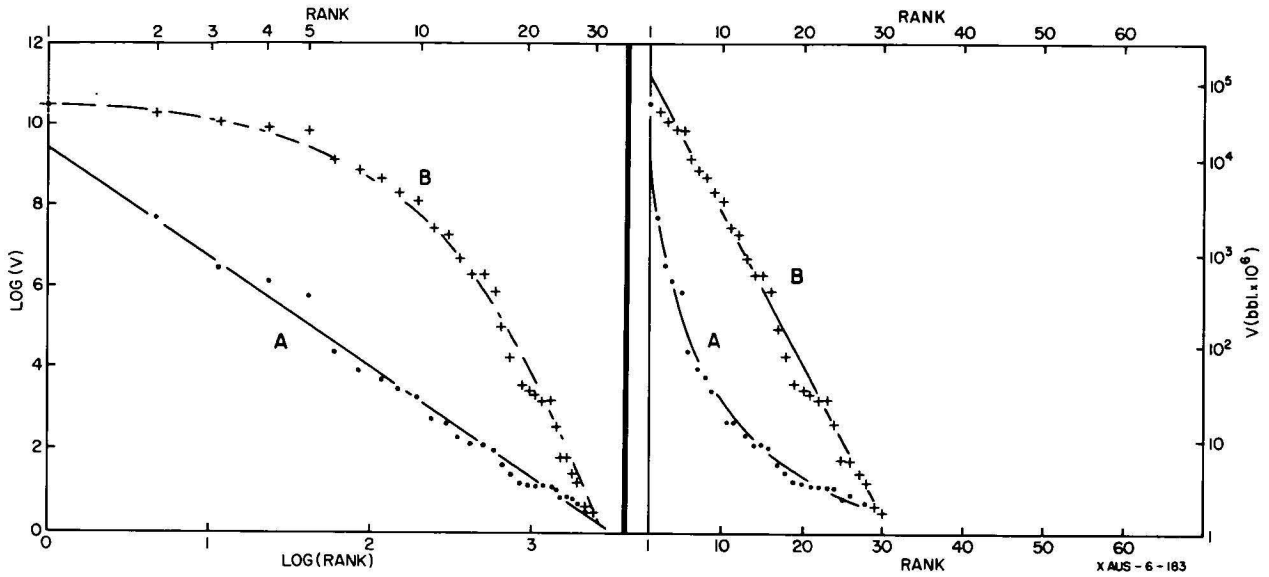

Figure 2. A—log-log distribution, B—log-linear distribution.

The log-log law appears the more valid and therefore the more useful of the two laws, as the larger (and usually the only economically significant) log-normal statistics do appear to fit this law reasonably well. Smaller values would be overestimated if this law were used, and perhaps the only way of determining if the undiscovered portion of the fields or ore bodies in an area fall into this category is to compare the discovered field (or ore body) sizes with those from a similar well-known geologically analagous area.

The log-linear law is less useful as both large and small field (or ore body) sizes are poorly estimated.

Acknowledgement

The figures were prepared by C. Johnson and G. Trott.

References

IVANHOE, L. F., 1976—Oil/gas potential in basins estimated. *The Oil and Gas Journal,* 6 December 1976, 154-6.

JEFFRIES, F. A., 1975—Australian oil exploration—a great lottery. *The APEA Journal,* **15**, 48-51.

KAUFMAN, G. M., BALCER, Y., & KRUYT, D., 1975—A probalistic model of oil and gas discovery. *AAPG Studies in Geology,* **1**, 113-42.

KRIGE, D. G., 1978—Log-normal de Wijsian Geostatistics for ore evaluation. *South African Institute of Mining and Metallurgy Monograph Series: Geostatistics* **1**, 24.

ROWLANDS, N. J., & SAMPEY, D., 1977—Zipf's Law—an aid to resource inventory prediction in partially explored areas. *Journal of the International Association for Mathematical Geology,* **9**, 383-91.

SARHAN, A. E., & GREENBERG, B. G., 1962—CONTRIBUTIONS TO ORDER STATISTICS, *John Wiley, New York.*

ZIPF, G. P., 1949—HUMAN BEHAVIOUR AND THE PRINCIPLE OF LEAST EFFORT. *Addison-Wesley, Reading, Massachussetts.*

Seventh BMR Symposium

The BMR Symposia are annual events, stressing work of relevance to industry. The Seventh Symposium was held in Canberra between 2 and 4 May 1978, and was opened by Mr A. J. Woods, Secretary of the Department of National Development, on behalf of the Hon. K. E. Newman, MP, Minister of the Department.

Sessions were held at the Academy of Science Building on 2 and 3 May. Talks presented, abstracts of which are given below, included results of completed projects, of work in progress, and some more general topics. A panel discussion was held on 'Assessment of 1:100 000 scale geological mapping of Precambrian terrains in northern and central Australia'.

There were two informal workshops on 4 May: one of them, on Involvement of government organisations in geochemical surveys, was held at CSIRO Head Office; the second, held at BMR, was on the Georgina Basin.

Australia's non-renewable energy resources

L. C. Ranford

Information on Australia's non-renewable energy resources was compiled at BMR in 1977 to assist the National Energy Advisory Committee (NEAC) in an assessment of the nation's energy resources. The work was conducted with the assistance and co-operation of other government organisations including the Joint Coal Board, the States Mines Departments and some oil companies.

The data on the various resources were classified into categories in terms of the certainty of occurrence and the economic feasibility of extraction using the 'McKelvey Box' as adopted by BMR. This classification system was judged to be the best available to present the data in a form suitable for national policy considerations, and to facilitate quantitative comparisons between the different energy resources.

Examination of the resource diagrams for the various energy raw materials and analysis of the data used in their compilation highlight a number of points about our energy resources and the available assessments.

On a percapita basis Australia is relatively rich in fossil and nuclear energy resources. However, we still have only very limited knowledge of our total energy resources and in fact, petroleum is the only energy commodity for which an assessment of total resources has yet been attempted. Australia's demonstrated, economic, recoverable resources of petroleum amount to a little more than 2 percent of our total non-renewable energy resources, but petroleum currently provides between 41 and 100 percent fo the energy requirements in the various Australian States, and provided 56 percent of the total Australian energy used in 1976/77.

Coal accounts for about 84 percent of the total non-renewable energy resources in the demonstrated economic category. These resources occur relatively close to the major population centres in Queensland, NSW, and Victoria.

Australia's uranium resources, if used in thermal nuclear reactors, represent about 14 percent of our recoverable demonstrated economic energy resources. About 85 percent of the uranium in this category occurs in the Northern Territory.

Oil shale deposits in Australia are subeconomic at current prices but identified resources are estimated to contain at least 500 times as much oil as has been identified in Australian oil fields to date. Some of this oil may be recovered with technology currently being developed.

The logic that underlies a feasibility study and calculations for mining projects

J. C. Erskine & E. L. Smith

The logical flow of information needed for a feasibility study is described, and then consideration is given to those parts of the study that can be done by computer. A flow chart is shown which puts into context those parts of the study which have to be done manually (the subjective parts) and those which the computer can handle (the objective parts).

The flow chart shows the logical flow starting with facts, going through geological, geostatistical and metallurgical studies, and ending with the formulation of several feasible conceptual plans, the detailed economic calculation and writing out of the economics of each of the plans, and the recommendation of one of the plans.

Two computer programs for use with mining feasibility studies are being designed at BMR. One is for geostatistical studies; the other, which will be described here, models (for each conceptual plan) the calculations of equipment and capital works requirements, and calculates capital costs, revenues, financial analysis and economic risk analysis. After the mining engineer has provided the basic mining and financing information, and metallurgical and location data, this program can calculate and print out the whole of the remainder of the information needed to decide on the relative economic desirability of each plan.

The steps which the program will go through are as follows:

- Access the capital cost data base. The data is being compiled to give capital costs at the mine of all major mining equipment and capital works; it will be updated annually to take account of inflation, and of changing equipment and mining methods.
- Calculate requirements of equipent and capital works, and their capital cost. (For example, it calculates numbers of drills, shovels, trucks, and totals their capital costs).
- Calculate and write out detailed schedules of inflated and uninflated depreciable and tax allowable capital costs for proving-up drilling, construction camp, mine development, concentrator and support facilities, civil engineering, power supply, workshop, store and inventory, and town construction.
- Calculate capital cost, including interest (if any) and working capital, and a cumulative total capital cost for each year.
- Calculate revenue (smelter return from data of concentrate grades, impurites, distance from smelter, metal prices, and exchange rates.
- With the above information available, and the addition of operating costs (at present to be

provided as data, but in later years to be calculated by the program) it is then relatively easy, in PROSPER computer language, to perform the financial analysis (printing out a year by year summary of the capital account, operating account tax account, annual cash flow and discounted cash flow rate of return).

- Draw the graphs for economic risk simulation (sensitivity analysis) to show how the discounted cash flow rate of return will vary with variations in the major parameters.

The calculation and expression of national estimates of inferred mineral resources

J. W. Cottle

Obtaining national estimates of inferred mineral resources for particular commodities involves the preparation of individual estimates for each deposit and the aggregation of these estimates to produce a national total.

Because inferred resources refer to possible extensions or repetitions of known bodies of mineralisation their estimation is based largely on a broad geological knowledge of the deposit with, if at all, only a few samples or measurements. As a result, the components that might comprise any particular deposit estimate (e.g. grade, volume, density) incorporate varying degrees of uncertainty. Estimation of any of these components by a single value (e.g. a grade of 3.5 percent) gives no indication of the probable accuracy (uncertainty) of the estimate and leads, ultimately, to a total national estimate, the probable accuracy of which is also unknown.

The problem of the uncertainty of the estimate can be overcome by the application of simple probability theory and simulation. This probabilistic approach embodies a flexibility that allows the uncertainty in each variable to be expressed and fully accounted for within the analysis. As will be demonstrated, this methodology ensures that the information content of the final national total estimate is greatly increased which, in turn, enables ensuing decisions to be more soundly based, because they can take account of the inherent uncertainty of the estimate.

An example of a national mineral appraisal: lead and zinc in Canada

D. F. Sangster (Geological Survey of Canada)

In 1972 and again in 1977, national appraisals of Canada's undiscovered lead and zinc resources were completed. The basic approach adopted was to carry out the *evaluation* in geological terms by deposit-type even though the *reporting* was in terms of commodities.

The techniques used and the problems encountered are described for two different deposit-types: (1) stratabound deposits of the "Mississippi Valley" type in carbonate rocks and (2) volcanogenic massive sulphide deposits in volcanic rocks.

Although in both cases an attempt was made to establish "type areas" and extrapolate from these to the target areas, this proved to be almost impossible for the Mississippi Valley deposit-type, largely because of lack of grade-tonnage data in the type areas.

In contrast to these difficulties, however, it was found that the distribution of volcanogenic massive sulphides was much more predictable. In seven type areas, centred around felsic volcanic accumulations, it was found that, per area, the range in numbers of deposits, total metal content, and grade were all relatively small. Furthermore, the distribution of deposits in each area conformed to a predictable pattern. Regularity and hence predictability such as this is necessary in resource estimation, and hence evaluation of undiscovered zinc and lead resources in volcanogenic massive sulphide deposits is relatively easier (and more accurate?) than in Mississippi Valley deposits.

Configuration and composition of the basement of the Pine Creek Geosyncline

D. H. Tucker, N. Sampath, & I. G. Hone

Most large uranium deposits discovered in the Pine Creek Geosyncline occur in Lower Proterozoic metasediments adjacent to granitic complexes. Accordingly, an interpretation of the regional geophysical data has been made to determine the location of shallow granitic complexes.

A study of the regional data and of measured rock densities indicates that most of the gravity features can be explained by the presence of low density granitic complexes within more dense Lower Proterozoic metasediments; some features can be explained by lateral variation in density of the metasediments themselves. Anomaly analyses indicate that the granitic complexes commonly slope outwards beneath the Lower Proterozoic sediments, and can be modelled as bodies with a depth extent generally less than 5000 m. In the main there appears to be no density or magnetic contrast between the granitic complexes and the basement of the Pine Geosyncline. Hence the modelled depth extent of the granitic complexes can be used to map the thickness of Lower Proterozoic sediments and the structure of the geosyncline.

A regional model based on this hypothesis suggests that a basement high runs south from the Alligator Rivers Uranium Field, through the Jim Jim Granite, and then eastwards beneath the Kombolgie Sandstone. Another basement high fringes Van Diemen Gulf. The South Alligator Valley Uranium Field appears to lie in a basement deep.

Except in a few localities, magnetic interpretation does not help in determining the deep basment configuration. However, as most of the magnetic anomalies are caused by near-surface sources within the Lower Proterozoic section, the magnetics provide depth estimates to the base of flat-lying cover rocks and surficial cover which blankets much of the area.

Subdivision of the Precambrian

K. A. Plumb

The IUGS Subcommission on Precambrian Stratigraphy is developing a world-wide subdivision of Precambrian time. The results of the Subcommission's meeting during 1977, and the prospects for achieving a satisfactory subdivision, will be discussed.

Discussion centres around the following points: geological history is episodic and essentially regional, whereas time is a continuum with no natural subdivisions; the first-order subdivision being sought is in fact, that of time; the agreement being sought is a convention, essentially a mechanism to promote international scientific communication without undue distortion. Therefore, world-wide fundamental geological significance must not be implied by the subdivisions chosen; it should be potentially practicable to use all indices of correlation within the framework of the subdivision.

The subdivision should: (1) be acceptable to the majority; (2) be as simple as possible; (3) not prejudice objectively; and, (4) must contain operationally objective criteria. (5) The boundaries should have geological significance in as many regions as possible (but the significance may differ between areas); but, (6) it is unrealistic to expect the boundaries to fit all regions exactly. (7) The method by which the Phanerozoic time-scale evolved provides no useful guidelines for Precambrian subdivision.

The following methods of subdivision have been discussed and rejected by the Subcommission: Arbitary (e.g., 500 m.y. units); Stratotypes; Tectono-magmatic cycles; Biostratigraphic; Palaeomagnetic;

and Theoretical Concepts of Earth Evolution.

The subdivision being sought is a geochronological subdivision of convenience, or best fit. From analysis of presently available data, time boundaries will be selected, to pass through major breaks in the stratigraphic record which are common to as many regions as possible.

The following decisions were reached by unanimous vote:

(1) A two-fold subdivision of the Precambrian into Archaean and Proterozoic is accepted by the Subcommission.
(2) As an operational criterion, the boundary between Archaean and Proterozoic is assigned a geochronological age of 2500 m.y.
(3) The terms Archaean and Proterozoic should have status as eons, equivalent in rank to Phanerozoic, though of considerably greater duration.

By majority vote, the Subcommission accepted, as one focus of future work, the review and acceptance of Precambrian Reference Sections. Criteria and procedures are being prepared.

The principal focus of the next meeting will be the subdivision of both the Proterozoic and Archaean.

Analysis of available data indicates that the prospects for agreement on further subdivision are good. I personally anticipate that boundaries will be selected at about 1000 m.y., 1800 m.y., and 2900 m.y. The units so defined may be further subdivided at about 1400 or 1600 m.y., 2000 m.y., and at the base of the late Proterozoic glacial successions. These boundaries would be very practical for use in Australia. The units so defined could be given new names.

I propose that no change should be made to the existing schemes in use in Australia until the Subcommission has completed its recommendations.

Advances in the understanding of the stratigraphy of the Pine Creek Geosyncline, Northern Territory

I. H. Crick, P. G. Stuart-Smith, & R. S. Needham

Significant uranium mineralisation in the Pine Creek Geosyncline is contained within three formations-the Cahill, Koolpin, and Golden Dyke Formations.

Because of the similar carbonate-carbonaceous rock assemblages and their association to uranium mineralisation, these three formations have been regarded as being facies and time equivalents. Recent work indicates that the Cahill Formation is older than the Koolpin Formation and that the Koolpin Formation is equivalent to the upper part of the Golden Dyke Formation. A tentative correlation is made between the lower Golden Dyke Formation which contains the uranium mineralisation in the Rum Jungle area and the lower Cahill Formation in which the large uranium deposits of the Alligator Rivers area are located.

The Cahill Formation consists of two members, a lower carbonate-carbonaceous-chlorite schist sequence and an upper quartz schist, feldspathic quartzite sequence. The formation overlies a thick sequence of continental arkose, quartzite, and conglomerate of the Mount Partridge Formation, or the Mount Basedow Gneiss-which form the base of the Lower Proterozoic succession in the Alligator Rivers area. These rocks are transitional into higher grade gneisses of the Nanambu Complex, and probably unconformably overlie Archaean granites as several granites within the Complex have Archaean ages.

The upper section of the Cahill Formation is correlated with the Mount Hooper Beds, the Coirwong Greywacke, and the Mundogie Sandstone, and is interpreted as representing a shallow marine transgressive sequence. Pebbles of silicified dolomite in conglomerates of the Mount Hooper Beds are evidence of an older carbonate sequence, probably the lower member of the Cahill Formation. The Koolpin Formation unconformably overlies the Mount Hooper Beds, Coirwong Greywacke, and Mundogie Sandstone. Changes in metamorphic grade from lower greenschist to amphibolite in the Cahill Formation can be explained simply by depth of burial.

Tuff has been recognised within the Golden Dyke Formation in the Burnside Granite area in the western part of the geosyncline. The Gerowie Chert in the South Alligator River valley, which was previously considered to be possibly a diagenetically altered dolomite, is composed mainly of tuff. Underlying the Gerowie Chert are iron-rich sediments of the Koolpin Formation; these are commonly chert-banded, lenticular, or nodular, ferruginous and carbonaceous siltstones; they are similar to iron-rich sediments commonly underlying the tuff in the Golden Dyke Formation.

The Gerowie Chert has previously been interpreted as interfingering to the west with the Koolpin Formation, and to the east with the Fisher Creek Siltstone, an interpretation now difficult to sustain as the Gerowie Chert is a time-stratigraphic unit.

The presence of an upfaulted Archaean basement ridge (the Stag Creek Volcanics) confining sedimentation of the South Alligator Group (the Koolpin Formation, Gerowie Chert, and Fisher Creek Siltstone) to an eastern basin, as has previously been proposed, now seems unlikely; Foy & Miezitis (1977) have found that the Stag Creek Volcanics are interbedded with sediments of the Masson Formation. We suggest therefore that the tuff and underlying iron-rich sediments of the Golden Dyke Formation are equivalent to the Gerowie Chert and Koolpin Formation.

A major revision of the lower Proterozoic stratigraphy of the Pine Creek Geosyncline is required.

Petroleum resource assessment methods

D. J. Forman

For most companies the purpose of petroleum resource assessment is to determine the likely amount of undiscovered petroleum in an area so that management may decide whether or not the petroleum is worth exploring for. Industry and government also require petroleum resource assessments for long-term planning.

A number of publications are available on methods of estimating the amount and value of discovered petroleum resources. In recent years there have also been a number of papers on methods of estimating undiscovered petroleum, but the methods presented are extremely diverse, some of them are invalid, and many are not applicable to Australian conditions.

Estimation of undiscovered resources requires that geological and historical data and inference are applied both objectively and subjectively, either in theoretical models or in comparisons, to solve two problems. One is to calculate the probability that hydrocarbons exist; the other is to estimate the volume of hydrocarbons that may exist.

The probability that a basin, play, or prospect does contain hydrocarbons is determined by risk analysis. The prospect-by-prospect, play methods, or volumetric methods may all be used to estimate the volume of petroleum that is likely to be discovered. Selection of the method or methods depends on how much is known about the geology of the area, the time available for study, and access to the necessary data and methodology. It is important to consider the location and field-size distribution of the undiscovered resources so that the economies of producing them may be assessed.

Maturation of petroleum source rocks in Australia: results of the BMR-CSIRO studies, 1977

J. D. Gorter

The aim of the continuing joint project was to provide basic data for petroleum resource assessment of

Australian basins for BMR basin studies groups, and provide a stimulus for industry. Emphasis was placed on previously written-off areas, and basins from which source rock work had not been done. An attempt to sample all geological periods, from late Precambrian to early Tertiary, and diverse sedimentary environments, was made.

The primary controlling factors determining the hydrocarbon potential of a basin are the total amount of organic carbon, type of organic material—whether of plant or animal origin—and the thermal history of the rocks. Recently developed techniques relating to hydrocarbon generation enable integration of these data into basin evaluation. Five parameters were selected to provide the basic data: total organic carbon content, solvent extractable organic content, hydrocarbon content, extract chromatography, and vitrinite reflectance.

During 1977 BMR submitted over 300 core samples to CSIRO, representing some 106 wells in 20 onshore basins. Subsidised wells, and BMR and State Survey stratigraphic drilling provided the bulk of the core samples submitted. This paper discusses the more interesting results, some of which are summarised below.

1. In the Canning Basin vitrinite reflectance data and moderately high total organic carbon values suggest that the Permian Noonkanbah Formation is a good source rock in the southeastern Fitzroy Graben. Reservoir and structure are expected to be present. Similarly, Ordovician rocks on the northeastern Broome Arch are at present mature, and of excellent source potential; however, disappointing results were obtained from wells in the same structural province. Oil in the Permian Grant Formation at Thangoo 1 is probably derived from the immediately underlying Ordovician.

2. Data from the Clarence-Moreton Basin suggest that the play is a gas prospect, with a source in the Triassic coal measures. It would have unnamed Upper Triassic sands (if permeable) as a reservoir and be sealed by the Walloon Coal Measures in post-Jurassic structures at a depth of no greater than 2000 m in the north and 1000 m in the south of the basin.

3. In the Hillsborough Basin very high total organic carbon values, low vitrinite reflectance values, and the chromatograph patterns, indicate typical oil-shale extracts.

4. Moderate total organic carbon values and submature reflectivities from the non-marine Lower Permian glacial sequence in the Murray-Darling Basin suggest that these rocks may be a potential gas source, if more deeply buried.

5. In the Laura Basin a large divergence between Lower Jurassic and Permian reflectivities is evident. This can be interpreted either as due to the removal of some 3500 m of Triassic rock before the Jurassic, or to a change in heat-flow regime.

Enhanced recovery: a general discussion with possible application to Australian oilfields

B. A. McKay

In the next ten years, many Western industrialised nations will be major importers of crude oil because of their imbalanced demand/indigenous supply situation. In 1990 for instance Australia will have to import about four times her currently projected production to meet her supply gap. Because of prolific discoveries in the North Sea, Great Britain is one of the fortunate few and will have crude for export in the 1980's.

In some undersupply situations, the problem is one of productivity and recovery efficiency. This is exemplified by the United States where over 300 billion barrels of liquid crude resources exist (sufficient for 50 years supply at current usage), but only about 10 percent of this is currently recoverable.

At projected crude oil prices of US$20/Bbl in 1990, the drain on foreign reserves for these imports will be a major economic concern for many nations in the same relative position.

Increased exploration may be the answer in some undersupply nations; however, improving recovery efficiency may offer the most viable means for (economically) increasing reserves and oil production. Currently, there are a number of enhanced recovery pilot schemes underway in various nations, foremost of which are in the USA. Techniques have been tailored to certain reservoirs, e.g., steam injection and in situ combustion for increasing production from heavy oil reservoirs, surfactant-micellar injection techniques for reservoirs benefiting from a lowering of interfacial tensions.

Many enhanced recovery schemes overseas are considered after using secondary techniques such as waterflooding in reservoirs having finite boundaries. Many Australian oil fields (particularly Bass Strait) have primary active water drive which affords good displacement efficiency, but being "open ended", have little scope for control or use of enhanced recovery. The Moonie oil reservoir in Queensland is in a somewhat similar position as Bass Strait, with a strong edge-water drive; however, the high residual oil saturation at depletion (65% of oil in place) makes Moonie a tempting prospect. The Petroleum Technology Laboratory of the BMR is currently investigating the use of polymer displacement in core samples from this field with the hope of assisting improved economic recovery.

However, Barrow Island may be the best candidate for enhanced recovery in Australia because of its finite reservoir system, low oil viscosity, and high oil saturation, although problems may ensue with low formation permeability.

Western Victoria, a geothermal energy prospect?

J. P. Cull

All heat contained within the Earth can be described as geothermal energy. However a geothermal resource can be defined only if heat can be extracted from crustal rocks and concentrated at the surface by fluid migration.

There are no hydrothermal fields in Australia but hot springs have been found in regions of recent volcanism. In addition there are many bores producing hot water in sedimentary basins. Resources of this type are conduction dominated, and maximum rates of heat extraction can be calculated only if heat flow is determined.

The Otway Basin is defined as a low enthalpy geothermal energy prospect. Large volumes of hot water can be readily obtained form high-yield aquifers. Flow rates of 70 L/s and temperatures greater than 50°C have been recorded. Heat can be extracted for process and space heating using existing bores near Portland. Additionally, steam may be made available from centres of recent volcanism within the basin. At Mount Gambier heat flow is 91.8 $\pm$ mW m^{-2}. An anomalous source of heat is indicated close to the crater.

A seismic investigation of the Eastern margin of the Galilee Basin, Queensland

J. Pinchin

Beneath the southeastern margin of the Galilee Basin lie the Drummond and Adavale Basins. The structural relationships of these three basins have an important bearing on the hydrocarbon potential of the area; gas has been discovered in the Adavale Basin and there have been gas and oil shows within the Galilee Basin. In addition, Permian coal measures of the Galilee Basin subcrop along the eastern margin and their depth and extent is of economic interest.

In 1976, BMR shot four six-fold c.d.p. seismic reflection traverses covering 219 km across the eastern

margin of the Galilee Basin in areas where there had been no previous seismic coverage. The first two traverses, about 50 km east of Hughenden, were to investigate the structure of the basin's northeastern margin with relevance to the extent of the coal measures, and Traverses 3 and 4 were to investigate the underlying Adavale and Drummond Basins in the Galilee-Jericho area.

The results from Traverse 1 showed that the northeast margin of the Galilee Basin has been affected by faulting as recently as Tertiary times, and a possible fault-bounded anticline probably trending parallel to the basin margin was crossed. Drummond Basin rocks thicken to 800 m at the west end of the traverse, where they are overlain by 2000 m of Galilee Basin sediments. No structures of any kind were intersected by Traverse 2, although a steep basin margin was expected from interpretation of aeromagnetic data; the observed magnetic anomaly is probably caused by intrabasement changes in rock type. The Permian coal measures dip gently from a depth of 750 m at the northwest end of the line to 1000 m at the southeast end. The Galilee Basin sediments are underlain by 600 m of Lower Carboniferous Drummond Basin sediments, hence the Drummond Basin is seen to extend further northwest than previously thought.

Traverse 3 extended a BMR 1971 seismic traverse to provide continuous seismic coverage from Lake Galilee 1 well eastwards to the outcrop of the Anakie Metamorphics. Results indicate that sedimentary rocks of the Drummond Basin, in particular the Mount Hall and Telemon Formations, extend westwards below the Galilee Basin; it is unlikely that the Adavale Basin extends this far north. The traverse crosses a prominent gravity high, the Donnybrook Gravity High, and this is thought to be caused by a dense intra-basement block rather than basement uplift. An alternative explanation for the gravity high, involving a reversed density contrast of dense sediments over less dense volcanics, is being considered. Results from the fourth traverse also show that Drummond Basin sediments extend far westwards beneath the Galilee Basin, and that the Adavale Basin, which is the more prospective of the two pre-Galilee basins, is restricted to the south.

Both coal and oil exploration in this area are going to prove difficult. The steep and faulted northeast margin of the Galilee Basin provides only a narrow strip where coal is likely to be found at mineable depths, and the pre-Galilee sediments below the basin's eastern margin look unprospective for petroleum because of their fluviatile origin. However, an area between Traverse 1 and Traverse 3, known as the Koburra Trough, contains a thick sequence of Permo-Carboniferous sediments, and its eastern margin is probably bounded by structures such as that crossed by Traverse 1; these structures could provide petroleum traps and it is on this area that exploration should now concentrate.

Lead and zinc in carbonate rocks—prospects in the Georgina Basin, Northern Territory and Queensland

J. J. Draper

The Georgina Basin contains a thick sequence of carbonate rocks, of Early Cambrian to Early Ordovician age, deposited in a series of subtidal to supratidal environments on an epicontinental shelf. These carbonate rocks unconformably overlie Vendian to Lower Cambrian glacigene and marine rocks in the southern part of the basin, and pre-Adelaidean rocks elsewhere (except where rare Lower Cambrian basalt is present). Lower to Middle Ordovician shallow marine siliciclastic rocks overlie the carbonate rocks in the southern part of the basin. During the Devonian, deformation of the basin was accompanied by dominantly freshwater sedimentation. Mesozoic and Tertiary rocks and Recent sediments obscure much of the basin. There are a number of prospective targets for lead and zinc mineralisation in the carbonate rocks, but two targets of particular importance are the Arrinthrunga Formation, together with its partial equivalent the Meeta Beds, and the post-Devonian to Mesozoic unconformity.

The *Arrinthrunga Formation and* Meeta Beds comprise subtidal to supratidal limestone and dolomite containing large quantities of algal material. Minor mineralisation occurs in the units at Box Hole (galena, barite, sphalerite) and BMR Huckitta Nos. 7 and 8 (minor scattered sphalerite), and anomalous values of lead, barium, and zinc are present in Alliance Mulga No. 1 at about the same stratigraphic level as at Box Hole. Fluorite is present in the unit, but is probably formed in an early stage of diagenesis. The Box Hole and Mulga No. 1 occurrences, as well as an occurrence of galena in the overlying Tomahawk Beds, coincide with positive gravity features. Part of the Arrinthrunga Formation was deposited in an arid supratidal environment, so that brines would be present and gypsum (often preserved as pseudomorphs) would provide a potential source of sulphur. Hydrocarbons are also present. One area of particular interest is around Alliance Mulga No. 1, where the Meeta Beds are (?)disconformably overlain by the Ninmaroo Formation which is strongly jointed (NE-SW). Another region worthy of consideration is the Marqua to Toomba Range area where shallow water, shoaling sediments pass laterally into fetid, dark, subtidal sediments; there is a good possibility of stratigraphic traps.

The *post-Devonian to Mesozoic unconformity* is a well developed karst surface which transects various shallow-water, shoaling sediments bonate rock units. The Mesozoic sequence overlying the unconformity is initially freshwater, overlain by a transgressive marine sequence. (In the Camooweal-Undilla area, apparently marine shales directly overlie the unconformity.) The post-Devonian to Mesozoic unconformity provides a suitable conduit for mineralising fluids and suitable ore traps. Pseudomorphs of pyrite are often associated with the unconformity. One feature of the present karst surface in the basin is the presence of manganese and iron concentrations with zinc values up to 0.65 percent and barium to 1.14 percent—this weathering concentration may be a suitable mechanism for pre-concentrating metals for later redeposition as Mississippi Valley Type deposits. Areas worthy of closer consideration are the Camooweal-Undilla area, Glenormiston-Alderly area and the eastern Burke River Structural Belt.

Gravity evidence for abrupt changes in mean crustal density at junctions of Australia's crustal blocks

P. Wellman

The major gravity anomalies in central and Western Australia occur as elongate dipoles, either in isolation or in a series. Each dipole can be explained by an abrupt change in mean crustal density across the junction of crustal blocks, and by the associated isostatic compensation. Typically a block has an anomalously high mean density in the upper or whole crust; this slowly reverts to normal away from the block boundary. Some dipoles are enhanced in amplitude by low density sediments and their compensation. The observed anomalies are consistent with the anomalous masses being isostatically compensated by variations in thickness of the crust; the variations are gradual, and extend to about 100 km from the boundaries of the anomalous bodies.

The crustal block boundaries inferred from dipole anomalies correspond in position with the crustal block boundaries inferred from geology, and approximately with the position of those inferred from the gravity trend pattern. At boundaries between younger and older blocks there is a tendency for the younger block to have high density material

forming its block edge, and for the older block to be covered with sediment; these features are likely to be caused by the process of formation of the younger block, or the joining of the younger block to the older block. The dipole anomalies on the Australian Precambrian crust are similar to those recognised at Precambrian province boundaries in Canada, and have similar tectonic positions.

The use of microfossils in Precambrian correlation: problems and principles

M. D. Muir

The intensive study of Precambrian microfossils is a comparatively recent development in palaeontology, and the use of Precambrian microfossils for stratigraphic correlation is in its infancy. At this early stage, there are few workers in the field and most of them lack experience in biostratigraphy. It is important to try to avoid making the kinds of mistakes that, because of excesses of enthusiasm, have characterised the early stages of other branches of palaeontology. Useful lessons can be learned by examining the development of ideas on the biostratigraphic application of palynology (the study of spores and pollen and other organic walled microfossils).

The problems that were encountered in the early days of stratigraphic palynology and that now face us in Precambrian stratigraphic micropalaeontology are strikingly similar. Correlation is required for kilometres of both outcrop section and of drillcore, on both regional and local scales. The morphology of the fossils is simple and they are very small, and require fairly sophisticated microscopical techniques for their understanding. Physical and chemical changes during incorporation into and diagenesis of the sediment can grossly alter the fossils' morphologies. The present-day equivalents are poorly known morphologically, and in terms of their ecological significance. The fossil assemblages are barely known. There may be large numbers of taxa in a single sample and extremely numerous individuals in a single microscope preparation, all of which makes the serious study of samples very time consuming.

One way of tackling the problem is to make a conscious effort *not* to try to identify fossils with living species, but to try to group fossils, as objectively as possible, into small units which are delineated by severe morphological and dimensional restraints. This will inevitably produce a very much larger number of 'taxa' than conventional palaeontological treatment, but it does produce data that can be treated numerically. Similar techniques were applied to the almost intractable problems of the stratigraphic palynology of the tropical Tertiary (Germeraad, Hopping, & Muller, 1968) with excellent results. Zonations on various scales of refinement were produced, and it proved possible to determine the controls over these zonations. Universal, long-ranging zones are probably a result of plant evolution, while fine-scale basinal zones are controlled by local ecological and edaphic conditions.

At present the outlines of broad, evolutionary zones in the Precambrian can be detected. Basin studies, currently in progress, will form the basis for local zonations which can be used for intra and eventually inter-basinal correlation. Because the Precambrian time scale is so long, a solid framework of isotopic age determinations is an essential substrate for biostratigraphy, as is also a thorough understanding of lithostratigraphy, facies analysis, and diagenesis. The microfossils are organic walled, and can be used colorimetrically as sensitive indicators of thermal diagenesis, and depth of burial. Microfossils have been recovered from rocks of biotite grade, so the possibilities for correlation in metamorphic terrains are available. This could be of considerable interest in the correlation of, say, the McArthur Basin, and the Mount Isa region.

Thus although the problems involved in such studies cannot be underestimated, they are not insuperable, provided a commonsense approach is taken.

GERMERAAD, J. H., HOPPING, C. A., & MULLER, J., 1968—Palynology of Tertiary sediments from tropical areas. *Review of Palaeobotany and Palynology*, **6**, 189-348.

Crustal structure in Australia from explosion seismology

D. Denham & D. M. Finlayson

All our mineral resources lie in the Earth's crust, and all of the crust is derived from the mantle, so it is important to look at the structure and physical properties of the crust and upper mantle.

Studies using man-made explosions show that in oceanic regions the crust is comparatively thin (10-15 km) and simple, whereas in continental areas the crust is thicker (30-50 km) and often extremely complicated. This situation arises because oceanic crust is ephemeral—at most lasting only 200 m.y.—and is generated in only one way. Hot mantle rises under mid-ocean ridges to form new oceanic lithosphere and this cools with a crust on top as it spreads away from the ridge.

In a continental environment we have to contend with several complicated and interactive processes, such as erosion, intrusion, granitisation, metamorphism and subduction, and on a much larger time scale—some continental rocks are at least 3800 m.y. It seems that once material is accreted to a continent it mostly stays in a continental environment in one form or another, almost indefinitely. In most of Australia we have no knowledge of intra-crustal structure below crystalline basement.

Because of the complications on land it is a difficult problem to determine the intra-crustal structure there. The most successful techniques have been those which use man-made explosions. These involve using refractions and wide-angle reflections from large explosions (3-500 t) and vertical reflection techniques developed for oil search purposes.

BMR has been involved in several crustal studies using explosions since the Maralinga atomic blasts of the 1950s. The results show that the upper crustal velocities beneath the sediments are very variable, ranging from 5.7-6.4 km/s. We always observe crustal velocities in this range. In the lower crust sometimes we observe velocities in the 6.5-7.5 km/s range, and sometimes we don't. This and other evidence suggest that there is great heterogeneity throughout the crust. Recent work in southeast Australia casts doubt on the simplistic two-layer crust formerly proposed, and suggests the possibility of local low-velocity layers and lower crustal velocities of 7.3-7.4 km/s before reaching normal mantle, which has a velocity of about 8 km/s.

The seismic structure of the upper mantle appears to be less variable, but seismic recording programs in recent years have demonstrated that the fine structure of the upper mantle is no less difficult to determine than that in the crust. In the western and central part of the continent reconnaissance surveys show the velocity of the upper mantle immediately beneath the crust falls in the range 8.2-8.3 km/s, while in the east the velocities range from 7.8-8.1 km/s. This change in velocity correlates well with the heat flow rates, which are low in the Archaean cratons of the west (40 mW/m^2) and high in the east (80 mW/m^2), and the ages of the crust, which range from about 3500 m.y. in the west to about 400 m.y. in the east.

The thickness of crustal rocks seem to lie mostly within the range 30-40 km, compared with a range of 25-50 km in North America and USSR. However, thicknesses of over 40 km have been interpreted from reconnaissance surveys in southwest Australia and beneath the Snowy Mountains. Refinements in instrumentation and interpretation methods within the last 10 years will undoubtedly lead to a revision of the

current simplistic models of intracrustal and upper mantle structure which no longer stand up to detailed examination.

Tectonic setting of kimberlites in southeastern Australia

John Ferguson & L. P. Black

Recent discoveries have established the existence of fourteen areas where kimberlitic rocks occur in southeastern Australia, in the States of New South Wales, Victoria, Tasmania and South Australia (Ferguson & Sheraton, 1977, and Stracke & others, 1977). One or more intrusives are found in each area, the maximum being twenty-seven. Rb-Sr dating on whole-rock samples and on phlogopite separates have established Permian and Jurassic ages for kimberlitic occurrences in northwestern New South Wales and South Australia, respectively. Field relations indicate that all the occurrences postdate the Proterozoic, and that some are as young as Tertiary.

In an attempt to relate the kimberlites and their associated rock types to a structural framework the following features were investigated: on and off-shore structures, igneous activity, earthquake activity, general tectonics, gravity, and magnetics. Postulated continental extensions of transform faults, stemming from both the Antarctic and Tasman Sea Ridges, appear to have played the major role in the location of the kimberlitic intrusives in southeastern Australia. The South Australian kimberlitic occurrences all lie on the continental projection of the oceanic fracture zone arising from present-day spreading associated with the Antarctic Ridge. This feature is in accord with the postulate that the sites of transform faults are probably dictated by pre-existing structural weaknesses in the pre-breakup continental crust. On the eastern seaboard, this southern spreading ridge is also thought to be responsible for the projected continental fracture zone which lies coincident with a broad belt of Cainozoic igneous activity, and is also approximately the edge of Cainozoic epeirogenic uplift and the Cainozoic mean line of hot-spot migration. All the kimberlitic occurrences near the eastern seaboard of Australia fall within this broad zone of activity. Their location also appears to have been governed by fracture patterns developed initially during pre-breakup times, which later became the sites of continental extensions of transform faulting during the Tasman Sea opening; this spreading commenced 80 m.y. ago, and aborted 60 m.y. ago. A number of the kimberlites on the eastern seaboard of Australia are located at the intersections of the projected continental transforms stemming from the two spreading centres.

FERGUSON, J., & SHERATON, J. W., 1977—Petrochemistry of kimberlitic rocks and associated xenoliths of southeastern Australia. Extended Abstracts, Second International Kimberlite Conference, Sante Fe, New Mexico, October 3-7, 1977.

STRACKE, K. J., FERGUSON, J., & BLACK, L. P., 1977—Structural setting of kimberlites in southeastern Australia. Extended Abstracts, Second International Kimberlite Conference, Sante Fe, New Mexico, October 3-7, 1977.

LANDSAT for geology—a review of current techniques and achievements

C. J. Simpson

The extensive research into satellite data technology that followed the launch of LANDSAT-1 (ERTS-1) in 1972 has resulted in progressive improvements to product quality and digital data analysis techniques. Improved image quality has direct significance to the many mineral and petroleum exploration organisations that are now routinely applying conventional photogeological interpretation techniques to LANDSAT multispectral scanner imagery.

Considerable effort has been directed to detection and analysis of LANDSAT lineaments. The USGS, for example, includes the results of LANDSAT lineament analysis in the synthesis of mineral resources assessment. To date, the only reported mineralisation discovery based solely on LANDSAT, resulted from visual interpretation of imagery.

Photogeological techniques will continue to be the main means of LANDSAT interpretation; however, even the best quality imagery may contain less than one quarter of the total information recorded. LANDSAT imagery is produced electronically from digital data recorded on magnetic tape. Each scene of each of the four spectral bands imaged by LANDSAT is composed of about 7.5 million picture elements (pixels). The ground brightness of each pixel (representing an effective area of 79 m x 56 m) is recorded by the scanner system on a scale which cannot be completely represented in a photographic image. Computer analysis techniques offer the only adequate means of analysing all the data in a LANDSAT scene.

Considerable progress has been made with computer analysis of LANDSAT digital data, and some techniques have definite application to mineral and petroleum exploration. Various computer enhancement techniques have been employed to reveal structural and lithological information not visible on conventional LANDSAT imagery or aerial photography. In specific environments direct detection of iron-weathering products associated with hydrothermal alteration has been achieved. Many techniques which are showing promise overseas have yet to be tested in the Australian environment.

The Ngalia basin—a reappraisal

A. T. Wells & J. Moss

The structure and palaeotectonics of a large part of the westerly trending, poorly exposed, wide, axial zone of the Ngalia Basin has been elucidated by an interpretation of seismic data, and has been integrated with the structure revealed in the narrow marginal strips of outcrops.

Three prominent reflection events of varying quality and continuity were plotted over the western zone of the basin but only the deepest event showed continuity into the central zone. The deepest reflector is interpreted as originating at or near the base of the sedimentary sequence; the intermediate reflector at the top of the Proterozoic sequence; and the shallow reflector at the base of the Upper Palaeozoic Sequence.

Major faults delineate three major structural divisions in the western zone—a northern terrace, a central trough and a southern shelf. A fourth structural division in the central zone of the basin is characterised by a series of horsts and grabens.

Interpretation of the sequence of major faulting using palinspastic restorations show several distinct movements, both normal and reverse, with the earliest occurring in the Proterozoic. Many of the structures in the north can be continued with the major structures apparent in outcrop but those in the south have no surface expression.

Lower Palaeozoic rocks, previously postulated as absent in the western part of the basin, are now considered to be represented by a wedge of sediments with a maximum thickness of 1700 m preserved in the central trough. Although structural closures are few, the strong indication of a thick Palaeozoic sequence considerably enhanced the petroleum potential of the basin.

THE BUREAU OF MINERAL RESOURCES, GEOLOGY AND GEOPHYSICS

BMR JOURNAL of Australian Geology & Geophysics

The BMR Journal is a quarterly publication. It contains results of work carried out by BMR, either alone or jointly with other organisations or individuals, and of work sponsored by BMR. In addition to articles the Journal may include short notes, and discussion. Discussion of material in the Journal is invited from anyone. Essentially the Journal is a research outlet, but it also records new information and developments, and reflects the varied roles and functions of the organisation. The Journal aims for rapid publication from a range of earth science activities. It forms an integral part of BMR's exchange system; it can also be purchased on subscription or, if available, as individual numbers.

Volume 3, Number 1 (March 1978) contains the following articles: Proterozoic microfossils from the Roper Group, Northern Territory, Australia; The stratigraphic and tectonic development of the Manokwari area, Irian Jaya; Triassic environments in the Canning Basin, Western Australia; The Proterozoic and Palaeozoic rocks of The Granites-Tanami region, Western Australia and Northern Territory, and inter-regional correlations; Lithological correlations of Adelaidean glaciogenic rocks in parts of the Amadeus, Ngalia and Georgina Basins; Hot-spot volcanism in St Andrew Strait, Papua New Guinea: geochemistry of a bimodal rock suite. It also includes the following notes: Clay modelling of the Fitzroy Graben; Delny-Mount Sainthill Fault System, eastern Arunta Block; Buried reef structures in the Lennard Shelf, Canning Basin, Western Australia.

Volume 3, Number 2 (June 1978) contains the following articles: Skeletal carbonate variation on the continental shelf of Australia; Mathematical modelling of experimental systems simulating metal chelating in reducing sedimentary environments; The Late Cainozoic evolution of the Carpentaria Plains, north Queensland; The sediments of the Argo abyssal plain and adjacent areas, northeast Indian Ocean; The Oenpelli Dolerite – a Precambrian continental tholeiitic suite from the Northern Territory; Nannofossil and planktic foraminiferal biostratigraphy across the Oligocene-Miocene boundary in parts of the Indo-Pacific region; Gravity evidence for abrupt changes in mean crustal density at the junction of Australian crustal blocks. It also includes the following notes: Stratigraphic significance of a discovery of Lower Proterozoic tuff in the Pine Creek Geosyncline, Northern Territory; A system for the simulation of sedimentary environments.

Subscription costs $10 (Australian) per annual volume; or if available $3 per individual number. All amounts are payable in advance. These sums cover the cost of ordinary postage only; airmail is extra – write for details. Subscriptions, made payable to the Receiver of Public Moneys, should be sent to the Director, Bureau of Mineral Resources, Geology and Geophysics, P.O. Box 378, Canberra City, A.C.T. 2601, Australia.

Subscription for Volume 3 – $10, Volumes 1, 2 & 3 – $30.

Two other BMR publications

AUSTRALIAN MINERAL INDUSTRY ANNUAL REVIEW 1976

The Australian Mineral Industry Annual Review 1976 includes information to 30 June 1977 and was published in August 1978. The yearbook provides a record of the growth of the Australian mineral industry, and reports production, consumption, treatment, trade, prices, new developments, exploration, and resources for all mineral commodities including fuels, and summarises equivalent developments abroad. Full statistical coverage is limited to 1976. With this edition the printing format has been redesigned, more illustrations have been incorporated in **Part 1,** and four new location maps, for mineral sands, salt fields, sulphur, and tungsten, in **Part 2.**

Part 1, **'General Review',** contains salient statistics of the Australian mineral industry as a whole, and provides an overview of the industry under the headings: World Summary, The Mineral Industry in Australia, The Industry in the National Economy, Important Recent Developments, Production, Overseas Trade, Prices, Mineral Exploration Expenditure, Structural Data (including Investment, Mining Census Summary, Wages and Salaries, Industrial Disputes, Taxation, Royalty Receipts), and Government Assistance, Legislation, and Controls. **Part 2, 'Commodity Review',** is the major section covering individual mineral commodities, from Abrasives to Zirconium. **Part 3, 'Mining Census',** tabulates statistics extracted from the Mining Census, and some mineral processing statistics from the Manufacturing Census. **Part 4, 'Mineral Production: State Mines Departments Statistics'** tabulates quantum and value data on mineral output provided by State Departments of Mines. Listed in **Appendices** are: Principal Mineral Producers; Ore Buyers and Mineral Dealers; Government Mining Services; Industry, Professional, and Development Organisations and Associations, etc.; and a Summary of Mineral Royalties payable in the States and Territories.

AUSTRALIAN MINERAL INDUSTRY QUARTERLY

The Australian Mineral Industry Quarterly—a joint publication of BMR and the Australian Bureau of Statistics—reviews developments in mineral and fuel commodities in Australia and records statistics of production, exports, and imports. **Number 4 of Volume 30,** was published in August 1978:

Part 1 (BMR)—'Quarterly Review'—contains a 'commodity review' of the principal mineral commodities in 1977, an article, 'Australian mineral resources 1977', and a list of metal, ore, and concentrate prices for the quarter ended 31 December 1977.

Part 2 (ABS)—'Quarterly Statistics'—contains production and trade figures for the quarter ended 30 September 1977. Summary tables of Australian mine, smelter, and refinery production of principal minerals and metals for the quarter ended 31 December 1977 are also included.

The article in **Volume 31, No. 1,** now in press, is 'Coal exploration in Australia', by R. Pratt.

The price of the 1976 Annual Review is $18.00; the price of one volume (4 numbers) of the Quarterly is $8.00. Subscription forms may be obtained by writing to the Director, Bureau of Mineral Resources Geology and Geophysics, P.O. Box 378, Canberra City, A.C.T. 2601, or phone (062) 49 9300.

Contents

Notes

Abstracts

R76/1403(3) Cat. No. 78 7635 8